District-scale landslide risk analysis of debris inundation for the Kaikōura District

CI Massey SJ de Vilder B Lukovic
DB Townsend BJ Rosser

GNS Science Consultancy Report 2021/89
October 2021

GNS SCIENCE
TE PŪ AO

DISCLAIMER

This report has been prepared by the Institute of Geological and Nuclear Sciences Limited (GNS Science) exclusively for and under contract to Environment Canterbury and Kaikōura District Council. Unless otherwise agreed in writing by GNS Science, GNS Science accepts no responsibility for any use of or reliance on any contents of this report by any person other than Environment Canterbury and Kaikōura District Council and shall not be liable to any person other than Environment Canterbury and Kaikōura District Council, on any ground, for any loss, damage or expense arising from such use or reliance.

Use of Data:

Date that GNS Science can use associated data: October 2021

BIBLIOGRAPHIC REFERENCE

Massey CI, de Vilder SJ, Lukovic B, Townsend DB, Rosser BJ. 2021. District-scale landslide risk analysis of debris inundation for the Kaikōura District. Lower Hutt (NZ): GNS Science. 117 p. Consultancy Report 2021/89.

CONTENTS

EXECUTIVE SUMMARY ..... **IV**

NOTATION ..... **VI**

1.0 INTRODUCTION **1**

1.1 Project Objectives 2
1.2 Report Structure 4
1.3 Personnel 4

2.0 DATA USED IN THIS STUDY **5**

3.0 RISK ANALYSIS METHODOLOGY **7**

3.1 Analysis Method Framework 8
3.2 Landslide Types and Locations Analysed 9
3.3 Probability of the Initiating Event and Landslide Intensity 10
3.3.1 Earthquake-Induced Landslides 10
3.3.2 Rainfall-Induced Landslides 13
3.4 Probability of the Landslide Hitting the Element at Risk ($P_{(T:L)}$) 17
3.5 Vulnerability ($V_{(D:T)}$): Probability of Being Killed if Present and in the Path of Landslide Debris 22
3.6 Local Personal Risk 24
3.6.1 Risk Model Scenarios 26

4.0 RISK ANALYSIS RESULTS **28**

4.1 LPR versus AIFR 28
4.2 General Results for the Study Area 31

5.0 DISCUSSION **33**

5.1 Consistency with Actual Experience 33
5.2 Sensitivity to Key Uncertainties 34
5.3 Comparison with Prehistorical Landslide Rates 38
5.4 Applying these Results 41

6.0 RISK IN CONTEXT **43**

7.0 CONCLUSIONS **44**

8.0 ACKNOWLEDGEMENTS **45**

9.0 REFERENCES **45**

FIGURES

Figure 1.1 Study area location. 2

Figure 3.1 Standard normal distribution displaying relationship between cumulative percentage of the data and standard deviations. 7

Figure 3.2 Earthquake-induced landslide susceptibility model inputs related to the 2016 Kaikōura earthquake and used to forecast landslide occurrence, adopting the logistic regression model from Massey et al. (forthcoming 2021). 11

Figure 3.3 Earthquake-induced landslide susceptibility model results for earthquake bands 1 to 4. 12

Figure 3.4 Rainfall-induced landslide susceptibility model results, adopting the historical 24-hour rainfall amounts, for bands 1 to 3. 16
Figure 3.5 Earthquake-induced landslide runout probability of exceedance (50% and 2.3%) Fahrböschung extents for given volume classes of open slope dry rock and debris avalanches for an example watershed (Watershed 12). 19
Figure 3.6 Rainfall-induced landslide runout probability of exceedance (50% and 2.3%) Fahrböschung extents for given volume classes of open slope wet debris avalanches and channelised wet debris flows and floods for an example watershed (Watershed 12) 20
Figure 4.1 Risk model results for mean scenarios 1 (a) to 4 (d), adopting different values for the variables used in the risk model 29
Figure 4.2 Risk model results for upper scenarios 5 (a) to 9 (e), adopting different values for the variables used in the risk model 30
Figure 4.3 Local personal risk maps for earthquake- and rainfall-induced landslides and all landslides for one watershed. 32
Figure 5.1 Polygons, showing the debris fans extending south from the Mt Fyffe range that were used to estimate their volumes 38
Figure 5.2 Difference models for the fans for which volumes were calculated 39

TABLES

Table 2.1 Summary of data types, sources and uses within this study. 5
Table 3.1 Annual frequency of a given PGA occurring in the study area obtained from the NSHM, and the representative event PGA for each earthquake band. 11
Table 3.2 Landslide volume classes and the assumed probability of an earthquake-induced landslide of a given volume class occurring in the 2016 Kaikōura earthquake, adopting Version 2.0 of the mapped landslide distribution 13
Table 3.3 Annual frequency of a given range of 24-hour rainfall amounts occurring in the study area based on historical data, obtained from the HIRDS V4 model, and the representative mean 24-hour rainfall amount for each band 16
Table 3.4 Landslide volume classes and the assumed probability of a rainfall-induced landslide of a given volume class occurring in the Cyclone Alison and ex-Tropical Cyclone Ita storms. 16
Table 3.5 Summary of Fahrböschung and ΔH/L values for each volume class of open slope dry debris and rock avalanches used in this project 18
Table 3.6 Summary of Fahrböschung and ΔH/L values for each volume class of open slope wet debris avalanches used in this project 18
Table 3.7 Summary of Fahrböschung and ΔH/L values for each volume class of channelised wet debris floods and flows used in this project 18
Table 3.8 Landslide intensity (debris height) and the adopted bio-physical vulnerability values used in the study. 23
Table 3.9 Landslide volume classes and runout exceedance with their assumed bio-physical vulnerability values used in the study. 24
Table 3.10 Risk model scenarios. 27
Table 5.1 Uncertainties and their implications for risk. 35
Table 5.2 Results of fan volume calculation. 40

APPENDICES

APPENDIX 1 EARTHQUAKE-INDUCED LANDSLIDE SUSCEPTIBILITY 51

APPENDIX 2 RAINFALL-INDUCED LANDSLIDE SUSCEPTBILITY.....52

A2.1 Datasets and Variables Used to Train the Rainfall-Induced Landslide Model 52

A2.2 The Logistic Regression RIL Model 57

A2.3 The Statistical Performance of the Rainfall-Induced Landslide Model.....57

A2.4 Rainfall-Induced Landslide Model Results 58

APPENDIX 3 LOCAL PERSONAL RISK MAPS: SCENARIO 2.....62

APPENDIX 4 LOCAL PERSONAL RISK MAPS: SCENARIO 7.....89

APPENDIX 5 EXAMPLE SITE-SPECIFIC ASSESSMENT FORM.....117

APPENDIX TABLES

Table A1.1 Logistic regression parameter estimates (coefficients) for each variable per GeolCode used to forecast earthquake-induced landslide susceptibility.....51

Table A2.1 Predictor variables used in the logistic regression model and their ID codes, descriptions and units. 54

Table A2.2 Logistic regression modelled scenarios trained per GeolCode, adopting data from Cyclone Alison (1975) and ex-Tropical Cyclone Ita (2014) rainfall-induced landslide inventories combined.....59

Table A2.3 Parameter estimates (coefficients) for each variable per GeolCode, adopting data from Cyclone Alison (1975) and ex-Tropical Cyclone Ita (2014) rainfall-induced landslide inventories combined.....59

APPENDIX FIGURES

Figure A2.1 24-hour rainfall from rain gauge records and the mapped landslide distributions associated with: Cyclone Alison (1975) and ex-Tropical Cyclone Ita (2014).....53

Figure A2.2 The variables used to train the logistic regression rainfall-induced landslide forecast model.....56

Figure A2.3 The cumulative number of landslides per square kilometre equal to or greater than a given landslide source area, plotted separately for Cyclone Alison and ex-Tropical Cyclone Ita.....56

Figure A2.4 GeolCode 1: CumF-R plot for the logistic regression model.....60

Figure A2.5 GeolCode 2: CumF-R plot for the logistic regression model.....60

Figure A2.6 GeolCode 3: CumF-R plot for the logistic regression model.....61

Figure A2.7 GeolCode 5: CumF-R plot for the logistic regression model.....61

EXECUTIVE SUMMARY

Canterbury Regional Council (CRC) and Kaikōura District Council (KDC) commissioned the Institute of Geological and Nuclear Sciences (GNS Science) to map areas of the KDC district that could potentially be affected by landslides triggered by earthquakes and/or rainfall.

GNS Science has carried out a district-scale quantified landslide risk analysis for the debris inundation areas, identified in Phase 1 of the project, triggered by earthquake and rainfall events. The objective of this Phase 2 study is to inform KDC and CRC of the spatial distribution of risk to life and the factors that most contribute to landslide risk in the study area.

The quantitative landslide risk analysis used in this Phase 2 study is based on risk-estimation methods that follow appropriate parts of the Australian Geomechanics Society framework for landslide risk management (Australian Geomechanics Society 2007a–d). It provides risk estimates suitable for use under SA/SNZ ISO1000: 2009. The risk analysis quantifies the risk to people – in this case, of loss of life – in the study area. The landslide risk metrics adopted for this study are: (i) the local personal risk (LPR) and (ii) the annual individual fatality risk (AIFR).

The LPRs calculated in this report assume that a person is present 100% of the time. To calculate the AIFR from landslide hazards to a person in a dwelling, the estimated LPR for a given dwelling is multiplied by the proportion of time that the person may spend in the dwelling per year. For example, if a person only spends 50% of their time a day (and per year) in the dwelling, then the AIFR would be 50% of the estimated LPR for the given dwelling (AIFR = LPR × 0.5).

The conclusions from this study are:

1. The LPR from landslide hazards depends on the proximity of a person or dwelling to the steeper slopes and/or whether they are on a debris flow fan.
2. The main contributor to the LPR is from rainfall-induced landslides (RIL). This is because RIL events occur more frequently than strong earthquakes.
3. The LPR from earthquake-induced landslides (EIL) tends to decrease more rapidly with increased distance from the toe of the steeper slopes than the LPR from RIL. This is because the debris from RIL is always wet and tends to travel further than the usually drier debris associated with EIL.
4. The LPR from RIL tends to be slightly higher around the Clarence Valley region and further north. This reflects:
    a. the slightly higher 24-hour rainfall amounts estimated around the Clarence Valley region and further north for the given rainfall bands from the High Intensity Rainfall Design System (HIRDS); and
    b. the more susceptible nature of the geological materials – mainly soils, sandstones, siltstones and limestones – compared to the stronger greywacke sandstones that form the majority of the slopes south of the Clarence Valley.
5. The LPR from EIL is highest along the steeper coastal sections of the Kaikōura district, especially along State Highway 1 to the north and south of Kaikōura and in the Mt Fyffe and Clarence River areas.

6. The sensitivity of the risk model to key uncertainties and the reliability of the assessments were investigated by changing some of the input variables used; these were: the number of landslides triggered by earthquake and 24-hour rainfall triggers; the impact of climate change on increasing the 24-hour rainfall amount forecast to occur at the given annual frequencies; the probability of landslide debris passing a given distance down the slope – runout probability of exceedance (POE) related to Fahrböschung; and the probability of a person present being hit and killed by landslide debris.
    a. These uncertainties are expressed as factors of difference. A factor of difference of 10 represents an order of magnitude change in the risk estimates, e.g. a factor of 10 increase changes the risk from 1×10^{-5} to 1×10^{-4}.
    b. These uncertainties combine to give a total factor of difference of between 8 and 10, which is up to an order of magnitude uncertainty between the risk estimates.
    c. This means that a location with an AIFR of 10^{-4} (1 chance in 10,000 of being killed per year) could feasibly have an AIFR as low as 10^{-5}, if all of the optimistic (non-conservative) values of the variables used in the risk model were adopted. Conversely, the AIFR at the same location may be as high as 10^{-3} if all of the pessimistic (conservative) values for the variables in the risk model were assumed. This difference is between the risk estimates that adopt all 'mean' (scenario 1) values versus those that adopt all upper (scenario 9) values for the variables used in the risk model.
7. The two most significant uncertainties in this analysis were: (i) the impact of climate change on increasing the 24-hour rainfall amounts that could occur at the given annual frequencies and (ii) the runout POE for each Fahrböschung extent. These two variables combine to give a total factor of difference between the risk estimates of between 5 and 6.

Recommended next steps for KDC and CRC are:

1. KDC and CRC consider establishing risk criteria for determining the tolerability or otherwise of landslide risk across the district, based on societal acceptance of comparable levels of risk arising from other sources. Such criteria should be based around a defined sustainable upper limit of tolerability of, for example, LPR or AIFR, that represents the risk level above which KDC and CRC does not consider it tolerable for there to be people at risk in their properties in the longer term.
2. From past examples, including the Port Hills, Canterbury, the sustainable threshold of AIFR should be set within a range from 3×10^{-5} to 1×10^{-3} per year, consistent with risk levels currently tolerated in New Zealand and with regulatory practice elsewhere. A suitable starting point for KDC and CRC's deliberation as to where to set their threshold within this range would be a level of 1×10^{-4} (1/10,000 per year) AIFR.
3. KDC and CRC could adopt a lower threshold of LPR or AIFR above which development is controlled to prevent accumulation of people in areas of substantial risk below the sustainable threshold of tolerability. Such a threshold could be set 10 times below the tolerability threshold for general property uses involving significant occupancy by people and 100 times below the tolerability threshold for particularly sensitive property uses (e.g. schools, care homes, hospitals).

NOTATION

$P_{(LOL)}$	The annual risk (probability) of loss of life (death) of a person from landslides.
$P_{(L)}$	The annual probability of the initiating event (landslide).
$P_{(T:L)}$	The probability of the landslide (e.g. the debris from a landslide of a given type) reaching the element at risk.
$P_{(S:T)}$	The spatio-temporal probability of the person at risk (the proportion of a year that the person is in the path of the landslide when it reaches or passes the element at risk).
$V_{(D:T)}$	The vulnerability of the person to the landslide event (the probability that the person will be killed if impacted by the landslide).
P_{UB}	Upper bound conditional probability used to calculate risk from landslides that occur during one triggering event.
VOLx:	A given volume class (e.g. 100 m³).
EILx	A representative earthquake band (e.g. Band 1).
RILx	A representative rainfall band (e.g. Band 1).
$N_{EQ:(VOLx:EILx)}$	The number of landslides of a given volume class occurring within each watershed and each earthquake band.
LSA_{EILx}	The forecast area of landslides in a watershed, if the representative earthquake band were to occur.
$P_{VOLx:EILx}$	The probability of a given earthquake-induced landslide volume class occurring, if the representative earthquake band were to occur.
A_{VOLx}	The source area of a landslide for a given volume class.
$N_{R:(VOLx:RILx)}$	The number of landslides of a given volume class occurring within each watershed and within each rainfall band.
LSA_{RILx}	The forecast area of landslides if the representative rainfall band were to occur.
$P_{VOLx:RILx}$	The probability of a given rainfall-induced landslide volume class occurring if the representative rainfall band were to occur.
P_{IN}	The probability of inundation.
$P_{IN:VOLx:50\%}$	The probability of inundation for a given volume class in the 50% runout probability of exceedance extent.
$P_{IN:VOLx:2.3\%}$	The probability of inundation for a given volume class in the 2.3% runout probability of exceedance extent.
$P_{IN:1(VOLx)}$	The probability of inundation within a source region from one landslide in each volume class.
$A_{VOL:100}$	The total area of the source region of the smallest landslide volume class (the 100 m^3 class) within the given watershed.
$P_{IN:N(VOLx)}$	The probability of inundation within a source region from all landslides in each volume class.
$P_{IN:N(VOLx:50\%)}$	The probability of debris from a landslide of a given volume class within the 50% runout probability of exceedance extent.
$P_{IN:N(VOLx:2.3\%)}$	The probability of debris from a landslide of a given volume class within the 2.3% runout probability of exceedance extent.
P_{DEATH}	The probability of death.

$P_{DEATH:VOLx:EILx:POEx}$	The probability of death for landslides in each volume class and within each earthquake band at a given runout probability of exceedance extent.
$P_{DEATH:ALL\_EILx}$	The probability of death for all landslides that occur within a given earthquake band.
$Af_{EIL\ x}$	The annual frequency for a given earthquake band.
$LPR_{EIL\ x}$	The local personal risk from landslides that occur within a given earthquake band.
$LPR_{EIL:Total}$	The local personal risk from landslides that are triggered by all earthquake bands.
$P_{DEATH:RILx:VOLx:POEx.}$	The probability of death for landslides in each volume class and within each rainfall band at given runout probability of exceedance extent.
$P_{DEATH:ALL\_RILx}$	The probability of death for all landslides that occur within a given rainfall band.
$LPR_{RIL\ x}$	The local personal risk from landslides that occur within a given rainfall band.
$LPR_{RIL:Total}$	The local personal risk from landslides that are triggered by all rainfall bands.

This page left intentionally blank.

1.0 INTRODUCTION

Canterbury Regional Council (CRC) and Kaikōura District Council (KDC) commissioned the Institute of Geological and Nuclear Sciences (GNS Science) to map areas of the KDC district that could potentially be affected by landslides triggered by earthquakes and/or rainfall. It is understood that the results from this project may be used to underpin parts of the KDC District Plan change with regard to their natural hazards provisions, which is being reviewed following the M_W7.8 14 November 2016 Kaikōura earthquake.

The work in this report was carried out under the agreed terms and conditions of the Approved Contractor Agreement, Contract No 1211-20/21 between CRC and GNS Science for the period May 2021 to April 2024.

The area covered by this study is shown in Figure 1.1.

This work is to be carried out in two phases:

- Phase 1: To provide a district-scale deterministic assessment of the locations within the project area that could be affected by landslide hazards.
- Phase 2: To provide a district-scale probabilistic analysis of the landslide hazards identified in Phase 1 and their risk to life.

Phase 2 required completion of Phase 1. Phase 1 was completed in March 2020 and the results are reported in CR2019/102 (Brideau et al. 2020). This report presents the results from Phase 2 of the work.

The scope of work, study area and budget for this Phase 2 work were outlined in Proposal number Q31199419, which was approved by CRC on 28 June 2021.

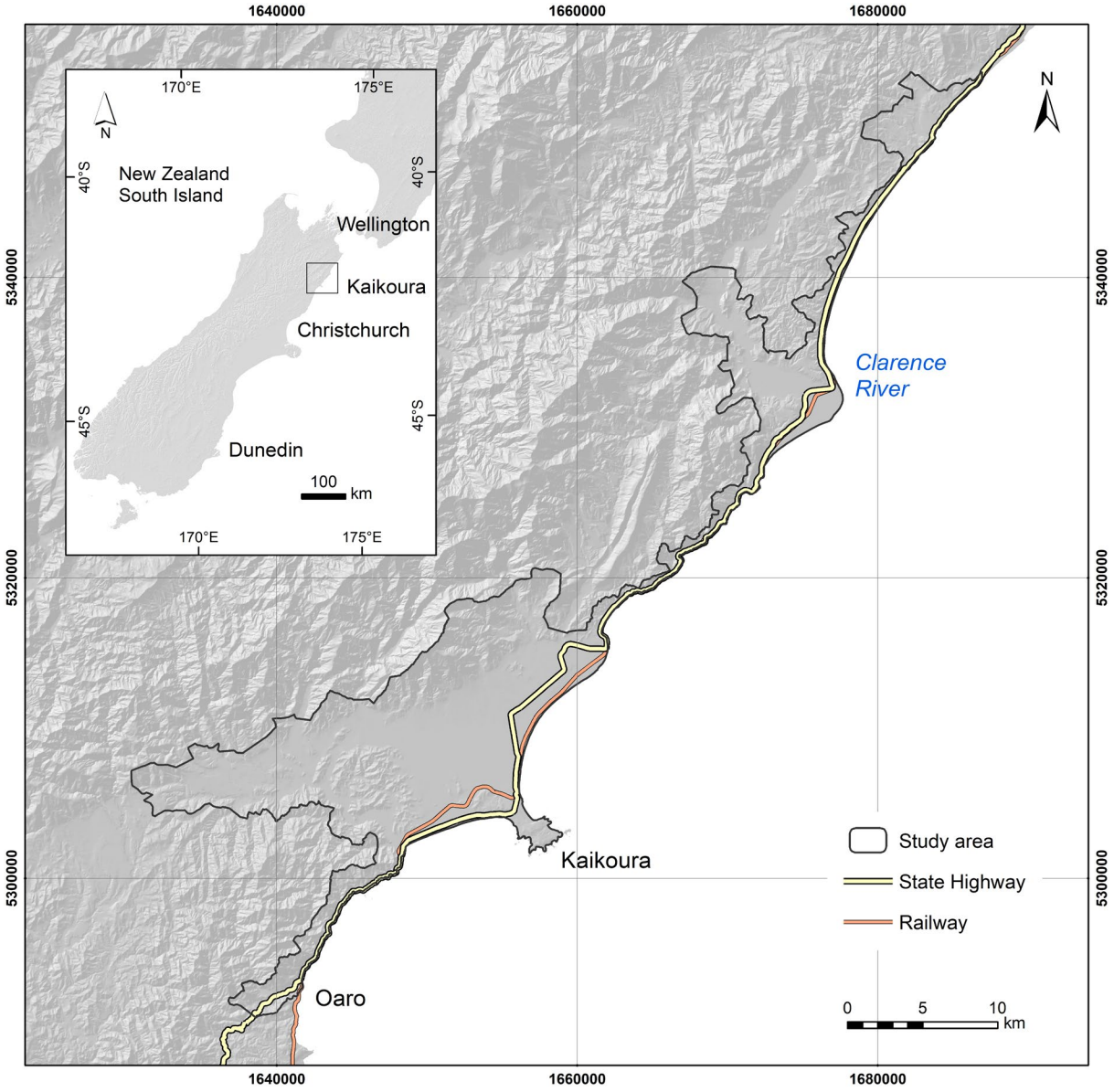


Figure 1.1 Study area location.

1.1 Project Objectives

The objective of this Phase 2 study is to inform KDC and CRC of the spatial distribution of risk to life and the factors that most contribute to landslide risk in the study area.

GNS Science has carried out a district-scale quantified landslide risk analysis for the debris inundation areas identified in Phase 1 of the project, as shown by the study area in Figure 1.1, that may be triggered by earthquake and rainfall events.

The quantitative landslide risk analysis is based on risk-estimation methods that follow appropriate parts of the Australian Geomechanics Society framework for landslide risk management (Australian Geomechanics Society 2007a–d). It provides risk estimates suitable for use under SA/SNZ ISO1000: 2009.

The risk analysis quantifies the risk to people – in this case, of loss of life – in the study area. The landslide risk metrics adopted for this study are local personal risk (LPR) and annual individual fatality risk (AIFR).

The LPR is a widely used risk metric (e.g. Massey et al. 2020a; Crowley et al. 2017; Jonkman et al. 2003) that represents the annual probability of death for a theoretical imaginary person present at a particular location for 100% of the time (24 hours a day and 365 days of the year). It is a useful metric to visualise the spatial distribution of risk in the study area and can be used to help plan and/or re-align buildings and roads.

The AIFR is expressed in terms of the fatality risk experienced by an individual (probability of death and can include life-threatening injuries) over one full year of living in a dwelling in the study area. The risk is calculated for a person that spends different amounts of time present in a dwelling per year. The units of AIFR are probability of fatality (loss of life) per year. Information on how to calculate AIFR from LPR data is provided in this report.

The uncertainties relating to the parameters used in the risk analyses, and their impact on the risk estimates, have also been quantified to give some indication of the precision of the risk results. This work does not include any assessment of the river-related (fluvial) flooding, erosion or debris flood hazards associated with the streams and rivers in the area (Figure 1.1) or the risk from other natural hazards, such as tsunami.

The project comprises the following tasks, which were carried out for the study area shown in Figure 1.1:

1. Collate historical rainfall and landslide records to develop rainfall-induced landslide (RIL) magnitude and annual frequency relationships.
2. Adopt the earthquake-induced landslide (EIL) susceptibility models developed by Massey et al. (forthcoming 2021) and develop landslide magnitude frequency relationships linked to earthquake ground shaking intensity.
3. Develop geospatial landslide risk models using the hazard footprints developed in Phase 1 of this work.
4. Carry out field validation of the risk analysis results.

This Phase 1 and Phase 2 work relies upon the datasets developed for the MBIE-funded Endeavour Programme, ‘Earthquake-induced landscape evolution’ (Contract Number: C05X1709).

1.2 Report Structure

The report has been structured into six sections:

- Section 1: Introduction and background to this report
- Section 2: Data used in this study
  - Description of the data used and their sources
- Section 3: Risk analysis methodology
  - Explanation and calculation of risk
- Section 4: Risk analysis results
  - Explanation of key risk drivers
- Section 5: Discussion
  - Consistency with actual experience
  - Sensitivity of the risk to key uncertainties
  - Comparison with prehistorical landslide rates
  - Applying the results
- Section 6: Risk in context.

1.3 Personnel

This report has been prepared by Chris Massey, Saskia de Vilder, Biljana Lukovic, Dougal Townsend and Brenda Rosser (GNS Science). The risk calculations and calculation route were reviewed by Rob Buxton (GNS Science). This report was independently reviewed by Dr Tim Davies (University of Canterbury). Members of the team visited the study areas on 29–30 September 2021 to carry out field validation surveys of the risk models and input data and to meet with KDC and CRC to discuss the results and input variables to be used in the risk model.

2.0 DATA USED IN THIS STUDY

Table 2.1 Summary of data types, sources and uses within this study.

Data	Description	Source	Date	Where Used in this Analysis
Light Detecting and Ranging (LiDAR), digital elevation model (DEM)	DEM derived from LiDAR survey (last return) sampled to 1 m ground resolution and subsequently resampled to a 3 m ground resolution.	AAM Ltd	2016	Used as base topography for the landslide runout modelling and risk modelling.
National New Zealand DEM	New Zealand DEM at 8 m resolution.	LINZ Data Service (2012)	2012	Used as the base topography for the earthquake- and rainfall-induced landslide susceptibility analyses. The DEM and its derivatives were resampled to 3 m resolution for this analysis.
Phase 1 Report: CR2019/102 (Brideau et al. 2020)	Identification of main landslide types affecting the study area.	Media reports, aerial photograph, local knowledge and survey data	2020	Used to estimate the volume and runout extent of landslides in the area
	Geospatial extents (maps) of landslide debris inundation areas.	-	2020	Used to identify the area affected by landslides of a given type and volume.
Empirical landslide runout models	Empirical relationships between landslide volume and runout for different types of landslide.	Brideau et al. (2021) – database of landslide types, volumes and runout, collated by GNS Science	2020	Used by Phase 1 report CR2019/102 to forecast the distance that different types and volumes of landslides will travel from the source areas within the study area. Also used in Phase 2 to generate additional runout areas for different statistical relationships to explore the sensitivity of the risk estimates to changes in landslide runout.
Mapping of pre-Kaikōura earthquake- and rainfall-induced landslides and the rainfall that triggered them.	Mapping of landslide distributions initiated by Cyclone Alison (11–12 March 1975) and ex-Tropical Cyclone Ita (17 April 2014). Compilation and modelling of rainfall data for these storms.	Aerial photography taken immediately after the events and rain gauge records for the events	2021	Used to establish a relationship between landslide occurrence and rainfall for the study area. This relationship was then used to forecast the number and volume of landslides that could be generated in future rainfall events.

Data	Description	Source	Date	Where Used in this Analysis
Volume characteristics of landslides triggered by the M_W7.8 2016 Kaikōura earthquake	The frequency, area and volume of landslides triggered by the Kaikōura earthquake.	Massey et al. (2020b)	2021	Used to forecast the number and volume of landslides that could be generated in future earthquakes.
Earthquake-induced landslide forecast tool for New Zealand: Version 2.0	Statistical model that forecasts the spatial distribution of earthquake-induced landslide probability over an area at the regional scale.	Massey et al. (forthcoming 2021)	2021	Used to estimate the susceptibility of a slope to generating landslides, and the landslide intensity, at different levels of earthquake ground shaking – peak ground acceleration.
High Intensity Rainfall (HIRDS V4)	The annual exceedance probability of different 24-hour amounts of rainfall using historical data and climate change scenarios.	NIWA https://niwa.co.nz/information-services/hirds	2021	Used to estimate the annual frequency of different amounts of rainfall, which is then linked to landslide occurrence/intensity.
The New Zealand National Seismic Hazard Model (NSHM)	The annual exceedance probability of different levels of peak ground acceleration for site class B (weathered rock).	Stirling et al. (2012)	2016	Used to estimate the annual frequency of different levels of earthquake shaking (peak ground acceleration), which is then linked to landslide occurrence/intensity.
1:250,000 Geological Map of New Zealand (QMAP)	Maps describing the geological units and materials present in New Zealand.	QMAP Seamless (Heron 2020)	2020	Used as an input within both the earthquake- and rainfall-induced landslide forecasts tools to estimate the susceptibility of slope to generating landslides.

3.0 RISK ANALYSIS METHODOLOGY

This report estimates the life-safety risk from landslide hazards to people in the study area. A hazard is a dangerous (or adverse) future event with the potential to cause harm. For this report, and within the study area, the dangerous future events of concern are landslides falling from the slopes onto people and dwellings and loss of land due to landslides beneath dwellings on slopes. While there are other hazards within the study area, these are not discussed in this report.

This report estimates the human life risk from debris avalanches, rock avalanches and debris flows (three types of landslide) to people in the study area (Figure 1.1). To account for the variability and uncertainty in estimating life risk, two 'risk scenarios' were adopted using the Mean and Upper estimates of the variables used in the risk analysis; these were:

1. Mean scenario – adopting the 50th% ('mean') estimates for the landslide susceptibility and production rates, debris runout and vulnerability.
2. Upper scenario – adopting the upper estimates for the landslide susceptibility and production rates, debris runout and vulnerability. This typically meant adopting the 84th% of the statistical relationships (which is equal to the the mean + 1 standard deviation interval, assuming a normal distribution) relating to landslide occurrence – how many landslides a rainfall or earthquake event might trigger – and how far the debris from a landslide might travel down a slope.

Throughout the report, we refer to statistical relationships of the 50th% ('mean') and 84th% ('upper'). We assume that the data is normally distributed, with the numbers referring to the cumulative percentage of the data, as represented by the mean (50th%) and mean + 1 standard deviation (84th%) of a normal distribution (Figure 3.2). The sensitivity of the risk model to changes in these and other variables used in the risk analyses was also examined to quantify the overall precision of the model.

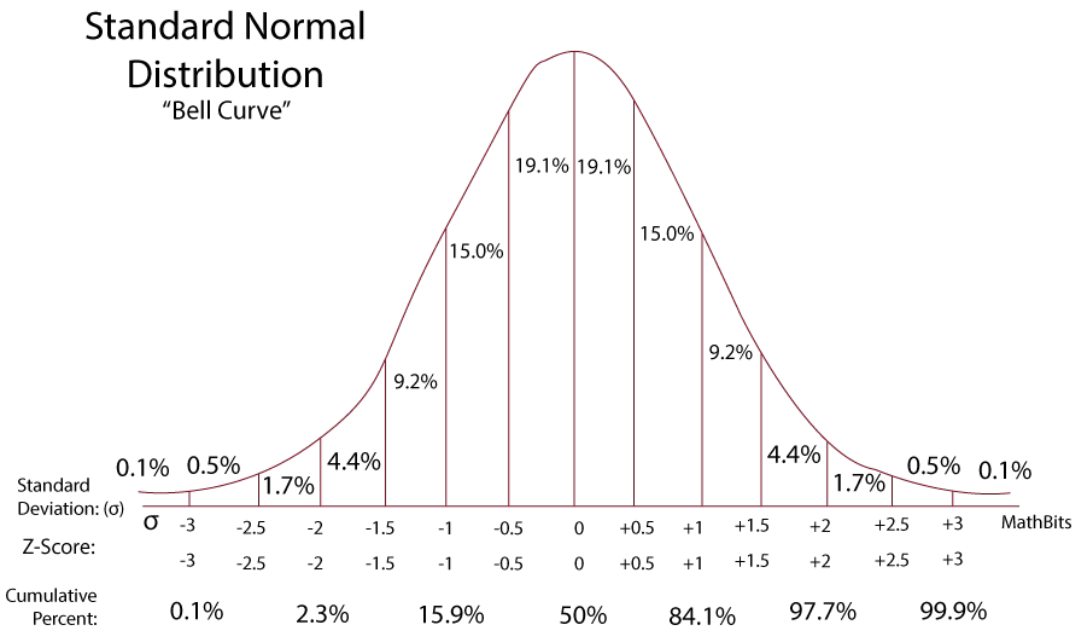


Figure 3.1 Standard normal distribution displaying relationship between cumulative percentage of the data and standard deviations.

3.1 Analysis Method Framework

The landslide risk assessment follows appropriate parts of the Australian Geomechanics Society framework for landslide risk management (Australian Geomechanics Society 2007a–d). A general overview of the risk calculation method is provided below, with more detailed information on the calculation route provided in Sections 3.4, 3.5 and 3.7. Using the Australian Geomechanics Society guidelines for landslide risk management, we calculated the annual probability of death (life risk) of an individual from:

$$P_{(LOL)} = P_{(L)} \, x \, P_{(T:L)} \, x \, P_{(S:T)} \, x \, V_{(D:T)} \qquad \text{Equation 3.1}$$

where:

- $P_{(LOL)}$ is the annual risk (probability) of **L**oss of **L**ife of a person from landslides;
- $P_{(L)}$ is the annual probability of the initiating event (**L**andslide);
- $P_{(T:L)}$ is the probability of the landslide (e.g. the debris from a landslide of a given type) reaching the element at risk;
- $P_{(S:T)}$ is the spatio-temporal probability of the person at risk (the proportion of a year that the person is in the path of the landslide when it reaches or passes the element at risk); and
- $V_{(D:T)}$ is the vulnerability of the person to the landslide event (the probability that the person will be killed if the dwelling is impacted by the landslide). Here, it is recommended that the vulnerability should also include the potential for a person to be aware of the hazard and take evasive action.

Within the study area, there are several situations where the risks from several landslide hazards have to be summed to give the total risk. These include:

- where the element at risk and persons are exposed to several types of landslides, e.g. debris flows, debris avalanches and rock avalanches;
- where the landslides may be triggered by more than one phenomenon, e.g. rainfall and earthquakes; and
- where the element at risk and persons are exposed to several different sizes of landslide of the same classification from different sources, e.g. debris avalanches of 100 m^3, 1000 m^3 and 100,000 m^3 volume.

In these cases, Equation 3.1 has been written as:

$$P_{(LOL)} = \sum_1^n (P_{(L)} x P_{(T:L)} \, x P_{(S:T)} x V_{(D:T)}) \qquad \text{Equation 3.2}$$

where *n* is the number of landslide hazards of a given type and volume triggered by a given phenomenon.

This assumes that the individual hazards are independent of each other, which may often not be correct. If one or more of the hazards may result from the same causative event, e.g. a single rainfall event or earthquake, then the probabilities are estimated using the theory of uni-modal bounds as follows:

The upper bound

From de Morgan's rule, the estimated upper bound conditional probability is:

$$P_{UB} = 1 - (1 - P_1) \times (1 - P_2) \ldots\ldots (1 - P_n)$$ Equation 3.3

where:

P_{UB} is the estimated upper bound conditional probability and P_1 to P_n is the estimate of several individual hazard conditional probabilities.

This calculation is carried out before applying the annual probability of the common causative event. If all of the conditional probabilities P_1 to P_n are small (<0.01), Equation 3.3 yields the same value, within acceptable accuracy, as obtained by adding all of the estimated conditional probabilities.

The lower bound

The lower bound estimate is the maximum individual conditional probability.

3.2 Landslide Types and Locations Analysed

The first step of the risk analysis is to delineate the types of landslides that occur at a given location, as the different landslide types have typical behaviours (e.g. velocity of displacement, re-occurrence, runout travel distance), which affects how hazardous they can be.

Based on the classification by Hungr et al. (2014), Phase 1 of this study (Brideau et al. 2020) analysed the potential locations and runouts of three types of rapidly moving landslides that occur in the study area. These were: (1) debris flows, (2) debris avalanches and (3) rock avalanches. These three types of landslide cover both slippage and falling debris hazards as defined in the Building Act (2004) (see Phase 1 report for definitions). Slippage or falling debris associated with slow-moving landslides, or from rockfalls, have not been assessed as part of this project.

The Phase 1 report determined the locations where landslides of different types and volumes are most likely to occur from potential source areas in the study area. This was calculated using empirical statistical relationships (see Phase 1 report [Brideau et al. 2020] for further information) using landslides generated during the Kaikōura earthquake. We have assumed that the same empirical statistical relationship applies to RIL, as the statistical relationships of landslides generated during the Kaikōura earthquake are within range of other international statistical relationships (cf. Massey et al. 2020).

In this Phase 2 study, the source areas and hazard footprints for the study area were taken from the Phase 1 study (Brideau et al. 2020). The watershed boundaries generated in Phase 1 were typically represented as second-order and third-order catchment boundaries. These were reviewed and modified where required to remove gaps and overlaps between adjacent watersheds. These modified watersheds are the starting point for the landslide risk analyses, with the risk being estimated for landslides sourcing from within each watershed. This was done to capture the physiographic differences between watersheds, which can affect the number, location and type of landslides generated within them.

In the Phase 1 study, a grid cell with a ground resolution of 3 m x 3 m was adopted for all modelling. In this Phase 2 study, we adopt the same 3 m x 3 m grid cell size for the landslide runout and risk modelling and a 32 m x 32 m grid cell size for the landslide susceptibility models (described in Sections 3.4.1 and 3.4.2).

3.3 Probability of the Initiating Event and Landslide Intensity

To estimate the $P_{(L)}$ term of the risk equation, a set of representative events (either earthquake peak ground acceleration [PGA] bands or 24-hour rainfall amount bands) is chosen to span the range of event severity from the lowest to the highest. The number and size of landslides (i.e. the landslide intensity) generated during each event band is estimated from empirical data. More information is provided in Section 3.4.1 for EIL and in Section 3.4.2 for RIL.

3.3.1 Earthquake-Induced Landslides

The probability of an EIL of a given volume occurring in each watershed at different levels of ground shaking intensity was determined using the EIL forecast model described by Massey et al. (2018; 2020c; forthcoming 2021). The landslide susceptibility model, adopting the logistic regression coefficients for the variables listed in Massey et al. (forthcoming 2021), was used to create forecast grids of landslide probability for the study area at a resolution of 32 m x 32 m.

For the modelling, four earthquake bands were adopted based on the annual exceedance probability (AEP, or annual frequency). These bands represent levels of earthquake shaking in the study area that have equivalent return intervals of approximately 100, 250, 500 and 1000 years (Table 3.1). The PGAs for these representative bands were obtained from the New Zealand National Seismic Hazard Model (NSHM; Stirling et al. 2012). The representative PGAs for each band vary spatially across the study area and were represented as a 10 km x 10 km (ground resolution) grid. These PGAs were used as inputs for the EIL susceptibility model.

The following steps were used to develop the EIL probability models for the study region:

- **Step 1:** Sample the NSHM PGAs within each representative earthquake band in ArcGIS for the study area.
- **Step 2:** Using the 10 km PGA grids from Step 1, estimate the EIL probability within each 32 m grid cell by including the given PGA for that grid cell, for each band, in the landslide forecast model, along with the other susceptibility variables required by the model (Figure 3.2). This was done to produce:
  - four 32 m EIL probability grids (one for each band) adopting the mean (50^{th}%) coefficients (Figure 3.3); and
  - four 32 m EIL probability grids adopting the upper (84^{th}%) of the coefficients for the variables used in the forecast tool (Appendix 1: the 84^{th}% coefficients are represented by the mean + 1 standard deviation, assuming a normal distribution).
- **Step 3:** Using the modified watershed boundaries, sum the landslide probabilities within each watershed separately for each EIL probability grid. The sum of the landslide probabilities represents the total number of grid cells that are forecast to generate landslides within the watershed, if the representative earthquake PGAs in the given band were to occur. By adopting the watershed boundaries, the difference in susceptibility to landslide triggering between them is captured, as some watersheds have higher susceptibility than others, meaning those that are more susceptible could generate more landslides during earthquake events.

Table 3.1 Annual frequency of a given PGA occurring in the study area obtained from the NSHM, and the representative event PGA for each earthquake band.

	Earthquake Band			
	Band 1	**Band 2**	**Band 3**	**Band 4**
PGA: Range (g)	0.2–0.3	0.3–0.5	0.5–0.7	>0.6
PGA: Mean (g) (Errors at 1σ)	0.24 (±0.01)	0.39 (±0.04)	0.54 (±0.06)	0.70 (±0.09)
Annual Exceedance Probability of Band	0.01	0.004	0.002	0.001
Equivalent Return Interval	100	250	500	1000

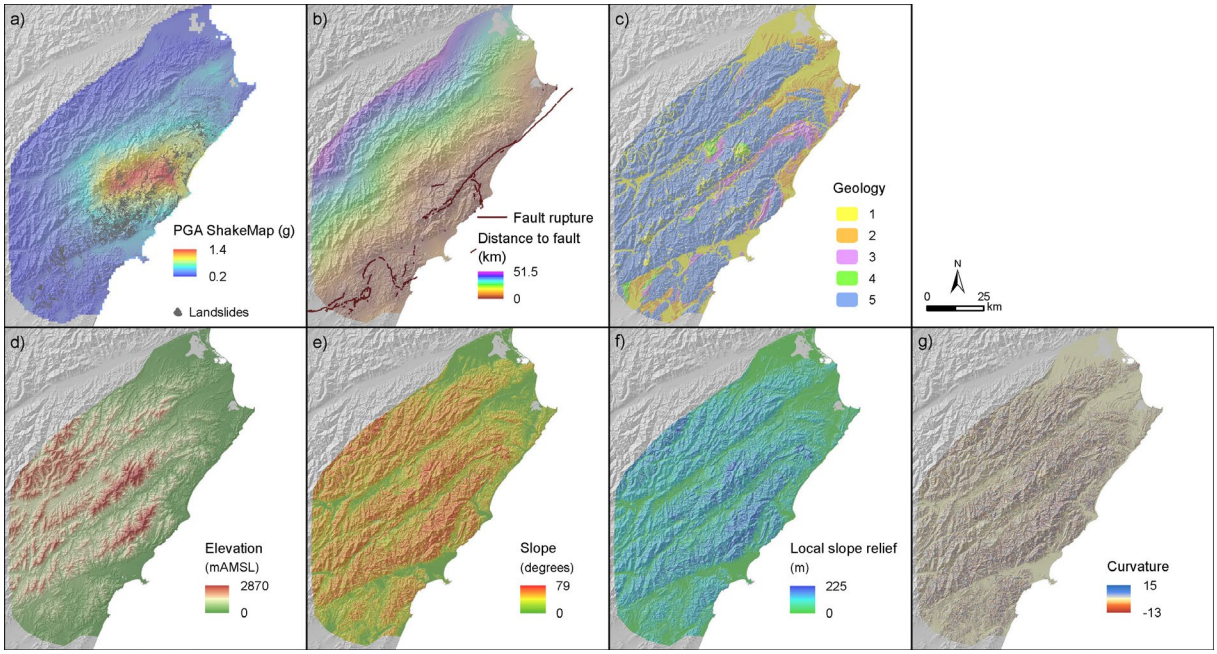


Figure 3.2 Earthquake-induced landslide susceptibility model inputs related to the 2016 Kaikōura earthquake and used to forecast landslide occurrence, adopting the logistic regression model from Massey et al. (forthcoming 2021).

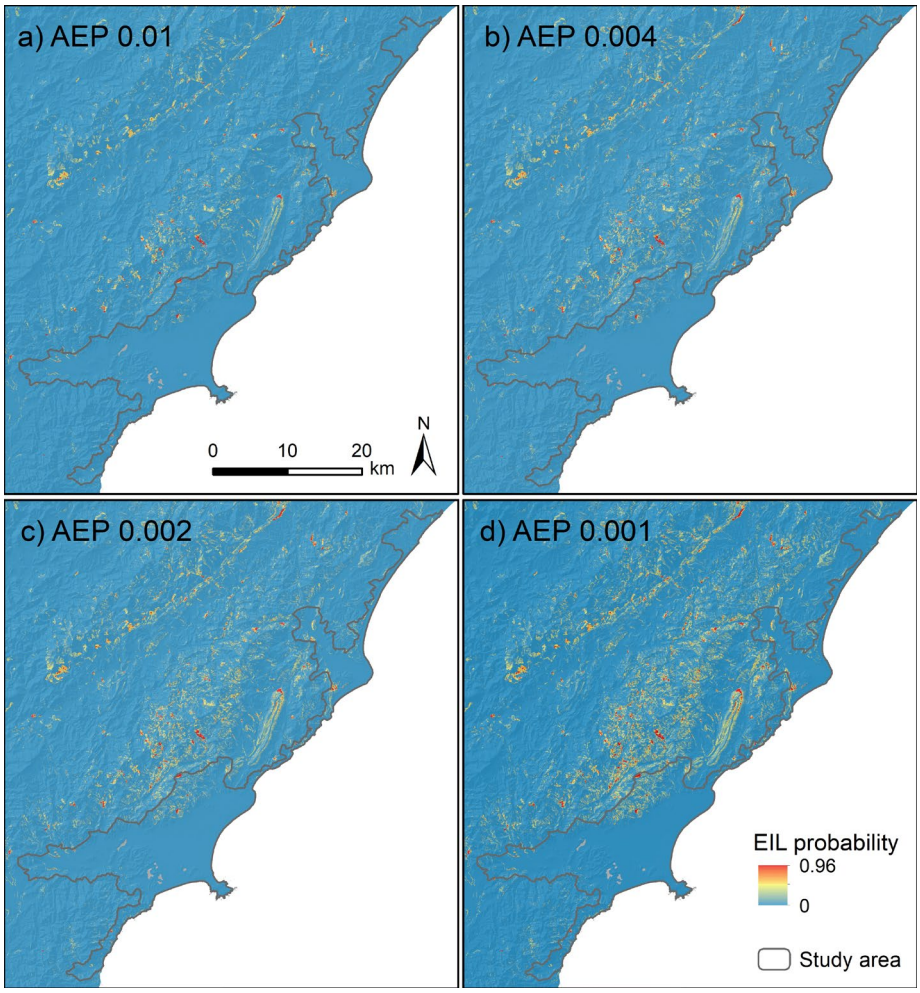


Figure 3.3 Earthquake-induced landslide susceptibility model results for earthquake bands 1 to 4.

- **Step 4:** Using the results from each EIL probability grid, multiply the number of forecast landslide grid cells by the area of a single grid cell (32 m × 32 m = 1024 m^2) to determine the area (in m^2) within each watershed that is forecast to become landslides if the PGA representing the given earthquake band were to occur (LSA_{EILx}).
- **Step 5:** For each watershed and earthquake band, determine the number of landslides of a given volume class occurring within it. The maximum credible landslide volume class that could occur within each watershed was determined during Phase 1 (which is the maximum volume source area region within each watershed). Seven volume classes of landslide were adopted, ranging from 10 m^3 to 10M m^3. Following discussions with CRC and KDC during Phase 1, landslide volumes in the 10 m^3 class, were not thought to be problematic for life safety, given their small volume. For this risk analysis, six volume classes – from 100, 1000, 10,000, 100,000, 1M and 10M m^3 – and their equivalent source areas (m^2) were adopted, as described in the Phase 1 report and shown in Table 3.2. The number of landslides of a given volume class (up to the maximum credible volume class) within each watershed for each band was then determined by:
  - Using the landslide frequency versus source area relationship taken from the Kaikōura earthquake Version 2.0 landslide inventory (Massey at al. 2020c) to estimate the probability distribution of landslides that occurred during this earthquake (Table 3.2).
  - Using this distribution to estimate the number of landslides of a given volume class occurring within each watershed and within each earthquake band ($N_{EQ(VOL:EIL)}$):

$$N_{EQ:(VOLx:EILx)} = (LSA_{EILx} \times P_{VOLx:EILx})/A_{VOLx}$$ Equation 3.4

where $P_{VOLx:EILx}$ is the probability of the given EIL volume class occurring if the representative earthquake PGA in the band were to occur, LSA_{EILx} is the forecast area of landslides from Step 4 and A_{VOLx} is the source area of a landslide for the given EIL volume class (see the Table 3.2).

Table 3.2 Landslide volume classes and the assumed probability of an earthquake-induced landslide (EIL) of a given volume class occurring in the 2016 Kaikōura earthquake, adopting Version 2.0 of the mapped landslide distribution (Massey et al. 2020c).

Landslide Volume Class (m^3)	Volume Class Range (m^3)	Source Area Mean (m^2)	Source Area Upper (m^2)	Data from the V2.0 Kaikōura EIL Inventory		
				Number of Landslides	Proportion of Landslides	Assumed Probability of an EIL Occurring ($P_{VOL:EIL}$)
(1) 100	32–316	70	85	4116	14%	0.3369*
(2) 1000	>316–3162	557	689	15,796	53%	0.3369
(3) 10,000	>3162–31,623	4443	5579	8481	29%	0.2870
(4) 100,000	>31,623–316,228	35,433	45,165	1074	4%	0.0363
(5) 1M	>316,228–3,162,278	282,563	365,653	78	0.3%	0.0026
(6) 10M	>3,162,278	2,253,353	2,960,288	3	0.01%	0.0001

* The landslide frequency – source area relationship of Massey et al. (2020c) displays a 'roll over' in the distribution at a source area of 500 m^2. The equivalent source area volume falls between landslide volume classes (1) and (2), indicating that the number of smaller landslides (with source areas <500 m^2) are under-represented in the distribution, probably due to the resolution of the original landslide mapping. Therefore, for volume class (1), it is assumed that $P_{VOL:EQ}$ is 50% of the sum of volume classes (1) and (2) combined.

3.3.2 Rainfall-Induced Landslides

Past rainstorms have triggered significant landslides in the region, e.g. Cyclone Alison (March 1975), ex--Tropical Cyclone Ita (April 2014), Cyclone Debbie (early April 2017), Cyclone Cook (mid-April 2017) and ex-Tropical Cyclone Gita (February 2018). The probability of a RIL of a given volume occurring in each watershed at different levels of rainfall intensity were determined using an RIL forecast model developed for this study. This was done using logistic regression, to train a forecast model on past RIL and the rainfall that triggered them, in the Kaikōura region. To do this, landslide distributions that were triggered by Cyclone Alison (1975) and ex-Tropical Cyclone Ita (2014) were used. These mapped by GNS Science for the EILD Endeavour Programme. A total of 19,963 landslide source areas were mapped for Cyclone Alison and 3813 for ex-Tropical Cyclone Ita. The method and data used to train the RIL model and statistical results from fitting the model to the data, along with the coefficients for the variables used in the final model, are described in Appendix 2.

Landslides generated during Cyclone Debbie (early April 2017), Cyclone Cook (mid-April 2017) and ex-Tropical Cyclone Gita (February 2018) were not used to train the forecast model for RIL. As these storms occurred after the 2016 Kaikōura earthquake, the number of landslides that were triggered by each storm appear to be elevated compared to those before the earthquake due to the landscape damage it generated. Increases in the rates of landsliding post-earthquake are often temporary and short-lived (e.g. 5–10 years; for example, Tang et al.

2016; Marc et al. 2015). Research and collection of landslide data relating to these storms is ongoing and incomplete at the time of writing this Phase 2 report. However, our use of pre-earthquake historical landslides currently represents the best estimate of how many landslides of a given volume occur during rainfall events.

The landslide susceptibility model, adopting the logistic regression coefficients for the variables listed in Appendix 2, was used to create forecast grids of landslide probability for the study area at a resolution of 32 m x 32 m. There were not enough landslide records occuring in igneous rocks (GeolCode 4 – see Appendix 2 for more information) to statistically fit a logistic regression model. This is because these materials only cover a small part of the area affected by landslides in both storms. For those small areas of the study area within igneous rocks (GeolCode 4), the greywacke (GeolCode 5) coefficients were instead adopted for landslide forecasting, with the rock mass properties of greywacke assumed to be comparable to that of igneous rocks.

For the modelling, three rainfall bands were adopted based on the AEPs of a given range of 24-hourly rainfall (cumulative rainfall for a 24-hour period) events occurring in the study area. These bands represent historical amounts of rainfall that have equivalent return intervals of approximately 50, 100 and 250 years (Table 3.3). The 24-hour rainfall amounts for these representative bands were obtained from HIRDS. The representative 24-hour rainfall amounts for each band taken from HIRDS vary geospatially across the study area and were represented as a 2 km x 2 km (ground resolution) grid. These 24-hour rainfall amounts were used as inputs for the RIL susceptibility model.

To account for the impact of climate change on the forecast 24-hour rainfall amounts, the historical HIRDS rainfall amounts were multiplied by a percentage change factor of 22% based on a projected 2.58°C of climate warning for the 2081–2100 period, adopting RCP8.5 (Carey-Smith et al. 2018). These values were chosen based on advice from CRC. The RIL probability was also estimated using these climate-change-adjusted 24-hour rainfall amounts as inputs.

The following steps were used to develop the RIL probability models for the study region:

- **Step 1:** Use the HIRDS V4 model to sample the 24-hour rainfall amounts for the study area at 2 km resolution for each of the three bands to create three GIS grids of 24-hour rainfall for the study area based on historical HIRDS data and three grids that adopt the climate change scenario (RCP8.5).
- **Step 2:** Using the 24-hour rainfall grids from Step 1, estimate the RIL probability for each rainfall band within each 32 m grid cell by including the given 24-hour rainfall amount for that grid cell, for each band, in the landslide forecast model, along with the other susceptibility variables required by the model. The RIL susceptibility model is described in Appendix 2. This was done to produce:
  - Six RIL probability grids (one for each band using the historical and climate-change-adapted rainfall amounts) that adopt the mean coefficients from the RIL susceptibility model (listed in Appendix 2). The probability model outputs adopting the historical 24-hour rainfall amounts are shown in Figure 3.4.
  - Six RIL probability grids that adopt the upper (84^{th}%) of the coefficients for the variables used in the RIL susceptibility model. These are listed in Appendix 2, where the 84% coefficients are represented by the mean + 1 standard deviation values.

- **Step 3:** Using the modified watershed boundaries, sum the landslide probabilities within each watershed separately for each RIL probability grid. The sum of the landslide probabilities represents the total number of grid cells that are forecast to generate landslides within the watershed, if the representative 24-hour rainfall amount in the given band were to occur. By adopting the watershed boundaries, the difference in susceptibility between them is captured, as some watersheds have higher susceptibility than others, meaning those that are more susceptible could generate more landslides during rainfall events.
- **Step 4:** Using the results from each RIL probability grid, multiply the number of forecast landslide grid cells by the area of a single grid cell (32 m × 32 m = 1024 m^2) to determine the area (in m^2) within each watershed that is forecast to be impacted by landslides if the 24-hour rainfall amount representing the given band were to occur (LSA_{RILx}).
- **Step 5:** For each watershed and 24-hour rainfall band, determine the number of landslides of a given volume class occurring within it. The maximum credible landslide volume class that could occur within each watershed was determined during Phase 1. These ranged from 10 to 1M m^3. Following discussions with CRC and KDC during Phase 1, landslide volumes in the 10 m^3 class were not thought to be problematic for dwellings, given their small volume. There are no RIL ≥1M m^3 known to have occurred within the study area. However, for this study, we assume that the 1M m^3 volume class could occur in a watershed where conditions allow (refer to the Phase 1 study and Table 3.4 for details). For this risk analysis, five volume classes – from 100, 1000, 10,000, 100,000 and 1M m^3 – and their equivalent source areas (m^2) were adopted, as described in Phase 1 and shown in Table 3.2. For this study, we assume that RIL have a similar source area to volume relationship as EIL, as we have limited data on RIL volumes. The probability of a landslide of given volume class (up to the maximum credible volume class) within each watershed was then determined by:
  - Using the landslide frequency versus source area relationship based on the Cyclone Alison (1975) and ex-Tropical Cyclone Ita (2014) landslide distributions to estimate the probability distribution of landslides that occurred during these storms (Table 3.4).
  - Using this distribution to estimate the number of landslides of a given volume class occurring within each watershed and within each 24-hour rainfall band ($N_{R(VOL:RIL)}$):

$$N_{R:(VOLx:RILx)} = (LSA_{RILx} \times P_{VOLx:RILx})/A_{VOLx} \quad \text{Equation 3.5}$$

    where $P_{VOLx:RILx}$ is the probability of the given RIL volume class occurring if the representative 24-hour rainfall amount within the band were to occur, LSA_{RILx} is the forecast area of landslides from Step 4, and A_{vox} is the source area of a landslide for the given RIL volume class (see Table 3.2).

Table 3.3 Annual frequency of a given range of 24-hour rainfall amounts occurring in the study area based on historical data, obtained from the HIRDS V4 model, and the representative mean 24-hour rainfall amount for each band. The range in rainfall values for each band is due to changes across the district. Rainfall amounts can be multiplied by a factor of 1.22 (22%) to determine RCP8.5 projected rainfall amounts.

	Rainfall Band		
	Band 1	**Band 2**	**Band 3**
24-hour Rainfall: Range (mm)	83–288	193–331	227–391
24-hour Rainfall (Historical): Mean (mm) (Errors at 1σ)	224 (±21)	258 (±25)	304 (±29)
Annual Exceedance Probability of Band	0.02	0.01	0.004
Equivalent Return Interval	50	100	250

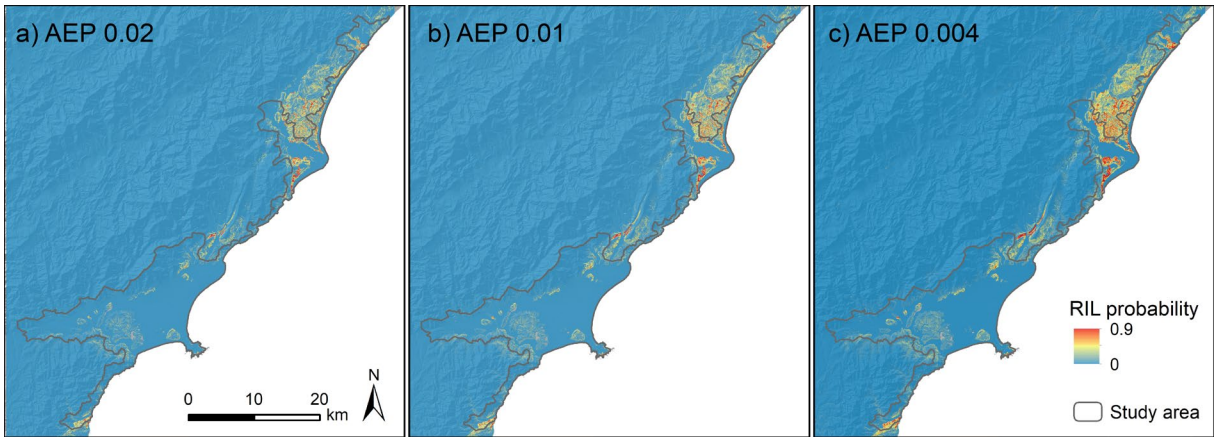


Figure 3.4 Rainfall-induced landslide susceptibility model results, adopting the historical 24-hour rainfall amounts, for bands 1 to 3.

Table 3.4 Landslide volume classes and the assumed probability of a rainfall-induced landslide (RIL) of a given volume class occurring in the Cyclone Alison and ex-Tropical Cyclone Ita storms.

Landslide Volume Class (m^3)	**Cyclone Alison (1975)**		**ex-Tropical Cyclone Ita (2014)**		**Assumed Probability of an RIL Occurring ($P_{VOL:RIL}$)**
	Number of Landslides	**Proportion of Landslides**	**Number of Landslides**	**Proportion of Landslides**	
(1) 100	10,944	54.8%	2105	55.2%	54.9%*
(2) 1000	8874	44.5%	1655	43.4%	44.3%
(3) 10,000	143	0.72%	53	1.39%	0.82%
(4) 100,000	2.0	0.010%	None	N/A	0.008%
(5) 1M	1.0**	0.0050%	None	N/A	0.0042%

* The landslide frequency – source area relationships (both RIL datasets) display a 'roll over' in the distributions at a source area of 100 m^2, indicating that the number of smaller landslides (with source areas <100 m^2) are potentially under-represented in the distribution.

** No landslides within this volume class occurred during these two storms. However, landslides of this volume have occurred post-2016 Kaikōura earthquake during ex-Tropical Cyclone Gita. Although rare, these are possibly caused in part due to the increased susceptibility of the slopes post-earthquake (as a result of earthquake-induced displacement and cracking of the slopes). Therefore, for this study, and only for channelised debris flows, it is assumed that a RIL within the 1M m^3 volume class could occur in a watershed where channelised debris flows are likely to occur. For wet open slope debris avalanches, it is assumed that the maximum volume of landslide that could occur is 100,000 m^3

3.4 Probability of the Landslide Hitting the Element at Risk ($P_{(T:L)}$)

The probability of a landslide reaching and hitting an element at risk ($P_{(T:L)}$) was estimated in this Phase 2 study using the landslide debris runout extents generated in Phase 1. The Phase 1 work:

- provided a district-scale deterministic assessment of locations within the project area that could be affected by debris and rock avalanches (slippage and falling debris hazards) triggered by earthquakes and rainfall; and
- delineated the location and extent of debris-flow fans within the project area and provided a district-scale deterministic assessment of potential debris inundation areas from debris flows triggered by rainfall.

In Phase 1, the landslide debris inundation areas were modelled in ArcGIS using a set of empirical relationships based on observations of landslides in New Zealand and worldwide.[1] The landslide debris inundation modelling was carried out for three landslide types: (1) debris flows, (2) debris avalanches and (3) rock avalanches. The landslide debris inundation extents reported in Phase 1 were estimated based on the 50% runout POE extent for a landslide type of a given volume. This assumes that, in 50% of cases, the landslide debris would extend further than estimated, and, in 50% of cases, the landslide debris would extend less than estimated. The potential landslide slippage areas were determined using the source area locations.

In Phase 2, the same empirical relationships and methods were used to generate an additional set of landslide debris inundation areas based on the 97.7% (mean + 2 standard deviations, see Figure 3.1) runout POE extent of a given landslide type of a given volume. These new extents assume that, in 2.3% of the cases, landslide debris would extend further than estimated. Debris inundation past the 2.3% runout exceedance extent has not been analysed.
In Phase 1, the debris inundation relationships were established for three types of landslide initiated under ‘dry’ or ‘wet’ conditions; these were: (1) open slope dry rock and debris avalanches (OSD), (2) open slope wet debris avalanches (OSW) and (3) channelised wet debris flows (CHW). Further information about the data and choice of empirical debris inundation relationships can be found in the Phase 1 report. In Phase 2, we assume that OSD rock and debris avalanches are those triggered by earthquakes and that OSW debris avalanches and CHW debris flows are those triggered by rainfall. The debris inundation Fahrböschung angles for both the 50^{th}% and 97.7^{th}% are shown in Table 3.5 for OSD, Table 3.6 for OSW and Table 3.7 for CHW.

Example runout POE extents for a given watershed are shown in Figure 3.5 for EIL and Figure 3.6 for RIL. Note that, for OSW, only Fahrböschung angles up to a volume class of 100,000 m^3 are used, and, for CHW, only Fahrböschung angles for volume classes between 1000 and 1M m^3 are used, as per the Phase 1 work.

1 These empirical relationships were based on the ‘Fahrböschung’, sometimes referred to as the ‘angle of reach’ or ‘runout angle’. Heim (1989) proposed that the distance a landslide travels is proportional to its fall height. The tangent of the ratio of the fall height (ΔH) to horizontal runout distance (L) between the crest of the source zone and toe of the deposit is known as the Fahrböschung, and it is usually expressed as an angle.

Table 3.5 Summary of Fahrböschung and ΔH/L values for each volume class of open slope dry debris and rock avalanches used in this project. See Phase 1 report for graphical representation of data considered.

Volume (m^3)	50% Runout Probability of Exceedance		2.3% Runout Probability of Exceedance	
	Fahrböschung (°)	ΔH/L	Fahrböschung (°)	ΔH/L
100	43	0.93	33	0.65
1000	41	0.87	31	0.60
10,000	38	0.78	29	0.55
100,000	30	0.58	16	0.29
1,000,000	23	0.42	12	0.21
10,000,000	18	0.32	9	0.15

Table 3.6 Summary of Fahrböschung and ΔH/L values for each volume class of open slope wet debris avalanches used in this project. See Phase 1 report for graphical representation of data considered.

Volume (m^3)	50% Runout Probability of Exceedance		2.3% Runout Probability of Exceedance	
	Fahrböschung (°)	ΔH/L	Fahrböschung (°)	ΔH/L
100	32	0.62	22	0.40
1000	28	0.52	19	0.34
10,000	24	0.45	16	0.29
100,000	21	0.38	14	0.24

Table 3.7 Summary of Fahrböschung and ΔH/L values for each volume class of channelised wet debris floods and flows used in this project. See Phase 1 report for graphical representation of data considered.

Volume (m^3)	50% Runout Probability of Exceedance		2.3% Runout Probability of Exceedance	
	Fahrböschung (°)	ΔH/L	Fahrböschung (°)	ΔH/L
100	33	0.65	18	0.32
1000	26	0.49	14	0.25
10,000	21	0.38	11	0.20
100,000	17	0.31	9	0.15
1,000,000	13	0.23	7	0.12

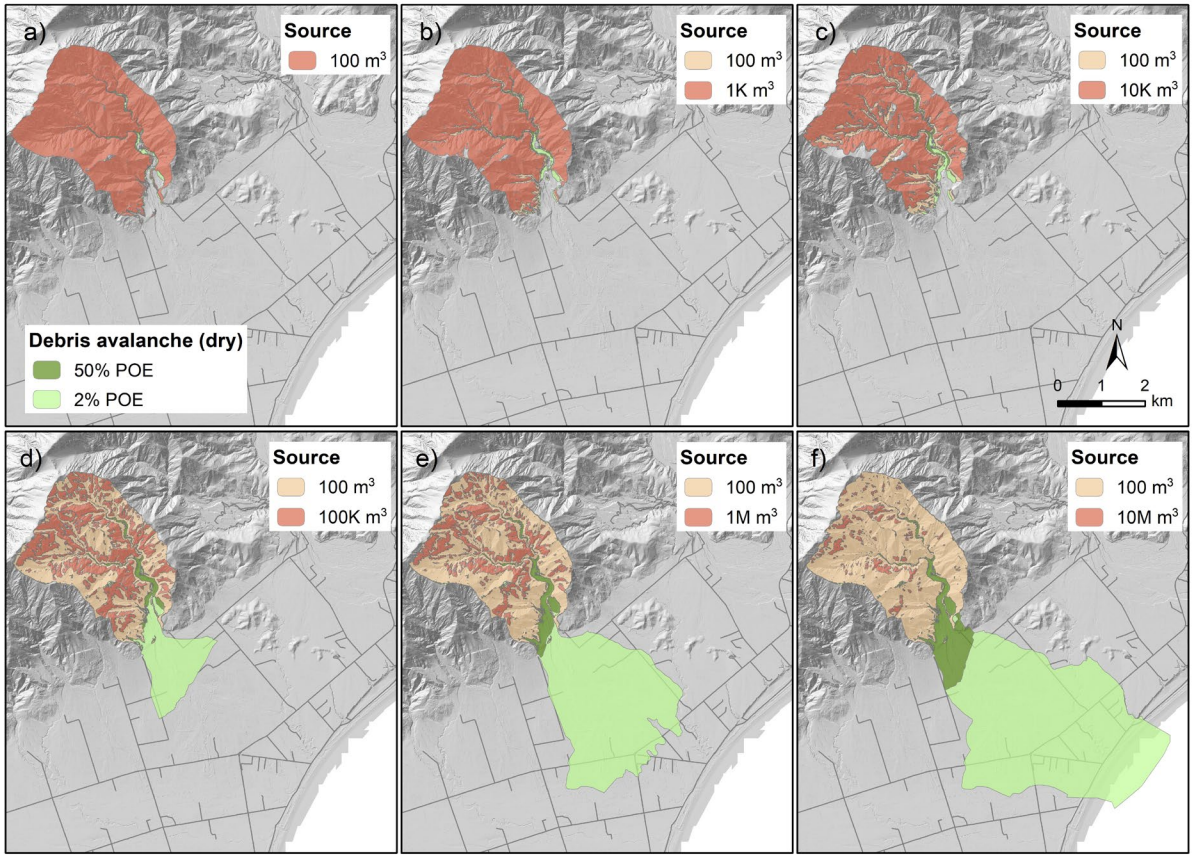


Figure 3.5 Earthquake-induced landslide runout probability of exceedance (50% and 2.3%) Fahrböschung extents for given volume classes of open slope dry rock and debris avalanches for an example watershed (Watershed 12).

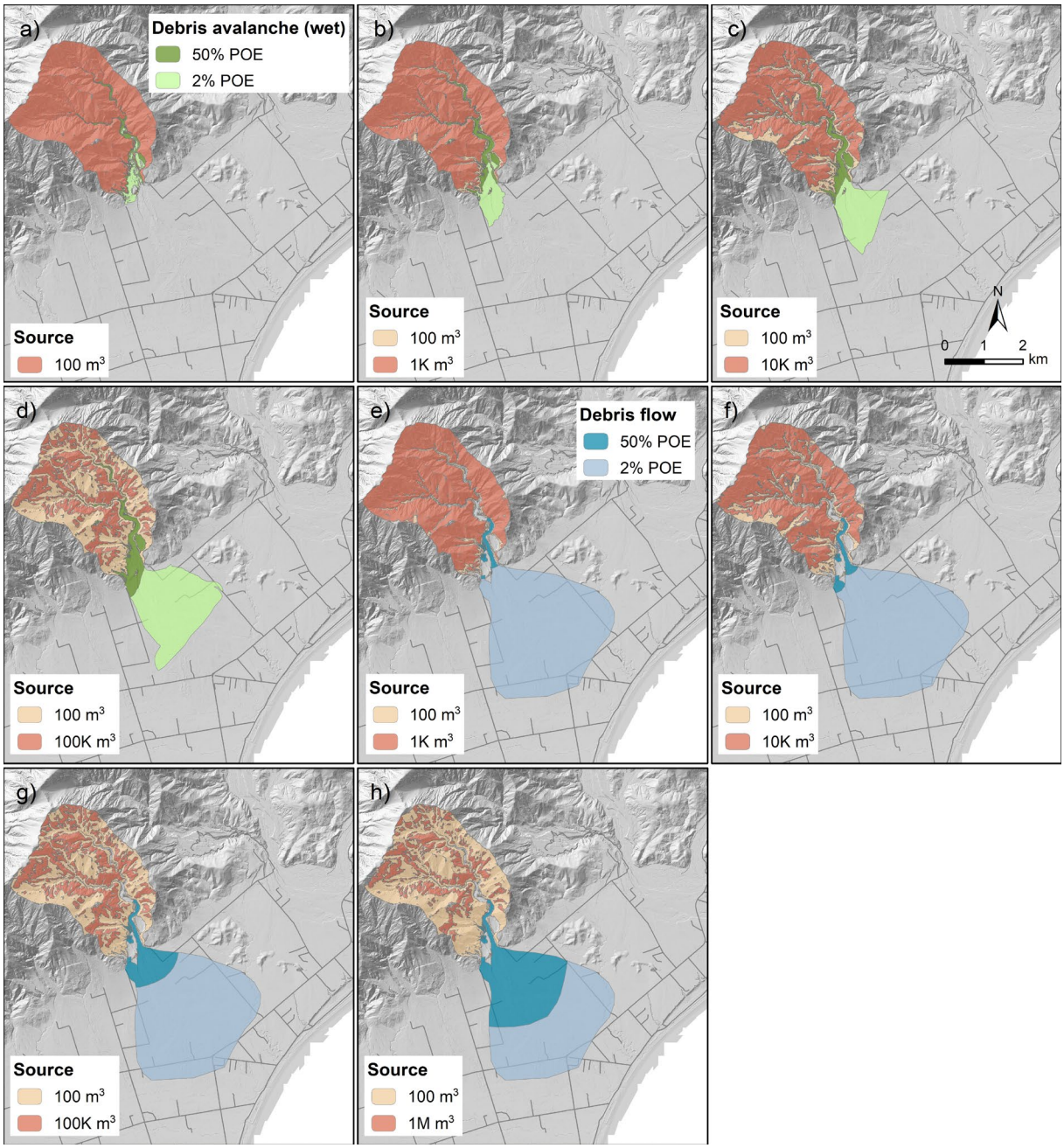


Figure 3.6 Rainfall-induced landslide runout probability of exceedance (50% and 2.3%) Fahrböschung extents for given volume classes of open slope wet debris avalanches and channelised wet debris flows and floods for an example watershed (Watershed 12). The difference in shape of the extents of the OSW and CHW are due to modelling methods – see the Phase 1 report for more information.

To represent the maximum inundation extent of CHW debris flows, the mapped extents of the debris fans were used instead of the Fahrböschung angles representing the 2.3% POE. This was done because these types of landslide may not have obvious source areas from which Fahrböschung angles can be projected, as such landslides can develop from the coalescing of debris from multiple landslides and/or by eroding and entraining debris from along their travel paths.

The following steps were taken to estimate the probability of a landslide of a given volume inundating (hitting) a given location:

- **Step 1:** For OSD and OSW, the probability of inundation (P_{IN}) was calculated using the Fahrböschung extents for the different volume classes from Phase 1, adopting either the 50% or 2.3% runout POE Fahrböschung angles, to create P_{IN} grids for each volume class ($P_{IN:VOLx:50\% \text{ or } 2.3\%}$).
- **Step 2:** Each grid was then split and assigned to each watershed to create a set of P_{IN} grids representing those source regions, of a given volume class, within each watershed.
- **Step 3:** The $P_{IN:1(VOLx)}$ within a source region from one landslide in each volume class, if it were to occur, was then calculated using the clipped grids from Step 2 using:

$$P_{IN:1(VOLx)} = \frac{A_{VOL:x}}{A_{VOL:100}} \quad \text{Equation 3.6}$$

  where $A_{VOL:x}$ is the area (m^2) of the source of the given landslide volume class (x) from Table 3.2 and $A_{VOL:100}$ is the total area of the source region of the smallest landslide volume class (the 100 m^3 class) within the given watershed. The source region of the smallest landslide volume class ($A_{VOL:100}$) was assumed to represent the potential source location of all landslides (all landslide volume classes) within the given watershed.
- **Step 4:** The probability of being inundated (hit) by a number of landslides ($P_{IN:N}$) within a source region, if the representative event band were to occur, was then calculated using:

$$P_{IN:N(VOLx)} = 1 - (1 - P_{IN:1(VOLx)})^N \quad \text{Equation 3.7}$$

  where $P_{IN:1(VOLx)}$ is from Step 3 and N is the number of landslides of the given volume class generated in each event band, calculated from Equation 3.4 for the earthquake bands and from Equation 3.5 for the 24-hour rainfall bands.
- **Step 5:** Steps 3 and 4 were then repeated for each of the runout POE Fahrböschung extents related to each landslide volume class, where, in Equation 3.6, $A_{VOL:100}$ was increased to account for the additional area of the potential inundation area within:
  - the 50% runout POE Fahrböschung extent – representing the area between the downslope extent of the source region and the extent of the 50% runout POE Fahrböschung region; and
  - the 2.3% runout POE Fahrböschung extent – representing the area between the downslope extent of the source region and the extent of the 2.3% runout POE Fahrböschung region.
- **Step 6:** If triggered, the probability of being inundated (hit) by a number of landslides ($P_{IN:N}$) within a source region was assumed to be 100%. In the 50% and 2.3% POE Fahrböschung regions, the probability of debris reaching anywhere within them was assumed to be 50% or 2.3%, respectively. To take this into account:
  - In the source region, for the Mean and Upper risk scenarios, the $P_{IN:N(VOLx)}$ (from Step 4) was assumed to be = 100% ($P_{IN:N(VOLx:100\%)}$).

- In the 50% POE Fahrböschung region, for the Mean risk scenario, the $P_{IN:N(VOLx)}$ (Step 5) was multiplied by 50% ($P_{IN:N(VOLx:50\%)}$), and, for the Upper scenario, the $P_{IN:N(VOLx)}$ was multiplied by 84% (0.84) ($P_{IN:N(VOLx:84\%)}$) and applied to the 50% POE Fahrböschung region only.
- In the 2.3% Fahrböschung region, the same approach was adopted, where, for the Mean scenario, the $P_{IN:N(VOLx)}$ was multiplied by 2.3% (0.023) ($P_{IN:N(VOLx:2.3\%)}$) and, for the Upper scenario, the $P_{IN:N(VOLx)}$ was multiplied by 16% (0.16) ($P_{IN:N(VOLx:16\%)}$) and applied to the 2.3% POE Fahrböschung region only.

Note: the rationale for using 2.3, 16, 50 and 84% values for the probability of inundation was because of the statistical limits of the POE Fahrböschung distributions between the mean + 1 or 2 standard deviation (assuming a normal distribution; see Figure 3.1).

- **Step 7:** For the CHW debris flows and floods, the debris fans mapped in Phase 1 were used. The fan extents were modified by extending them upstream into the watersheds, stopping them when the channels became narrow and where little or no debris was apparent in the channels. For those fans classified in Phase 1 as predominantly debris floods and debris flows (Melton ratios typically ≥ 0.3), the following was applied:
  - 50% runout POE Fahrböschung extent – representing the area between the downslope extent of the source region and the extent of the 50% runout POE Fahrböschung extent but confined to the maximum extent of the fan. For the Mean scenario, the $P_{IN:N(VOLx)}$ was assumed to be 50% ($P_{IN:N(VOLx:50\%)}$) from Step 6, and, for the Upper scenario, the $P_{IN:N(VOLx)}$ was assumed to be 84% ($P_{IN:N(VOLx:84\%)}$).
  - 2.3% runout POE Fahrböschung region – representing the area between the downslope extent of the 50% runout POE Fahrböschung extent and the remaining mapped extent of the fan. For the Mean scenario, the $P_{IN:N(VOLx)}$ was assumed to be 2.3% ($P_{IN:N(VOLx:2.3\%)}$) and, for the Upper scenario, the $P_{IN:N(VOLx)}$ was assumed to be 16% ($P_{IN:N(VOLx:16\%)}$).
  - For those fans classified as being predominantly fluvial in Phase 1 (Melton ratios <0.3), and/or fans without any modelled debris flow extents for different volume classes, it was assumed that debris flows may still occur but are more likely to be debris floods and the debris hyper-concentrated, given the lack of geomorphic features associated with past debris flows being observed on them. For these fans, P_{IN} was assumed to be 2.3% and 16% for the Mean and Upper Scenarios, respectively, due to the longer runout tendency. These regions were defined as being the area between the downslope extent of the source region and the mapped extent of the fan.

3.5 Vulnerability ($V_{(D:T)}$): Probability of Being Killed if Present and in the Path of Landslide Debris

The bio-physical vulnerability ($V_{(D:T)}$) is the probability of a person being killed, if present and in the path of a landslide, considering both: (a) the likelihood of being killed if struck/ buried and (b) the possibility of being able to take evasive action and avoid being struck/ buried. Bio-physical vulnerability depends on the landslide intensity, the characteristics of the elements at risk (here being people) and the impact of the landslide (Du et al. 2013). Vulnerability ranges between 0 and 1 and, for fatality risk, combines the likelihood of an injury sustained by the individual (if struck) being fatal (=1) and the possibility of getting out of the way to avoid being struck (Massey et al. 2019).

For bio-physical vulnerability, there is very little information published in the literature on how people die when they are in buildings hit by landslide debris. The available literature (e.g. Massey et al. 2019; Pollock and Wartman 2020) indicates that, for a person to be impacted by a landslide, they must firstly be present in the building; the debris needs to enter the building or cause the building to collapse on them, but, if the person is cognitively aware of the hazard, then they have a chance to avoid being hit.

The ability of a person to take evasive action depends mainly on the intensity of the landslide. Landslide intensity is a function of the volume or height of debris passing through a given location and its velocity. For this study, people are assumed to be inside their dwellings; therefore, the dwelling will offer them some protection from being struck/buried by debris. However, conversely, by being inside, a person may not be aware that a landslide may have occurred and thus be unable to take evasive action if the debris enters the dwelling. In this study, because of the absence of data to do otherwise, we adopt variable bio-physical vulnerability values linked to landslide intensity; in this case, the volume class of the landslide and the probability of inundation. To derive these values, the relationship between debris height and probability of death presented by Pollock and Wartman (2020) was adopted. We then linked debris heights and associated vulnerabilities to the landslide volume class by inferring debris heights for different volume classes at different locations; in this case, whether a dwelling is located in the source region ($P_{IN:N(VOLx:100\%)}$ from Step 6 in Section 3.5) or within the 50% or 2.3% POE Fahrböschung extents. The linkages between debris height, bio-physical vulnerability, landslide volume class and the POE extents are summarised in Tables 3.8 and 3.9.

In general, debris height will decrease with distance from the source area. For smaller landslide volumes (<100,000 m³), we assumed that this will result in lower vulnerability values with increased distance from the source area. For landslide volumes >100,000 m³, we assumed that the debris height will not decrease significantly enough with distance from the source area to result in lower vulnerability values. To estimate vulnerability to slippage in the source area, we related the source area depth (m) to the ability to take evasive action.

Following discussions with CRC, risk models adopting vulnerability factors of 1.0 for all landslide volume classes and POE Fahrböschung regions were also calculated. Where a constant vulnerability value of 100% was applied in the risk models, the metric calculated is the annual frequency of a grid cell being hit by landslide debris – or the probability of impact – not risk.

Table 3.8 Landslide intensity (debris height) and the adopted bio-physical vulnerability values used in the study.

Debris Height (m^3)	Bio-Physical Vulnerability (%)	Description
<1	0.1	Debris unlikely to enter the dwelling.
1	0.3	Debris unlikely to enter the dwelling but could enter through structural weak points, such as windows and doors.
2	0.5	Debris can enter via structural weak points and may even demolish the dwelling.
3	0.6	
5	0.8	
>5	1.0	Debris can enter; dwelling might be demolished.

Table 3.9 Landslide volume classes and runout exceedance with their assumed bio-physical vulnerability values used in the study.

Representative Landslide Volume (x) (m^3)	Vulnerability			Description
	Source ($P_{IN:N(VOLx:100\%)}$)	$P_{IN:N(VOLx:50\%)}$	$P_{IN:N(VOLx:2.3\%)}$	
100	0.5	0.3	0.1	The debris is unlikely to enter the dwelling and is limited in impact area, so a person could take evasive action.
1000	0.8	0.5	0.1	Debris could enter dwellings through structural weak points but is limited in extent, so a person could still take evasive action.
10,000	1	0.8	0.3	Debris is high enough to enter the dwelling and possibly even demolish it. The debris starts to cover a large enough area to make it difficult for a person to take evasive action.
100,000	1	1	0.5	
1,000,000	1	1	1	Given the large volume of debris and its extent, it could demolish a dwelling; it is unlikely that a person could take evasive action.
10,000,000	1	1	1	

3.6 Local Personal Risk

The LPR is calculated by assuming that a person is present in every grid cell 100% of the time and is calculated for each grid cell using the following steps:

For EIL:

- **Step 1:** Calculate the probability of death (P_{DEATH}) for landslides in each volume class and within each earthquake band at a given runout POE. The P_{DEATH} for a given landslide volume within a given earthquake band is then multiplied by the corresponding assumed vulnerability (V) value for that volume class of landslide and at the given probability of inundation location (Table 3.9), assuming a person is present. For example, for a 100 m^3 landslide triggered under earthquake band 1, the probability of death for a person located within the source region would be calculated as:

$$P_{DEATH:EIL1:VOL100:POE100} = P_{IN:N(VOL100:100\%)} \times V_{(D:T)} \quad \text{Equation 3.8}$$

- **Step 2:** P_{DEATH} is attached in ArcGIS to the relevant polygons, e.g. the source region and 50% and 2.3% POE extents, to produce grids of $P_{DEATH:EILx:VOLx:POEx}$. The polygons were turned into a single probability-of-death grid for each volume class and each earthquake band ($P_{DEATH:EILx:VOLx}$). A total of 24 $P_{DEATH:EILx:VOLx}$ grids were produced for earthquake triggers, i.e. four earthquake bands and six landslide volume classes.
- **Step 3:** To account for the possibility that multiple landslides of different volumes could be triggered at the same time, if the representative earthquake in a given band were to occur, the probability of death is calculated using de Morgan's rule (Equation 3.3) where:

$$P_{DEATH:ALL\_EILx} = 1 - \left(1 - P_{DEATH:VOL\_100}\right) \times \left(1 - P_{DEATH:VOL\_1000}\right) \times \left(1 - P_{DEATH:VOL\_n\ldots}\right) \quad \text{Equation 3.9}$$

$P_{DEATH:ALL\_EILx}$ is calculated in ArcGIS for each earthquake band by sampling the six $P_{DEATH:VOLx:EILx}$ grids (created in Step 2) that may intersect a given grid cell. This is done for each earthquake band to create four $P_{DEATH:ALL:EIL1–4}$ summary grids.

- **Step 4:** $P_{DEATH:ALL\_EIL1}$ is then multiplied by the annual frequency (*Af*) of the representative earthquake PGA for the given band (Table 3.1) to calculate the LPR at each grid cell for each band:

$$LPR_{EIL\ x} = P_{DEATH:\ ALL\_EIL\ x} \times Af_{EIL\ x} \quad \text{Equation 3.10}$$

- **Step 5:** The $LPR_{EIL\ x}$ values for each of the four earthquake bands are then added together for each grid cell to create a grid of $LPR_{EIL:Total}$.

These steps (1 to 5) are followed for the Mean and Upper risk scenarios separately to produce grids of LPR that represent each scenario.

For RIL:

The LPR is calculated in a similar way as for EIL; it is calculated for each grid cell using the following steps:

- **Step 1:** Calculate the probability of death (P_{DEATH}) for landslides in each volume class and within each 24-hour rainfall band at a given runout POE.
- **Step 2:** P_{DEATH} is calculated for each 24-hour rainfall band, landslide volume class and location and then attached in ArcGIS to the relevant polygon, e.g. the source region and 50% and 2.3% POE extents, to produce grids of $P_{DEATH:RILx:VOLx:POEx}$. The polygons were turned into a single probability-of-death grid for each volume class and each 24-hour rainfall band, separately for the OSW and CHW runout extents. A total of 12 P_{DEATH} grids were produced for rainfall triggers in each group, i.e. three 24-hour rainfall bands for OSW (volumes 100–100,000 m^3) and four landslide volume classes for CHW (volumes 1000–1M m^3. The maximum of the two probability-of-death grids (OSW and CHW) was chosen as a representative P_{DEATH} value for each of five volume classes (100–1M m^3) and for each of three rainfall bands. This resulted in 15 $P_{DEATH:VOLx:RILx}$ grids that were taken into the next step.
- **Step 3:** $P_{DEATH:ALL\_RILx}$ is calculated in ArcGIS for each 24-hour rainfall band by sampling the five $P_{DEATH:VOLx:RILx}$ grids (created in Step 2) that may intersect a given grid cell. This is done for each 24-hour rainfall band to create three $P_{DEATH:ALL:RIL1–3}$ summary grids.
- **Step 4:** $P_{DEATH:ALL\_RILx}$ is then multiplied by the annual frequency (*Af*) of the representative 24-hour rainfall amount for the given band (Table 3.3) to calculate the LPR at each grid cell for each band.
- **Step 5:** The LPR_{RILx} values for each of the three 24-hour rainfall bands are then added together for each grid cell to create a grid of $LPR_{RIL:Total}$.

These steps (1 to 5) are followed for the Mean and Upper risk scenarios separately to produce grids of LPR that represent each scenario. The final step is to sum the $LPR_{EIL:Total}$ and $LPR_{RIL:Total}$ to produce a grid of LPR_{Total} for each scenario. Information on calculating AIFR from LPR is provided in Section 4.2.

3.6.1 Risk Model Scenarios

Using the methodology discussed in the previous sections, GNS Science ran multiple risk models that adopted different estimates of the values for the variables used in the model; these are described in Table 3.10. The preliminary results from risk model scenarios 2 and 5 (Table 3.10) were used as the basis of discussions with KDC and CRC at a workshop held in Kaikōura on 29 September and discussion with Prof. Davies (external reviewer) on 11 October 2021. Following these discussions, further risk model scenarios were developed, assuming different rainfall models and a fixed vulnerability value.

For rainfall, KDC and CRC requested that risk model scenarios should be run using revised annual frequencies of the given 24-hour rainfall amounts to consider climate change projections. These projections were based on the HIRDS estimates, assuming RCP8.5 and a 2.58°C temperature increase over the next 80 years.

For vulnerability, KDC and CRC requested that the risk model scenarios should be run using a fixed vulnerability value of 1.0 (100%). This assumes that, if a grid cell is hit by debris, any person present is either killed or sustains a life-threatening injury. However, this is not likely to occur given that bio-physical vulnerability varies with landslide intensity, e.g. Table 3.9. Therefore, by assuming a vulnerability of 1.0 and a probability of a person being present of 1.0 (100%), the risk model can be used to calculate the annual frequency of a grid cell (building and or person) being hit by a landslide. This represents the annual frequency of a person being affected, e.g. as a result of a building and themselves (bio-physical) being impacted by landslides.

Table 3.10 Risk model scenarios.

Scenario		RIL	EIL	Debris Runout	Person Present	Vulnerability
1	MEAN	Mean (50th%) landslide probability estimates and historical 24-hour rainfall annual frequencies	Mean (50th%) landslide probability estimates	Mean (50th%) estimates	67% (0.67)	Variable as per Table 3.9
2	MEAN	Mean (50th%) landslide probability estimates and historical 24-hour rainfall annual frequencies	Mean (50th%) landslide probability estimates	Mean (50th%) estimates	100% (1.0)	Variable as per Table 3.9
3	MEAN	Mean (50th%) landslide probability estimates, with RCP8.5 Climate Change (CC) annual frequencies	Mean (50th%) landslide probability estimates	Mean (50th%) estimates	100% (1.0)	Variable as per Table 3.9
4	MEAN	Mean (50th%) landslide probability estimates, with RCP8.5 Climate Change (CC) annual frequencies	Mean (50th%) landslide probability estimates	Mean (50th%) estimates	100% (1.0)	100% (1.0)
5	UPPER	84th% landslide probability estimates with historical 24-hour rainfall annual frequencies	84th% landslide probability estimates	84th% POE Fahrböschung	100% (1.0)	Variable as per Table 3.9
6	UPPER	84th% landslide probability estimates with historical 24-hour rainfall annual frequencies	84th% landslide probability estimates	84th% POE Fahrböschung	100% (1.0)	100% (1.0)
7	UPPER	84th% landslide probability estimates with RCP8.5 Climate Change (CC) annual frequencies	84th% landslide probability estimates	84th% POE Fahrböschung	100% (1.0)	Variable as per Table 3.9
8	UPPER	84th% landslide probability estimates with RCP8.5 Climate Change (CC) annual frequencies	84th% landslide probability estimates	84th% POE Fahrböschung	100% (1.0)	100% (1.0)
9	UPPER	84th% landslide probability estimates with RCP8.5 Climate Change (CC) annual frequencies	84th% landslide probability estimates	Adopting OSW (wet) POE Fahrböschung extents for EIL	100% (1.0)	100% (1.0)

4.0 RISK ANALYSIS RESULTS

The results from the modelling of risk scenarios 1 to 9 (Table 3.10) are shown in Figure 4.1 for the mean scenarios and Figure 4.2 for the upper scenarios. The risk metrics calculated in this study are generally very small numbers, with large uncertainties (more detail is provided in Section 5.2). This report makes extensive use of the scientific number format of expressing risk in terms of powers of 10. For example, the number 10^{-4} (10 to the power of minus 4) is the fraction 1/10,000 and the decimal number 0.0001; it may also be expressed as 0.01%. The units of risk are a dimensionless probability of a given outcome (e.g. death) per unit of activity or time.

Figures 4.1 and 4.2 show the impact on the risk estimates based on the different values selected for the variables used in the model. Risk scenario 1 (Table 3.10, Figure 4.1a) is the least conservative – or most optimistic – based on the values adopted for the variables in the risk model. Conversely, risk scenario 9 (Table 3.10, Figure 4.2e) is the most pessimistic, or conservative, as it adopts the RCP8.5 climate change 24-hour rainfall annual frequencies, the upper (84^{th}%) statistical relationships for landslide production rates and debris runout POE Fahrböschung extents, as well as fixed values of 1.0 for the probability of a person being present and for vulnerability.

4.1 LPR versus AIFR

The results in Figure 4.1b–d and Figure 4.2 are presented in terms of LPR (risk model scenarios 2–9 in Table 3.10). The results from risk model scenario 1 (Figure 4.2a, Table 3.10) are presented as AIFR, as the probability of a person being present 67% of the time was assumed, based on previous work carried out in the Port Hills of Christchurch (Massey et al. 2021; Taig et al. 2015). The AIFR can be calculated from the LPR by estimating the probability of a person being present. This is the probability that an individual is present on the portion of the slope/ground when landslide debris moves through it. It is a function of the proportion of time spent by a person at a particular location each day and can range from 0% if the person is not present to 100% if the person is present all of the time.

For planning and regulatory purposes, it is established practice to consider individual risk to a ‘critical group’ of more highly exposed-to-risk people (Taig et al. 2012). For example, there are clearly identifiable groups of people (with significant numbers in the groups) who spend most of their time in their homes – the very old, the very young, the disabled and the sick.

For risk model scenarios 2–9 (Table 3.10), the LPR represents a person present 100% of the time in every grid cell and therefore does represent the AIFR if a person were to be present in a dwelling for 100% of the time, thus representing the most exposed person. However, in most situations, people do not spend 100% of their time in one location and, given that Kaikōura has many holiday homes that are not lived in all year round, the amount of time that an ‘average’ person spends at home could be considerably lower.

Other values have been adopted for people at home in dwellings, with values ranging from 58% (for a person spending 14 hours a day at home) to 83% (for a person spending 20 hours a day at home) (cf. Corominas et al. 2005). In the Port Hills of Christchurch, GNS Science (Massey et al. 2012) assumed that an average person spends 16 hours a day at home on average (16/24 = 0.67 or 67%), 365 days of the year. However, the most exposed person is still likely to be present for 100% of their time,

The LPRs calculated in this report assume that a person is present 100% of the time; therefore, these LPR values are equivalent to AIFR if a person is present 100% of the time, i.e. the person most exposed. To calculate the AIFR from landslide hazards to a person in a dwelling, the estimated LPR for a given dwelling is multiplied by the proportion of time that the person may spend in the dwelling per year. For example, if a person only spends 50% of their time a day (and per year) in the dwelling, then the AIFR would be 50% lower than the estimate LPR for the given dwelling (AIFR = LPR × 0.5).

In this report, we have calculated the AIFR assuming that a person is present 67% of the time to demonstrate how the risk can change when different values are adopted. The impact of such changes in the risk model are shown in Figure 4.1a and b. Figure 4.1a shows risk scenario 1 results, which assume that a person is present 67% of the time, while Figure 4.1b shows risk scenario 2 results, which assume that a person is present 100% of the time. All other values used for the other variables in both risk model scenarios are the same. The impact of such changes means that, for example, the number of buildings that fall within the 10^{-4} to 10^{-3} risk class increases from risk model scenario 1 to 2, as the boundary between the different risk changes on the ground. Given this uncertainty, we recommend that, for this district-scale analysis, the LPR risk metrics should be adopted based on the most exposed person who spends 100% of their time at home.

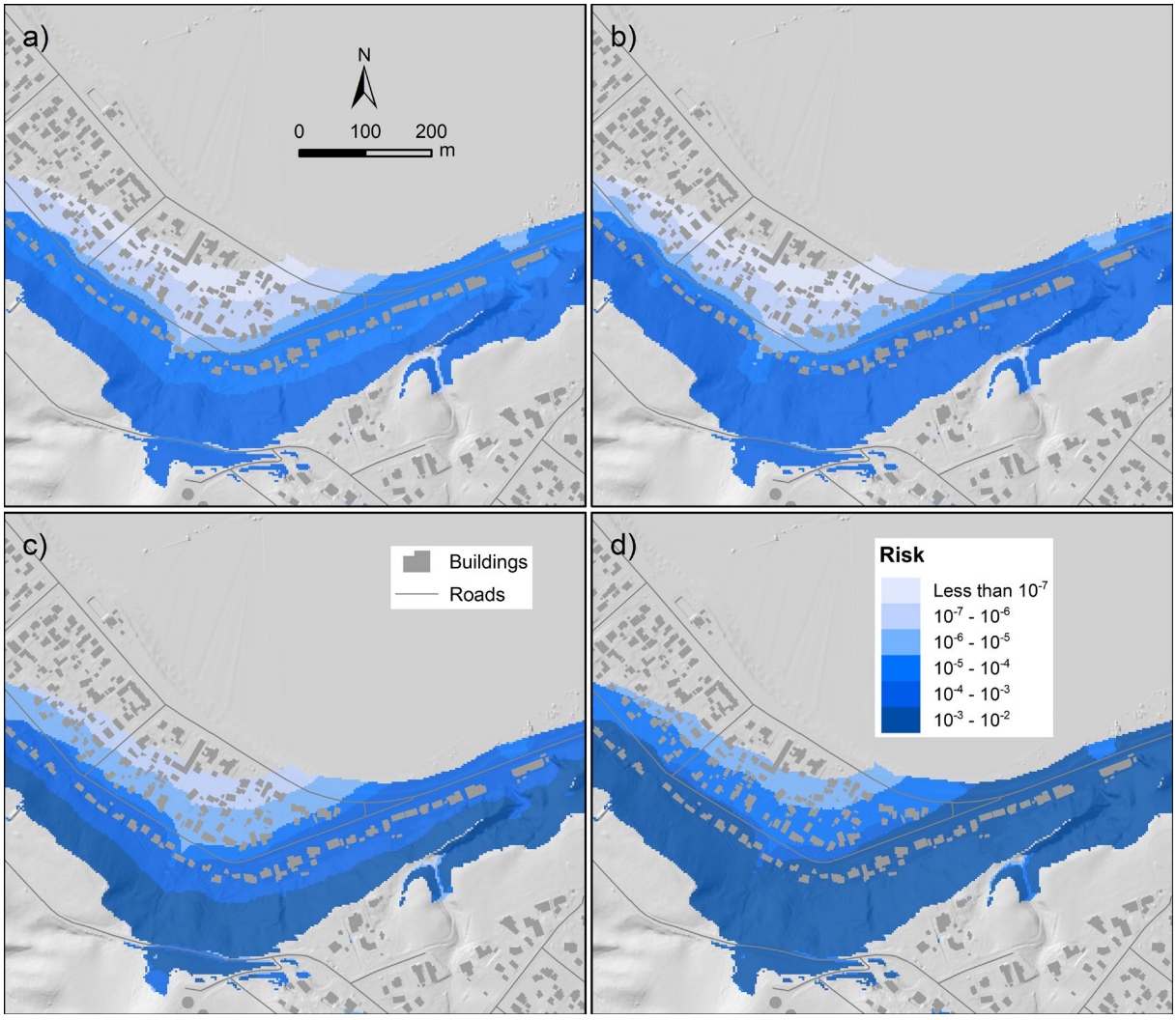


Figure 4.1 Risk model results for mean scenarios 1 (a) to 4 (d), adopting different values for the variables used in the risk model (listed in Table 3.10). The figure shows the impact on the risk estimates based on the different values selected for the variables used in the model. Risk scenario 1 (a) is the least conservative and risk scenario 4 (d) is the most conservative.

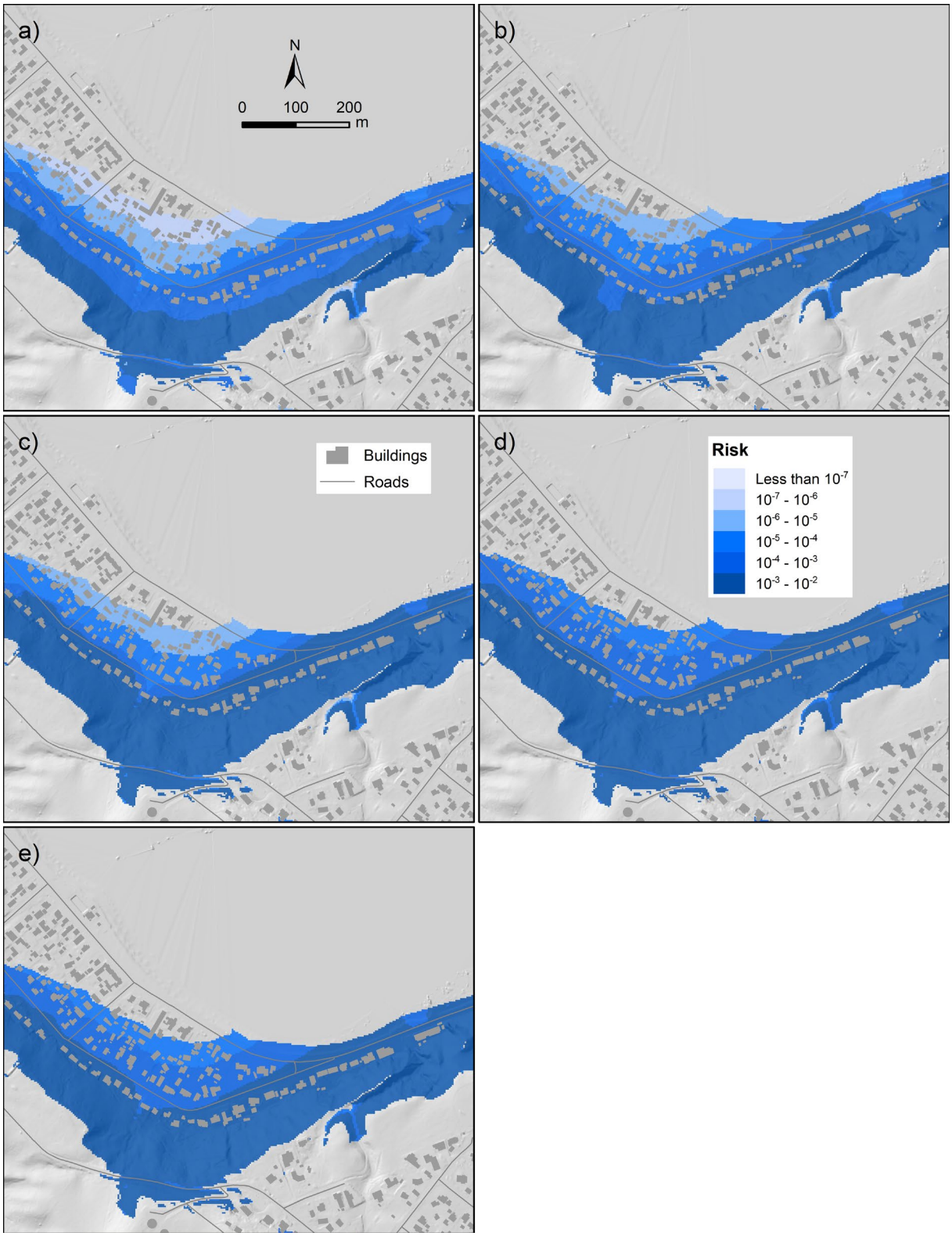


Figure 4.2 Risk model results for upper scenarios 5 (a) to 9 (e), adopting different values for the variables used in the risk model (listed in Table 3.10). The figure shows the impact on the risk estimates based on the different values selected for the variables used in the model. Risk scenario 5 (a) is the least conservative and risk scenario 9 (e) is the most conservative.

4.2 General Results for the Study Area

Maps showing the LPR adopting Scenario 2 (Table 3.10), are shown for the entire study area in Appendix 3. They are based on 'mean' (50th%) estimates of landslide production rates and debris runout and adopt historical 24-hour rainfall annual frequencies and variable vulnerability values. They are slightly conservative, as they assume that a person is present 100% of the time. The probability of a person being present is uncertain and is hard to quantify, as there is no information for the Kaikōura district to help determine what the 'mean' value might be. Therefore, in our opinion, risk model scenario 2 provides the 'best' estimate of the LPR to those people in the study area who are currently exposed to landslide hazards. These LPR values are equivalent to the AIFR, assuming that a person is present 100% of the time.

The risk model results show that:

1. The LPR varies as a function of the proximity of, for example, a dwelling or person to the steeper slopes and where they are on a debris flow fan.
2. The main contributor to the LPR is from RIL, although the EIL probabilities are higher than the RIL ones for the same annual frequency of triggering event (e.g. Figure 4.3). There is a factor of increase of about eight between the EIL and RIL risk model results, indicating that the LPR risk is almost one order of magnitude (a factor of 10) higher for RIL than EIL. This is because:
   - landslide-triggering rainfall events occur more frequently than strong earthquakes.
   - the LPR from EIL tends to decrease rapidly with increased distance from the toe of the steeper slopes, relative to the LPR from RIL. This is because the debris from RIL is wet and tends to travel further than the usually drier debris associated with EIL.
3. The LPR extends furthest downslope from the steeper slopes in areas where there are mapped debris fans.
4. The LPR from RIL tends to be slightly higher in the north of the study area. This reflects:
   - the slightly higher 24-hour rainfall amounts estimated for the given rainfall bands from HIRDS; and
   - the more susceptible nature of the geological materials, mainly soils, sandstones, siltstones and limestones, compared to the stronger greywacke sandstones that form most of the slopes in the central and southern parts of the study area.
5. The LPR from EIL is highest along the steeper coastal sections of the study area, especially along State Highway 1 to the north and south of Kaikōura and in the Mt Fyffe and Clarence River areas.

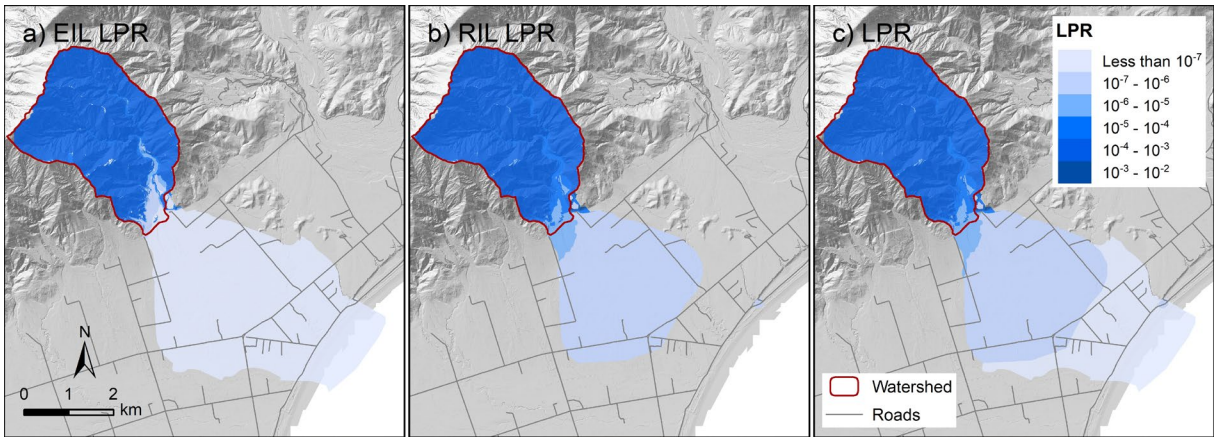


Figure 4.3 Local personal risk maps for earthquake- and rainfall-induced landslides and all landslides for one watershed.

5.0 DISCUSSION

5.1 Consistency with Actual Experience

To the authors' knowledge, there were no deaths in the study area from landslides triggered by the 2016 Kaikōura earthquake. The GNS Science landslide fatality database documents no deaths for the region since the 1880s; however, there is a gap in the data between 1950 and 1961.

About five dwellings are known to have been impacted by landslide debris triggered by the 2016 Kaikōura earthquake. Using the risk model for Band 4, which best represents the PGAs associated with the 2016 Kaikōura earthquake (Kaiser et al. 2017), the modelled 'forecast' number of house hits and deaths can be compared to the observed number of house hits and deaths. Observed house hits are defined as the number of dwellings hit by debris from landslides triggered by the 2016 Kaikōura earthquake (Massey et al. 2020c). The national LINZ building footprint database was used to represent the building locations. It should be noted that these footprints also include structures such as garages, barns, sheds and commercial buildings, as well as dwellings, and there are many buildings within individual land parcels. Therefore, only the largest single building was sampled from each land parcel, and these were assumed to be dwellings. However, it is noted that, in rural areas like this, such large buildings may be farm sheds or barns, so there is large uncertainty about whether those buildings selected are dwellings and the occupancy rates within a dwelling (i.e. the number of people in a dwelling and their probability of being present).

The modelled building hits and probabilities of death were calculated using Equations 3.7 and 3.9. The expected numbers of buildings hit from landslides triggered in Band 4 was estimated by using Equation 3.9 to calculate the probability of each assumed dwelling being hit within the risk model footprints. These were then summed to estimate the number of dwellings forecast to have been hit by debris, which were then compared to the observed number of dwellings hit. Equation 3.9 was also used (adopting variable vulnerability values given in Table 3.9) to estimate the probability of death of a person within each dwelling within the risk model footprints and multiplying this by the probability of a person being present in the dwelling (assuming day-time occupancy) and the mean and upper estimates of the number of people who live in a dwelling (1 and 2.7 people per dwelling, based on Taig et al. 2015).

The EIL risk model forecasts (Scenario 2, Table 3.9), adopting Band 4, indicate between 1 and 10 dwelling hits and zero deaths from landslides, which compares to the five known dwelling hits and zero recorded deaths from EIL triggered by the 2016 Kaikōura earthquake.

The RIL risk model forecasts (Scenario 2) between one death every 60 years (assuming an occupancy of one person being present in each dwelling within the landslide risk model extent) and one death every 30 years, if two people are assumed to be present. If the climate change scenario is adopted (Scenario 3), the model forecasts one death every 15–30 years, assuming an occupancy of either two or one persons, respectively.

5.2 Sensitivity to Key Uncertainties

In this section, the sensitivity of the risk model to key uncertainties and the reliability of the assessments are identified.

The sensitivity of the estimated risk to changes in the following values for the variables used in the risk model has been assessed:

- The number of landslides triggered by both earthquake and 24-hour rainfall triggers.
  - For EIL and RIL, the mean and upper estimates of landslide susceptibility within each watershed were used to account for any uncertainty in the relationship between PGA and 24-hour rainfall and the landslide probability and the number of grid cells forecast to be landslides, and therefore the number of landslides generated. This was done adopting the mean and 84% (upper) statistical landslide susceptibility model coefficients for the variables used.
  - The relationship between landslide source volume and area, which affects the number of landslides than can occur in a watershed. The statistical relationship from Massey et al. (2020c) was varied, adopting the mean (50%) and upper (84%) estimates of the landslide source volume (m^3) to area (m^2) statistical fits based on Version 2.0 of the Kaikōura EIL inventory.
- The impact of climate change on increasing the 24-hour rainfall amount forecast to occur at the given annual frequencies. The risk model was run using rainfall forecasts based on RCP8.5 and a 2.58°C temperature increase over the next 80 years and their results compared with the model adopting the rainfall amounts for the same annual frequencies but based on historical data.
- The probability of landslide debris passing a given distance down the slope (runout POE per Fahrböschung). For EIL (OSD) and RIL (OSW and CHW), the probability of landslide debris reaching/passing a grid cell was varied using the statistical relationship between landslide volume and runout POE for each Fahrböschung, adopting 50% and 2.3% for the Mean scenario and 84% and 16% for the upper scenario (from Phase 1).
- The impact of an earthquake occurring after a major rainstorm. The upper EIL production rates capture the likely increase in EIL frequency that may occur in such a scenario. However, if this scenario were to occur, then the EIL debris may travel further downslope, as it would be wetter. This was evaluated by adopting the OSW runout POE per Fahrböschung values for EIL rather than the OSD values.
- The vulnerability of a person present in an affected building was assumed to be 1, irrespective of landslide volume and runout POE for each Fahrböschung region.

Potentially significant uncertainties are noted, with their likely implications for risk summarised, in Table 5.1. These uncertainties are expressed as factors of difference. A factor of difference of 10 represents an order of magnitude change in the risk estimates, e.g. the risk changes from 1×10^{-5} to 1×10^{-4}. These uncertainties combine to give a total factor of difference of between 8 and 10, which is up to an order of magnitude uncertainty between the risk estimates. This means that a location with an AIFR of 10^{-4} (1 chance in 10,000 of being killed per year) could feasibly have an AIFR as high as 10^{-3} (1 in 1000 chance of being killed per year) if all of the pessimistic (conservative) values for the variables in the risk model were assumed. This difference is between the risk estimates that adopt all 'mean' (scenario 1) values versus those that adopt all upper (scenario 9) values for the variables used in the risk model.

The input variables of climate change 24-hour rainfall amount and the landslide debris runout POE for each Fahrböschung are considered to be the two most significant uncertainties in this assessment, with each input variable having a factor of difference of 2 to 3 (see Table 5.1). These differences are shown in map form in Figures 4.1 and 4.2 for the different risk model scenarios listed in Table 3.10.

The risks presented in this report do not include any consideration of the potential reduction or increase in risk caused by site-specific factors that may mitigate/promote the effects of landslides impacting a location. This is a potentially significant uncertainty within the risk analyses. At the district scale, such impacts are unquantifiable as they relate to site-specific factors. An example process that may be used by engineering consultants to identify such factors (at the site-specific scale) and assess their impact on the district-scale risk results has been summarised in Appendix 5.

The increase in landslide volume 'bulking', caused by a landslide entraining material from along its flow path, has not been included specifically in this analysis. Such landslides might initiate as relatively small volume ones (e.g. <100 m^3) but could increase their volume by several orders of magnitude (e.g. 10,000 m^3) as they entrain more material. Modelling such landslides at the district scale is not possible. However, such landslides are indirectly accounted for as multiple volume classes of landslide are modelled, and such landslides tend to be initiated by rainfall and therefore deposit on fans. The mapped extent of the fans in the study area have been used in this risk analysis.

The number of landslides that were triggered by rainstorms post-earthquake appear to be elevated compared to pre-earthquake rates of landsliding due to landscape damage generated during an earthquake. However, increases in the rates of landsliding post-earthquake are temporary and short-lived (e.g. 5–10 years; Tang et al. 2016; Marc et al. 2015). This risk analysis does not include the cascading and conditional effect of increased landsliding following large earthquakes, though our use of pre-earthquake historical landslides represents the best estimate of how many landslides of a given volume occur during rainfall events. This may under-estimate risk from RIL immediately post-earthquake (Table 5.1).

Additionally, this risk analysis does not consider landslides that are not triggered by earthquakes or rainfall (e.g. they occur without a discernible trigger). A lack of data on such landslides in the Kaikōura district hinders the ability to incorporate landslides that occur without a discernible trigger within the risk analysis. The risk results for all scenarios therefore underestimate the risk (Table 5.1).

Table 5.1 Uncertainties and their implications for risk.

Issue	Direction and Scale of Uncertainty	Implications for Risk
a. Under-prediction of annual frequency for a given PGA by the NSHM.	Increasing. However, the contribution to risk from RIL is higher than EIL.	Risk due to earthquakes could be slightly under-estimated. The risk models should be re-run using the updated NSHM once available
b. Under-prediction of landslides that occur without a discernible trigger (e.g. not under earthquake or rainfall conditions)	Increasing. However, the contribution to risk from both RIL and EIL is likely to be higher.	Risk due to landslides occurring without a trigger could be under-estimated.

Issue	Direction and Scale of Uncertainty	Implications for Risk
c. Under-prediction of RILs that occur immediately post-earthquake	Increasing. However, the increase in RILs post-earthquake is likely to be short-lived and temporary.	Risk due to RILs occurring immediately following post-earthquake could be under-estimated.
d. Under-prediction of the rainfall amount (24-hour rainfall) occurring at a given annual frequency by HIRDS as a result of climate change.	Increasing. There is a significant difference between the historical and future rainfall forecasts for the same annual frequencies as a result of climate change. The rainfall amounts occurring at the given annual frequencies adopted in this study are forecast to increase by 22% by the end of the century, adopting RCP8.5 and a 2.58°C temperature increase over the next 80 years (HIRDS V4).	A mean factor of about 2–3 increase between models adopting the historical rainfall amounts (scenarios 2 and 5) and those models adopting the climate change forecast rainfall amounts (scenarios 3 and 7).
e. EIL susceptibility and the numbers of landslides produced in each earthquake band.	The data are well constrained for EIL, as the risk model used region-specific data. The slopes are also now damaged as a result of the strong ground shaking caused by the 2016 Kaikōura earthquake. This means that many slopes might be more susceptible to landslides than they were before the 2016 earthquake. A future strong earthquake, if it were to occur in the region within the next decade or two, might lead to an increased number of landslides (more than occurred in the 2016 earthquake), given the pre-conditioning. The largest uncertainty in the EIL forecast model is the level and geospatial extent of shaking in a future earthquake.	A mean factor of about 1.2 between the Mean (Scenario 2) and Upper scenario (Scenario 5).
f. RIL susceptibility and the numbers of landslides produced in each 24-hour rainfall band.	The data are well constrained for RIL, as the risk model uses region-specific data. However, pre-conditioning (cracking and past EIL) caused by the 2016 Kaikōura earthquake may have increased the susceptibility of the slopes to future RIL for a period of time (decade?) after the 2016 earthquake. This impact is currently being investigated as part of the EILD Endeavour Programme.	A mean factor of about 1.5 between the Mean (Scenario 2) and Upper scenarios (Scenario 5).

Issue	Direction and Scale of Uncertainty	Implications for Risk
g. The relationship between landslide source volume and area, which effects the number of landslides that can occur in a watershed.	The data are well constrained for EIL; however, for RIL, the source volume to area relationships do not exist for the datasets used in this study (Cyclone Alison and ex-Tropical Cyclone Ita). The statistical relationship from Massey et al. (2020c) was varied, adopting the 50% and upper 84% estimates of the landslide source volume (m^3) to area (m^2) statistical fits based on Version 2.0 of the Kaikōura EIL inventory.	Difficult to quantify, as few data are available for RIL source volume to area relationships. However, it is unlikely to be significant, as the risk is mainly calculated by adopting landslide source areas, which are well constrained from mapping.
h. Runout probability of exceedance for each Fahrböschung.	A large uncertainty but linked to the total volume of material leaving the slope and the nature of the material in which the landslide initiates. The POE values were applied to the whole area of the runout polygon rather than interpolating the POE values between the source area and runout extent. This underestimates the probability of spatial impact closer to the base of a slope.	A mean factor of about 2–3 between Mean (scenarios 2–4) and Upper scenarios (scenarios 5–8).
i. Adopting the OSW runout POE per Fahrböschung values for EIL rather than the OSD values.	The impact of an earthquake occurring after a major rainstorm could mean that the debris from EIL can travel further downslope, as it would be wetter. EIL models were run adopting OSW runout POE Fahrböschung values.	A mean factor of 1.3 between risk model scenarios 8 and 9.
j. Vulnerability: Probability that a person is killed, if struck by debris.	Could make a significant difference for the mid-volume classes of landslide (1000 to 100,000 m^3), based on the possibility that a person may be aware of a landslide and take evasive action, or by being upstairs or located in the downslope part of their dwelling and thus protected by it. However, the vulnerability values will always be large for the larger landslides, given the volumes of debris involved, and it is unlikely that people could outrun or 'dodge' such large volumes of debris, hence the recorded injuries.	A mean factor of about 2.0 between models adopting variable vulnerability values based on landslide volume and inferred debris height (scenarios 2, 3, 5 and 7) and those assuming fixed vulnerability values of 1 (scenarios 4, 6 and 8).

5.3 Comparison with Prehistorical Landslide Rates

To validate the number of landslides triggered during earthquake and rainfall events, some of the larger prehistoric debris fans in the Kaikōura district were mapped and their volume estimated to determine prehistorical landside rates, which are a proxy for the number of landslides that could have occurred in the past.

It is important to validate this, as the risk model is sensitive to the number of landslides triggered in future earthquake and rainfall events, especially as rainfall is expected to increase as a result of climate change. The risk model results show that the LPR from RIL is higher than EIL, therefore future climate change – and the forecast increasing rainfall amounts associated with it – suggest that RIL are likely to become even more predominant over the next 80 years.

The risk analysis in this study relies upon landslide data that represent a relatively short period in time. However, given the presence of several large debris fans on the foothills below Mt Fyffe, and the presence of multiple active faults – especially the Hope Fault that runs along the toe of the range front, landslides have certainly occurred prehistorically across most of the study area. These debris fans could therefore provide an indication of the prehistorical landslide debris accumulation rates, which could then be compared to the landslide production rates estimated in this study from historical values (provided below).

To do this, a geomorphic map of the seaward side of the Mt Fyffe range was made by interpreting the LiDAR Digital Elevation Model (DEM) in ArcMap and ArcPro. The geomorphic units include various hillslope, mass movement, depositional and tectonic features, following the GNS Science Urban Mapping schema (Figures 5.1 and 5.2). Emphasis was placed on mapping the alluvial fans, with a view to calculating their volumes and estimating the ages of the surface on which they are interpreted to have been deposited (Table 5.2).



Figure 5.1 Polygons, showing the debris fans (blue outline) extending south from the Mt Fyffe range that were used to estimate their volumes. Catchment areas are outlined in purple.

The debris accumulation rates were estimated for each of the mapped fans to allow comparison with the modelled debris accumulation rates from the same watersheds, using the estimated landslide production rates forecast by the landslide susceptibility models (RIL and EIL combined). This was done by using Equation 3.5 to estimate the number of landslides of a given volume class occurring in each earthquake and historical or climate change RCP8.5 24-hour rainfall band. These numbers of landslides of a given volume class were then multiplied by their representative volumes and summed and multiplied by the annual frequency of the given band (from Tables 3.1 and 3.3) to produce an annual landslide production rate per band. These productions rates from all bands were then summed for the watersheds that could contribute debris to a mapped fan for those fans that could be clearly linked to watersheds (Table 5.2). This allows the forecast landslide production rates to be compared to their equivalent prehistorical debris accumulation rates. However, this assumes that landslide and not fluvial processes dominated the prehistorical deposition of debris and that all of the forecast landslide debris generated in each watershed reaches a fan and remains on it indefinitely. It is not possible to separate the prehistorical debris accumulated by earthquake- or rainfall-triggered landslides.

However, given the listed (above) assumptions and uncertainties, in both the forecast susceptibility models and the way in which the fan volumes were estimated, the results (in Table 5.2) show that the prehistorical debris accumulation rates are more closely aligned, within the same order of magnitude, with the forecast landslide production rates, adopting the climate change RCP8.5 scenario. These results indicate a general similarity between the prehistorical and future rates adopting the climate change scenario, albeit with considerable uncertainty, given the methods used to estimate both.

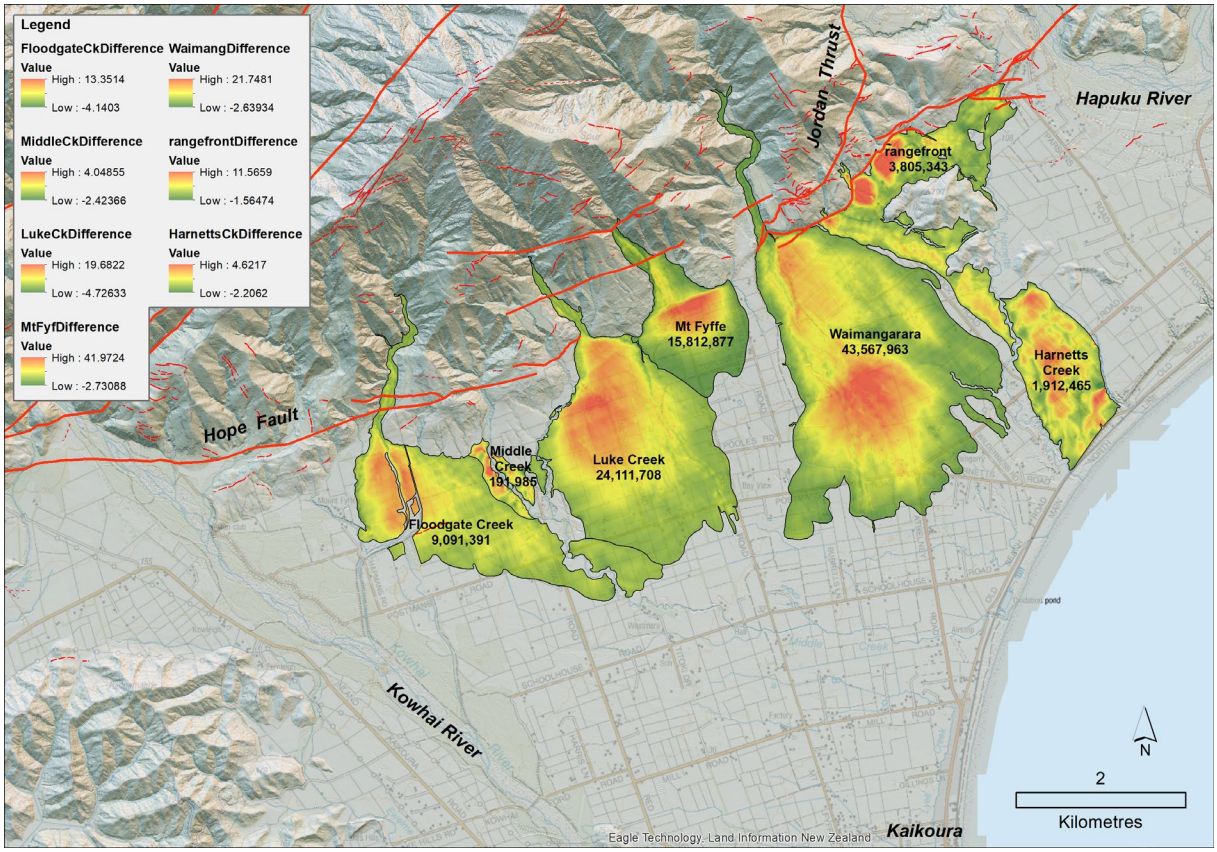


Figure 5.2 Difference models for the fans for which volumes were calculated. The volumes are calculated using the difference between the fan surface and the projected surface beneath the fan. See Table 5.2 for volume results (volumes given in m^3).

Table 5.2 Results of fan volume calculation.

Name	Watershed ID	Fan Area (m^2)	Fan Volume (m^3)	Approximate Age of Fan	Prehistorical Debris Accumulation Rate (m^3/yr)	Forecast Landslide Production Rate: RCP8.5 (m^3/yr)	Forecast Landslide Production Rate: Historical (m^3/yr)
Floodgate Creek	18 and 17	2,854,277	9,091,391	Late Holocene	2165	3750	908
Middle Creek*	-	232,207	191,985	Early Holocene	16	N/A	N/A
Luke Creek	14, 15 and part of 16	4,115,608	24,111,708	Late Holocene	5741	7884	1782
Mt Fyffe Walk	13	1,439,181	15,812,877	Late Holocene	3765	1035	146
Waimangarara	12	6,579,378	43,567,963	Early Holocene – Late Holocene	5313	4714	601
Waimangarara young	12	3,623,450.	27,137,812	Late Holocene	6461		
Rangefront fan*	10	1,921,309	3,805,342	Early Holocene – Late Holocene	464	N/A	N/A
Harnett's Creek*	10 and 12	1,459,159.	1,912,465	Early Holocene	163	N/A	N/A

*The forecast landslide production rates for these fans are uncertain, as the watersheds that could provide debris to them are not easily linked.

5.4 Applying these Results

The major uncertainties in the risk model relate to the input variables of (1) the expected time-varying frequency of a 24-hour rainfall amount occurring based on climate change projections and (2) the runout distance that landslide debris may travel downslope.

The confidence limits on the analysed risk levels are estimated to be marginally less than an order of magnitude (higher or lower) in terms of the absolute risk levels presented in this report. That is, an assessed risk of 10^{-4} per year could reasonably range from 10^{-3} per year to 10^{-5} per year.

When faced with uncertainties in assessing life safety risk, it is standard practice to take a precautionary view. That is, to base decisions on a risk value toward the upper, rather than the central or lower, end of the range emerging from the risk analysis. Typically (e.g. in the Building Code) an 84th percentile (84th%) value is used rather than the 50th percentile (50th%, or 'mean' estimate).

The LPR maps (Appendix 3) provide the 'best' estimate of the LPR to those people in the study area who are currently exposed to landslide hazards (risk model scenario 1, Table 3.10), as they are based on 'mean' (50th%) estimates of landslide production rates and debris runout and adopt historical 24-hour rainfall annual frequencies and variable vulnerability values. They are slightly conservative, as they assume that a person is present 100% of the time. These LPR values are equivalent to the AIFR, assuming that a person is present 100% of the time.

For future decision-making, the results from risk model scenario 7 (Appendix 4) might be more appropriate for KDC and CRC to use when considering a more precautionary approach. These LPR values can be assumed to be equivalent to AIFR, assuming that a person is present 100% of the time. They provide risk estimates based on more conservative values for the variables used in the risk model, which are:

- 24-hour rainfall amounts for the given annual frequencies, adopting the HIRDS estimates based on RCP8.5 and a 2.58°C temperature increase over the next 80 years;
- 84th% statistical estimates of the landslide production rates (RIL and EIL) and debris runout distances; and
- 100% occupancy, i.e. a person is present 100% of the time.

KDC should now consider how to utilise the risk maps in the District Plan. To do this, risk thresholds will need to be defined on which the hazard zones and planning rules associated with them can then be based. Some guidance around how to set such risk tolerability thresholds is given in Taig et al. (2012; forthcoming 2021a, 2021b).

Digital GIS-based layers containing the risk results for each of the modelled scenarios (1–9, Table 3.10) have been provided to KDC and CRC with this report. KDC and CRC may want to consider the results from these other risk model scenarios when choosing the most appropriate one(s) to use. However, by adopting risk model scenarios with a constant vulnerability value of 100%, the metric calculated is the annual frequency of a grid cell being hit by landslide debris, or the probability of impact, not of risk. Therefore, setting risk thresholds using such metrics becomes difficult.

Given the district scale of the risk models, a provision should be included whereby site-specific information for a site/dwelling could be used to re-evaluate the landslide risk, thus allowing the given site to be reclassified (e.g. changing its high hazard area status through a certification process). This process was allowed for in Christchurch City Council's replacement District Plan (Quigley et al. 2020). In 2016, the Independent Hearings Panel agreed to this provision, provided that any re-assessment should follow the same method and approach adopted for the district-wide assessments. Some information about how such site-specific factors could be incorporated into and modify the risk model are contained in Appendix 5.

6.0 RISK IN CONTEXT

Risk criteria used in other contexts and information on New Zealand natural hazard and other risks can be used to inform the nature of the risk metrics and criteria that KDC and CRC might adopt in relation to landslide risk in the study area. Such information can be used to define the quantitative ranges within which such criteria should be set in order to be consistent with practice elsewhere and with New Zealanders' apparent tolerance (or otherwise) for risk associated with other hazards (e.g. Taig et al. 2012; Taig, forthcoming 2021b; Clarke et al. 2021).

Recommended next steps for KDC and CRC are:

1. KDC and CRC consider establishing risk criteria for determining the tolerability or otherwise of landslide risk across the district, based on societal acceptance of comparable levels of risk arising from other sources. Such criteria should be based around a defined sustainable upper limit of tolerability of, for example, LPR or AIFR that represents the risk level above which KDC and CRC does not consider it tolerable for there to be people at risk in their properties in the longer term.
2. From past examples, including the Port Hills, Canterbury, the sustainable threshold of AIFR should be set within a range from 3×10^{-5} to 1×10^{-3} per year, consistent with risk levels currently tolerated in New Zealand and with regulatory practice overseas. A suitable starting point for KDC and CRC's deliberation as to where to set their threshold within this range would be a level of 1×10^{-4} (1/10,000 per year) AIFR.
3. KDC and CRC could adopt a lower threshold of LPR or AIFR above which development is controlled to prevent accumulation of people in areas of substantial risk below the sustainable threshold of tolerability. Such a threshold could be set 10 times below the tolerability threshold for general property uses, involving significant occupancy by people, and 100 times below the tolerability threshold for particularly sensitive property uses (e.g. schools, care homes, hospitals).

7.0 CONCLUSIONS

The conclusions from this study are:

1. The Local Personal Risk (LPR) has been estimated for landslide hazards – debris inundation and/or falling debris – that could occur within the study area from earthquake and rainfall triggers.
2. The LPR from landslide hazards varies as a function of the proximity of a person or dwelling to the steeper slopes and whether or not they are on a debris flow fan.
3. The main contributor to the LPR is from rainfall-induced landslides (RIL). This is because rainfall-triggering landslide events occur more frequently than strong earthquakes.
4. The LPR from earthquake-induced landslides (EIL) tends to decrease rapidly with increased distance from the toe of the steeper slopes, relative to the LPR from RIL. This is because the debris from RIL is wet and tends to travel further than the usually drier debris associated with EIL.
5. The LPR from RIL tends to be slightly higher in the north of the study area. This reflects:
   - the slightly higher 24-hour rainfall amounts estimated for the given rainfall bands from HIRDS; and
   - the more susceptible nature of the geological materials – mainly soils, sandstones, siltstones and limestones compared to the stronger greywacke sandstones that form most of the slopes in the central and southern parts of the study area.
6. The LPR from EIL is highest along the steeper coastal sections of the study area, especially along State Highway 1 to the north and south of Kaikōura and in the Mt Fyffe and Clarence River areas.
7. The sensitivity of the risk model to key uncertainties and the reliability of the assessments was investigated by changing some of the input variables used. These were: the number of landslides triggered by both earthquake and 24-hour rainfall triggers, the impact of climate change on increasing the 24-hour rainfall amount forecast to occur at the given annual frequencies, the probability of landslide debris passing a given distance down the slope (runout probability of exceedance for each Fahrböschung) and the vulnerability of a person present to being hit and killed by landslide debris.
8. These uncertainties combine to give a total factor of difference of between 8 and 10, which is up to an order of magnitude uncertainty on the risk estimates. This difference is between the risk estimates that adopt the Mean scenario inputs versus those that adopt all of the Upper scenario inputs. They are based on ranges of the input variables that are thought to be reasonable.
9. The two most significant uncertainties in this analysis are: (i) the impact of climate change on increasing the 24-hour rainfall amounts that could occur at the given annual frequencies and (ii) the runout POE for each Fahrböschung extent. These two variables combine to give a total factor of difference, between the risk estimates, of between 5 and 6.

8.0 ACKNOWLEDGEMENTS

The authors would like to acknowledge reviews by Dr Tim Davies (University of Canterbury), Dr. Andrea Wolter (GNS Science) and Scott Kelly (GNS Science) and input provided by Dr Trevor Carey-Smith (NIWA).

9.0 REFERENCES

Australian Geomechanics Society. 2007a. Commentary on guideline for landslide susceptibility, hazard and risk zoning for land use management. *Australian Geomechanics*. 42(1):37–62.

Australian Geomechanics Society. 2007b. Commentary on practice note guidelines for landslide risk management. *Australian Geomechanics*. 42(1):115–158.

Australian Geomechanics Society. 2007c. Guideline for landslide susceptibility, hazard and risk zoning for land use management. *Australian Geomechanics*. 42(1):13–36.

Australian Geomechanics Society. 2007d. Practice note guidelines for landslide risk management. *Australian Geomechanics*. 42(1):63–114.

Brideau M-A, de Vilder S, Massey C, Mitchell A, McDougall S, Aaron J. 2021. Empirical relationships to estimate the probability of runout exceedance for various landslide types. In: Guzzetti F, Mihalić Arbanas S, Reichenbach P, Sassa K, Bobrowsky PT, Takara K, editors. *Understanding and reducing landslide disaster risk. Volume 2: from mapping to hazard and risk zonation*. Cham (CH): Springer International Publishing. p. 321–327.

Brideau M-A, Massey CI, Lukovic B, Morgenstern R. 2020. Deterministic mapping of potential landslide debris inundation in the Kaikoura District. Lower Hutt (NZ): GNS Science. 37 p. Consultancy Report 2019/102. Prepared for Canterbury Regional Council.

Carey-Smith T, Henderson R, Singh S. 2018. High Intensity Rainfall Design System: version 4. Wellington (NZ): National Institute of Water & Atmospheric Research Ltd. 73 p. Client Report 2018022CH. Prepared for Envirolink.

Clarke LB, Kelly SD, FitzGerald T, Pondard N, Wilson-Rooy M. 2021. Stocktake of existing risk tolerance frameworks. Auckland (NZ): GNS Science. 81 p. Consultancy Report 2021/71. Prepared for the Ministry for the Environment.

Corominas J, Copons R, Moya J, Vilaplana JM, Altimir J, Amigó J. 2005. Quantitative assessment of the residual risk in a rockfall protected area. *Landslides*. 2(4):343–357. doi:10.1007/s10346-005-0022-z.

Corominas J, Einstein H, Davis T, Strom A, Zuccaro G, Nadim F, Verdel T. 2015. Glossary of terms on landslide hazard and risk. In: Lollino G, Giordan D, Crosta GB, Corominas J, Azzam R, Wasowski J, Sciarra N, editors. *Engineering Geology for Society and Territory – Volume 2*. Cham (CH): Springer International Publishing. p. 1775–1779.

Crowley H, Polidoro B, Pinho R, van Elk J. 2017. Framework for developing fragility and consequence models for Local Personal Risk. *Earthquake Spectra*. 33(4):1325–1345. doi:10.1193/083116eqs140m.

de Vilder SJ, Massey CI. 2020. Guidelines for natural hazard risk analysis on public conservation lands and waters – Part 3: analysing landslide risk to point and linear sites. Lower Hutt (NZ): GNS Science. 52 p. Consultancy Report 2020/52. Prepared for Department of Conservation.

Du J, Yin K, Nadim F, Lacasse S. 2013. Quantitative vulnerability estimation for individual landslides. In: Delage P, Desrues P, Frank R, Puech A, Schlosser F, editors. *Proceedings of the 18th International Conference on Soil Mechanics and Geotechnical Engineering, Paris 2013: challenges and innovations in geotechnics*. Paris (FR): Presses de Ponts. p. 2181–2184.

Fawcett T. 2006. An introduction to ROC analysis. *Pattern Recognition Letters*. 27(8):861–874. doi:10.1016/j.patrec.2005.10.010.

Heim A. 1989. Landslides & human lives. Skermer N, translator. Vancouver (CA): BiTech Publishers. 195 p.

Heron DW, custodian. 2020. Geological map of New Zealand: digital vector data [map]. 3rd ed. Lower Hutt (NZ): GNS Science. 1 USB, scale 1:250,000. (GNS Science geological map; 1).

Hungr O, Leroueil S, Picarelli L. 2014. The Varnes classification of landslide types, an update. *Landslides*. 11(2):167–194. doi:10.1007/s10346-013-0436-y.

Jonkman SN, van Gelder PHAJM, Vrijling JK. 2003. An overview of quantitative risk measures for loss of life and economic damage. *Journal of Hazardous Materials*. 99(1):1–30. doi:10.1016/S0304-3894(02)00283-2.

Kaiser AE, Balfour NJ, Fry B, Holden C, Litchfield NJ, Gerstenberger MC, D'Anastasio E, Horspool NA, McVerry GH, Ristau J, et al. 2017. The 2016 Kaikoura, New Zealand, earthquake: preliminary seismological report. *Seismological Research Letters*. 88(3):727–739. doi:10.1785/0220170018.

LINZ Data Service. 2012. NZ 8m Digital Elevation Model (2012). Wellington (NZ): Land Information New Zealand; [updated 2016 Aug 18; accessed 2021 Aug 26]. https://data.linz.govt.nz/layer/51768-nz-8m-digital-elevation-model-2012/

Lombardo L, Mai PM. 2018. Presenting logistic regression-based landslide susceptibility results. *Engineering Geology*. 244:14–24. doi:10.1016/j.enggeo.2018.07.019.

LRIS Portal. 2020. Lincoln (NZ): Landcare Research New Zealand. LCDB v5.0 – Land Cover Database version 5.0, mainland New Zealand. [updated 2020 Jan 29; accessed 2021 Oct]; [map]. https://lris.scinfo.org.nz/layer/104400-lcdb-v50-land-cover-database-version-50-mainland-new-zealand/

Marc O, Hovius N, Meunier P, Uchida T, Hayashi S. 2015. Transient changes of landslide rates after earthquakes. *Geology*. 43(10):883–886. doi:10.1130/g36961.1.

Massey CI, Gerstenberger MC, McVerry GH, Litchfield NJ. 2012. Canterbury earthquakes 2010/11 Port Hills slope stability: additional assessment of the life-safety risk from rockfalls (boulder rolls). Lower Hutt (NZ): GNS Science. 18 p. Consultancy Report 2012/214. Prepared for Christchurch City Council.

Massey CI, Lukovic B, de Vilder SJ, Archibald GC, Abbott ER. 2020a. Landslide risk analysis for Clifton Beach, Cape Kidnappers, Hawke's Bay. Lower Hutt (NZ): GNS Science. 101 p. Consultancy Report 2020/28. Prepared for Hastings District Council; Department of Conservation.

Massey CI, Lukovic B, Huso R, Buxton R, Potter SH. Forthcoming 2021. Earthquake-induced landslide forecast tool for New Zealand: version 2.0. Lower Hutt (NZ): GNS Science. (GNS Science report; 2018/08).

Massey CI, Thomas K-L, King AB, Singeisen C, Taig T, Horspool NA. 2019. SLIDE (Wellington): vulnerability of dwellings to landslides (Project No. 16/SP740). Lower Hutt (NZ): GNS Science. 76 p. (GNS Science report; 2018/27).

Massey CI, Townsend DB, Jones KE, Lukovic B, Rhoades DA, Morgenstern R, Rosser BJ, Ries W, Howarth JD, Hamling IJ, et al. 2020b. Volume characteristics of landslides triggered by the M_w 7.8 2016 Kaikōura Earthquake, New Zealand, derived from digital surface difference modelling. *Journal of Geophysical Research: Earth Surface*. 125(7):e2019JF005163. doi:10.1029/2019jf005163.

Massey CI, Townsend DT, Lukovic B, Morgenstern R, Jones K, Rosser B, de Vilder S. 2020c. Landslides triggered by the M_W7.8 14 November 2016 Kaikōura earthquake: an update. *Landslides*. 17(10):2401–2408. doi:10.1007/s10346-020-01439-x.

Massey CI, Townsend DB, Rathje E, Allstadt KE, Lukovic B, Kaneko Y, Bradley B, Wartman J, Jibson RW, Petley DM, et al. 2018. Landslides triggered by the 14 November 2016 Mw 7.8 Kaikoura earthquake, New Zealand. *Bulletin of the Seismological Society of America*. 108(3B):1630–1648. doi:10.1785/0120170305.

Parker RN, Hancox GT, Petley DN, Massey CI, Densmore AL, Rosser NJ. 2015. Spatial distributions of earthquake-induced landslides and hillslope preconditioning in the northwest South Island, New Zealand. *Earth Surface Dynamics*. 3(4):501–525. doi:10.5194/esurf-3-501-2015.

Pollock W, Wartman J. 2020. Human vulnerability to landslides. *GeoHealth*. 4(10):e2020GH000287. doi:10.1029/2020GH000287.

Quigley MC, Saunders W, Massey C, Van Dissen R, Villamor P, Jack H, Litchfield N. 2020. The utility of earth science information in post-earthquake land-use decision-making: the 2010–2011 Canterbury earthquake sequence in Aotearoa New Zealand. *Natural Hazards and Earth System Sciences*. 20(12):3361–3385. doi:10.5194/nhess-20-3361-2020.

Stirling MW, McVerry GH, Gerstenberger MC, Litchfield NJ, Van Dissen RJ, Berryman KR, Barnes P, Wallace LM, Villamor P, Langridge RM, et al. 2012. National seismic hazard model for New Zealand: 2010 update. *Bulletin of the Seismological Society of America*. 102(4):1514–1542. doi:10.1785/0120110170.

Taig T. Forthcoming 2021a. Risk comparisons for DOC visitors and staff. Cheshire (GB): TTAC Limited. 119 p.

Taig T. Forthcoming 2021b. Guidelines for DOC on dealing with natural hazard risk. Cheshire (GB): TTAC Limited. 78 p.

Taig T, Massey CI, Taig M, Becker JS, Heron DW. 2015. Validating the rockfall risk models developed for the Port Hills of Christchurch, New Zealand. In: Cubrinovski M, Bradley BA, Price C, Chin CY, editors. *6th International Conference on Earthquake Geotechnical Engineering, 1–4 November 2015, Christchurch, New Zealand*. Wellington (NZ): New Zealand Geotechnical Society (NZGS). p. 1353–1361.

Taig T, Massey CI, Webb TH. 2012. Canterbury earthquakes 2010/11 Port Hills slope stability: principles and criteria for the assessment of risk from slope instability in the Port Hills, Christchurch. Lower Hutt (NZ): GNS Science. 45 p. Consultancy Report 2011/319. Prepared for Christchurch City Council.

Tang C, Van Westen CJ, Tanyas H, Jetten VG. 2016. Analysing post-earthquake landslide activity using multi-temporal landslide inventories near the epicentral area of the 2008 Wenchuan earthquake. *Natural Hazards and Earth System Sciences*. 16(12):2641–2655. doi:10.5194/nhess-16-2641-2016.

TIBCO Software Inc. 2020. Logistic regression formula guide. Version 14.0. Palo Alto (CA): TIBCO Software Inc.; [accessed 2021 Aug]. https://docs.tibco.com/pub/stat/14.0.0/doc/pdf/TIB_stat_14.0_logistic_regression.pdf?id=7

von Ruette J, Papritz A, Lehmann P, Rickli C, Or D. 2011. Spatial statistical modeling of shallow landslides – validating predictions for different landslide inventories and rainfall events. *Geomorphology*. 133(1–2):11–22. doi:10.1016/j.geomorph.2011.06.010.

APPENDICES

This page left intentionally blank.

APPENDIX 1 EARTHQUAKE-INDUCED LANDSLIDE SUSCEPTIBILITY

Table A1.1 Logistic regression parameter estimates (coefficients) for each variable per GeolCode used to forecast earthquake-induced landslide susceptibility (see Massey et al. [forthcoming 2021] for explanation of variables).

Variable ID	GeolCode 1		GeolCode 2		GeolCode 3		GeolCode 4		GeolCode 5	
	Estimate	Std. Dev.	Estimate	Std. Dev.	Estimate	Std. Dev.	Estimate	Std. Dev.	Estimate	Std. Dev.
Intercept	-6.30	0.04	-8.16	0.03	-7.09	0.04	-7.00	0.04	-9.11	0.02
Elevation	-0.0011	0.00002	0.0019	0.00002	-0.00024	0.00003	-0.00040	0.00003	-0.00038	0.00001
Slope	0.059	0.001	0.056	0.001	0.035	0.001	0.011	0.001	0.043	0.001
LSR	0.048	0.001	0.021	0.000	0.025	0.001	0.030	0.001	0.035	0.000
Curvature	-0.154	0.012	-0.127	0.005	-0.122	0.007	-0.136	0.007	-0.104	0.003
FaultDist	-0.00015	0.000002	-0.00009	0.000001	-0.00005	0.000001	-0.00004	0.000001	-0.00003	0.0000002
PGA	0.15	0.03	1.25	0.02	1.37	0.03	1.75	0.03	1.63	0.01
Pseudo R^2	0.38		0.30		0.16		0.12		0.19	

APPENDIX 2 RAINFALL-INDUCED LANDSLIDE SUSCEPTBILITY

We have used a logistic regression model to create a landslide susceptibility model to forecast the spatial distribution of rainfall-induced landslides (RIL) in the study area. Logistic regression models estimate the landslide probability (0 to 1, where 1 = landslide occurrence) at the regional scale, where regional scale is defined as being between 1:25,000 and 1:250,000 (Corominas et al. 2015) and is referred to as the 'district' scale in this report. Susceptibility models and maps are a fundamental input to hazard analysis, as they can be used to determine the most probable locations of where landslides may initiate (de Vilder and Massey 2020). Susceptibility maps are typically based on information from landslide inventories, along with any pre-disposing 'susceptibility' factors, developed for a specific triggering event. The logistic regression model was 'trained' using two RIL datasets, specific to the district (Figure A2.1). These were:

- Cyclone Alison (11–12 March 1975) and associated landslides, and
- ex-Tropical Cyclone Ita (17 April 2014) and associated landslides.

The aim of the modelling in this study is to create a statistically robust model that can be used to forecast landslide probability as an input for the risk analysis.

A2.1 Datasets and Variables Used to Train the Rainfall-Induced Landslide Model

The predictor variables used to train the models were chosen based on variables previously found to influence landslide occurrence (e.g. von Ruette et al. 2011; Lombardo and Mai 2018). Based on these studies, we reduced the number of predictor variables used in model training to the following, in no particular order: (1) 24-hour rainfall amount, (2) land cover code (LCC), (3) geology, (4) elevation, (5) slope, (6) local slope relief (LSR), (7) curvature and (8) aspect.

These predictor variables and the methods used to calculate them are described in Table A2.1 and shown in Figure A2.2. To undertake the modelling, a sample grid at 32 m ground resolution was defined and an input grid for each variable was created and aligned with the sample grid. The 32 m resolution grid size was chosen, as it was much less than the typical hillslope lengths in the regions used for modelling, which can vary from 100 to >>1000 m. This resolution was identified as fulfilling the needs of the stakeholders. It also allowed easy aggregation of the inputs derived from the elevation data based upon the NZ 8 m Digital Elevation Model (2012) obtained from the Land Information New Zealand (LINZ) Data Service. For this analysis, only landslide source areas, not debris trails, from each inventory were used. To reduce sample bias; (1) it was assumed that a grid cell is defined as being a landslide source (LS = 1) if its centroid falls within a landslide source area, even if the grid cell is not fully occupied by the landslide source; and (2) all landslides within each dataset were used, regardless of their size. The minimum mapped landslide source areas within the datasets used are <10 m^2 for both Cyclone Alison and ex-tropical Cyclone Ita landslide inventories. The 'roll-overs' in the landslide source frequency-area plots are 100 m^2 for both Alison and Ita datasets, suggesting that landslides smaller than these were unlikely to have been systematically mapped and are therefore under-represented in these inventories (Figure A2.3).

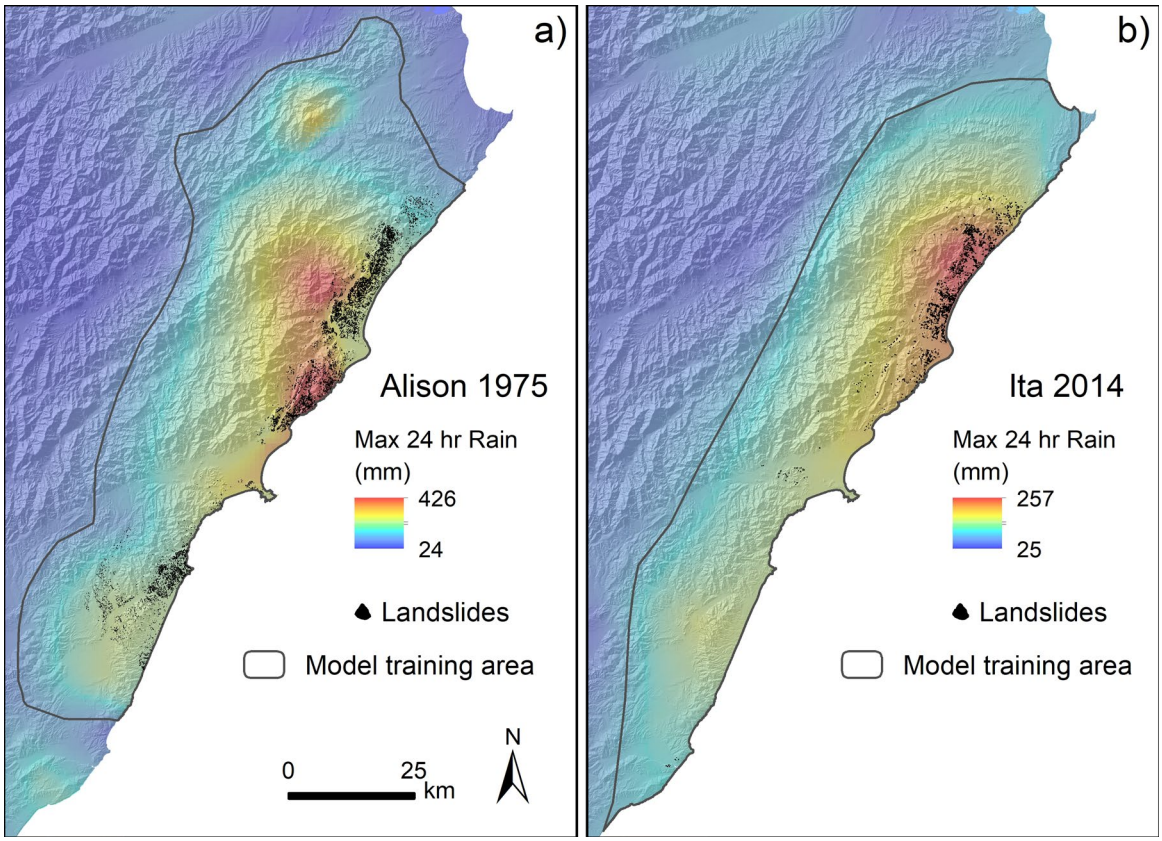


Figure A2.1 24-hour rainfall from rain gauge records and the mapped landslide distributions associated with: (a) Cyclone Alison (1975) and (b) ex-Tropical Cyclone Ita (2014).

Table A2.1 Predictor variables used in the logistic regression model and their ID codes, descriptions and units.

Variable Type	Variable ID	Description	Units
Landslide susceptibility	Geology 1 (GeolCode 1)	Quaternary sands, silts and gravels. These materials typically form terrace deposits on the top of the steep coastal cliffs, as well as on inland gentle slopes adjacent to the main rivers of the area. Many of these terraces have been incised by rivers.	N/A
	Geology 2 (GeolCode 2)	Neogene limestones, sandstones and siltstones, which are typically weak. They occur along sections of the coast north of Kaikōura.	N/A
	Geology 3 (GeolCode 3)	Upper Cretaceous to Paleogene rocks, including limestones, sandstones, siltstones and minor volcanic rocks. These are typically weak and easily erodible, and they can contain thin clay seams that are volcanic in origin. They are typically exposed in narrow strips overlying the greywacke basement rocks in the Kaikōura region.	N/A
	Geology 4 (GeolCode 4)	All intrusive and extrusive igneous rocks, ranging in age from Jurassic to Quaternary. Includes andesites, basalts, rhyolites, ignimbrites, dacites, granites and granodiorites.	N/A
	Geology 5 (GeolCode 5)	Lower Cretaceous Torlesse (Pahau terrane) 'basement' rocks are predominantly sandstones and argillite, also known as greywacke. The greywacke rocks are typically moderately to well bedded and tend to be closely jointed. They form many of the coastal slopes, as well as the steeper inland Kaikōura mountain ranges, and are the dominant rock type affected by the Kaikōura earthquake.	N/A
	$Slope_{MEAN}$	Local hillslope gradient generated in ArcGIS from the LINZ 8 m resolution DEM, adopting the mean value of all 8 m cells that fall within each cell of the 32 m sample grid. This variable is a proxy for the static shear stresses in the slope.	Degrees (°)
	Land Cover Code 1 (LCC1)	Taken from the Land Cover Database (LCDB; LRIS Portal 2020). This code represents exotic and indigenous forest.	N/A
	Land Cover Code 2 (LCC2)	Taken from the LCDB. This code represents bare ground, transport (such as roads) and urban.	N/A
	Land Cover Code 3 (LCC3)	Taken from the LCDB. This code represents alpine vegetation, grassland and scrub.	N/A

Variable Type	Variable ID	Description	Units
	$Elev_{MEAN}$	Local hillslope elevation taken from the LINZ 8 m resolution DEM, adopting the mean value of all 8 m cells that fall within each cell of the 32 m sample grid. This variable represents the observation that topography can limit the size of the landslides. For example, slopes that are higher in elevation tend to have larger surface areas and can therefore generate larger landslides than slopes at lower elevations, which tend to have smaller surface areas (Massey et al. 2020c). It could also represent different climatic conditions and erosion processes, which could dominate at different elevations.	Metres above mean sea level (mAMSL)
	$Curv_{MEAN}$	Curvature generated in ArcGIS from the LINZ 8 m resolution DEM. For each cell, the curvature value is calculated as a second derivative of the surface fitted through that cell and its eight surrounding neighbours. A negative value indicates that the surface is upwardly convex at that cell. A positive profile indicates that the surface is upwardly concave at that cell. A value of 0 indicates that the surface is flat. Curvature was aggregated to 32 m resolution, adopting the mean value of all 8 m cells that fell within each cell of the 32 m sample grid. This variable is a proxy for slope depressions and areas that may accumulate water.	One hundredth (1/100) of a z-unit
	LSR_{MAX}	Local slope relief generated from the LINZ 8 m resolution DEM using focal statistics in ArcGIS. It is calculated at 8 m resolution as the difference in elevation between a given grid cell and the lowest in elevation grid cell within an 80 m (10 cells) radius. LSR was aggregated to 32 m resolution, adopting the maximum value of all 8 m cells that fell within each cell of the 32 m sample grid. LSR represents the local height of the sample grid cell. It presents locally steeper and potentially more unstable slopes at a scale larger than the 32 m grid cell size.	Metres (m)
Landslide (earthquake) forcing	$Aspect_{MEAN}$	Generated in ArcGIS from the LINZ 8 m resolution DEM using 1° aspect bins. The mean was calculated by adopting the mean value of all 8 m cells that fall within each cell of the 32 m sample grid. The aspect is a proxy for the likely soil moisture of the cell, as certain aspects are more shaded (e.g. the south-facing aspects) compared to the northern ones that are exposed to more solar radiation and are thus assumed to be drier.	Degrees (m)
	24-hr Rain	The 24-hour maximum rainfall amount calculated from the gauge data over the length of each storm. The rain gauge data was interpolated between gauges using the natural neighbour function in ArcGIS.	mm

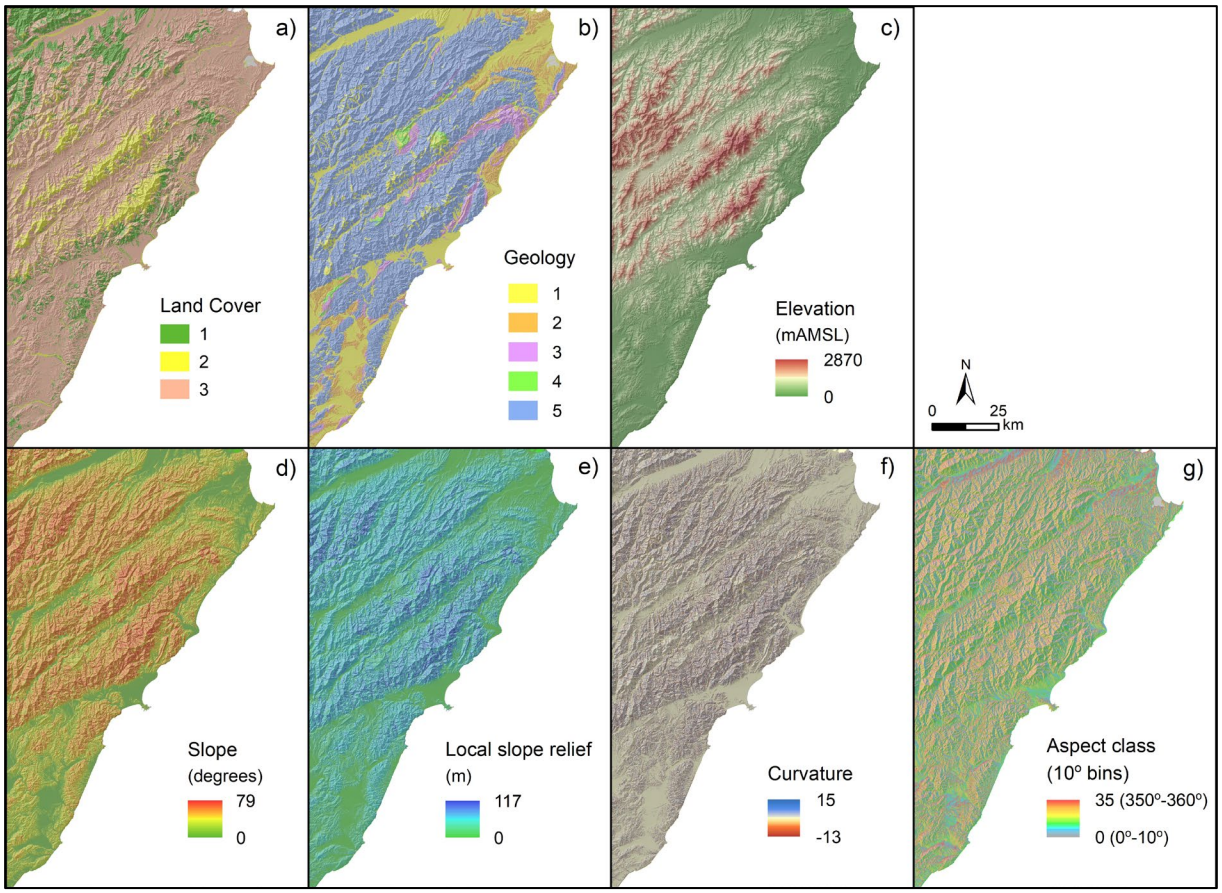


Figure A2.2 The variables used to train the logistic regression rainfall-induced landslide forecast model.

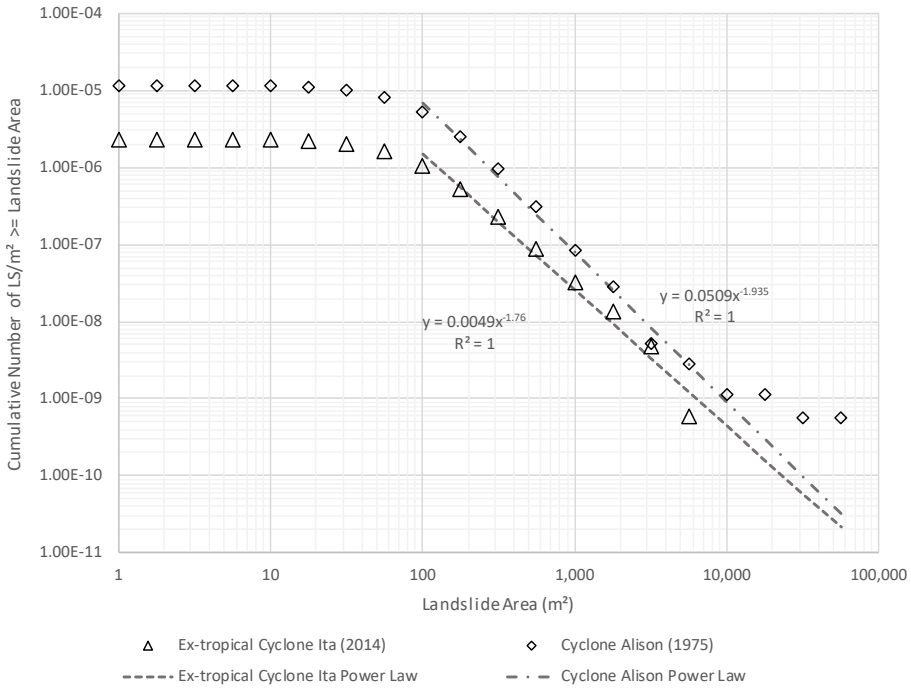


Figure A2.3 The cumulative number of landslides per square kilometre equal to or greater than a given landslide source area, plotted separately for Cyclone Alison (diamonds) and ex-Tropical Cyclone Ita (triangles). The power law trend lines are fitted to the data for landslide source areas >100 m^2.

A2.2 The Logistic Regression RIL Model

Logistic regression is routinely used to forecast landslide occurrence (e.g. Lombardo and Mai 2018) by calculating landslide probability from a series of input 'predictor' variables. The method is used to estimate the coefficients for predicting the probability (P_{LS}) that $Y = 1$, given the values of one or more predictor variables. Here, the condition $Y = 1$ corresponds to the occurrence of a landslide and $Y = 0$ corresponds to no landslide within a sample grid cell on the ground. The regression coefficients are estimated using a maximum likelihood criterion. For this work, we independently derived models that were fitted to the continuous predictor variables grouped by GeolCode, where landslide probability ($P_{LS:\ Geology\ x}$) for each geology group (GeolCode) is given by the following equation:

$$P_{LS:Geology\ x} = \frac{1}{1+exp\left(-\left(\begin{matrix} C_{Intercept}+C_{RAIN_{24hr}}.RAIN_{24hr}+C_{Elev_{MEAN}}.Elev_{MEAN}+C_{Aspect}.Aspect+ \\ +C_{Slope_{MEAN}}.Slope_{MEAN}+C_{LSR_{MAX}}.LSR_{MAX}+C_{Curve_{MEAN}}.Curve_{MEAN}+LLC \end{matrix}\right)\right)} \quad \text{Equation A2.1}$$

Land Cover Code was included in the regression as a categorical variable. The regression coefficients were derived by 'training' on the two RIL datasets using the Statistica software (TIBCO Software Inc. 2020). For model fitting, we used an unbalanced dataset, given that the occurrence of a landslide ($Y = 1$) is much rarer than not ($Y = 0$). Therefore, our datasets are inherently biased toward no landslides ($Y = 0$) and, as a result, are naturally unbalanced.

For a predictor variable to be included in the model, it must have a logical and statistically significant influence on P_{LS}. We used a significance level (p-value) of $p < 0.05$ (using the Wald statistic) as the threshold for inclusion in the model.

A2.3 The Statistical Performance of the Rainfall-Induced Landslide Model

The statistical performance of the logistic regression were compared using two approaches: (1) the ROC curve and AUC and (2) the cumulative forecast probability versus the cumulative landslide record, referred to as the 'CumF-R'. ROC curves (e.g. Fawcett 2006; Lombardo and Mai 2018) are graphical plots based on the analysis of 'non-failing' and 'failing' predictions. The ROC curve is created by plotting the true positive rate (TPR) against the false positive rate (FPR) at various threshold settings. The TPR is also known as 'sensitivity' in machine learning. The FPR is known as 'probability of false alarm' and can be calculated as (1 − specificity), where specificity is true negative rate (TNR). The ROC curves illustrate the diagnostic ability of a binary classifier system, as its discrimination threshold is varied. The shape of the curve is used to evaluate the goodness of fit for a binary classifier – in this case, whether a grid cell is a landslide or not ($Y = 1$ or $Y = 0$) – where the class prediction for each instance is based on the continuous random variable; in this case, the landslide probability. The TPR defines how many correct positive results (in this case, landslides, or cells where $Y = 1$) occur among all positive samples (total number of landslide cells). FPR, on the other hand, defines how many incorrect positive results (non-landslides, or cells where $Y = 0$) occur among all negative samples (total number of cells with $Y = 0$). The number of landslide (true positive) and non-landslide (false positive) cells was counted for all cells where the landslide probability was greater than a threshold, where the threshold is a varying parameter.

An ROC curve demonstrates the following: (1) the trade-off between TPR and FPR; (2) that the closer the curve follows the left y-axis border and then the top x-axis border of the ROC space (AUC close to 1), the more informative the prediction may be; and (3) that the closer the curve comes to the 45° diagonal of the ROC space (AUC = 0.5), the less informative the prediction may be. Therefore, a model result with an AUC >0.9 indicates that the ability of

the model to forecast landslide probability is ‘excellent’, and an AUC <0.70 indicates that the ability of the model to forecast landslide probability is ‘poor’ (Lombardo and Mai 2018).

The TPR (sensitivity), FPR (1-specificity) and AUC were calculated for each modelled scenario in the following way:

- **Step 1:** Forecasting. Using the logistic regression models fitted to each GeolCode, the ‘forecast’ probability was calculated for each grid cell in the dataset based on the variables for the given cell. The data was then ordered from high to low forecast probability.
- **Step 2:** TPR (Sensitivity). This is the cumulative number (forecast probability sorted from high to low, Step 1) of correctly predicted landslides (cells where Y = 1) divided by the total number of cells classified as being a landslide (Y = 1) in the given dataset.
- **Step 3:** FPR (1 – Specificity). This is the cumulative number (forecast probability sorted from high to low, Step 1) of non-landslides predicted as landslides (cells where Y = 0) divided by the total number of cells classified as not being a landslide (Y = 0).
- **Step 4:** Area under the curve (AUC). The area was calculated from a histogram created by plotting the TPR on the y-axis against the FPR on the x-axis for each forecast probability, sorted from hight to low (Step 1).
- **Step 5:** ROC was also plotted and AUC calculated using the Python scikit-learn library.

The CumF-R relationship is a way to show whether the forecast model is under- or over-predicting the number of grid cells that are forecast as being a landslide. It therefore shows the ‘consistency’ of the modelled forecast probabilities against the actual grid cells recorded as being landslides (Parker et al. 2015; Massey et al. 2018). These are calculated as the cumulative sum of forecast landslide probability values for each sample grid cell, sorted from low to high probability. The corresponding recorded *Y*-values, i.e. $Y = 1$ (landslide) or $Y = 0$ (no landslide) are also summed on the sorted dataset, providing the cumulative sum of grid cells classified as being a landslide ($Y = 1$). A well-performing model should plot as a ‘straight’ line and close to the line of equality in cumulative forecast versus cumulative record space. A poorly performing model will not be a straight line and will either over- or under-forecast the cumulative number of landslide cells.

A2.4 Rainfall-Induced Landslide Model Results

The results from the logistic regression model are shown in Table A2.2. The parameter estimates (coefficients) for each variable are listed in Table A2.3. These results represent parameter estimates for each variable based on logistic regression models fitted to all records within each GeolCode from both RIL inventories combined (Cyclone Alison and ex-Tropical Cyclone Ita). There were not enough landslide records in GeolCode 4 to statistically fit a logistic regression model, so models were only fitted to GeolCodes 1, 2, 3 and 5. The results from the modelling show that the logistic regression model trained using the two RIL inventories are robust and can be used to forecast RIL probability.

The CumF-R plots are shown in Figures A2.4–A2.7, and show that, in general, the relationships between the cumulative record and cumulative forecast probabilities display a good fit to the line of equality. This shows that the modelled probabilities are broadly consistent with the data, that the observed and predicted probabilities display a good fit to the line of equality and that the fitted models generally have no apparent biases in any part of their range.

To investigate the rank order of importance of the different variables used in the models, the Wald statistic was used (Tibco Software Inc. 2020). In order of importance, from most to least important, the variables used in all GeolCode models were: (1) 24-hour Rain, (2) Elevation, (3) Slope, (4) Aspect, (5) LLC, (6) LSR and (7) Curvature.

Table A2.2 Logistic regression modelled scenarios trained per GeolCode, adopting data from Cyclone Alison (1975) and ex-Tropical Cyclone Ita (2014) rainfall-induced landslide inventories combined. For the percentage difference column, negative values would indicate that the given model scenario under-estimates the number of cells where *Y* =1, and positive values would indicate an over-estimate.

Model Scenario	Total N Grid Cells Y=1 (Landslide)	Total N Grid Cells Y=0 (Non-Landslide)	Pseudo R^2	ROC: AUC
GeolCode 1	1366	1,845,830	0.25	0.94
GeolCode 2	8223	842,276	0.24	0.91
GeolCode 3	4188	777,163	0.21	0.89
GeolCode 5	7477	5,106,994	0.22	0.93

Table A2.3 Parameter estimates (coefficients) for each variable per GeolCode, adopting data from Cyclone Alison (1975) and ex-Tropical Cyclone Ita (2014) rainfall-induced landslide inventories combined. For the categorical variable of Land Cover Code (LCC), LCC3 was used as the reference within all GeolCode models.

Variable ID	GeolCode 1		GeolCode 2		GeolCode 3		GeolCode 5	
	Estimate	Std. Dev.	Estimate	Std. Dev.	Estimate	Std. Dev.	Estimate	Std. Dev.
Intercept	-10.5	0.1	-9.81	0.07	-8.6	0.1	-8.0	0.1
24-hr Rain	0.0160	0.0004	0.0241	0.0002	0.0159	0.0002	0.0136	0.0001
Elevation	-0.0083	0.0003	-0.0050	0.0001	-0.0062	0.0001	-0.0058	0.0001
Slope	0.140	0.007	0.082	0.003	0.107	0.004	0.074	0.003
Aspect	-0.046	0.003	0.002	0.001	-0.013	0.002	-0.024	0.001
LSR	-0.04	0.01	-0.042	0.006	-0.10	0.01	-0.08	0.01
Curvature	0.09	0.03	0.01	0.01	0.03	0.02	0.09	0.01
LCC1	0.43	0.09	-0.12	0.04	-0.35	0.05	0.22	0.06
LCC2	-1.2	0.1	-0.06	0.06	-0.2	0.1	-1.0	0.1
LCC3	1	-	1	-	1	-	1	-
Pseudo R^2	0.94		0.91		0.89		0.93	

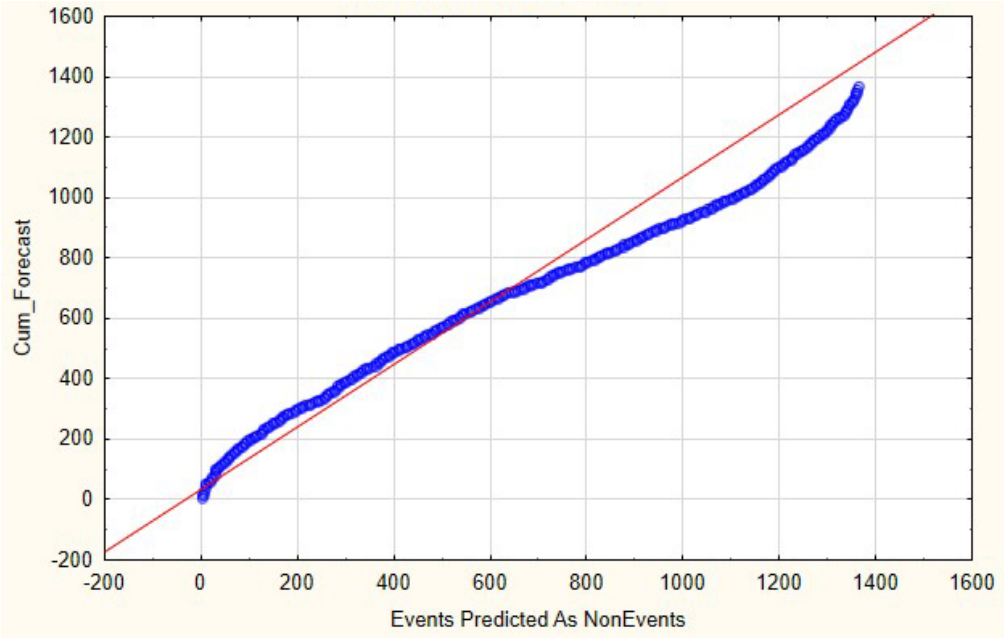


Figure A2.4 GeolCode 1: CumF-R plot for the logistic regression model. The results are based on a model fitted to Cyclone Alison (1975) and ex-Tropical Cyclone Ita (2014) rainfall-induced landslide inventories. The Cum_Forecast (y-axis) is the Sensitivity (true positive rate), and the x-axis is the cumulative record, Events Predicted as NonEvents, which is also the Specificity (false positive rate).

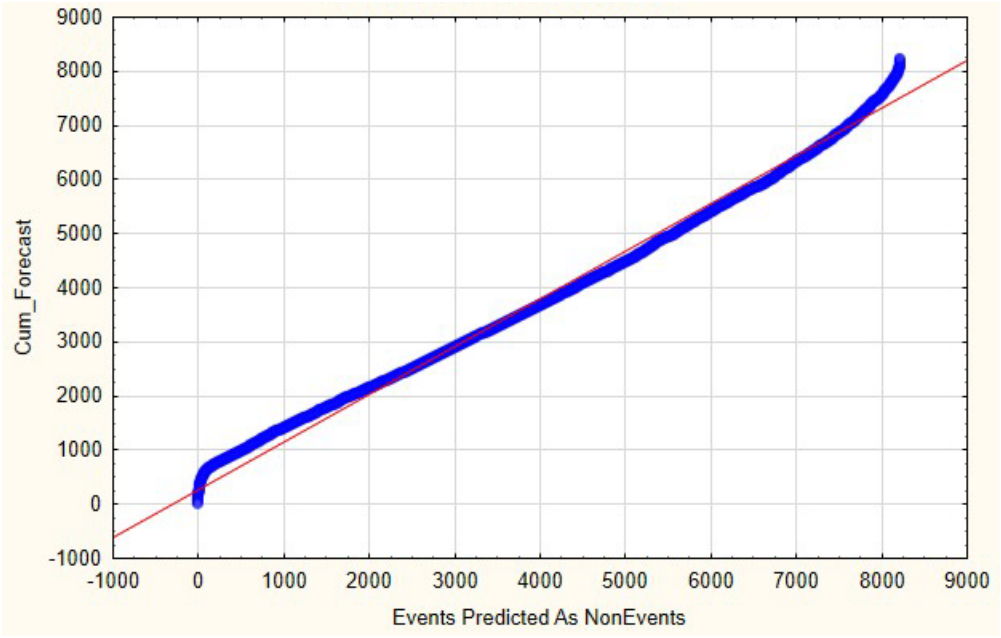


Figure A2.5 GeolCode 2: CumF-R plot for the logistic regression model. The results are based on a model fitted to Cyclone Alison (1975) and ex-Tropical Cyclone Ita (2014) rainfall-induced landslide inventories. The Cum_Forecast (y-axis) is the Sensitivity (true positive rate), and the x-axis is the cumulative record, Events Predicted as NonEvents, which is also the Specificity (false positive rate).

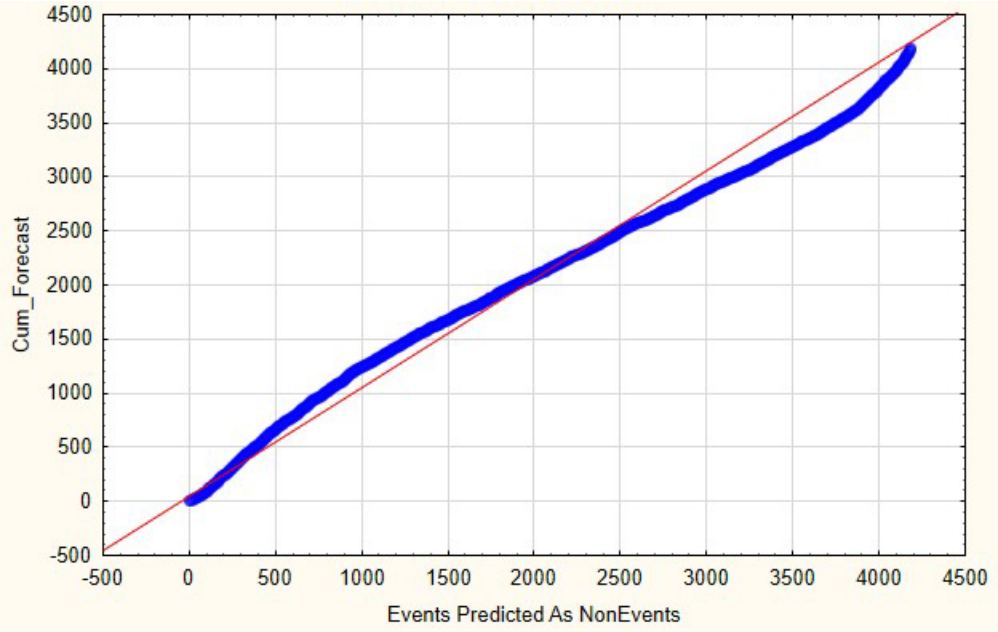


Figure A2.6 GeolCode 3: CumF-R plot for the logistic regression model. The results are based on a model fitted to Cyclone Alison (1975) and ex-Tropical Cyclone Ita (2014) rainfall-induced landslide inventories. The Cum_Forecast (y-axis) is the Sensitivity (true positive rate), and the x-axis is the cumulative record, Events Predicted as NonEvents, which is also the Specificity (false positive rate).

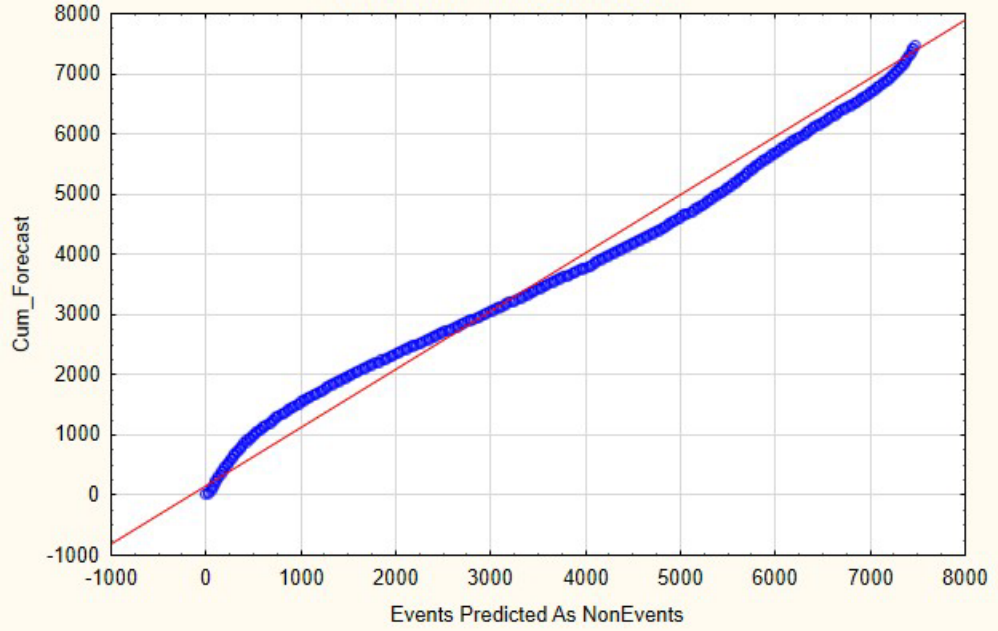
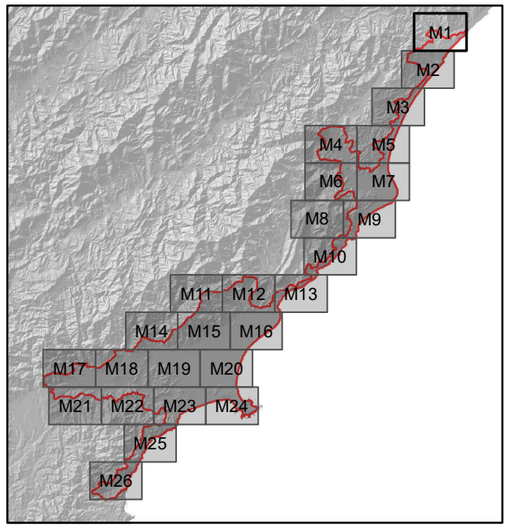
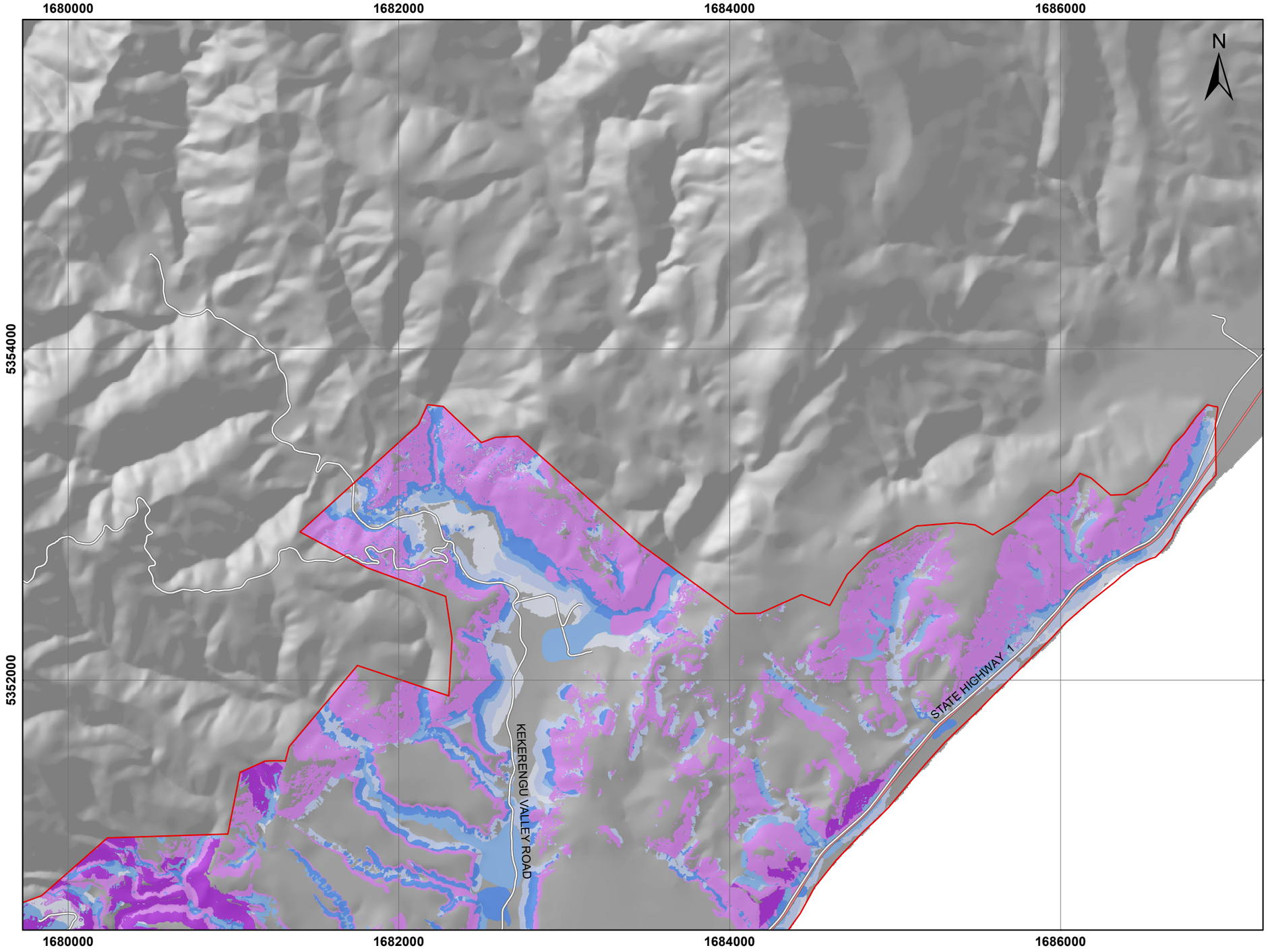


Figure A2.7 GeolCode 5: CumF-R plot for the logistic regression model. The results are based on a model fitted to Cyclone Alison (1975) and ex-Tropical Cyclone Ita (2014) rainfall-induced landslide inventories. The Cum_Forecast (y-axis) is the Sensitivity (true positive rate), and the x-axis is the cumulative record, Events Predicted as NonEvents, which is also the Specificity (false positive rate).

APPENDIX 3

LOCAL PERSONAL RISK MAPS: SCENARIO 2





Local personal risk

- 10^{-2} - 10^{-1}
- 10^{-3} - 10^{-2}
- 10^{-4} - 10^{-3}
- 10^{-5} - 10^{-4}
- 10^{-6} - 10^{-5}
- 10^{-7} - 10^{-6}
- Less than 10^{-7}

Roads

Railway

Study area

SCALE BAR: 0 0.5 1 km

EXPLANATION:

The model is based on mean landslide probability estimates and historical 24-hour rainfall annual frequencies. It uses a variable value for the vulnerability of a person if hit by a landslide, based on the landslide size and the person's distance from the source.

Background shade model derived from 8 m New Zealand Digital Elevation Model (LINZ Data Service 2012). PROJECTION: New Zealand Transverse Mercator 2000.

DRW: BL

CHK: CM, SDV

GNS SCIENCE TE PŪ AO

Confidential 2021

LOCAL PERSONAL RISK from earthquake- and rainfall-induced landslides Mean scenario

Regional Landslide Risk Analysis Kaikōura

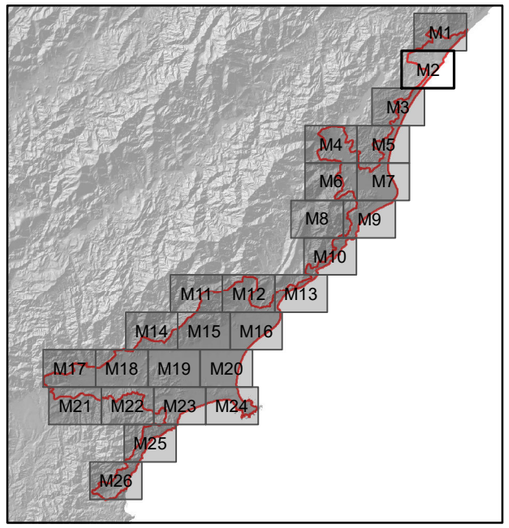
Appendix 3

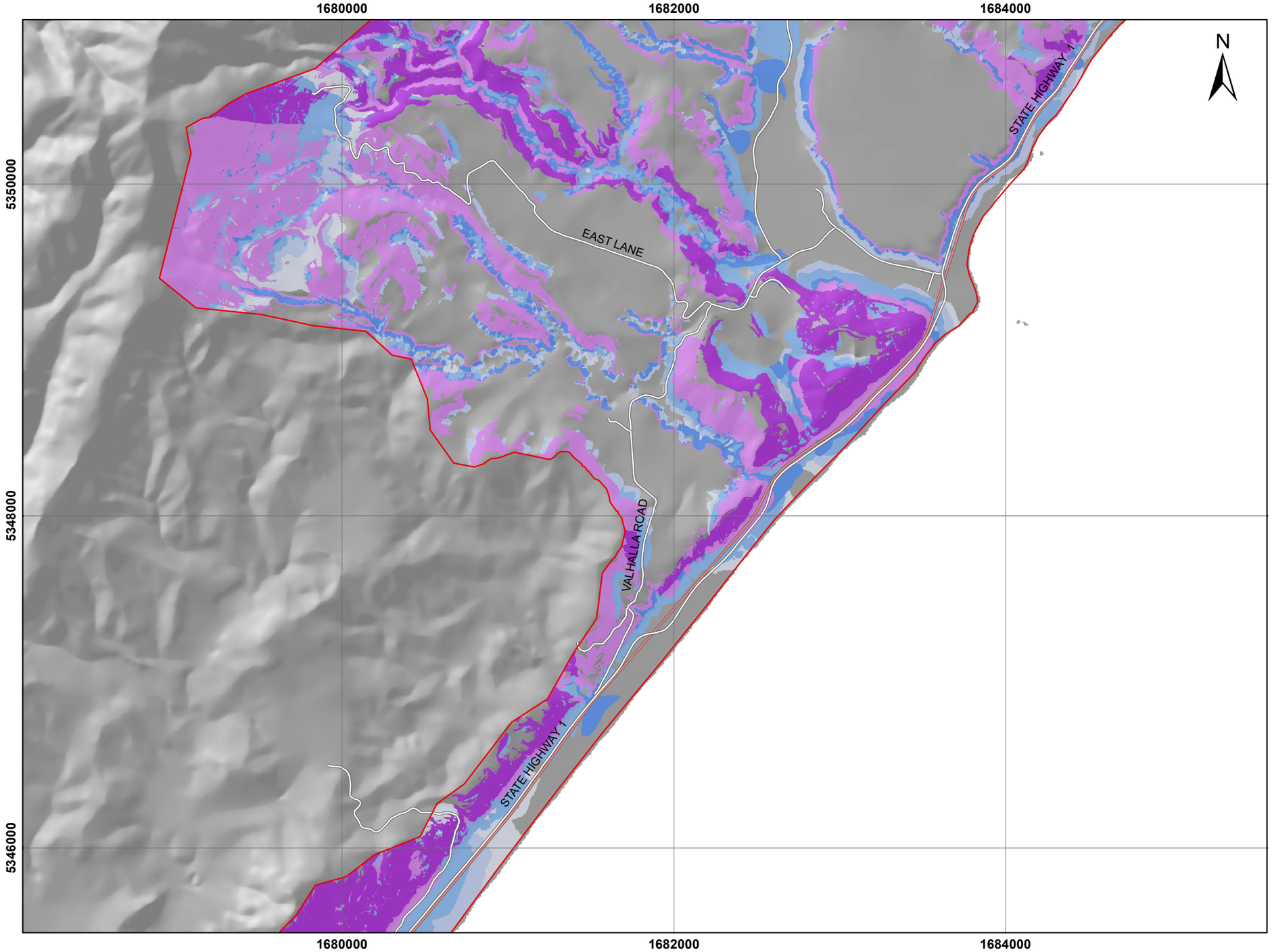
Map 1

FINAL

REPORT: CR2021/89

DATE: Oct 2021





Local personal risk

- 10^{-2} - 10^{-1}
- 10^{-3} - 10^{-2}
- 10^{-4} - 10^{-3}
- 10^{-5} - 10^{-4}
- 10^{-6} - 10^{-5}
- 10^{-7} - 10^{-6}
- Less than 10^{-7}

- Roads
- Railway
- Study area

SCALE BAR: 0 0.5 1 km

EXPLANATION:

The model is based on mean landslide probability estimates and historical 24-hour rainfall annual frequencies. It uses a variable value for the vulnerability of a person if hit by a landslide, based on the landslide size and the person's distance from the source.

Background shade model derived from 8 m New Zealand Digital Elevation Model (LINZ Data Service 2012). PROJECTION: New Zealand Transverse Mercator 2000.

DRW: BL

CHK: CM, SDV

GNS SCIENCE TE PŪ AO

Confidential 2021

LOCAL PERSONAL RISK from earthquake- and rainfall-induced landslides Mean scenario

Regional Landslide Risk Analysis Kaikōura

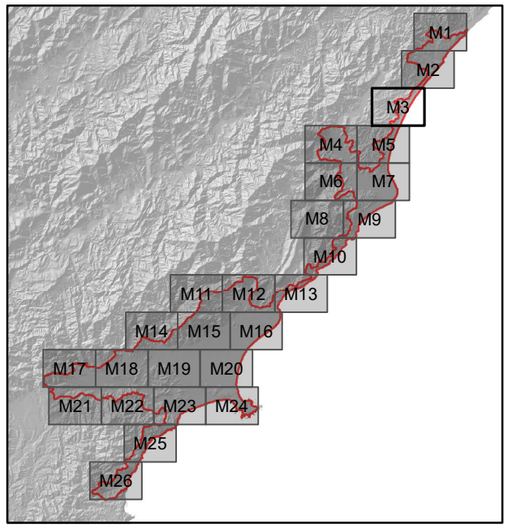
Appendix 3

Map 2

FINAL

REPORT: CR2021/89

DATE: Oct 2021



1676000 1678000 1680000

5344000

5342000

N

STATE HIGHWAY 1

Local personal risk

- 10^{-2} - 10^{-1}
- 10^{-3} - 10^{-2}
- 10^{-4} - 10^{-3}
- 10^{-5} - 10^{-4}
- 10^{-6} - 10^{-5}
- 10^{-7} - 10^{-6}
- Less than 10^{-7}

Roads

Railway

Study area

SCALE BAR: 0 0.5 1 km

EXPLANATION:

The model is based on mean landslide probability estimates and historical 24-hour rainfall annual frequencies. It uses a variable value for the vulnerability of a person if hit by a landslide, based on the landslide size and the person's distance from the source.

Background shade model derived from 8 m New Zealand Digital Elevation Model (LINZ Data Service 2012). PROJECTION: New Zealand Transverse Mercator 2000.

DRW: BL

CHK: CM, SDV

GNS SCIENCE TE PŪ AO

Confidential 2021

LOCAL PERSONAL RISK from earthquake- and rainfall-induced landslides Mean scenario

Regional Landslide Risk Analysis Kaikōura

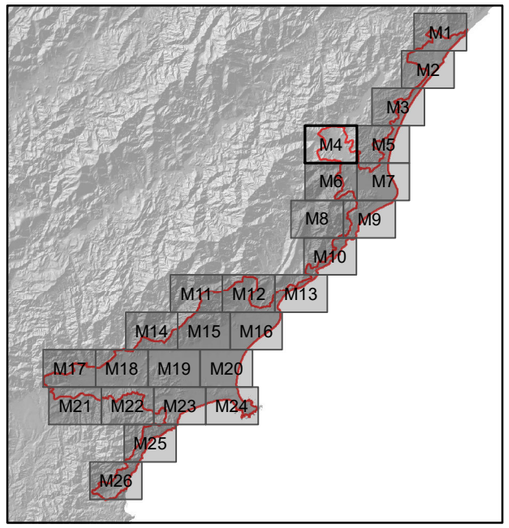
Appendix 3

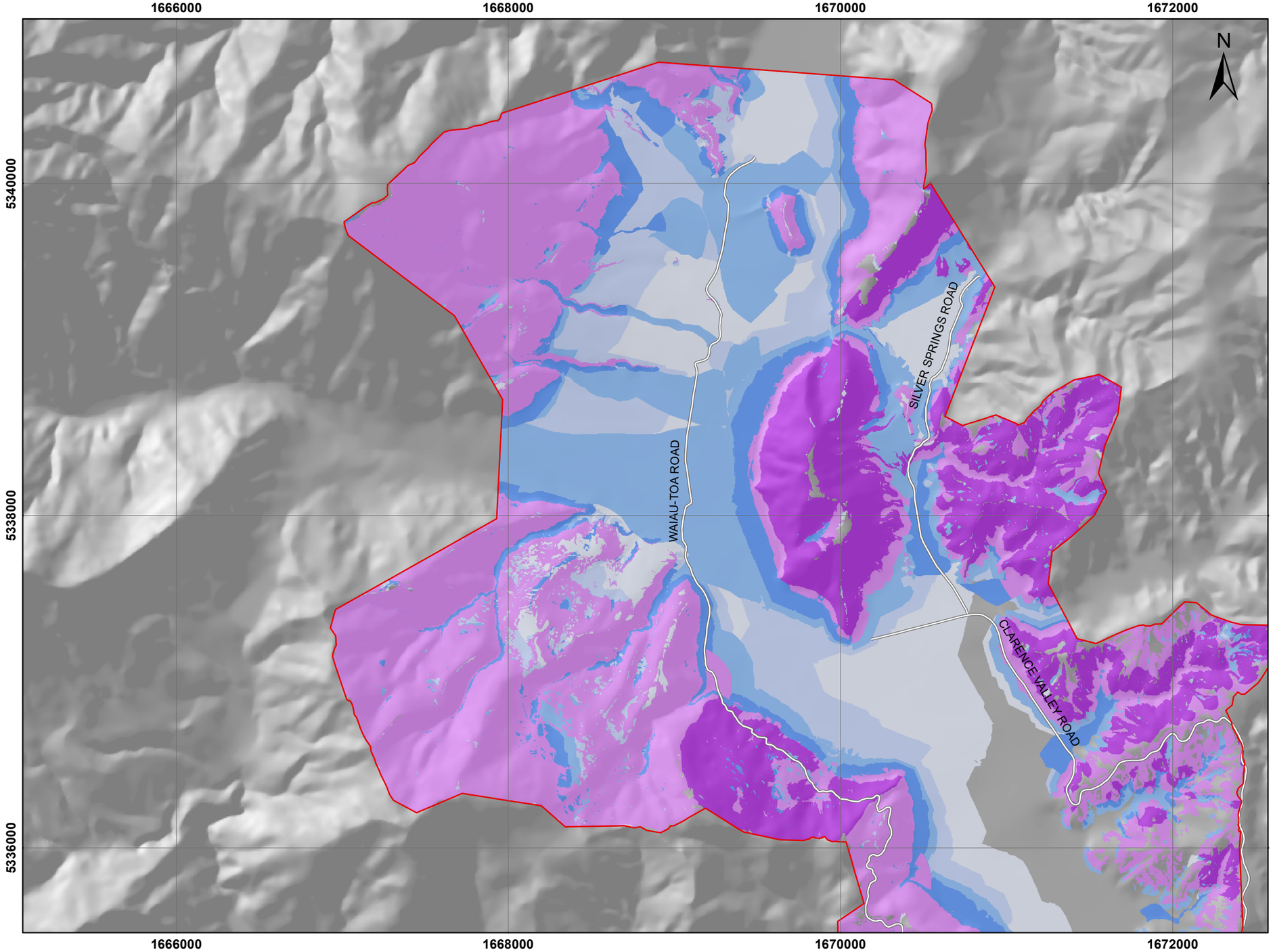
Map 3

FINAL

REPORT: CR2021/89

DATE: Oct 2021





Local personal risk

- 10^{-2} - 10^{-1}
- 10^{-3} - 10^{-2}
- 10^{-4} - 10^{-3}
- 10^{-5} - 10^{-4}
- 10^{-6} - 10^{-5}
- 10^{-7} - 10^{-6}
- Less than 10^{-7}

- Roads
- Railway
- Study area

SCALE BAR: 0 0.5 1 km

EXPLANATION:

The model is based on mean landslide probability estimates and historical 24-hour rainfall annual frequencies. It uses a variable value for the vulnerability of a person if hit by a landslide, based on the landslide size and the person's distance from the source.

Background shade model derived from 8 m New Zealand Digital Elevation Model (LINZ Data Service 2012). PROJECTION: New Zealand Transverse Mercator 2000.

DRW: BL

CHK: CM, SDV

GNS SCIENCE TE PŪ AO

Confidential 2021

LOCAL PERSONAL RISK from earthquake- and rainfall-induced landslides Mean scenario

Regional Landslide Risk Analysis Kaikōura

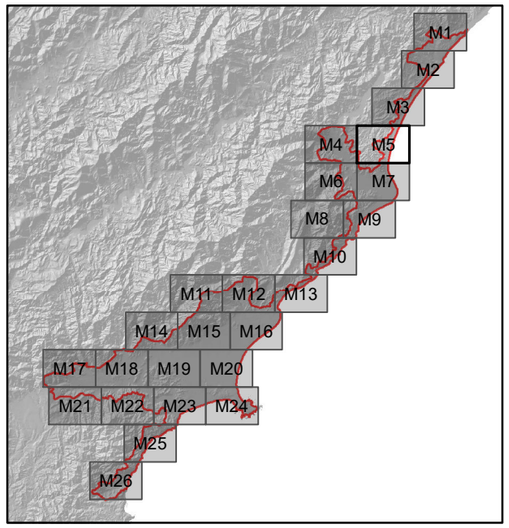
Appendix 3

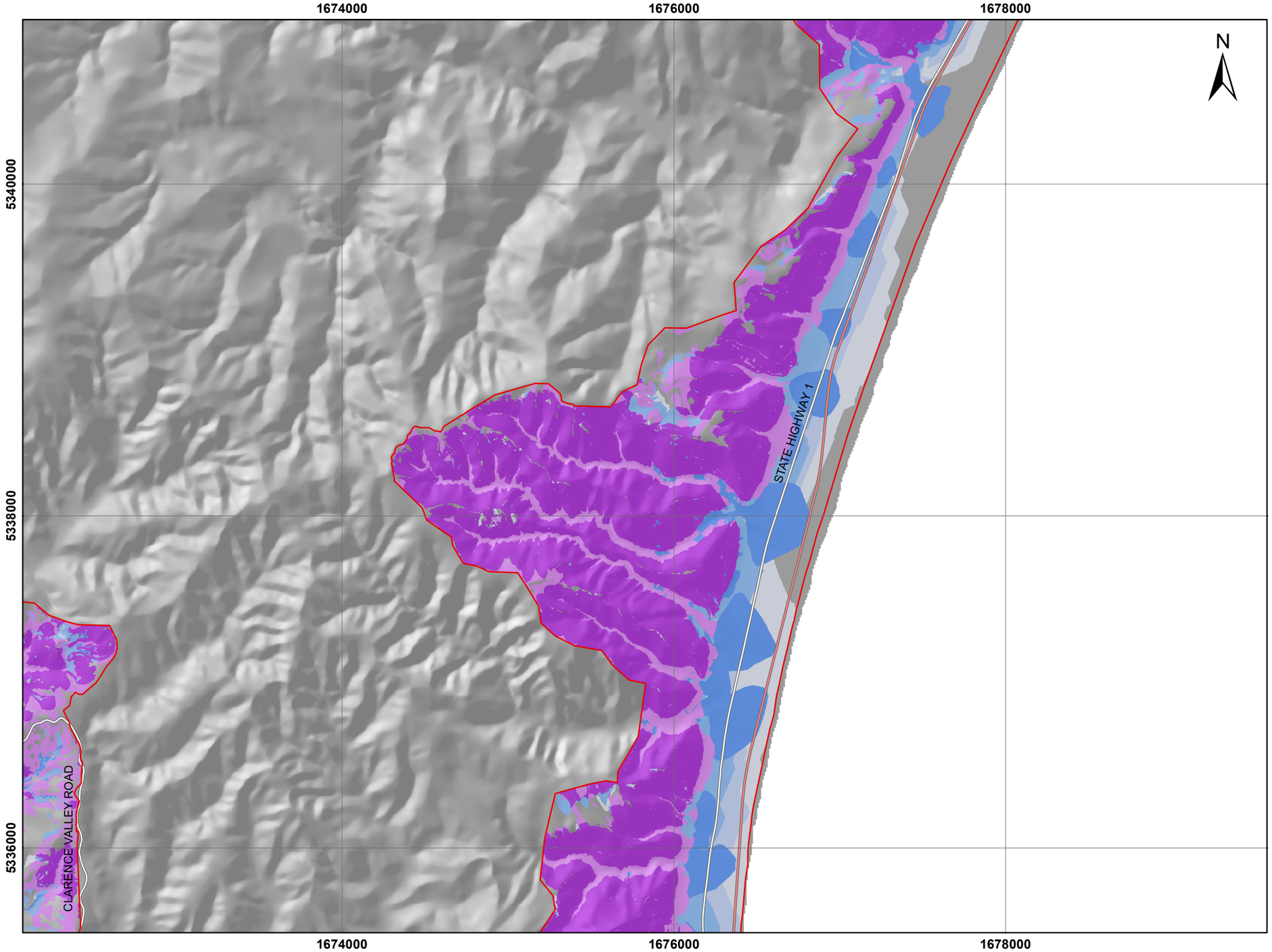
Map 4

FINAL

REPORT: CR2021/89

DATE: Oct 2021





Local personal risk

- 10^{-2} - 10^{-1}
- 10^{-3} - 10^{-2}
- 10^{-4} - 10^{-3}
- 10^{-5} - 10^{-4}
- 10^{-6} - 10^{-5}
- 10^{-7} - 10^{-6}
- Less than 10^{-7}

Roads

Railway

Study area

SCALE BAR: 0 0.5 1 km

EXPLANATION:

The model is based on mean landslide probability estimates and historical 24-hour rainfall annual frequencies. It uses a variable value for the vulnerability of a person if hit by a landslide, based on the landslide size and the person's distance from the source.

Background shade model derived from 8 m New Zealand Digital Elevation Model (LINZ Data Service 2012). PROJECTION: New Zealand Transverse Mercator 2000.

DRW: BL

CHK: CM, SDV

GNS SCIENCE TE PŪ AO

Confidential 2021

LOCAL PERSONAL RISK from earthquake- and rainfall-induced landslides Mean scenario

Regional Landslide Risk Analysis Kaikōura

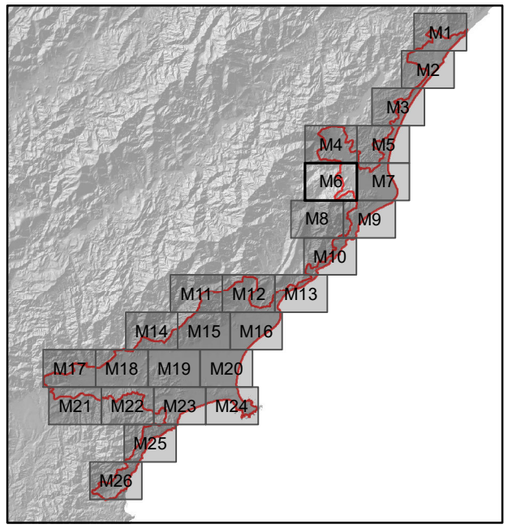
Appendix 3

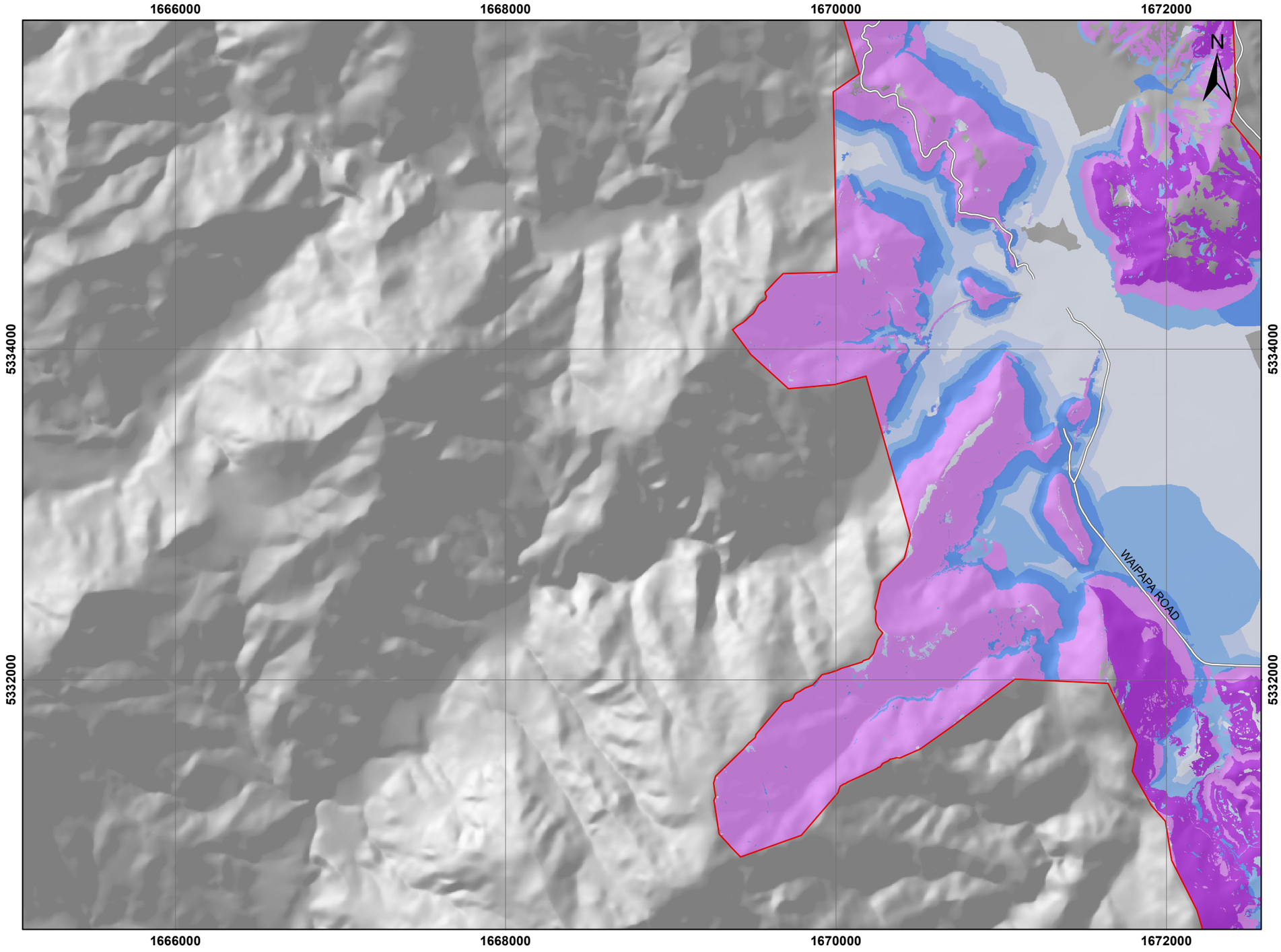
Map 5

FINAL

REPORT: CR2021/89

DATE: Oct 2021





Local personal risk

- 10^{-2} - 10^{-1}
- 10^{-3} - 10^{-2}
- 10^{-4} - 10^{-3}
- 10^{-5} - 10^{-4}
- 10^{-6} - 10^{-5}
- 10^{-7} - 10^{-6}
- Less than 10^{-7}

Roads

Railway

Study area

SCALE BAR: 0 0.5 1 km

EXPLANATION:

The model is based on mean landslide probability estimates and historical 24-hour rainfall annual frequencies. It uses a variable value for the vulnerability of a person if hit by a landslide, based on the landslide size and the person's distance from the source.

Background shade model derived from 8 m New Zealand Digital Elevation Model (LINZ Data Service 2012). PROJECTION: New Zealand Transverse Mercator 2000.

DRW: BL

CHK: CM, SDV

GNS SCIENCE TE PŪ AO

Confidential 2021

LOCAL PERSONAL RISK
from earthquake- and rainfall-induced landslides
Mean scenario

Regional Landslide Risk Analysis
Kaikōura

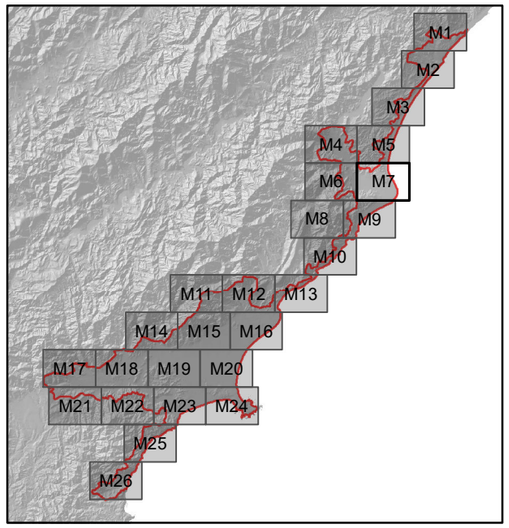
Appendix 3

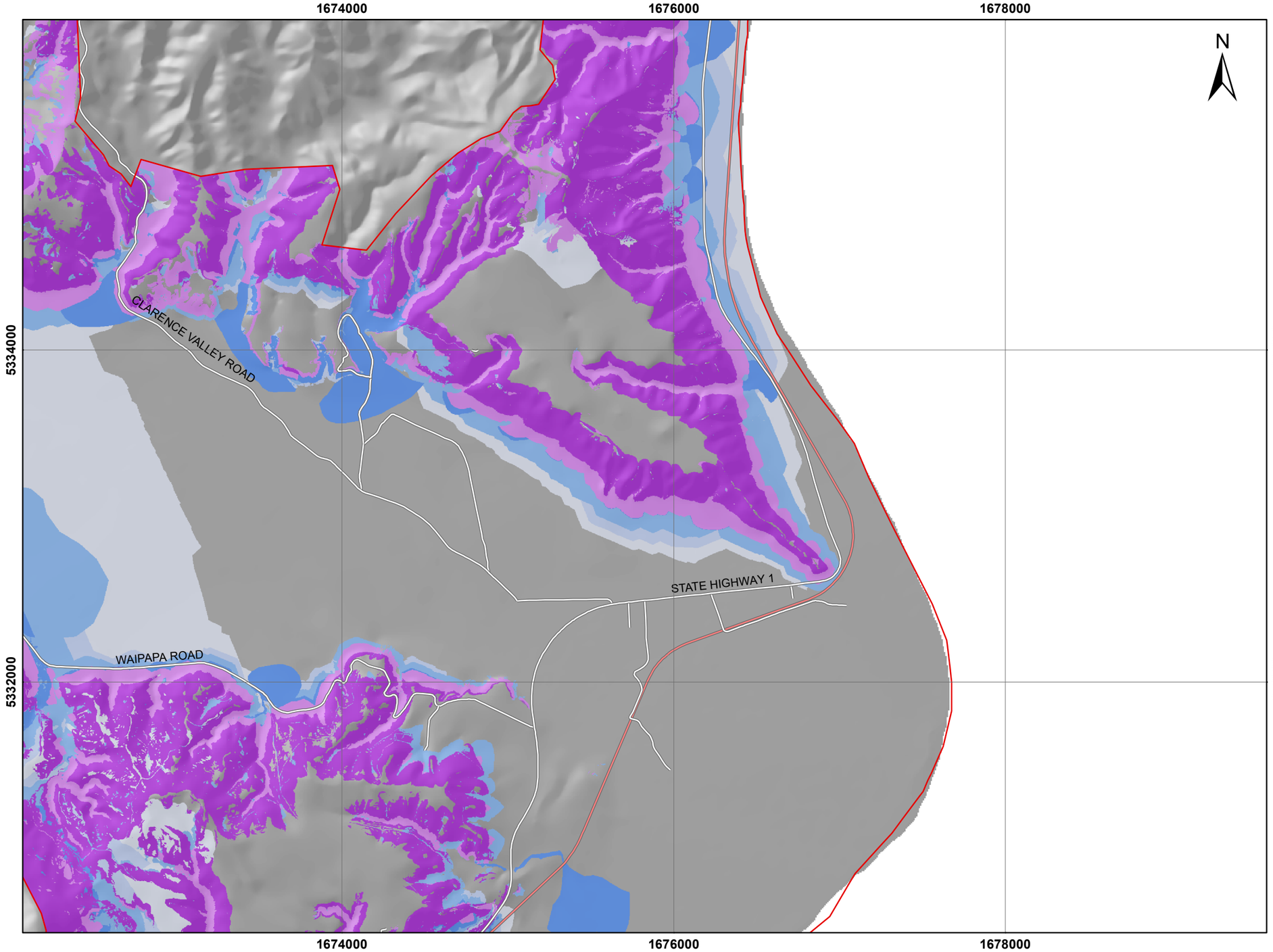
Map 6

FINAL

REPORT: CR2021/89

DATE: Oct 2021





Local personal risk

- 10^{-2} - 10^{-1}
- 10^{-3} - 10^{-2}
- 10^{-4} - 10^{-3}
- 10^{-5} - 10^{-4}
- 10^{-6} - 10^{-5}
- 10^{-7} - 10^{-6}
- Less than 10^{-7}

- Roads
- Railway
- Study area

SCALE BAR: 0 0.5 1 km

EXPLANATION:

The model is based on mean landslide probability estimates and historical 24-hour rainfall annual frequencies. It uses a variable value for the vulnerability of a person if hit by a landslide, based on the landslide size and the person's distance from the source.

Background shade model derived from 8 m New Zealand Digital Elevation Model (LINZ Data Service 2012). PROJECTION: New Zealand Transverse Mercator 2000.

DRW: BL

CHK: CM, SDV

GNS SCIENCE TE PŪ AO

Confidential 2021

LOCAL PERSONAL RISK from earthquake- and rainfall-induced landslides Mean scenario

Regional Landslide Risk Analysis Kaikōura

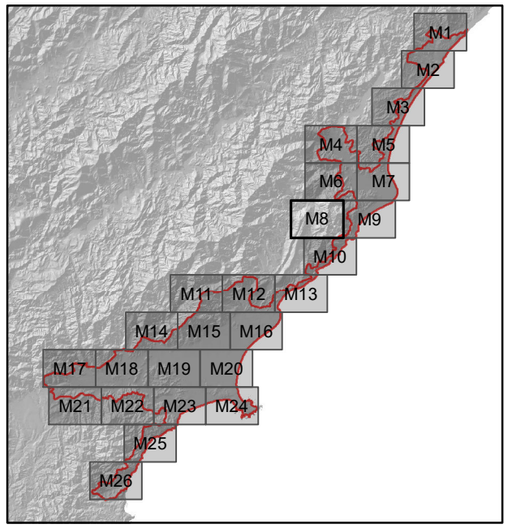
Appendix 3

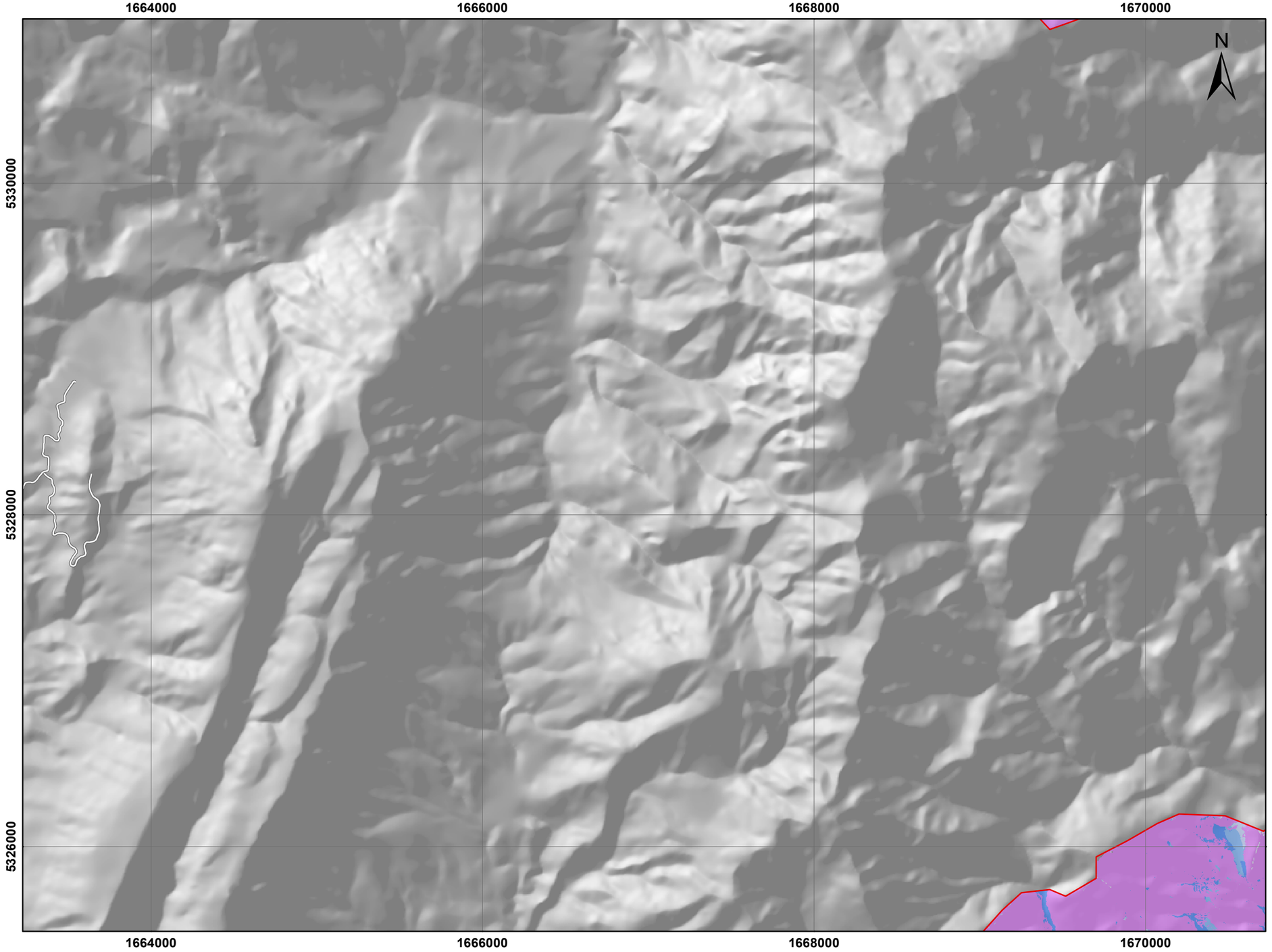
Map 7

FINAL

REPORT: CR2021/89

DATE: Oct 2021





Local personal risk

- 10^{-2} - 10^{-1}
- 10^{-3} - 10^{-2}
- 10^{-4} - 10^{-3}
- 10^{-5} - 10^{-4}
- 10^{-6} - 10^{-5}
- 10^{-7} - 10^{-6}
- Less than 10^{-7}

Roads

Railway

Study area

SCALE BAR: 0 0.5 1 km

EXPLANATION:

The model is based on mean landslide probability estimates and historical 24-hour rainfall annual frequencies. It uses a variable value for the vulnerability of a person if hit by a landslide, based on the landslide size and the person's distance from the source.

Background shade model derived from 8 m New Zealand Digital Elevation Model (LINZ Data Service 2012). PROJECTION: New Zealand Transverse Mercator 2000.

DRW: BL

CHK: CM, SDV

GNS SCIENCE TE PŪ AO

Confidential 2021

LOCAL PERSONAL RISK from earthquake- and rainfall-induced landslides Mean scenario

Regional Landslide Risk Analysis Kaikōura

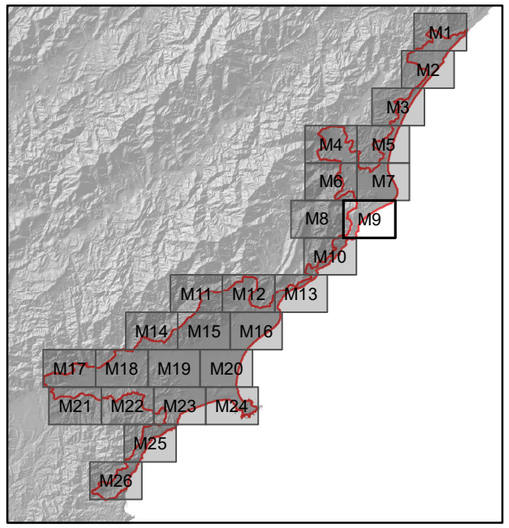
Appendix 3

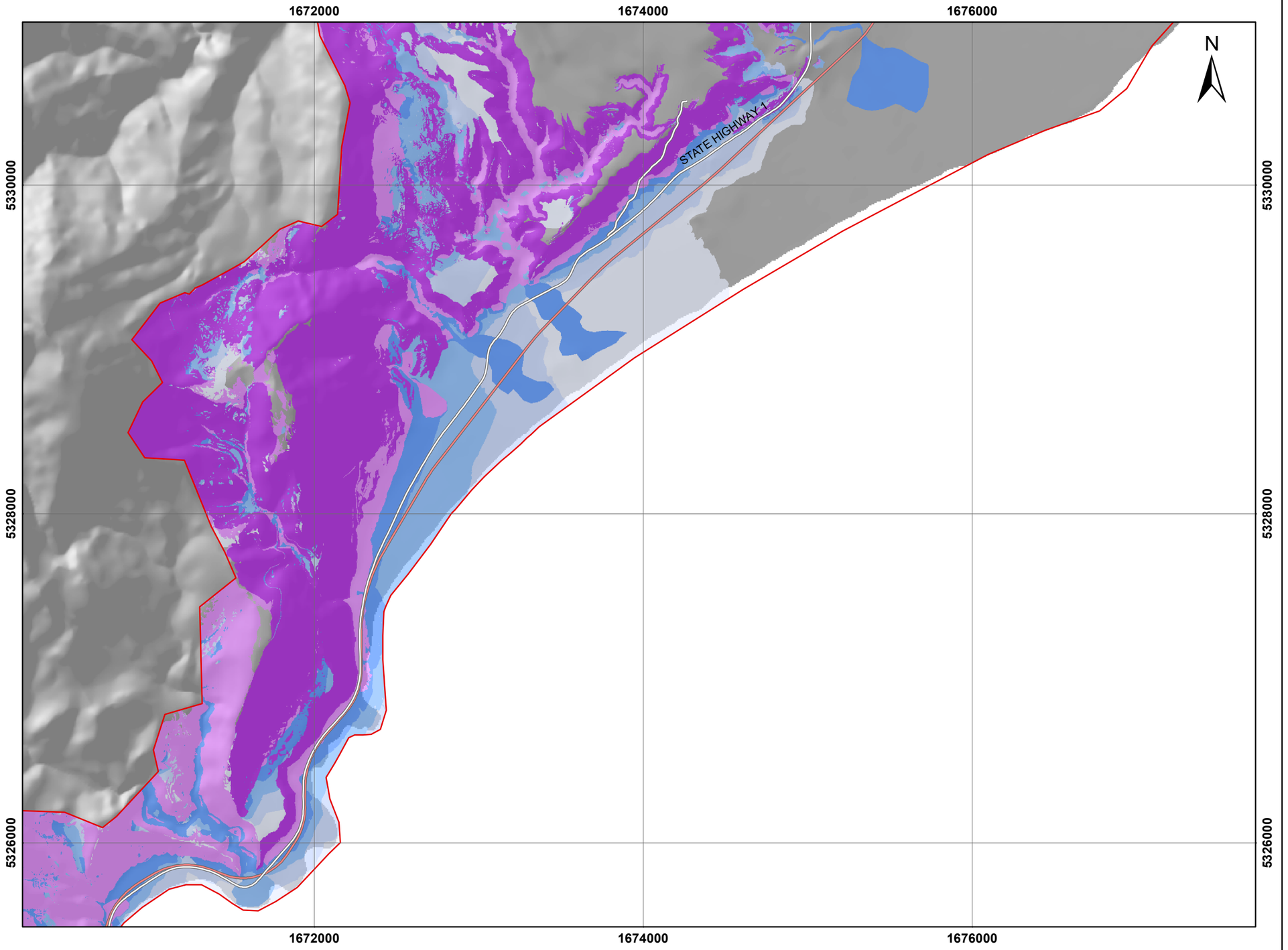
Map 8

FINAL

REPORT: CR2021/89

DATE: Oct 2021





Local personal risk

- 10^{-2} - 10^{-1}
- 10^{-3} - 10^{-2}
- 10^{-4} - 10^{-3}
- 10^{-5} - 10^{-4}
- 10^{-6} - 10^{-5}
- 10^{-7} - 10^{-6}
- Less than 10^{-7}

- Roads
- Railway
- Study area

SCALE BAR: 0 0.5 1 km

EXPLANATION:

The model is based on mean landslide probability estimates and historical 24-hour rainfall annual frequencies. It uses a variable value for the vulnerability of a person if hit by a landslide, based on the landslide size and the person's distance from the source.

Background shade model derived from 8 m New Zealand Digital Elevation Model (LINZ Data Service 2012). PROJECTION: New Zealand Transverse Mercator 2000.

DRW: BL

CHK: CM, SDV

GNS SCIENCE TE PŪ AO

Confidential 2021

LOCAL PERSONAL RISK from earthquake- and rainfall-induced landslides Mean scenario

Regional Landslide Risk Analysis Kaikōura

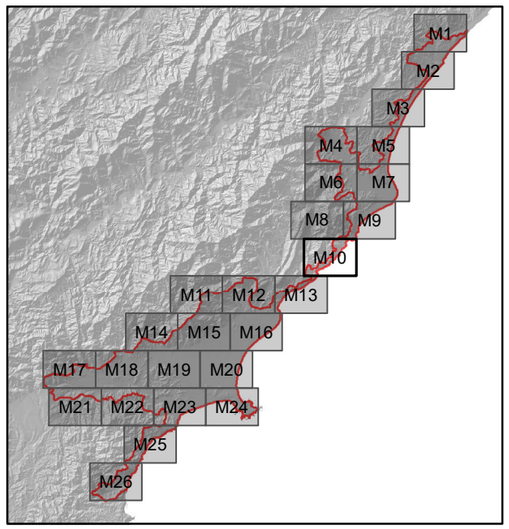
Appendix 3

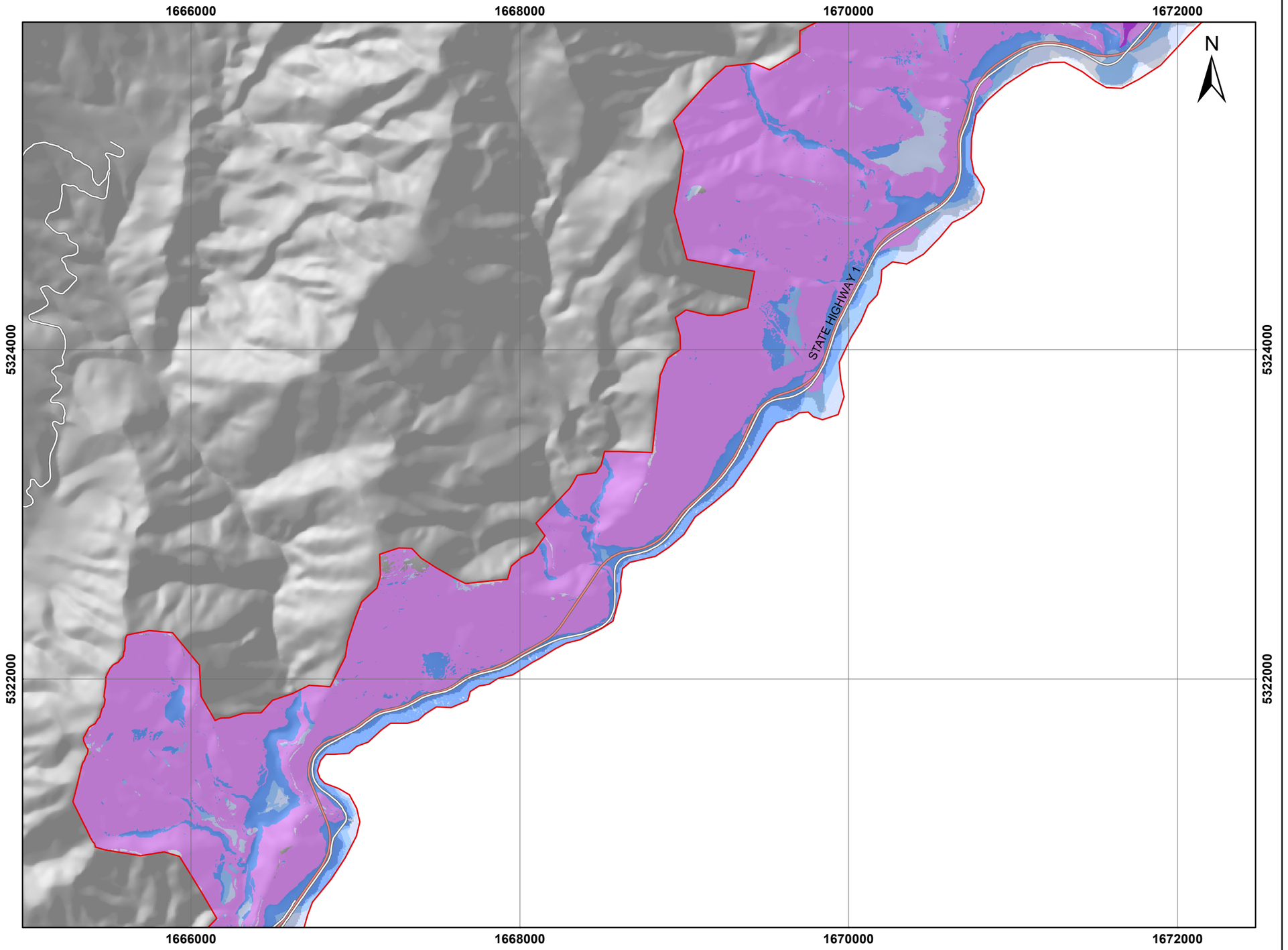
Map 9

FINAL

REPORT: CR2021/89

DATE: Oct 2021





Local personal risk

- 10^{-2} - 10^{-1}
- 10^{-3} - 10^{-2}
- 10^{-4} - 10^{-3}
- 10^{-5} - 10^{-4}
- 10^{-6} - 10^{-5}
- 10^{-7} - 10^{-6}
- Less than 10^{-7}

- Roads
- Railway
- Study area

SCALE BAR: 0 0.5 1 km

EXPLANATION:

The model is based on mean landslide probability estimates and historical 24-hour rainfall annual frequencies. It uses a variable value for the vulnerability of a person if hit by a landslide, based on the landslide size and the person's distance from the source.

Background shade model derived from 8 m New Zealand Digital Elevation Model (LINZ Data Service 2012). PROJECTION: New Zealand Transverse Mercator 2000.

DRW: BL

CHK: CM, SDV

GNS SCIENCE TE PŪ AO

Confidential 2021

LOCAL PERSONAL RISK from earthquake- and rainfall-induced landslides Mean scenario

Regional Landslide Risk Analysis Kaikōura

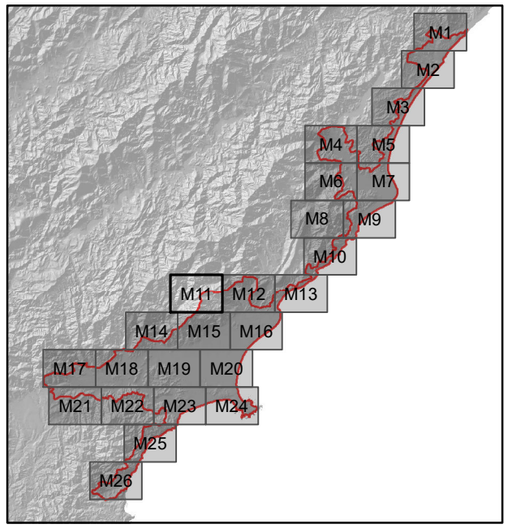
Appendix 3

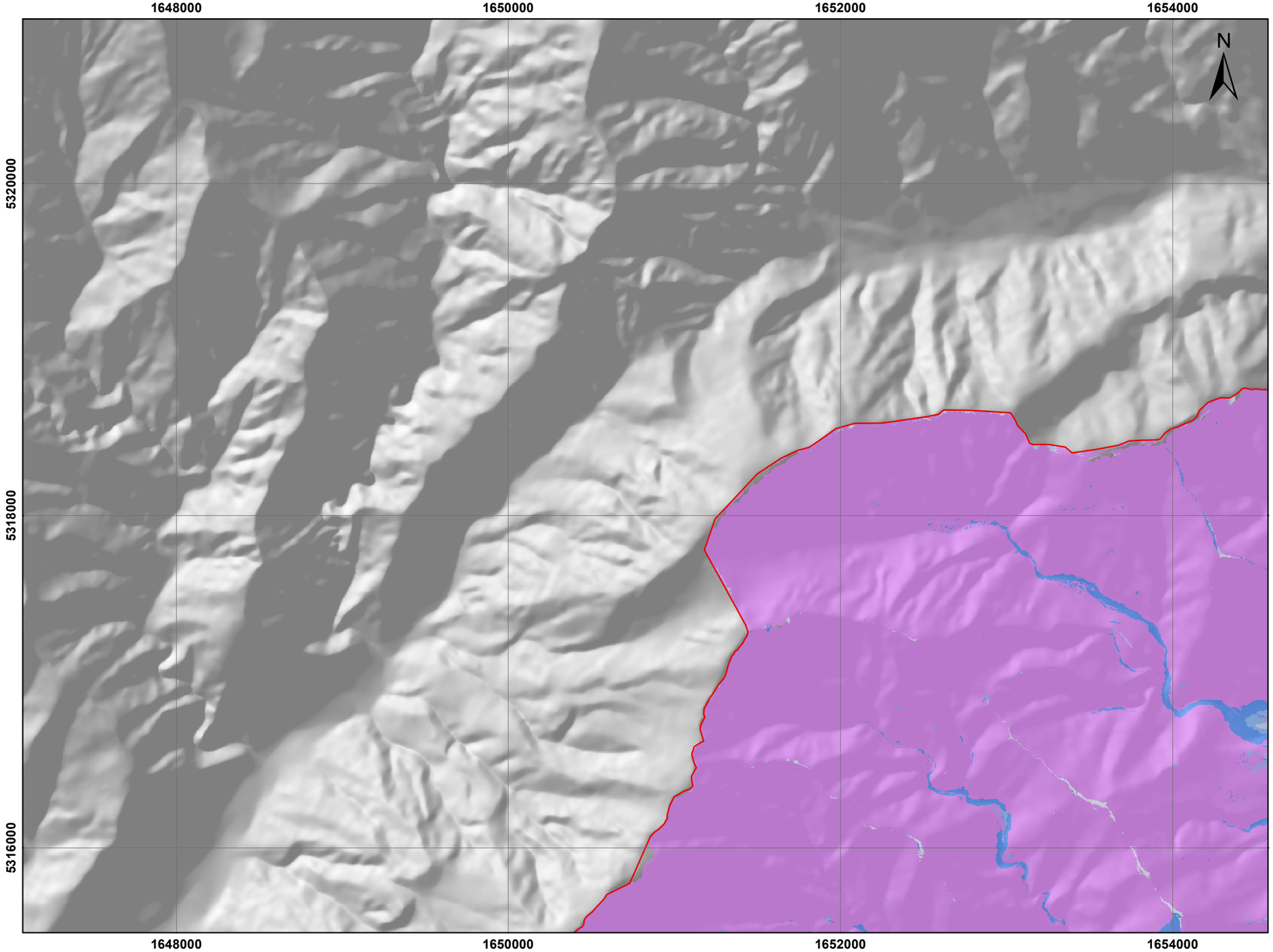
Map 10

FINAL

REPORT: CR2021/89

DATE: Oct 2021





Local personal risk

- 10^{-2} - 10^{-1}
- 10^{-3} - 10^{-2}
- 10^{-4} - 10^{-3}
- 10^{-5} - 10^{-4}
- 10^{-6} - 10^{-5}
- 10^{-7} - 10^{-6}
- Less than 10^{-7}

- Roads
- Railway
- Study area

SCALE BAR: 0 0.5 1 km

EXPLANATION:

The model is based on mean landslide probability estimates and historical 24-hour rainfall annual frequencies. It uses a variable value for the vulnerability of a person if hit by a landslide, based on the landslide size and the person's distance from the source.

Background shade model derived from 8 m New Zealand Digital Elevation Model (LINZ Data Service 2012). PROJECTION: New Zealand Transverse Mercator 2000.

DRW: BL

CHK: CM, SDV

GNS SCIENCE TE PŪ AO

Confidential 2021

LOCAL PERSONAL RISK from earthquake- and rainfall-induced landslides Mean scenario

Regional Landslide Risk Analysis Kaikōura

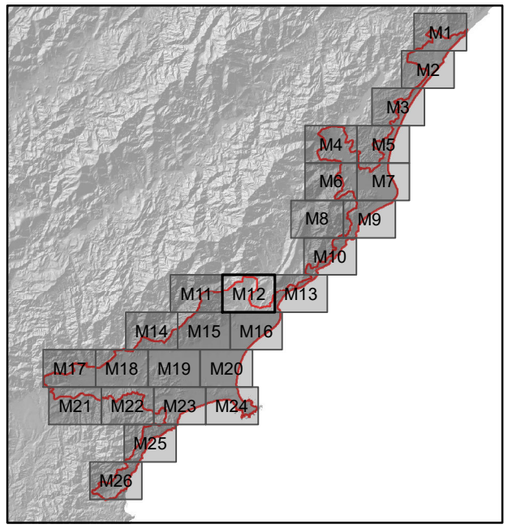
Appendix 3

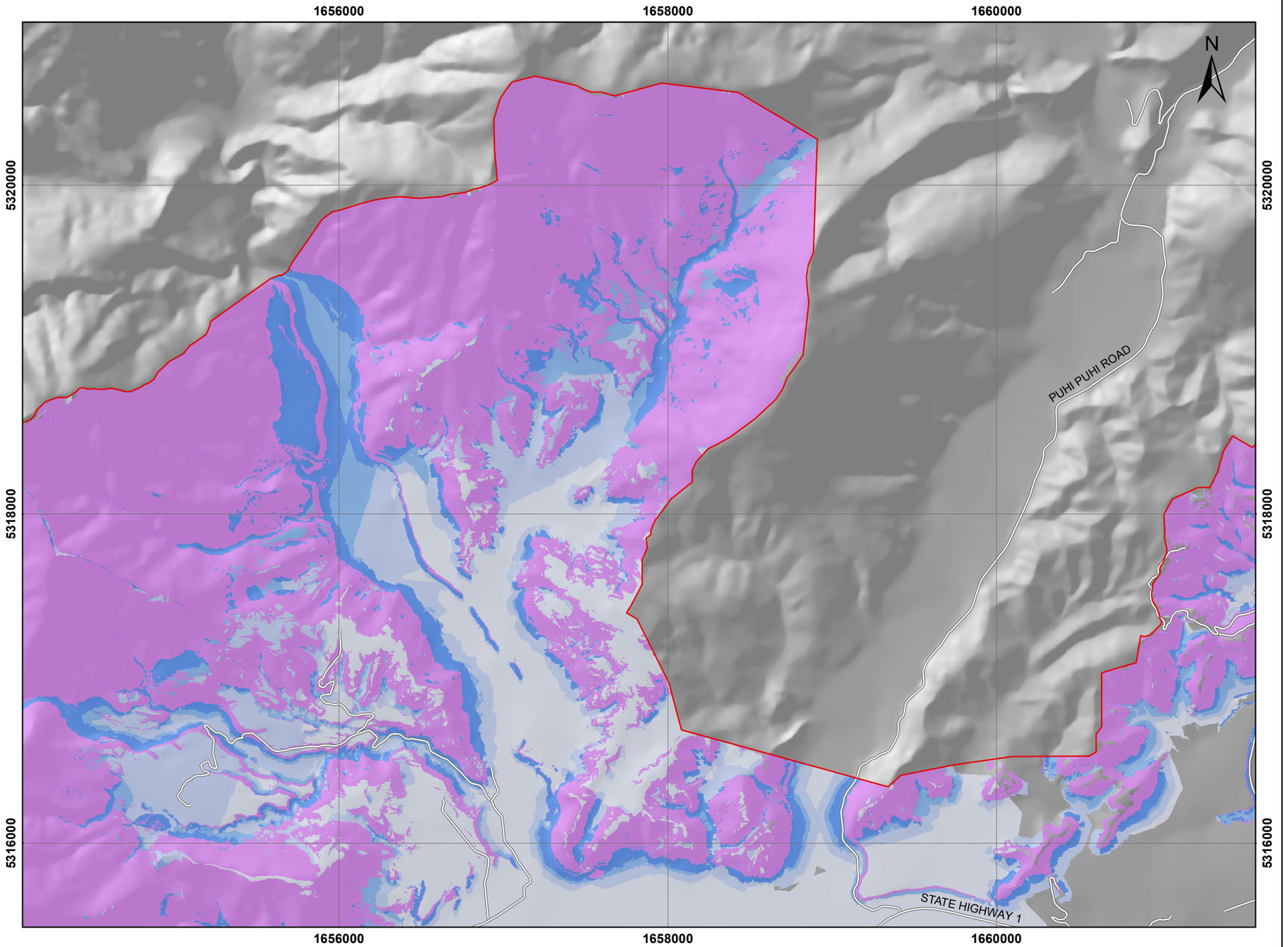
Map 11

FINAL

REPORT: CR2021/89

DATE: Oct 2021





Local personal risk

- 10^{-2} - 10^{-1}
- 10^{-3} - 10^{-2}
- 10^{-4} - 10^{-3}
- 10^{-5} - 10^{-4}
- 10^{-6} - 10^{-5}
- 10^{-7} - 10^{-6}
- Less than 10^{-7}

Roads

Railway

Study area

SCALE BAR: 0 0.5 1 km

EXPLANATION:

The model is based on mean landslide probability estimates and historical 24-hour rainfall annual frequencies. It uses a variable value for the vulnerability of a person if hit by a landslide, based on the landslide size and the person's distance from the source.

Background shade model derived from 8 m New Zealand Digital Elevation Model (LINZ Data Service 2012). PROJECTION: New Zealand Transverse Mercator 2000.

DRW: BL

CHK: CM, SDV

GNS SCIENCE TE PŪ AO

Confidential 2021

LOCAL PERSONAL RISK from earthquake- and rainfall-induced landslides Mean scenario

Regional Landslide Risk Analysis Kaikōura

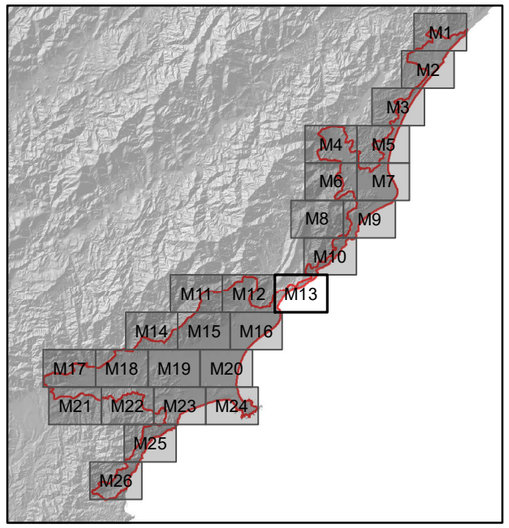
Appendix 3

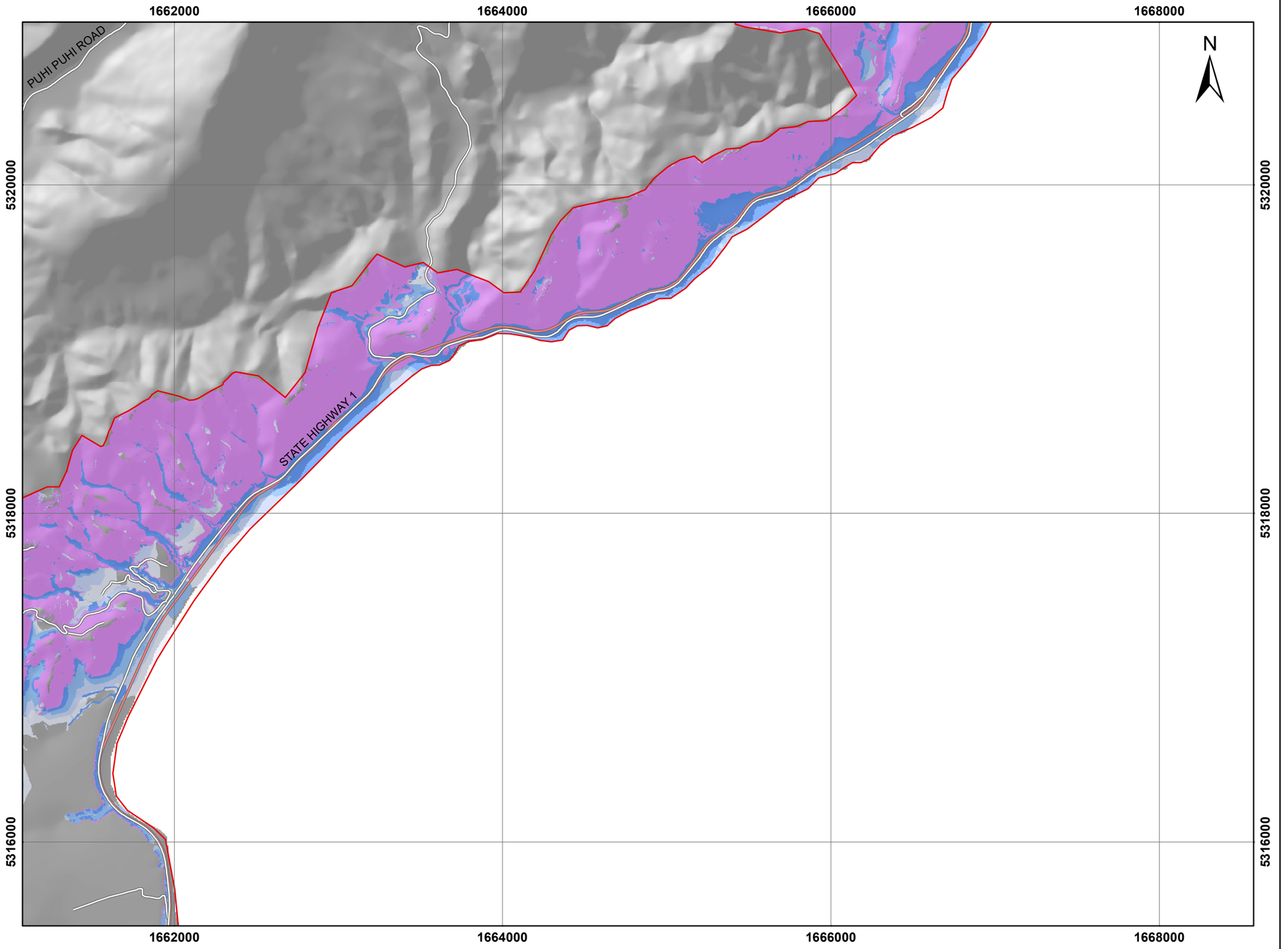
Map 12

FINAL

REPORT: CR2021/89

DATE: Oct 2021





Local personal risk

- 10^{-2} - 10^{-1}
- 10^{-3} - 10^{-2}
- 10^{-4} - 10^{-3}
- 10^{-5} - 10^{-4}
- 10^{-6} - 10^{-5}
- 10^{-7} - 10^{-6}
- Less than 10^{-7}

- Roads
- Railway
- Study area

SCALE BAR: 0 0.5 1 km

EXPLANATION:

The model is based on mean landslide probability estimates and historical 24-hour rainfall annual frequencies. It uses a variable value for the vulnerability of a person if hit by a landslide, based on the landslide size and the person's distance from the source.

Background shade model derived from 8 m New Zealand Digital Elevation Model (LINZ Data Service 2012). PROJECTION: New Zealand Transverse Mercator 2000.

DRW: BL

CHK: CM, SDV

GNS SCIENCE TE PŪ AO

Confidential 2021

LOCAL PERSONAL RISK
from earthquake- and rainfall-induced landslides
Mean scenario

Regional Landslide Risk Analysis
Kaikōura

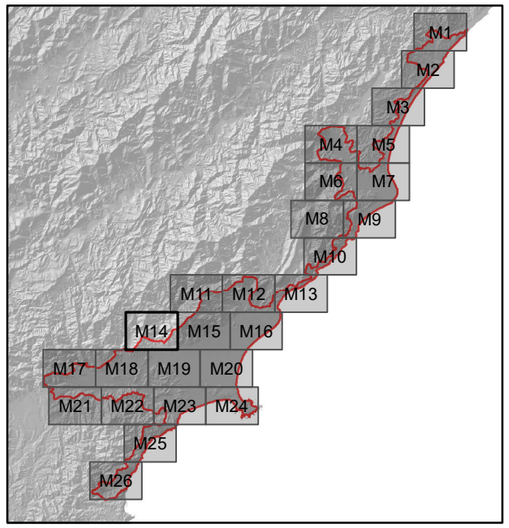
Appendix 3

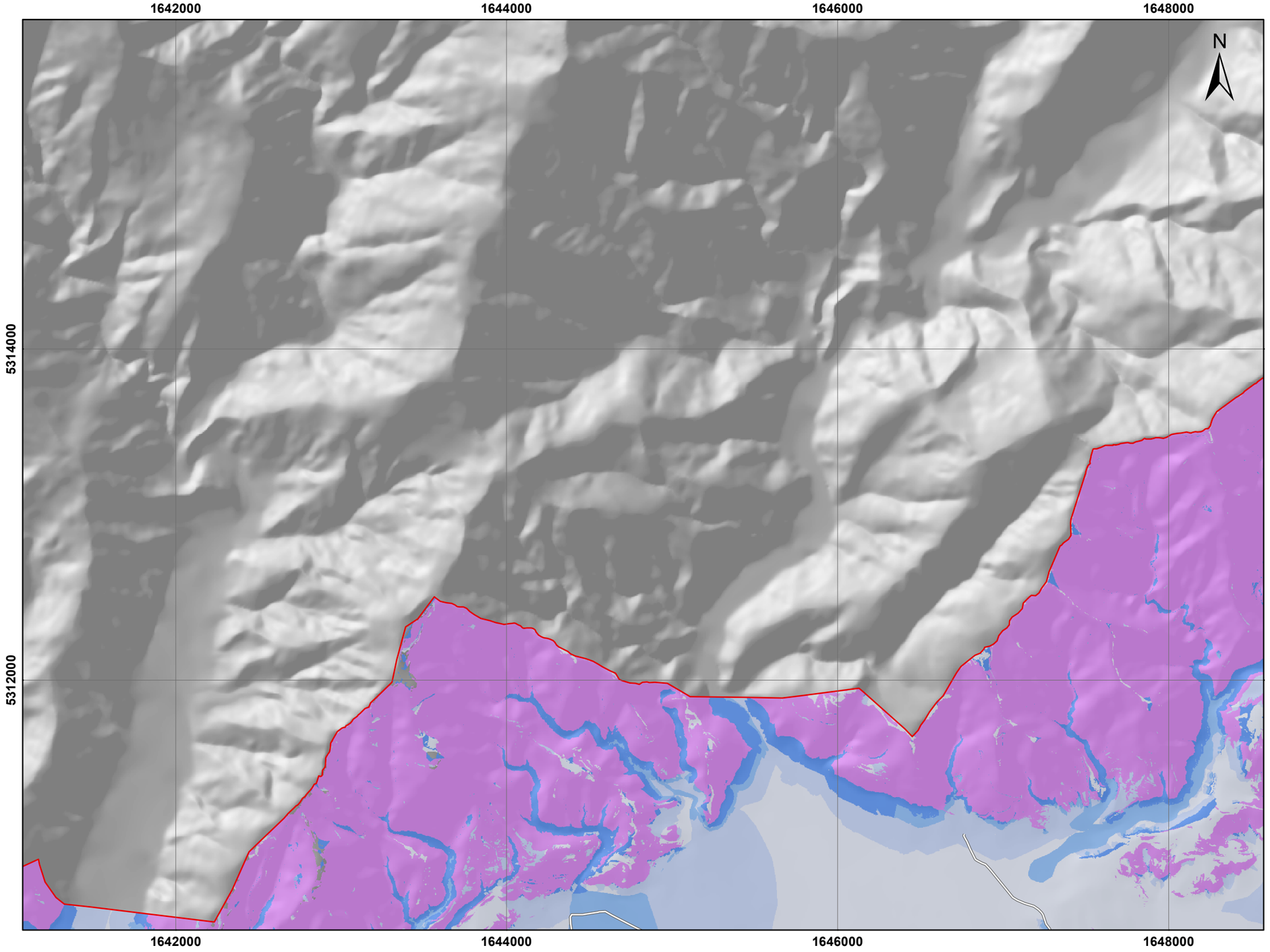
Map 13

FINAL

REPORT: CR2021/89

DATE: Oct 2021





Local personal risk

- 10^{-2} - 10^{-1}
- 10^{-3} - 10^{-2}
- 10^{-4} - 10^{-3}
- 10^{-5} - 10^{-4}
- 10^{-6} - 10^{-5}
- 10^{-7} - 10^{-6}
- Less than 10^{-7}

- Roads
- Railway
- Study area

SCALE BAR: 0 0.5 1 km

EXPLANATION:

The model is based on mean landslide probability estimates and historical 24-hour rainfall annual frequencies. It uses a variable value for the vulnerability of a person if hit by a landslide, based on the landslide size and the person's distance from the source.

Background shade model derived from 8 m New Zealand Digital Elevation Model (LINZ Data Service 2012). PROJECTION: New Zealand Transverse Mercator 2000.

DRW: BL

CHK: CM, SDV

GNS SCIENCE TE PŪ AO

Confidential 2021

LOCAL PERSONAL RISK from earthquake- and rainfall-induced landslides Mean scenario

Regional Landslide Risk Analysis Kaikōura

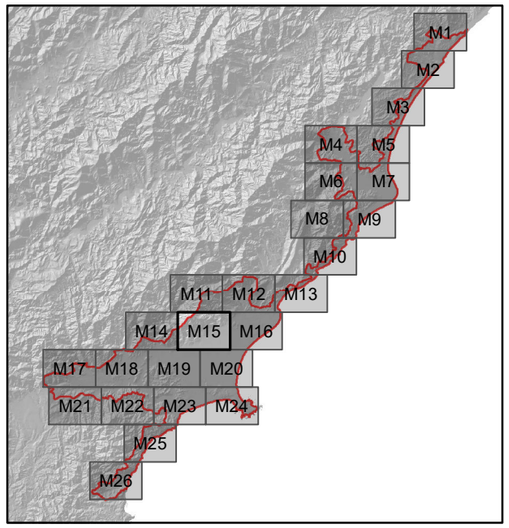
Appendix 3

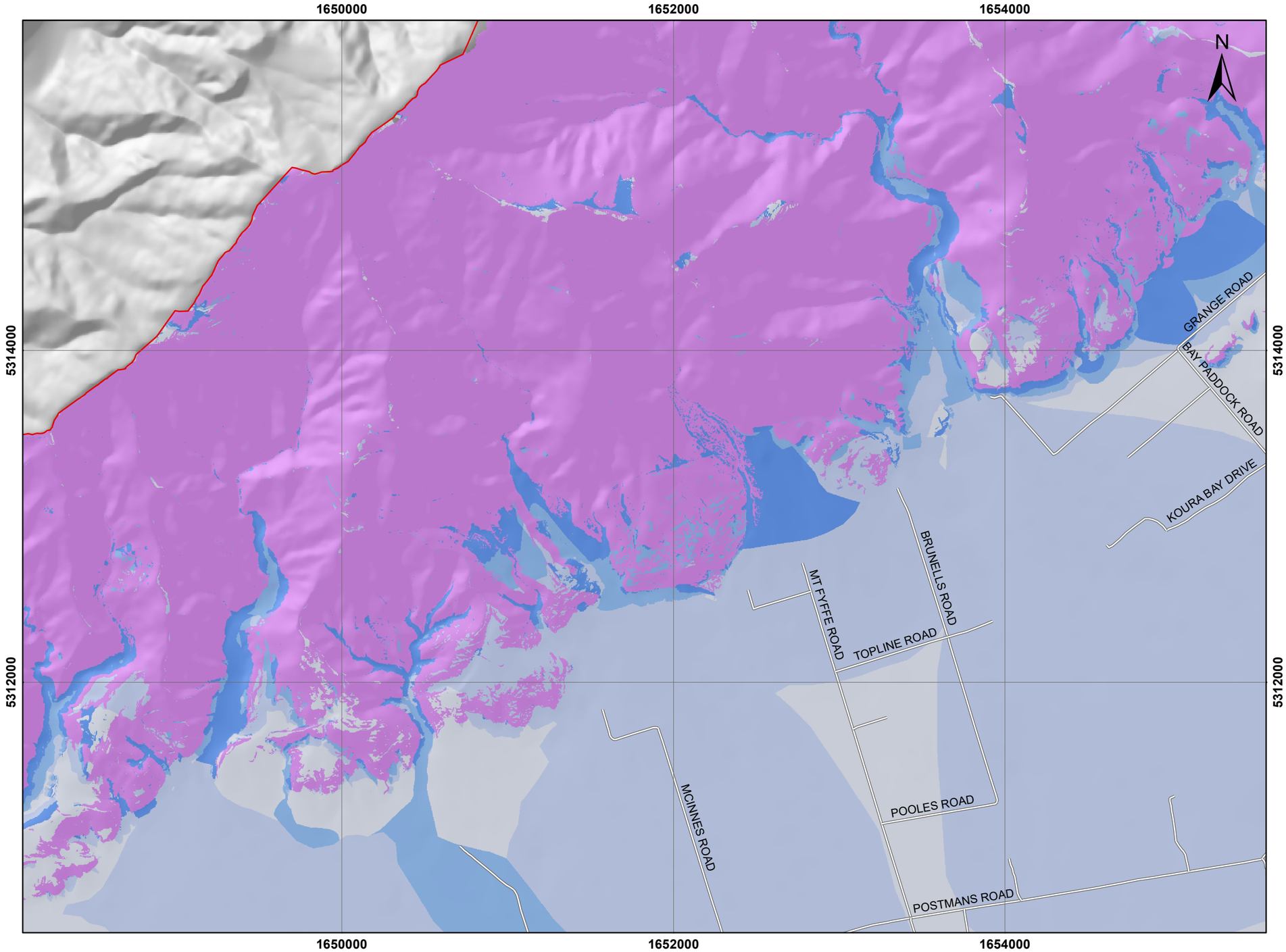
Map 14

FINAL

REPORT: CR2021/89

DATE: Oct 2021





Local personal risk

- 10^{-2} - 10^{-1}
- 10^{-3} - 10^{-2}
- 10^{-4} - 10^{-3}
- 10^{-5} - 10^{-4}
- 10^{-6} - 10^{-5}
- 10^{-7} - 10^{-6}
- Less than 10^{-7}

- Roads
- Railway
- Study area

SCALE BAR: 0 0.5 1 km

EXPLANATION:

The model is based on mean landslide probability estimates and historical 24-hour rainfall annual frequencies. It uses a variable value for the vulnerability of a person if hit by a landslide, based on the landslide size and the person's distance from the source.

Background shade model derived from 8 m New Zealand Digital Elevation Model (LINZ Data Service 2012). PROJECTION: New Zealand Transverse Mercator 2000.

DRW: BL

CHK: CM, SDV

GNS SCIENCE TE PŪ AO

Confidential 2021

LOCAL PERSONAL RISK from earthquake- and rainfall-induced landslides Mean scenario

Regional Landslide Risk Analysis Kaikōura

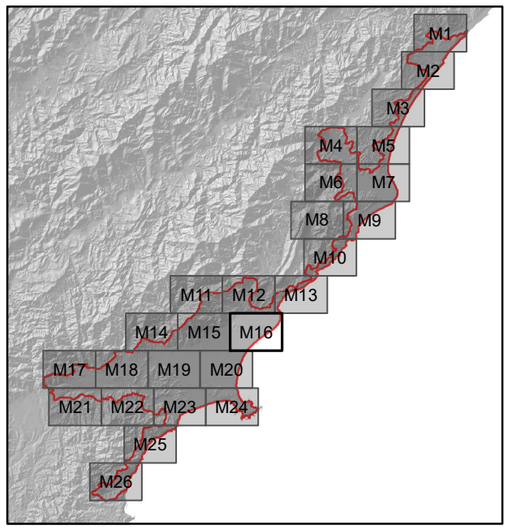
Appendix 3

Map 15

FINAL

REPORT: CR2021/89

DATE: Oct 2021



1656000 1658000 1660000 1662000

5314000

5312000

N

PARSONS ROAD
GRANGE ROAD
STATE HIGHWAY 1
STATION ROAD
KIWA ROAD
LOVERS LANE
KINCAID ROAD
FACTORY ROAD
BAY PADDOCK ROAD
OLD BEACH ROAD
WILDERNESS ROAD
HARNETTS ROAD

Local personal risk

- 10^{-2} - 10^{-1}
- 10^{-3} - 10^{-2}
- 10^{-4} - 10^{-3}
- 10^{-5} - 10^{-4}
- 10^{-6} - 10^{-5}
- 10^{-7} - 10^{-6}
- Less than 10^{-7}

Roads
Railway
Study area

SCALE BAR: 0 0.5 1 km

EXPLANATION:
The model is based on mean landslide probability estimates and historical 24-hour rainfall annual frequencies. It uses a variable value for the vulnerability of a person if hit by a landslide, based on the landslide size and the person's distance from the source.

Background shade model derived from 8 m New Zealand Digital Elevation Model (LINZ Data Service 2012). PROJECTION: New Zealand Transverse Mercator 2000.

DRW: BL
CHK: CM, SDV

GNS SCIENCE TE PŪ AO

Confidential 2021

LOCAL PERSONAL RISK
from earthquake- and rainfall-induced landslides
Mean scenario

Regional Landslide Risk Analysis
Kaikōura

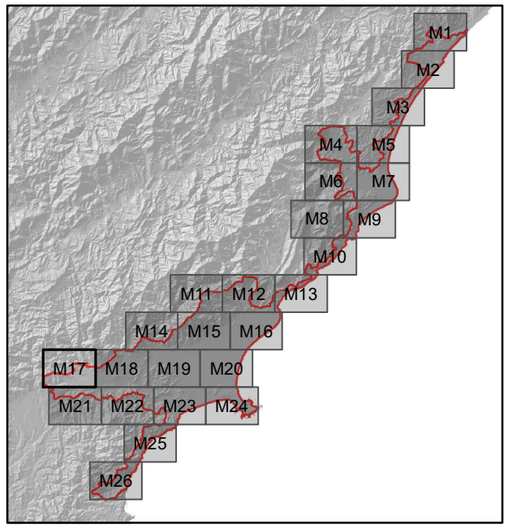
Appendix 3

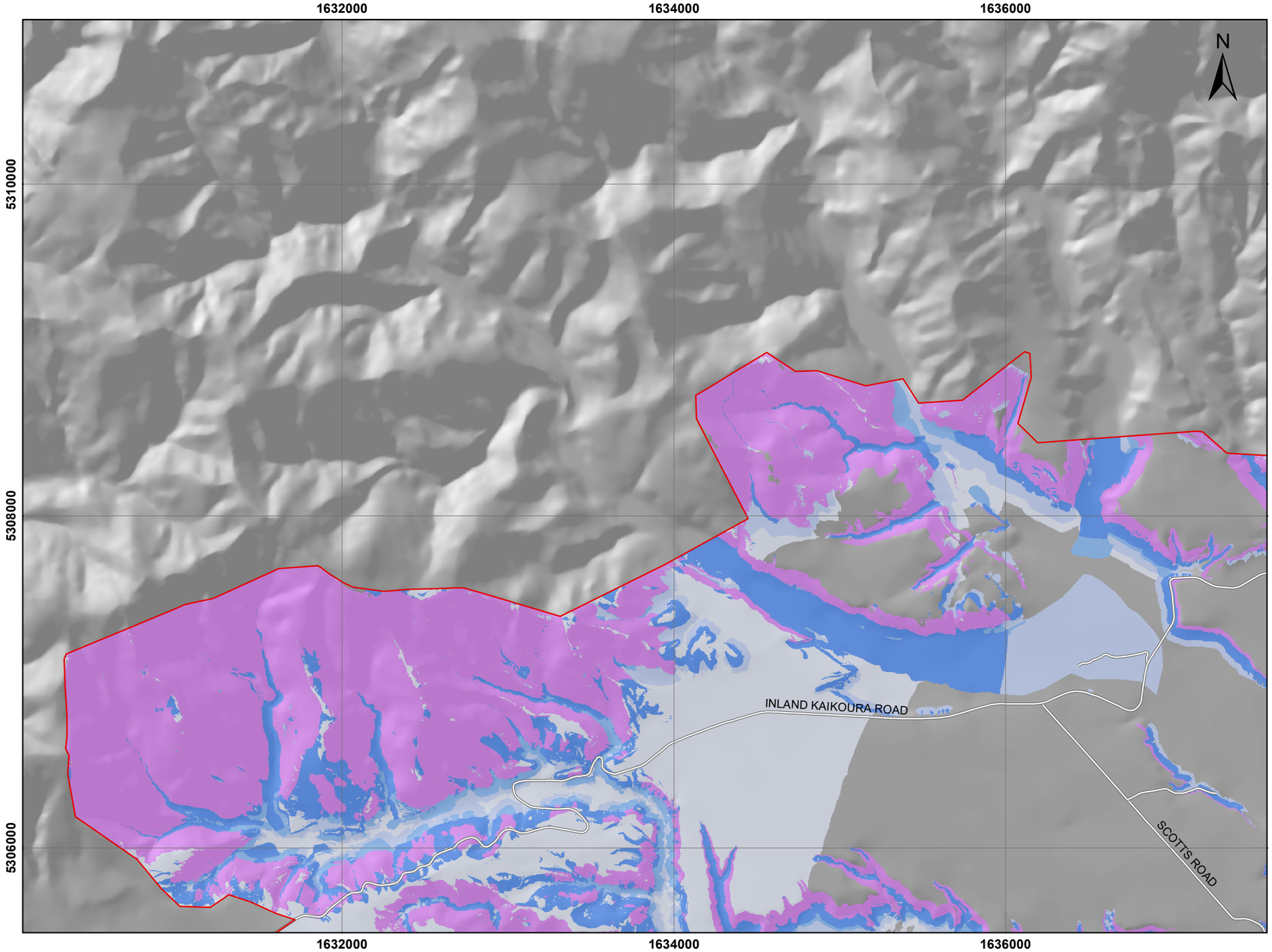
Map 16

FINAL

REPORT: CR2021/89

DATE: Oct 2021





Local personal risk

- 10^{-2} - 10^{-1}
- 10^{-3} - 10^{-2}
- 10^{-4} - 10^{-3}
- 10^{-5} - 10^{-4}
- 10^{-6} - 10^{-5}
- 10^{-7} - 10^{-6}
- Less than 10^{-7}

Roads

Railway

Study area

SCALE BAR: 0 0.5 1 km

EXPLANATION:

The model is based on mean landslide probability estimates and historical 24-hour rainfall annual frequencies. It uses a variable value for the vulnerability of a person if hit by a landslide, based on the landslide size and the person's distance from the source.

Background shade model derived from 8 m New Zealand Digital Elevation Model (LINZ Data Service 2012). PROJECTION: New Zealand Transverse Mercator 2000.

DRW: BL

CHK: CM, SDV

GNS SCIENCE TE PŪ AO

Confidential 2021

LOCAL PERSONAL RISK from earthquake- and rainfall-induced landslides Mean scenario

Regional Landslide Risk Analysis Kaikōura

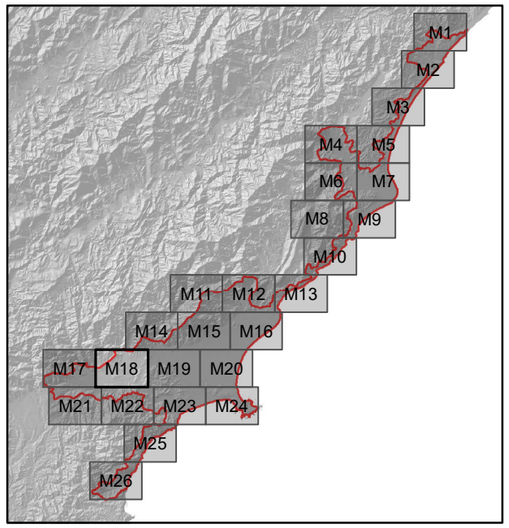
Appendix 3

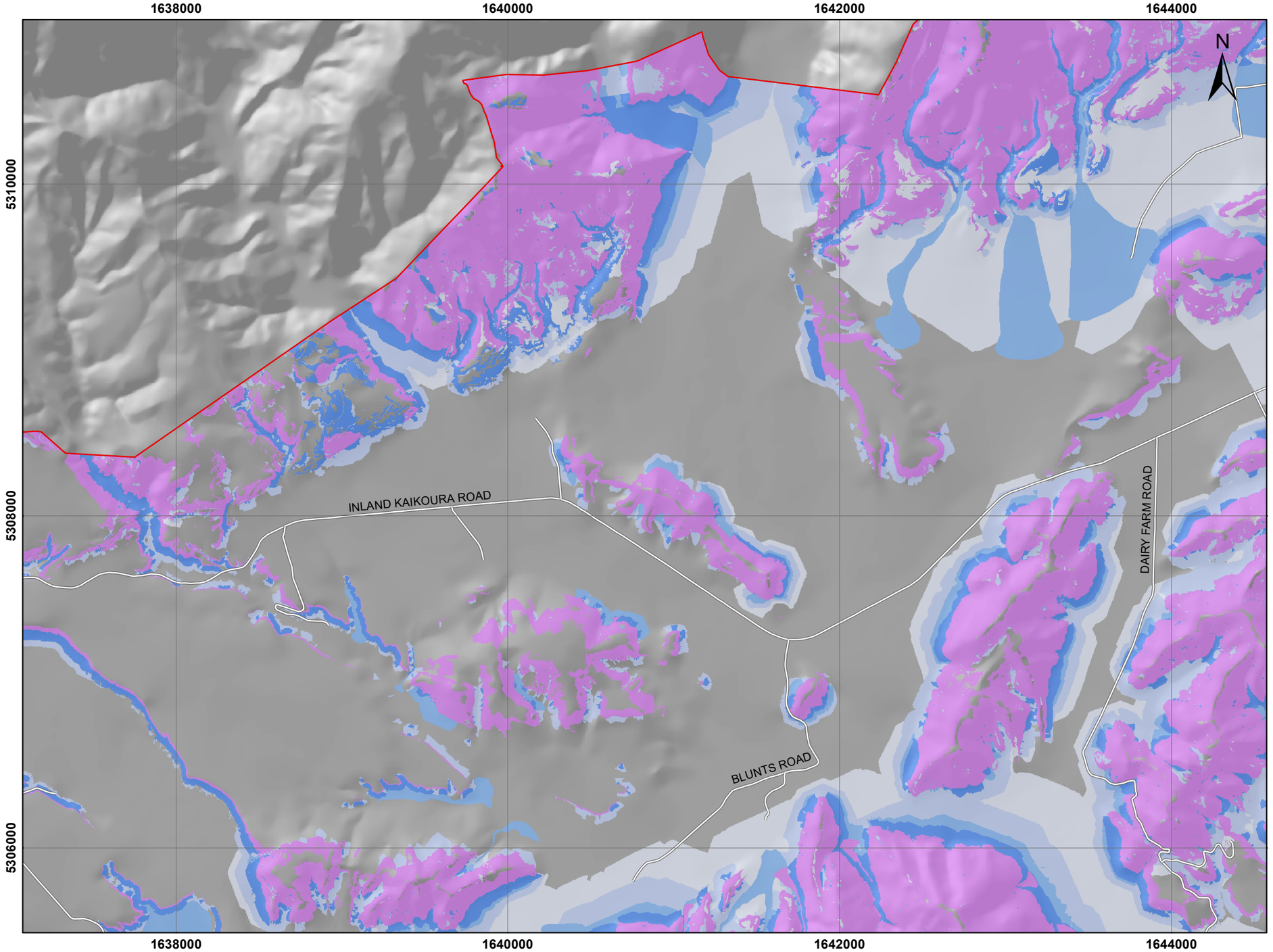
Map 17

FINAL

REPORT: CR2021/89

DATE: Oct 2021





Local personal risk

- 10^{-2} - 10^{-1}
- 10^{-3} - 10^{-2}
- 10^{-4} - 10^{-3}
- 10^{-5} - 10^{-4}
- 10^{-6} - 10^{-5}
- 10^{-7} - 10^{-6}
- Less than 10^{-7}

- Roads
- Railway
- Study area

SCALE BAR: 0 0.5 1 km

EXPLANATION:

The model is based on mean landslide probability estimates and historical 24-hour rainfall annual frequencies. It uses a variable value for the vulnerability of a person if hit by a landslide, based on the landslide size and the person's distance from the source.

Background shade model derived from 8 m New Zealand Digital Elevation Model (LINZ Data Service 2012). PROJECTION: New Zealand Transverse Mercator 2000.

DRW: BL

CHK: CM, SDV

GNS SCIENCE TE PŪ AO

Confidential 2021

LOCAL PERSONAL RISK
from earthquake- and rainfall-induced landslides
Mean scenario

Regional Landslide Risk Analysis
Kaikōura

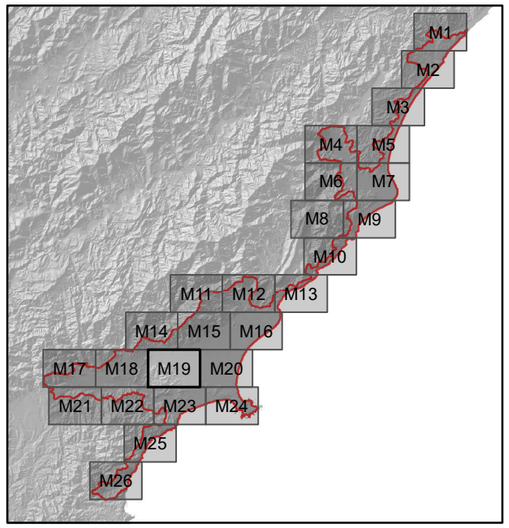
Appendix 3

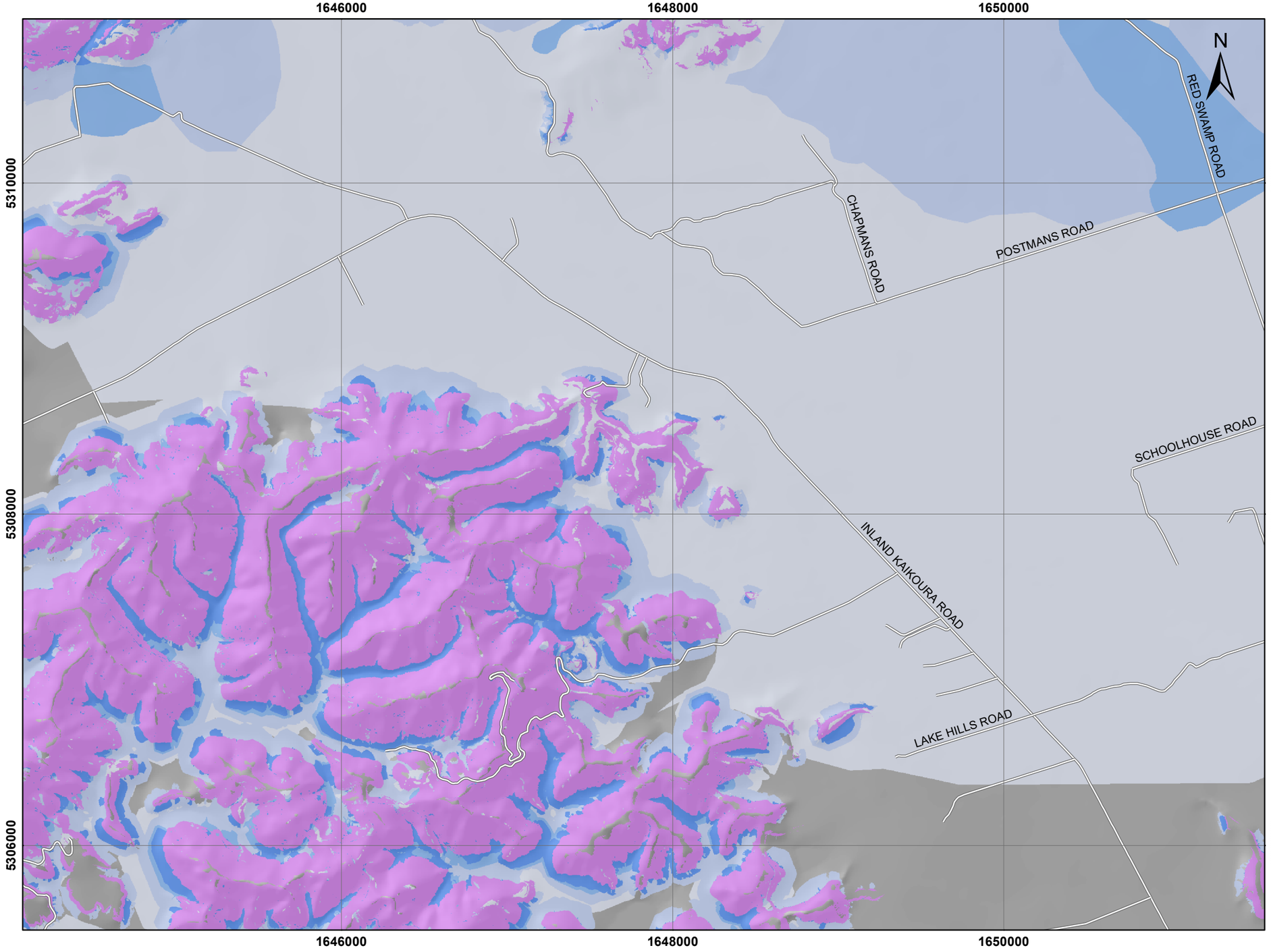
Map 18

FINAL

REPORT: CR2021/89

DATE: Oct 2021





Local personal risk

- 10^{-2} - 10^{-1}
- 10^{-3} - 10^{-2}
- 10^{-4} - 10^{-3}
- 10^{-5} - 10^{-4}
- 10^{-6} - 10^{-5}
- 10^{-7} - 10^{-6}
- Less than 10^{-7}

Roads

Railway

Study area

SCALE BAR: 0 0.5 1 km

EXPLANATION:

The model is based on mean landslide probability estimates and historical 24-hour rainfall annual frequencies. It uses a variable value for the vulnerability of a person if hit by a landslide, based on the landslide size and the person's distance from the source.

Background shade model derived from 8 m New Zealand Digital Elevation Model (LINZ Data Service 2012). PROJECTION: New Zealand Transverse Mercator 2000.

DRW: BL

CHK: CM, SDV

GNS SCIENCE TE PŪ AO

Confidential 2021

LOCAL PERSONAL RISK from earthquake- and rainfall-induced landslides Mean scenario

Regional Landslide Risk Analysis Kaikōura

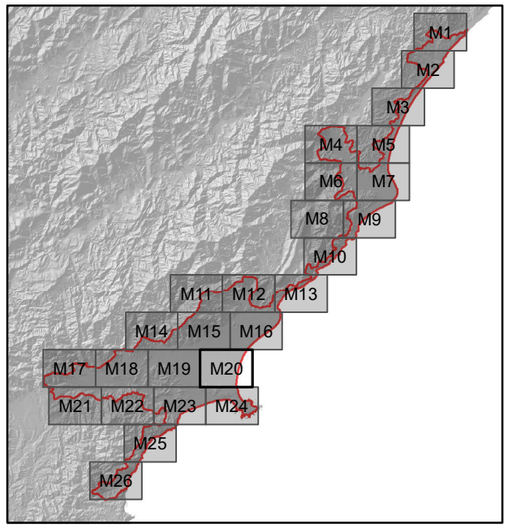
Appendix 3

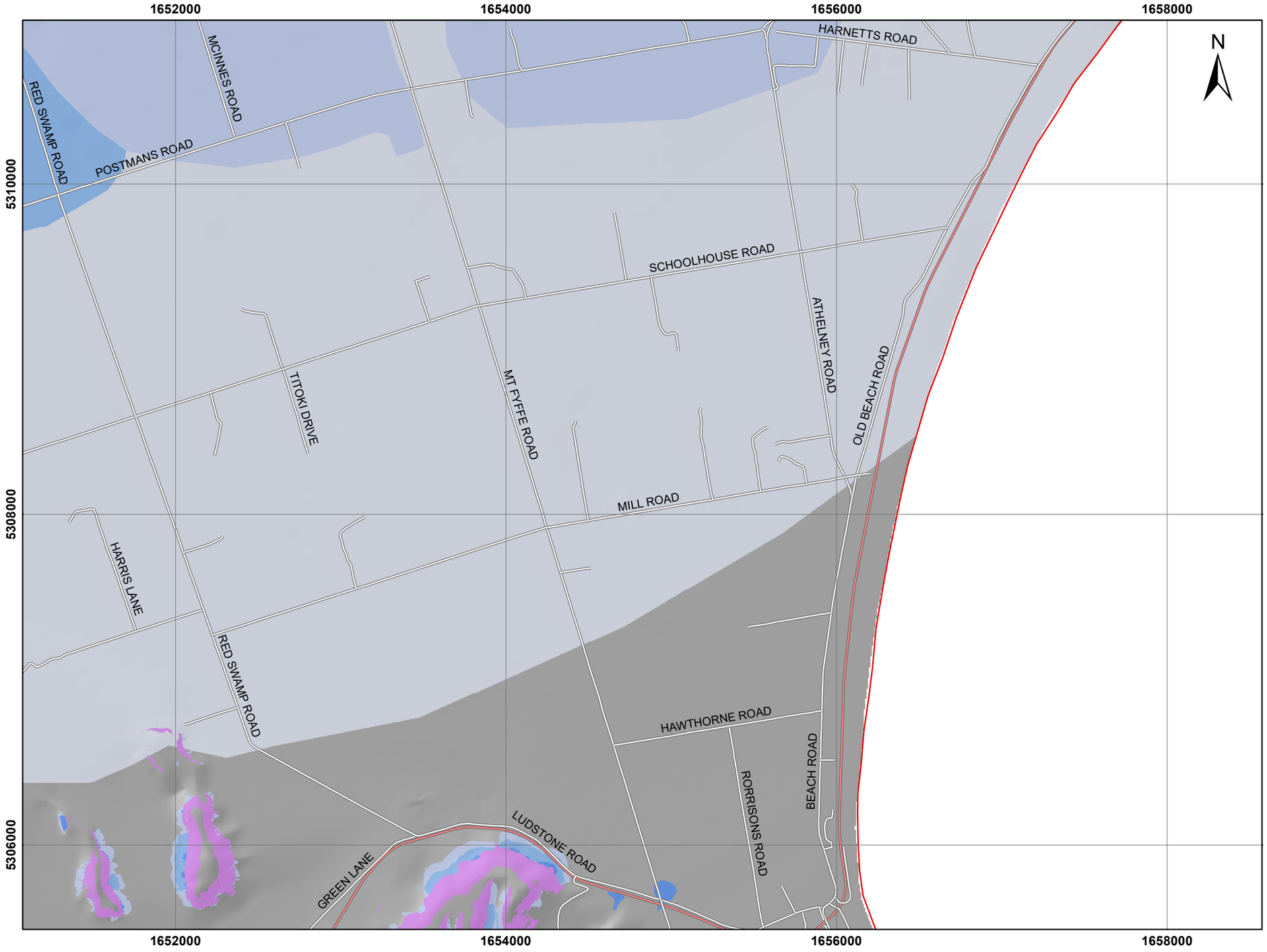
Map 19

FINAL

REPORT: CR2021/89

DATE: Oct 2021





Local personal risk

- 10^{-2} - 10^{-1}
- 10^{-3} - 10^{-2}
- 10^{-4} - 10^{-3}
- 10^{-5} - 10^{-4}
- 10^{-6} - 10^{-5}
- 10^{-7} - 10^{-6}
- Less than 10^{-7}

- Roads
- Railway
- Study area

SCALE BAR: 0 0.5 1 km

EXPLANATION:

The model is based on mean landslide probability estimates and historical 24-hour rainfall annual frequencies. It uses a variable value for the vulnerability of a person if hit by a landslide, based on the landslide size and the person's distance from the source.

Background shade model derived from 8 m New Zealand Digital Elevation Model (LINZ Data Service 2012). PROJECTION: New Zealand Transverse Mercator 2000.

DRW: BL

CHK: CM, SDV

Confidential 2021

LOCAL PERSONAL RISK
from earthquake- and rainfall-induced landslides
Mean scenario

Regional Landslide Risk Analysis
Kaikōura

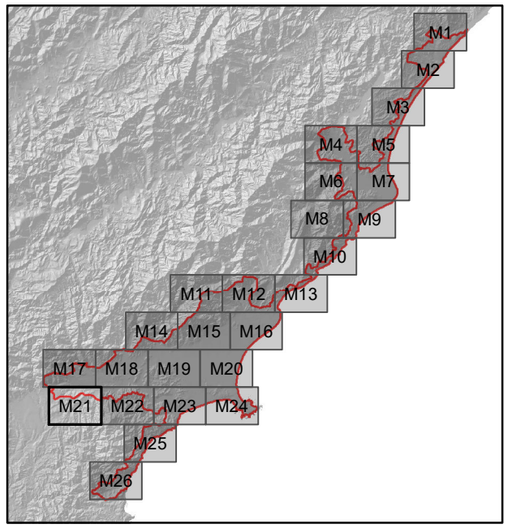
Appendix 3

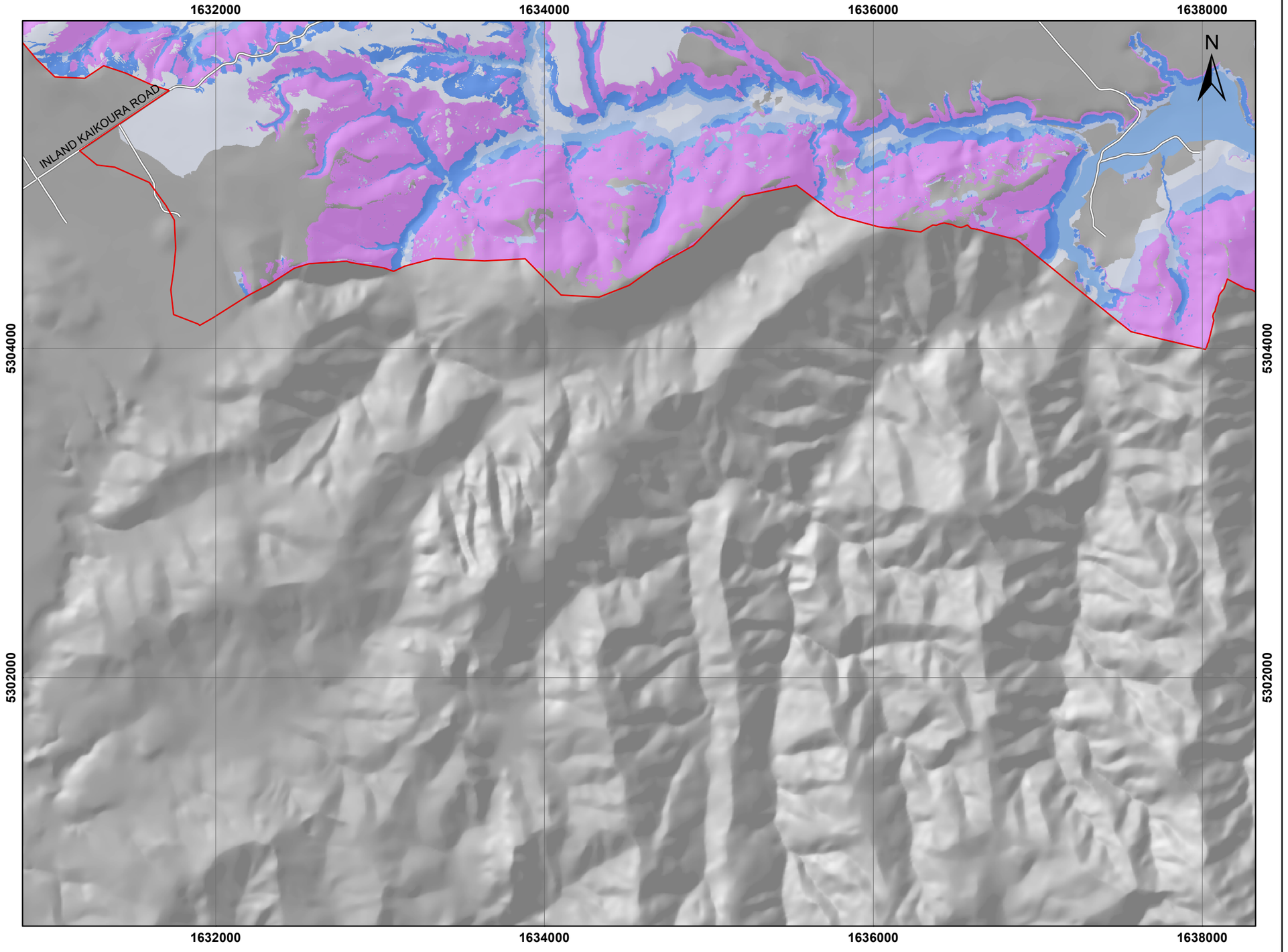
Map 20

FINAL

REPORT: CR2021/89

DATE: Oct 2021





Local personal risk

- 10^{-2} - 10^{-1}
- 10^{-3} - 10^{-2}
- 10^{-4} - 10^{-3}
- 10^{-5} - 10^{-4}
- 10^{-6} - 10^{-5}
- 10^{-7} - 10^{-6}
- Less than 10^{-7}

- Roads
- Railway
- Study area

SCALE BAR: 0 0.5 1 km

EXPLANATION:

The model is based on mean landslide probability estimates and historical 24-hour rainfall annual frequencies. It uses a variable value for the vulnerability of a person if hit by a landslide, based on the landslide size and the person's distance from the source.

Background shade model derived from 8 m New Zealand Digital Elevation Model (LINZ Data Service 2012). PROJECTION: New Zealand Transverse Mercator 2000.

DRW: BL

CHK: CM, SDV

GNS SCIENCE TE PŪ AO

Confidential 2021

LOCAL PERSONAL RISK
from earthquake- and rainfall-induced landslides
Mean scenario

Regional Landslide Risk Analysis
Kaikōura

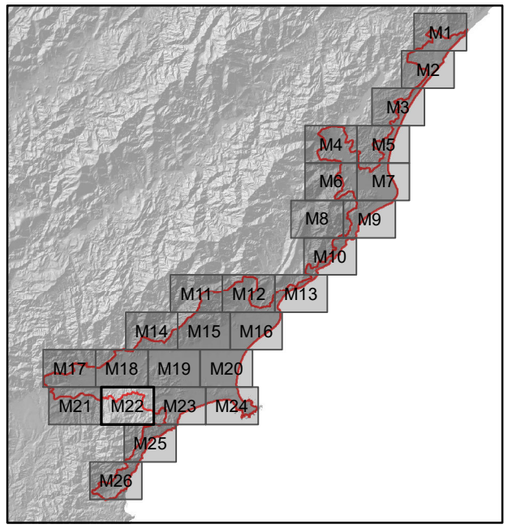
Appendix 3

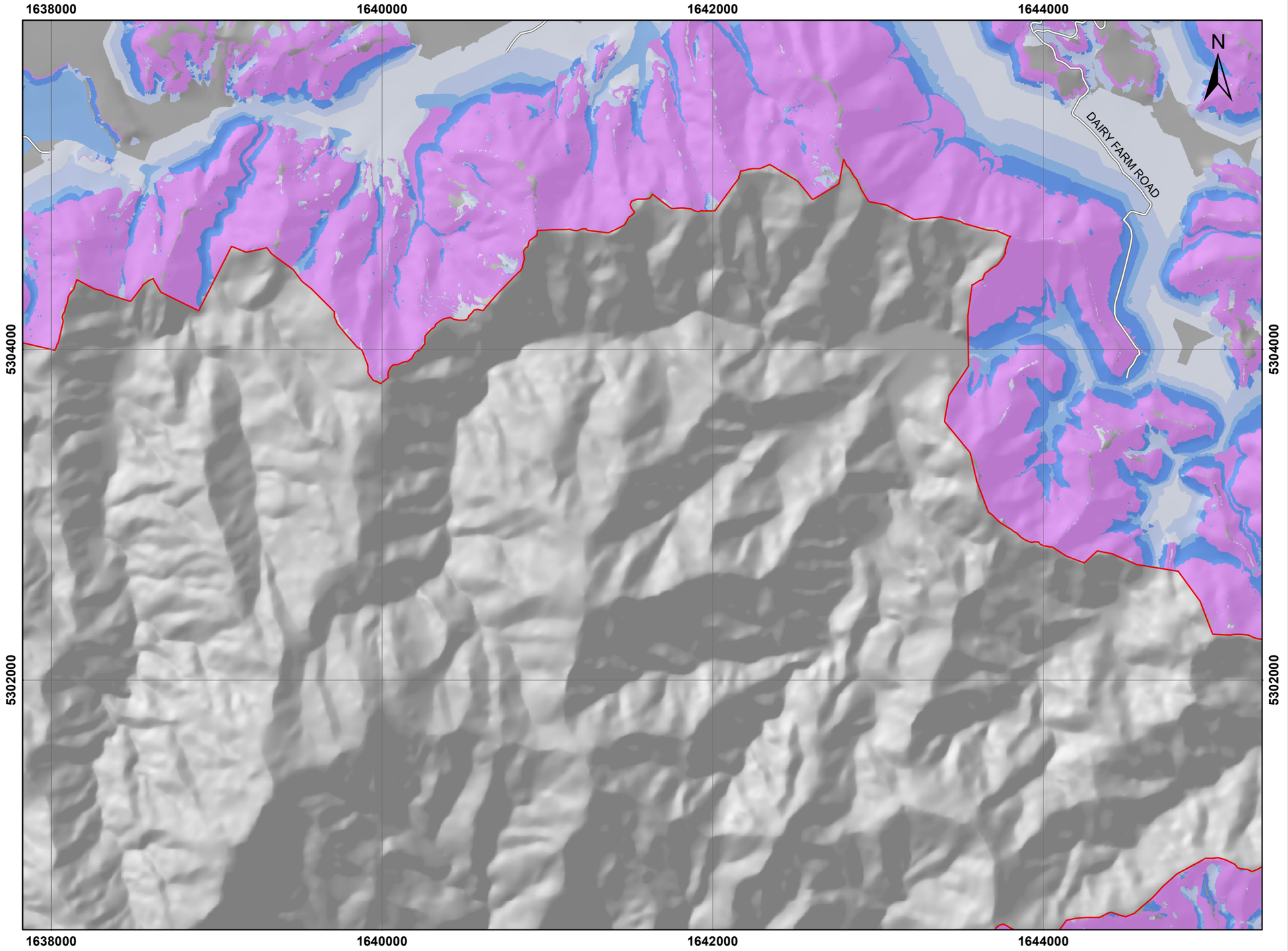
Map 21

FINAL

REPORT: CR2021/89

DATE: Oct 2021





Local personal risk

- 10^{-2} - 10^{-1}
- 10^{-3} - 10^{-2}
- 10^{-4} - 10^{-3}
- 10^{-5} - 10^{-4}
- 10^{-6} - 10^{-5}
- 10^{-7} - 10^{-6}
- Less than 10^{-7}

Roads

Railway

Study area

SCALE BAR: 0 0.5 1 km

EXPLANATION:

The model is based on mean landslide probability estimates and historical 24-hour rainfall annual frequencies. It uses a variable value for the vulnerability of a person if hit by a landslide, based on the landslide size and the person's distance from the source.

Background shade model derived from 8 m New Zealand Digital Elevation Model (LINZ Data Service 2012). PROJECTION: New Zealand Transverse Mercator 2000.

DRW: BL

CHK: CM, SDV

GNS SCIENCE TE PŪ AO

Confidential 2021

LOCAL PERSONAL RISK
from earthquake- and rainfall-induced landslides
Mean scenario

Regional Landslide Risk Analysis
Kaikōura

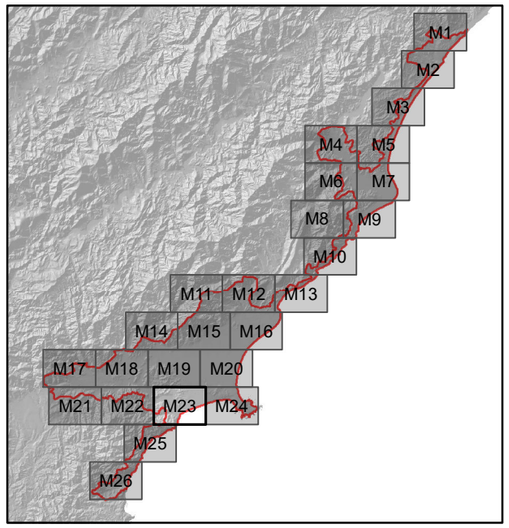
Appendix 3

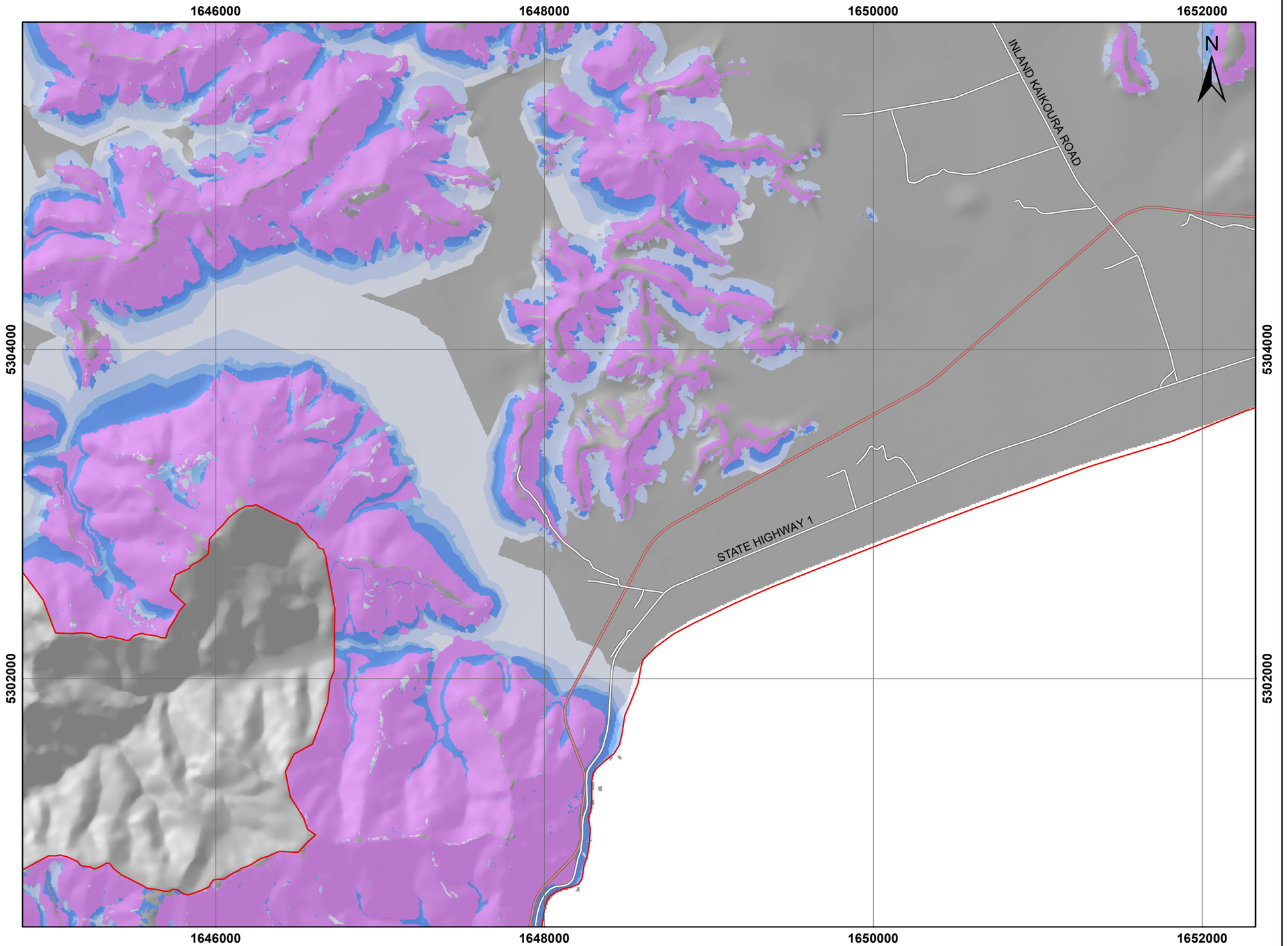
Map 22

FINAL

REPORT: CR2021/89

DATE: Oct 2021





Local personal risk

- 10^{-2} - 10^{-1}
- 10^{-3} - 10^{-2}
- 10^{-4} - 10^{-3}
- 10^{-5} - 10^{-4}
- 10^{-6} - 10^{-5}
- 10^{-7} - 10^{-6}
- Less than 10^{-7}

- Roads
- Railway
- Study area

SCALE BAR: 0 0.5 1 km

EXPLANATION:

The model is based on mean landslide probability estimates and historical 24-hour rainfall annual frequencies. It uses a variable value for the vulnerability of a person if hit by a landslide, based on the landslide size and the person's distance from the source.

Background shade model derived from 8 m New Zealand Digital Elevation Model (LINZ Data Service 2012). PROJECTION: New Zealand Transverse Mercator 2000.

DRW: BL

CHK: CM, SDV

GNS SCIENCE TE PŪ AO

Confidential 2021

LOCAL PERSONAL RISK from earthquake- and rainfall-induced landslides Mean scenario

Regional Landslide Risk Analysis Kaikōura

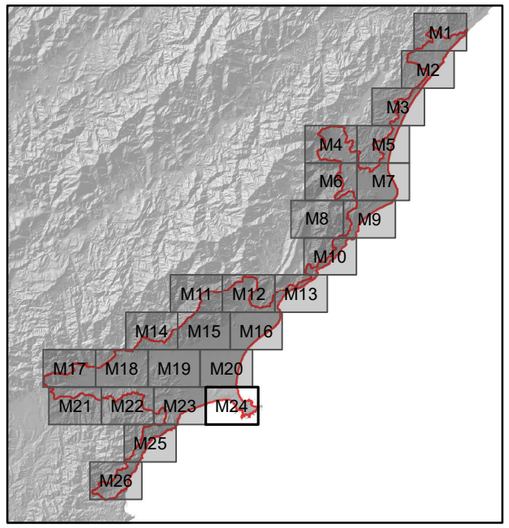
Appendix 3

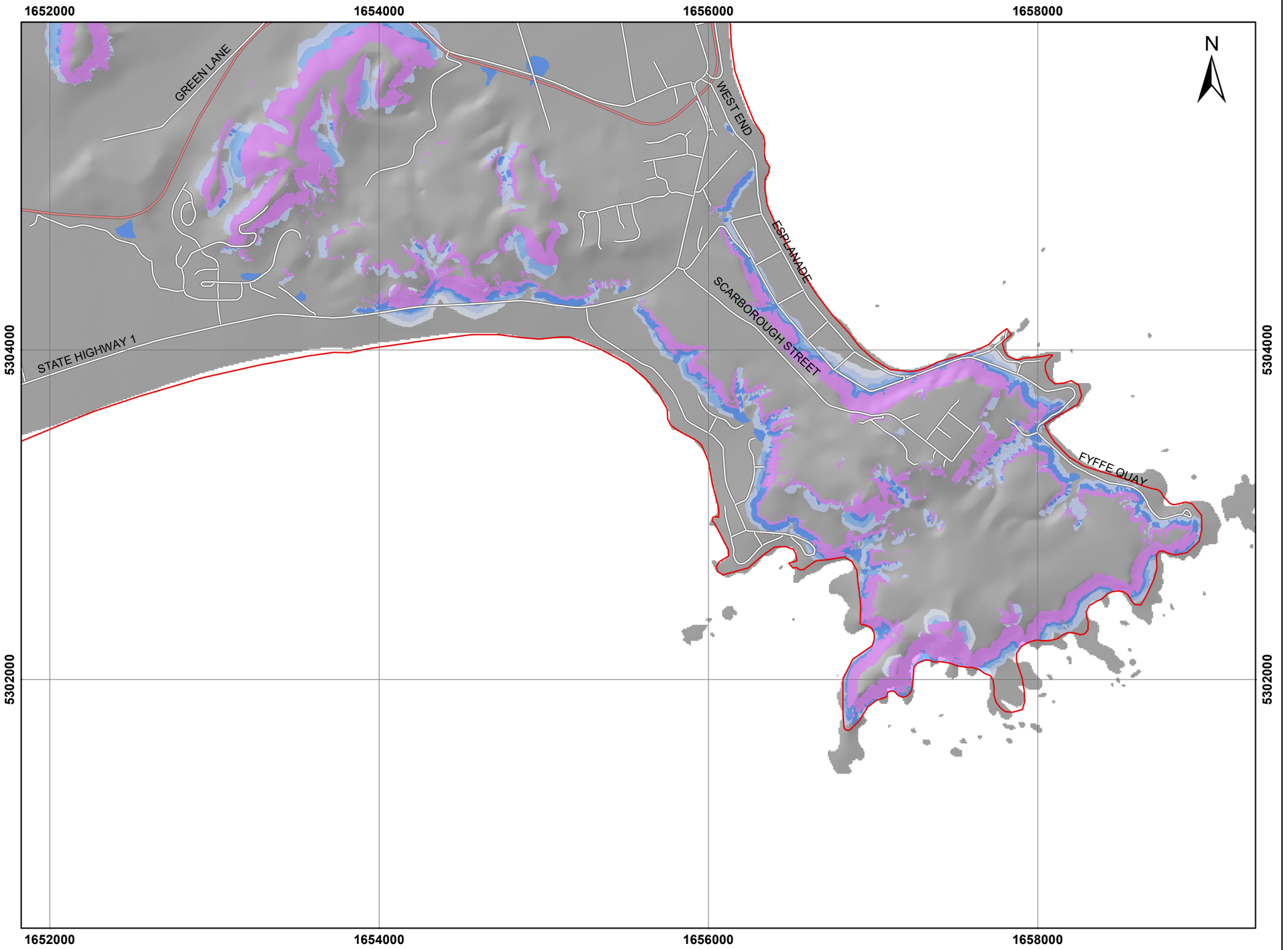
Map 23

FINAL

REPORT: CR2021/89

DATE: Oct 2021





Local personal risk

- 10^{-2} - 10^{-1}
- 10^{-3} - 10^{-2}
- 10^{-4} - 10^{-3}
- 10^{-5} - 10^{-4}
- 10^{-6} - 10^{-5}
- 10^{-7} - 10^{-6}
- Less than 10^{-7}

- Roads
- Railway
- Study area

SCALE BAR: 0 0.5 1 km

EXPLANATION:

The model is based on mean landslide probability estimates and historical 24-hour rainfall annual frequencies. It uses a variable value for the vulnerability of a person if hit by a landslide, based on the landslide size and the person's distance from the source.

Background shade model derived from 8 m New Zealand Digital Elevation Model (LINZ Data Service 2012). PROJECTION: New Zealand Transverse Mercator 2000.

DRW: BL

CHK: CM, SDV

GNS SCIENCE TE PŪ AO

Confidential 2021

LOCAL PERSONAL RISK from earthquake- and rainfall-induced landslides Mean scenario

Regional Landslide Risk Analysis Kaikōura

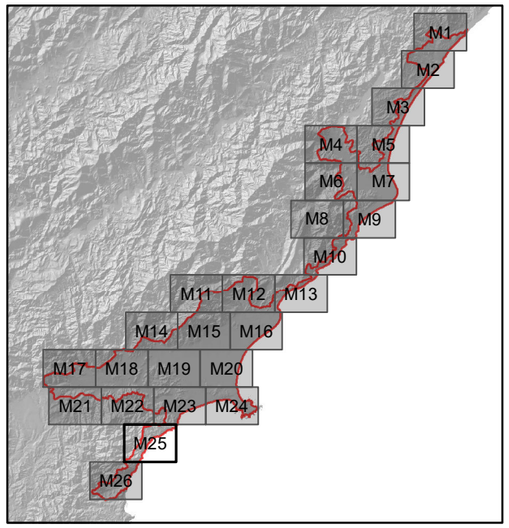
Appendix 3

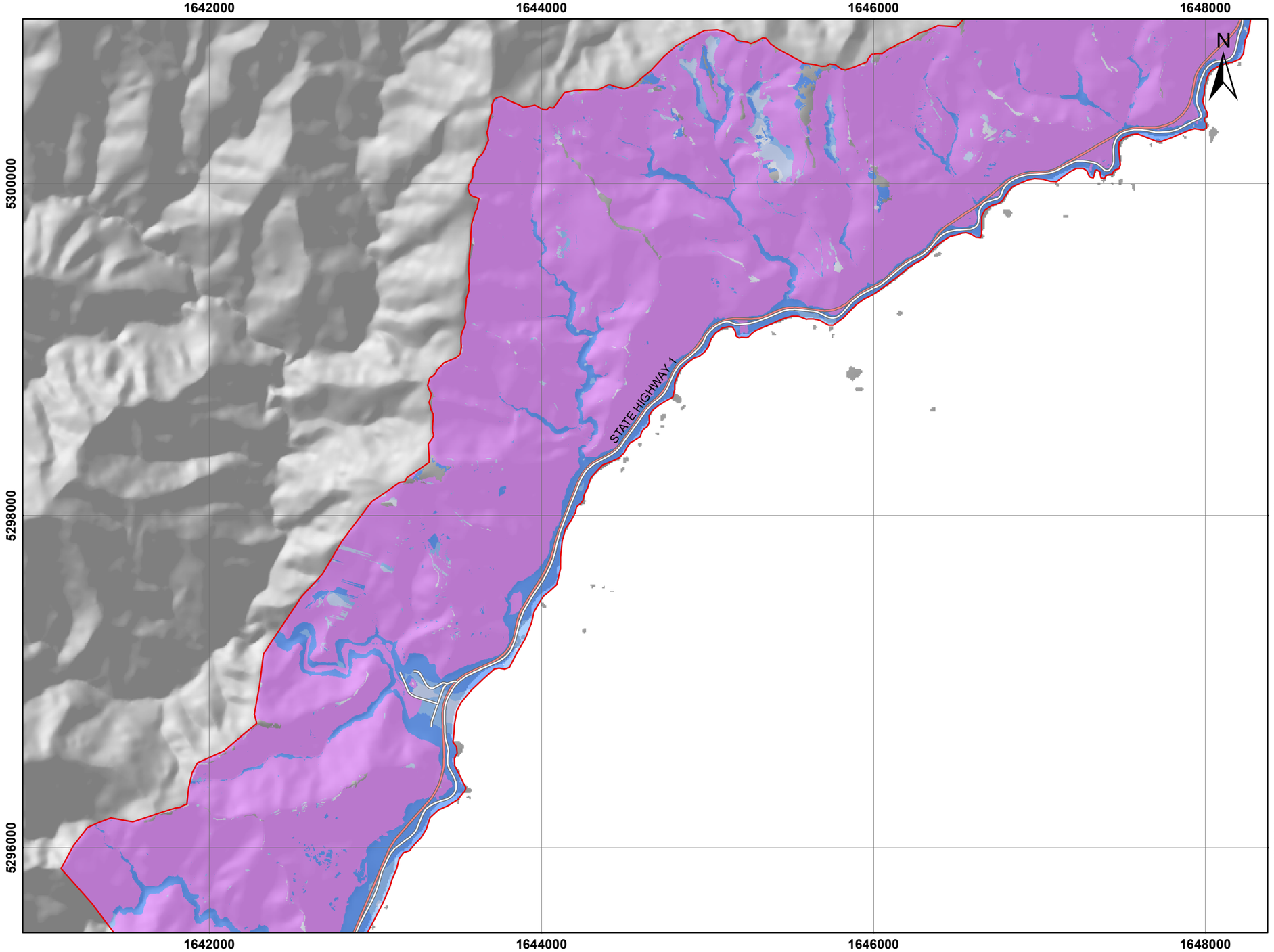
Map 24

FINAL

REPORT: CR2021/89

DATE: Oct 2021





Local personal risk

- 10^{-2} - 10^{-1}
- 10^{-3} - 10^{-2}
- 10^{-4} - 10^{-3}
- 10^{-5} - 10^{-4}
- 10^{-6} - 10^{-5}
- 10^{-7} - 10^{-6}
- Less than 10^{-7}

- Roads
- Railway
- Study area

SCALE BAR: 0 0.5 1 km

EXPLANATION:

The model is based on mean landslide probability estimates and historical 24-hour rainfall annual frequencies. It uses a variable value for the vulnerability of a person if hit by a landslide, based on the landslide size and the person's distance from the source.

Background shade model derived from 8 m New Zealand Digital Elevation Model (LINZ Data Service 2012). PROJECTION: New Zealand Transverse Mercator 2000.

DRW: BL

CHK: CM, SDV

GNS SCIENCE TE PŪ AO

Confidential 2021

LOCAL PERSONAL RISK from earthquake- and rainfall-induced landslides Mean scenario

Regional Landslide Risk Analysis Kaikōura

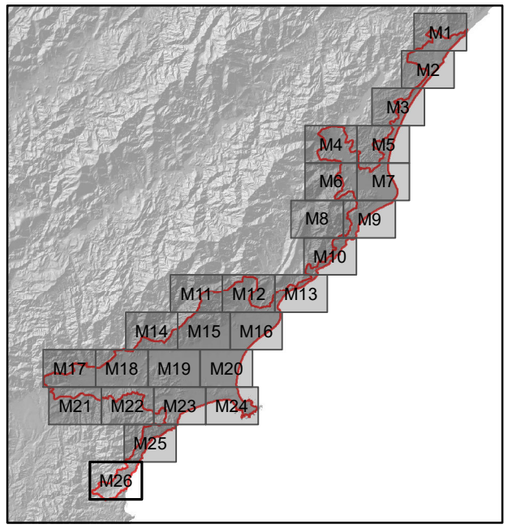
Appendix 3

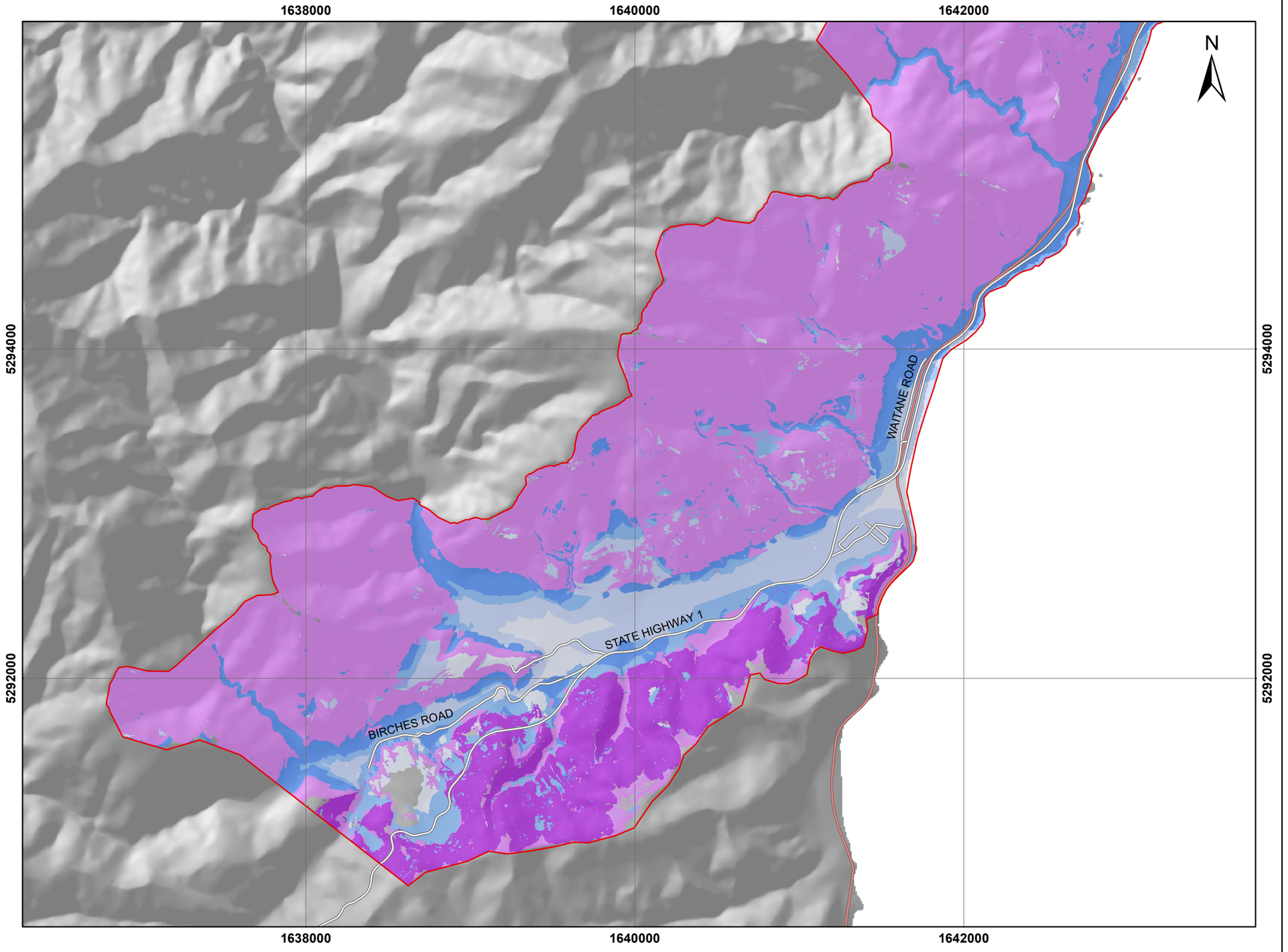
Map 25

FINAL

REPORT: CR2021/89

DATE: Oct 2021





Local personal risk

- 10^{-2} - 10^{-1}
- 10^{-3} - 10^{-2}
- 10^{-4} - 10^{-3}
- 10^{-5} - 10^{-4}
- 10^{-6} - 10^{-5}
- 10^{-7} - 10^{-6}
- Less than 10^{-7}

Roads

Railway

Study area

SCALE BAR: 0 0.5 1 km

EXPLANATION:

The model is based on mean landslide probability estimates and historical 24-hour rainfall annual frequencies. It uses a variable value for the vulnerability of a person if hit by a landslide, based on the landslide size and the person's distance from the source.

Background shade model derived from 8 m New Zealand Digital Elevation Model (LINZ Data Service 2012). PROJECTION: New Zealand Transverse Mercator 2000.

DRW: BL

CHK: CM, SDV

GNS SCIENCE TE PŪ AO

Confidential 2021

LOCAL PERSONAL RISK from earthquake- and rainfall-induced landslides Mean scenario

Regional Landslide Risk Analysis Kaikōura

Appendix 3

Map 26

FINAL

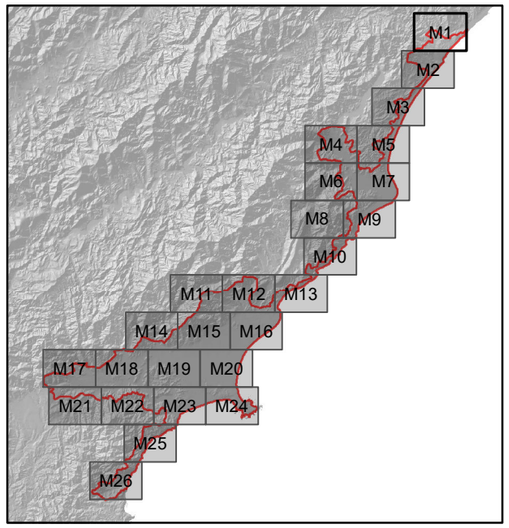
REPORT: CR2021/89

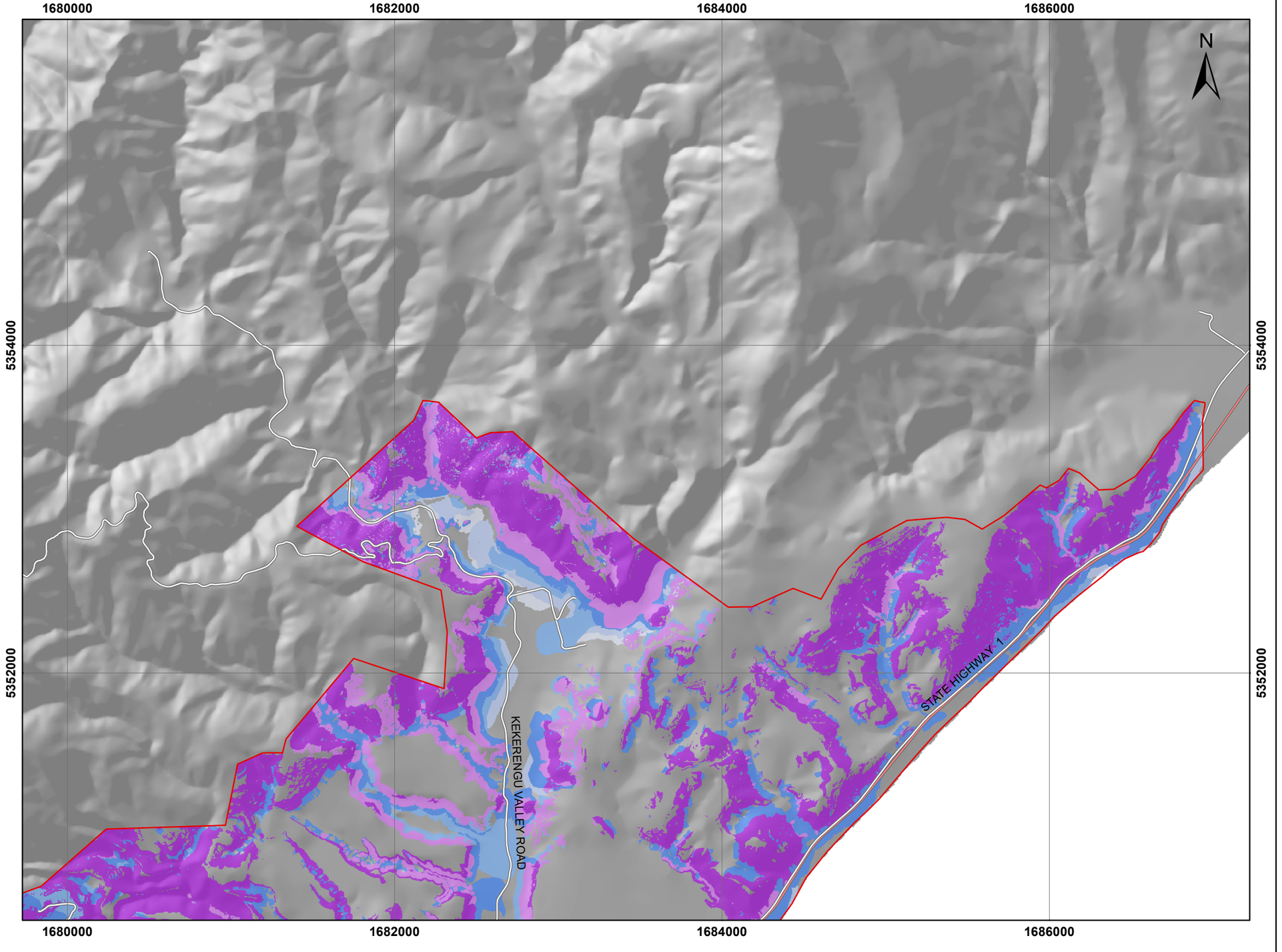
DATE: Oct 2021

APPENDIX 4

LOCAL PERSONAL RISK MAPS: SCENARIO 7

This page left intentionally blank.





Local personal risk

- 10^{-2} - 10^{-1}
- 10^{-3} - 10^{-2}
- 10^{-4} - 10^{-3}
- 10^{-5} - 10^{-4}
- 10^{-6} - 10^{-5}
- 10^{-7} - 10^{-6}
- Less than 10^{-7}

Roads

Railway

Study area

SCALE BAR: 0 0.5 1 km

EXPLANATION:
The model is based on 84% landslide probability estimates and annual frequencies for 24-hour rainfall adapted for Climate Change as per RSP 8.5 model. It uses a variable value for the vulnerability of a person if hit by a landslide, based on the landslide size and the person's distance from the source.

Background shade model derived from 8 m New Zealand Digital Elevation Model (LINZ Data Service 2012). PROJECTION: New Zealand Transverse Mercator 2000.

DRW: BL

CHK: CM, SDV

GNS SCIENCE TE PŪ AO

Confidential 2021

LOCAL PERSONAL RISK from earthquake- and rainfall-induced landslides Upper scenario

Regional Landslide Risk Analysis Kaikōura

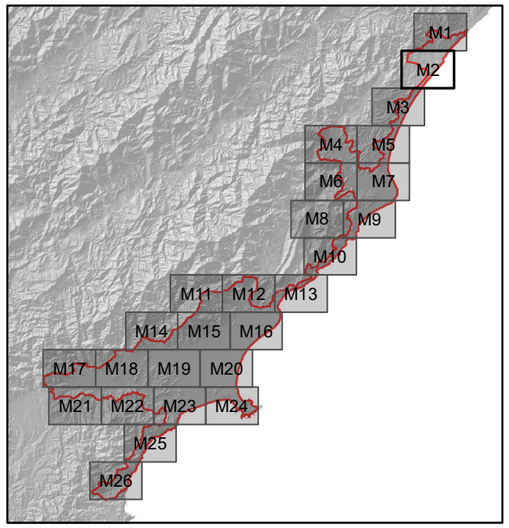
Appendix 4

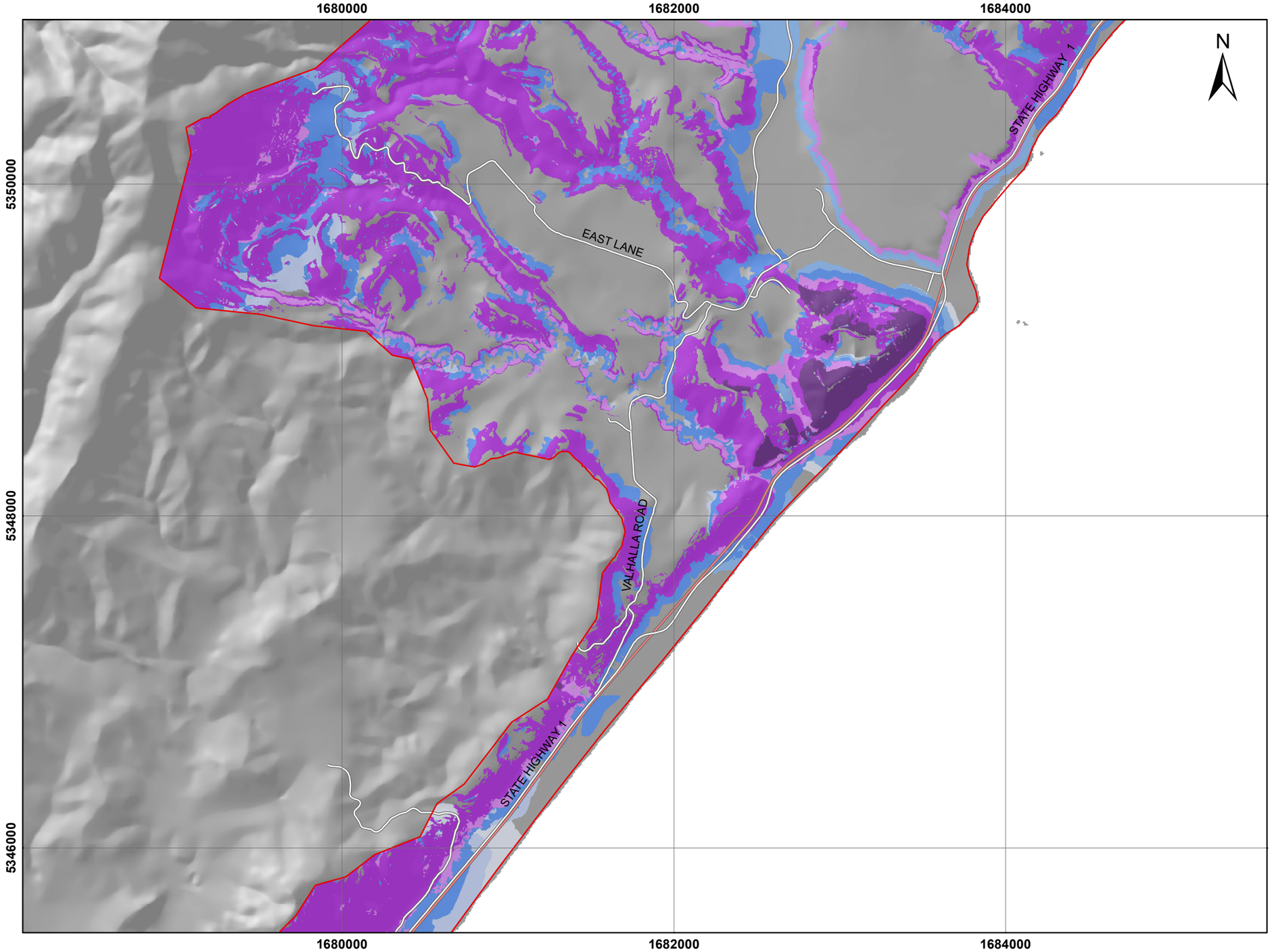
Map 1

FINAL

REPORT: CR2021/89

DATE: Oct 2021





Local personal risk

- 10^{-2} - 10^{-1}
- 10^{-3} - 10^{-2}
- 10^{-4} - 10^{-3}
- 10^{-5} - 10^{-4}
- 10^{-6} - 10^{-5}
- 10^{-7} - 10^{-6}
- Less than 10^{-7}

- Roads
- Railway
- Study area

SCALE BAR: 0 0.5 1 km

EXPLANATION:
The model is based on 84% landslide probability estimates and annual frequencies for 24-hour rainfall adapted for Climate Change as per RSP 8.5 model. It uses a variable value for the vulnerability of a person if hit by a landslide, based on the landslide size and the person's distance from the source.

Background shade model derived from 8 m New Zealand Digital Elevation Model (LINZ Data Service 2012). PROJECTION: New Zealand Transverse Mercator 2000.

DRW: BL

CHK: CM, SDV

GNS SCIENCE TE PŪ AO

Confidential 2021

LOCAL PERSONAL RISK from earthquake- and rainfall-induced landslides Upper scenario

Regional Landslide Risk Analysis Kaikōura

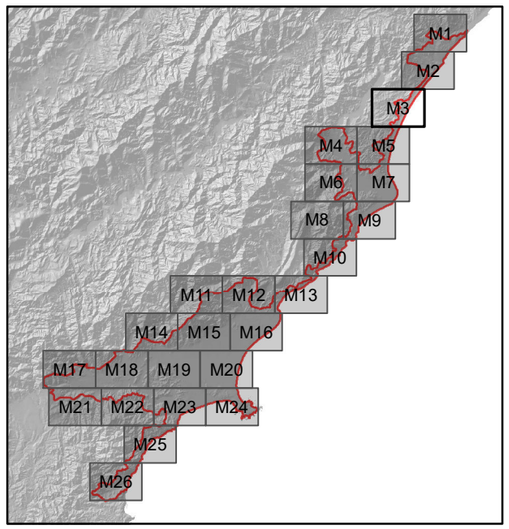
Appendix 4

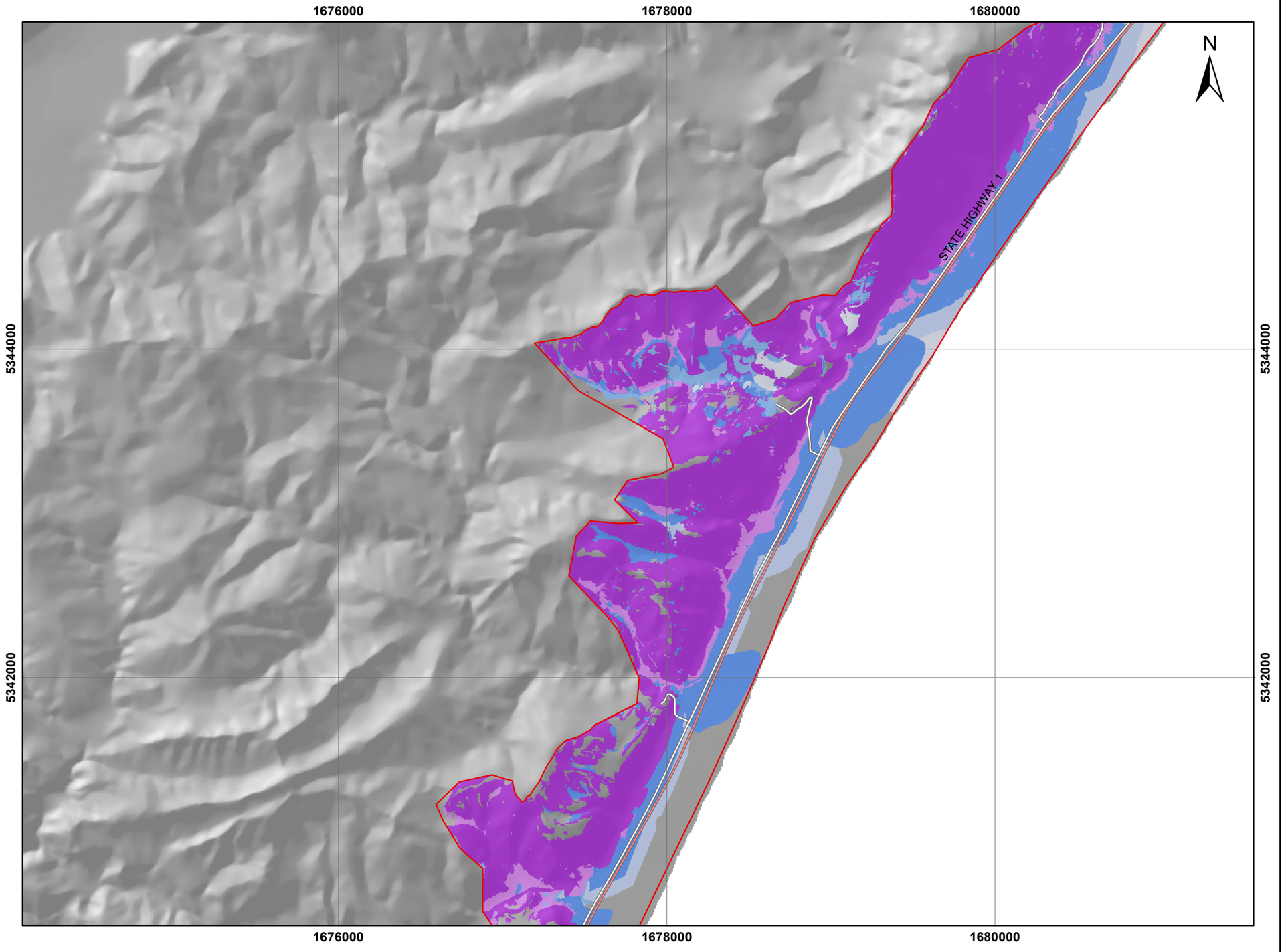
Map 2

FINAL

REPORT: CR2021/89

DATE: Oct 2021





Local personal risk

- 10^{-2} - 10^{-1}
- 10^{-3} - 10^{-2}
- 10^{-4} - 10^{-3}
- 10^{-5} - 10^{-4}
- 10^{-6} - 10^{-5}
- 10^{-7} - 10^{-6}
- Less than 10^{-7}

Roads

Railway

Study area

SCALE BAR: 0 0.5 1 km

EXPLANATION:

The model is based on 84% landslide probability estimates and annual frequencies for 24-hour rainfall adapted for Climate Change as per RSP 8.5 model. It uses a variable value for the vulnerability of a person if hit by a landslide, based on the landslide size and the person's distance from the source.

Background shade model derived from 8 m New Zealand Digital Elevation Model (LINZ Data Service 2012). PROJECTION: New Zealand Transverse Mercator 2000.

DRW: BL

CHK: CM, SDV

GNS SCIENCE TE PŪ AO

Confidential 2021

LOCAL PERSONAL RISK from earthquake- and rainfall-induced landslides Upper scenario

Regional Landslide Risk Analysis Kaikōura

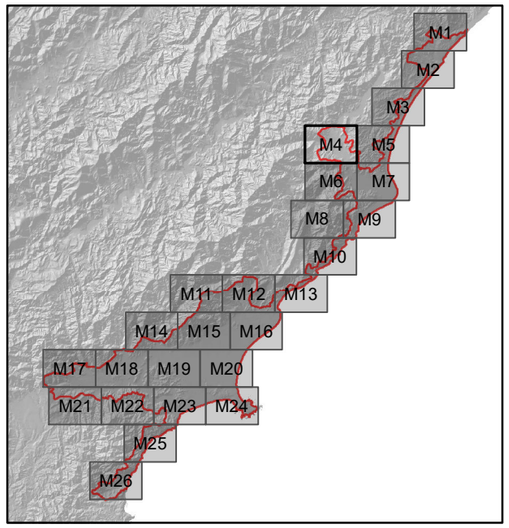
Appendix 4

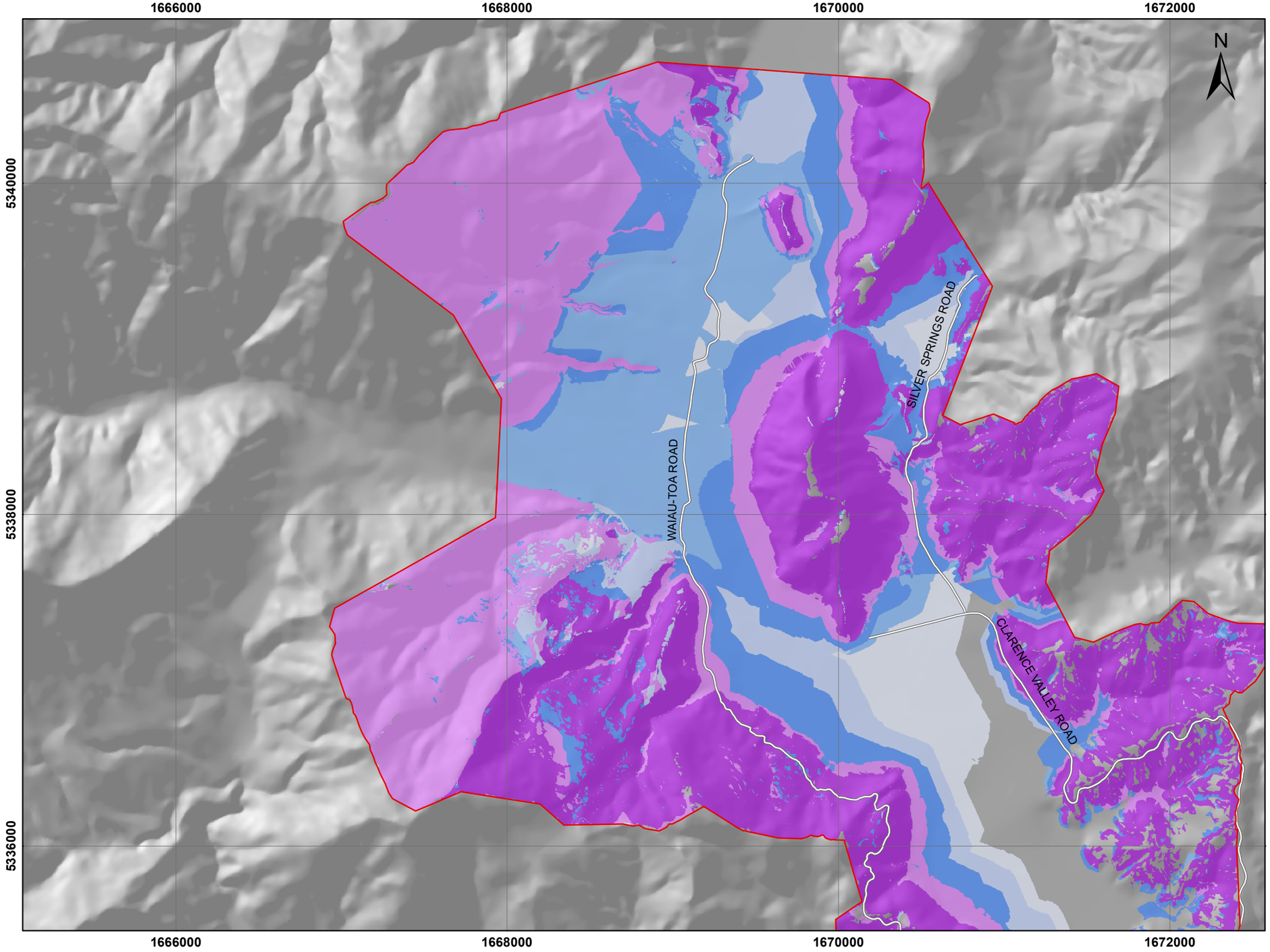
Map 3

FINAL

REPORT: CR2021/89

DATE: Oct 2021





Local personal risk

- 10^{-2} - 10^{-1}
- 10^{-3} - 10^{-2}
- 10^{-4} - 10^{-3}
- 10^{-5} - 10^{-4}
- 10^{-6} - 10^{-5}
- 10^{-7} - 10^{-6}
- Less than 10^{-7}

Roads

Railway

Study area

SCALE BAR: 0 0.5 1 km

EXPLANATION:
The model is based on 84% landslide probability estimates and annual frequencies for 24-hour rainfall adapted for Climate Change as per RSP 8.5 model. It uses a variable value for the vulnerability of a person if hit by a landslide, based on the landslide size and the person's distance from the source.

Background shade model derived from 8 m New Zealand Digital Elevation Model (LINZ Data Service 2012). PROJECTION: New Zealand Transverse Mercator 2000.

DRW: BL

CHK: CM, SDV

GNS SCIENCE TE PŪ AO

Confidential 2021

LOCAL PERSONAL RISK
from earthquake- and rainfall-induced landslides
Upper scenario

Regional Landslide Risk Analysis
Kaikōura

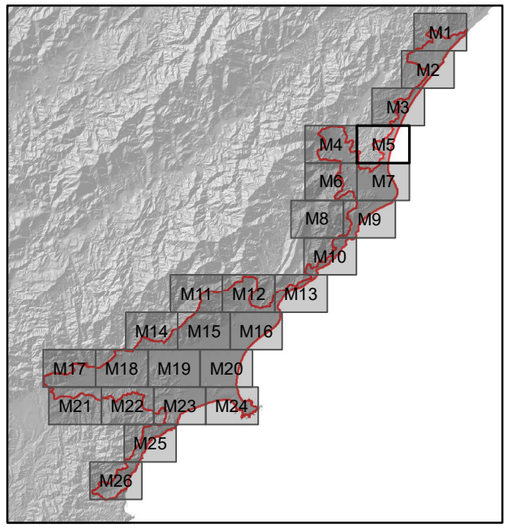
Appendix 4

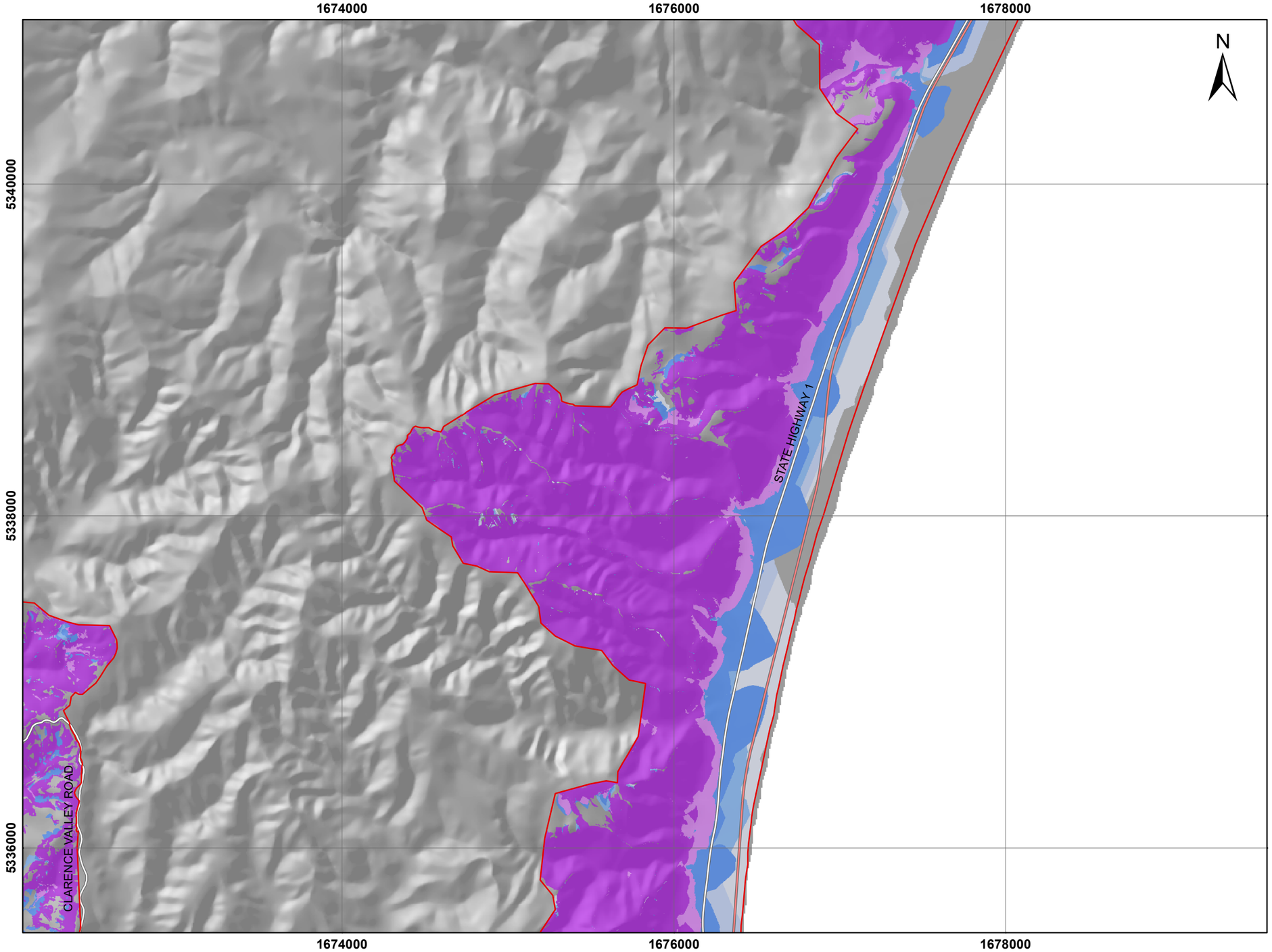
Map 4

FINAL

REPORT: CR2021/89

DATE: Oct 2021





Local personal risk

- 10^{-2} - 10^{-1}
- 10^{-3} - 10^{-2}
- 10^{-4} - 10^{-3}
- 10^{-5} - 10^{-4}
- 10^{-6} - 10^{-5}
- 10^{-7} - 10^{-6}
- Less than 10^{-7}

Roads

Railway

Study area

SCALE BAR: 0 0.5 1 km

EXPLANATION:

The model is based on 84% landslide probability estimates and annual frequencies for 24-hour rainfall adapted for Climate Change as per RSP 8.5 model. It uses a variable value for the vulnerability of a person if hit by a landslide, based on the landslide size and the person's distance from the source.

Background shade model derived from 8 m New Zealand Digital Elevation Model (LINZ Data Service 2012). PROJECTION: New Zealand Transverse Mercator 2000.

DRW: BL

CHK: CM, SDV

GNS SCIENCE TE PŪ AO

Confidential 2021

LOCAL PERSONAL RISK from earthquake- and rainfall-induced landslides Upper scenario

Regional Landslide Risk Analysis Kaikōura

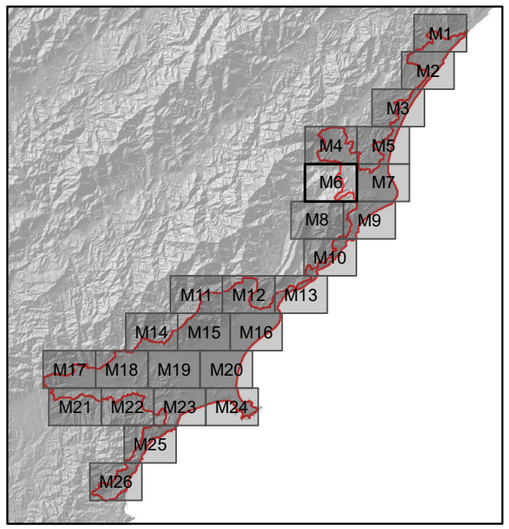
Appendix 4

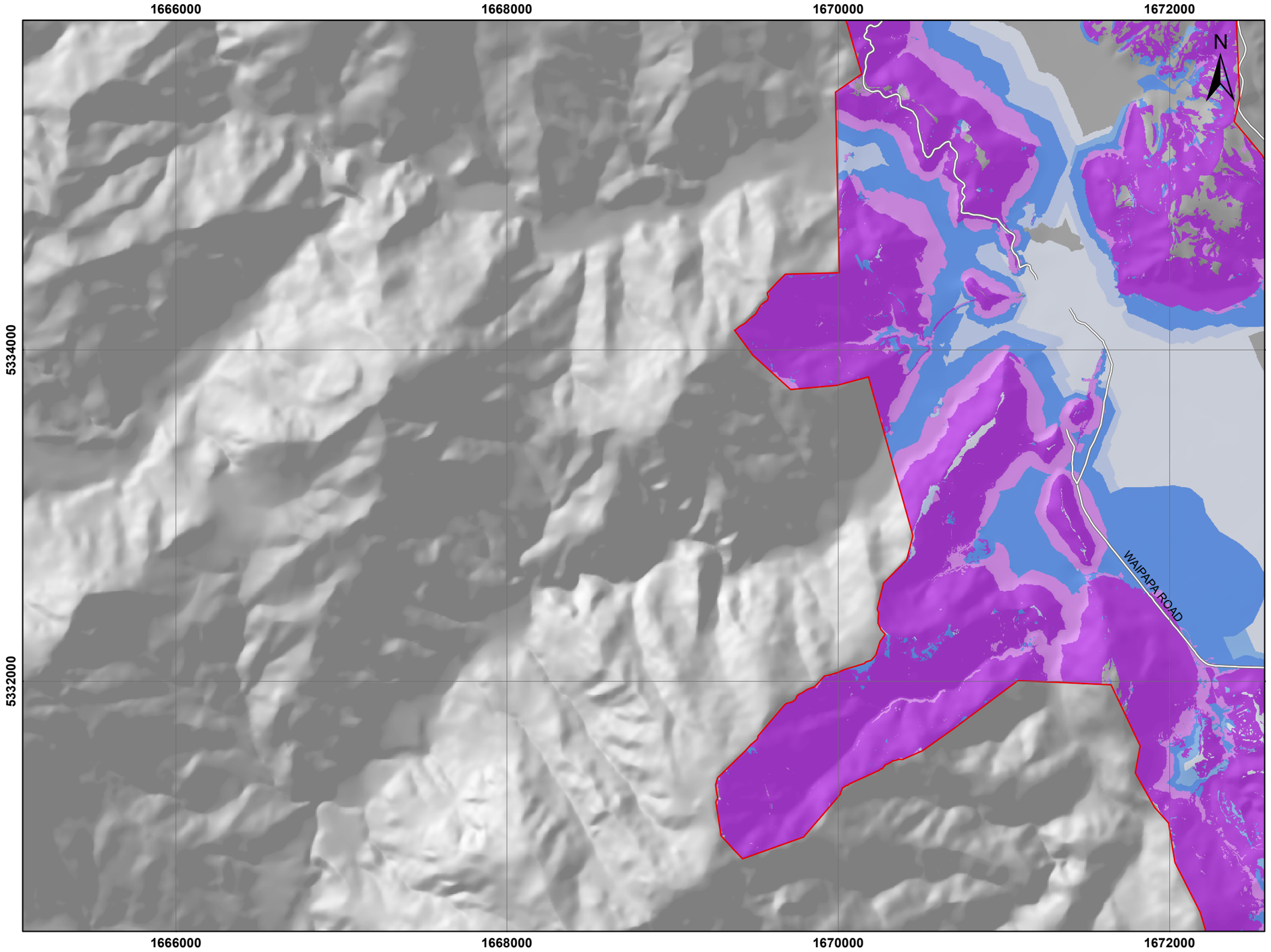
Map 5

FINAL

REPORT: CR2021/89

DATE: Oct 2021





Local personal risk

- 10^{-2} - 10^{-1}
- 10^{-3} - 10^{-2}
- 10^{-4} - 10^{-3}
- 10^{-5} - 10^{-4}
- 10^{-6} - 10^{-5}
- 10^{-7} - 10^{-6}
- Less than 10^{-7}

Roads

Railway

Study area

SCALE BAR: 0 0.5 1 km

EXPLANATION:

The model is based on 84% landslide probability estimates and annual frequencies for 24-hour rainfall adapted for Climate Change as per RSP 8.5 model. It uses a variable value for the vulnerability of a person if hit by a landslide, based on the landslide size and the person's distance from the source.

Background shade model derived from 8 m New Zealand Digital Elevation Model (LINZ Data Service 2012). PROJECTION: New Zealand Transverse Mercator 2000.

DRW: BL

CHK: CM, SDV

GNS SCIENCE TE PŪ AO

Confidential 2021

LOCAL PERSONAL RISK from earthquake- and rainfall-induced landslides Upper scenario

Regional Landslide Risk Analysis Kaikōura

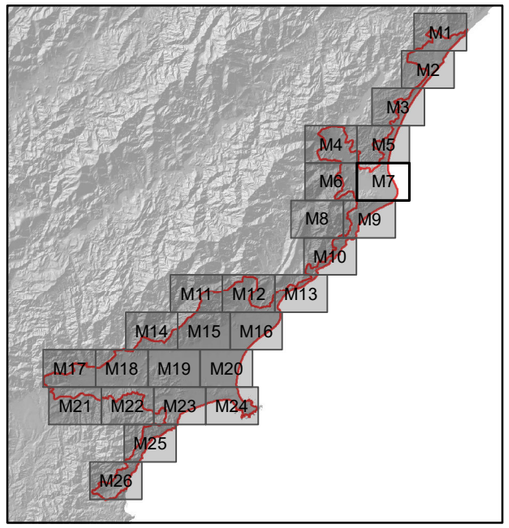
Appendix 4

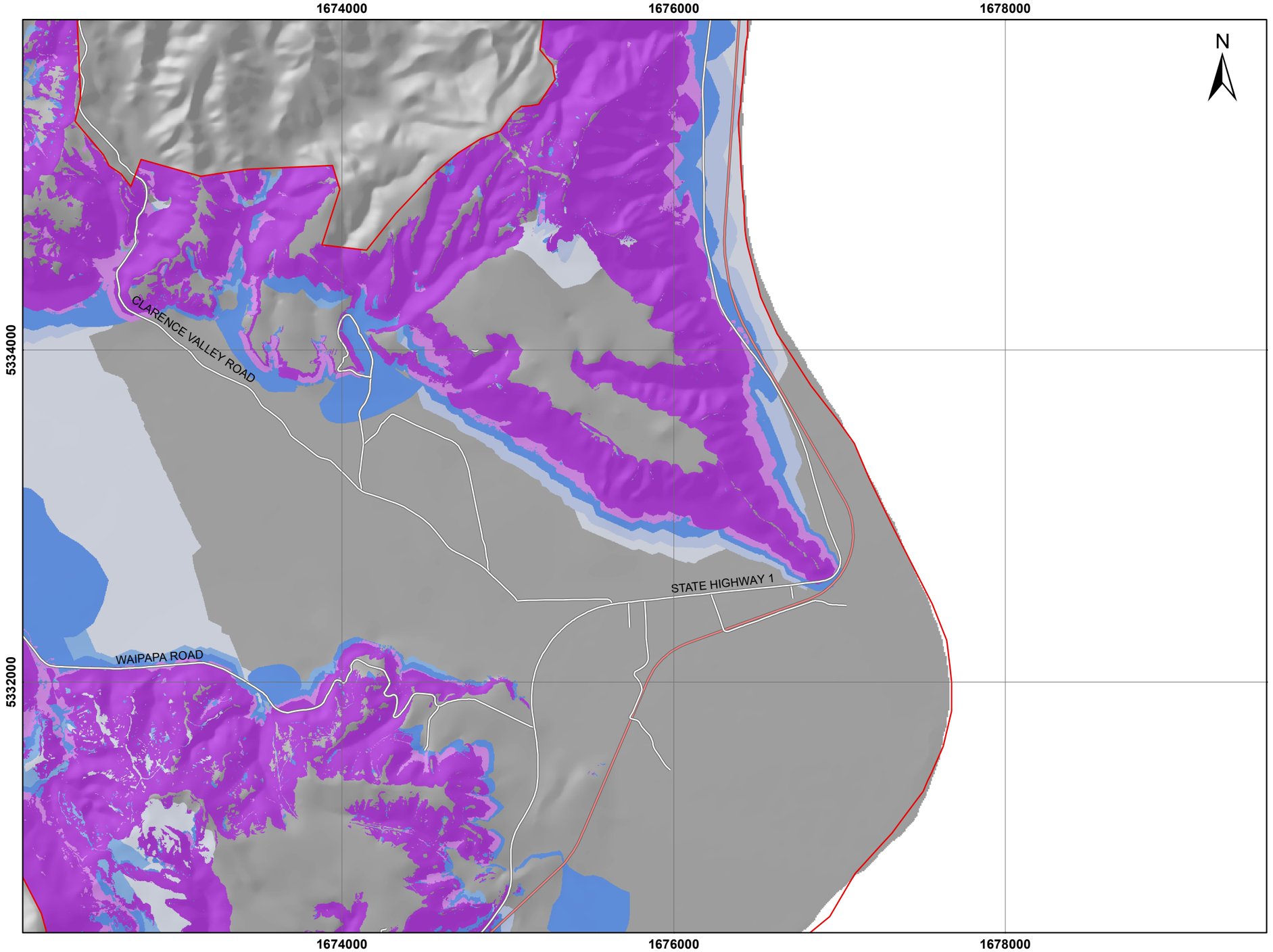
Map 6

FINAL

REPORT: CR2021/89

DATE: Oct 2021





Local personal risk

- 10^{-2} - 10^{-1}
- 10^{-3} - 10^{-2}
- 10^{-4} - 10^{-3}
- 10^{-5} - 10^{-4}
- 10^{-6} - 10^{-5}
- 10^{-7} - 10^{-6}
- Less than 10^{-7}

- Roads
- Railway
- Study area

SCALE BAR: 0 0.5 1 km

EXPLANATION:

The model is based on 84% landslide probability estimates and annual frequencies for 24-hour rainfall adapted for Climate Change as per RSP 8.5 model. It uses a variable value for the vulnerability of a person if hit by a landslide, based on the landslide size and the person's distance from the source.

Background shade model derived from 8 m New Zealand Digital Elevation Model (LINZ Data Service 2012). PROJECTION: New Zealand Transverse Mercator 2000.

DRW: BL

CHK: CM, SDV

GNS SCIENCE TE PŪ AO

Confidential 2021

LOCAL PERSONAL RISK from earthquake- and rainfall-induced landslides Upper scenario

Regional Landslide Risk Analysis Kaikōura

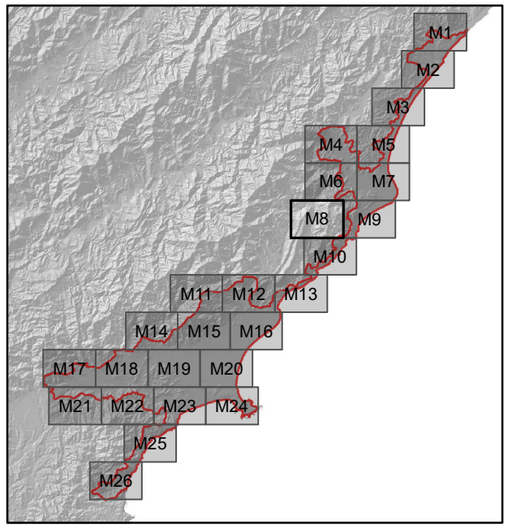
Appendix 4

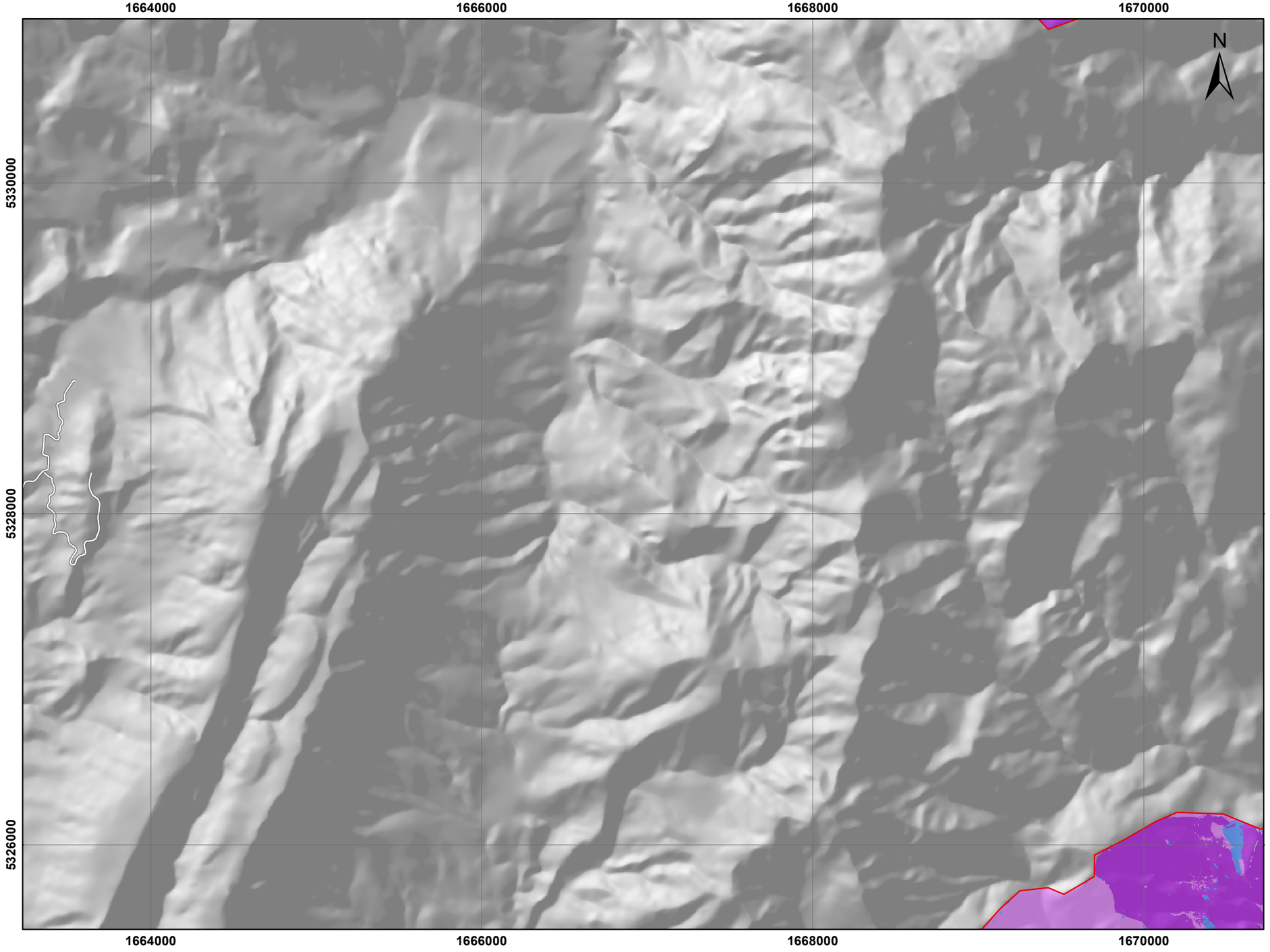
Map 7

FINAL

REPORT: CR2021/89

DATE: Oct 2021





Local personal risk

- 10^{-2} - 10^{-1}
- 10^{-3} - 10^{-2}
- 10^{-4} - 10^{-3}
- 10^{-5} - 10^{-4}
- 10^{-6} - 10^{-5}
- 10^{-7} - 10^{-6}
- Less than 10^{-7}

Roads

Railway

Study area

SCALE BAR: 0 0.5 1 km

EXPLANATION:

The model is based on 84% landslide probability estimates and annual frequencies for 24-hour rainfall adapted for Climate Change as per RSP 8.5 model. It uses a variable value for the vulnerability of a person if hit by a landslide, based on the landslide size and the person's distance from the source.

Background shade model derived from 8 m New Zealand Digital Elevation Model (LINZ Data Service 2012). PROJECTION: New Zealand Transverse Mercator 2000.

DRW: BL

CHK: CM, SDV

GNS SCIENCE TE PŪ AO

Confidential 2021

LOCAL PERSONAL RISK from earthquake- and rainfall-induced landslides Upper scenario

Regional Landslide Risk Analysis Kaikōura

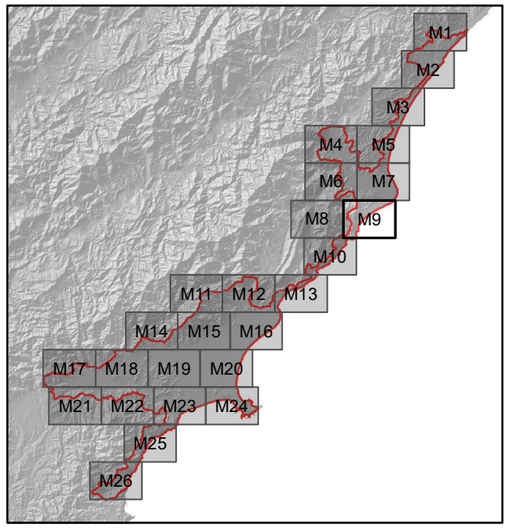
Appendix 4

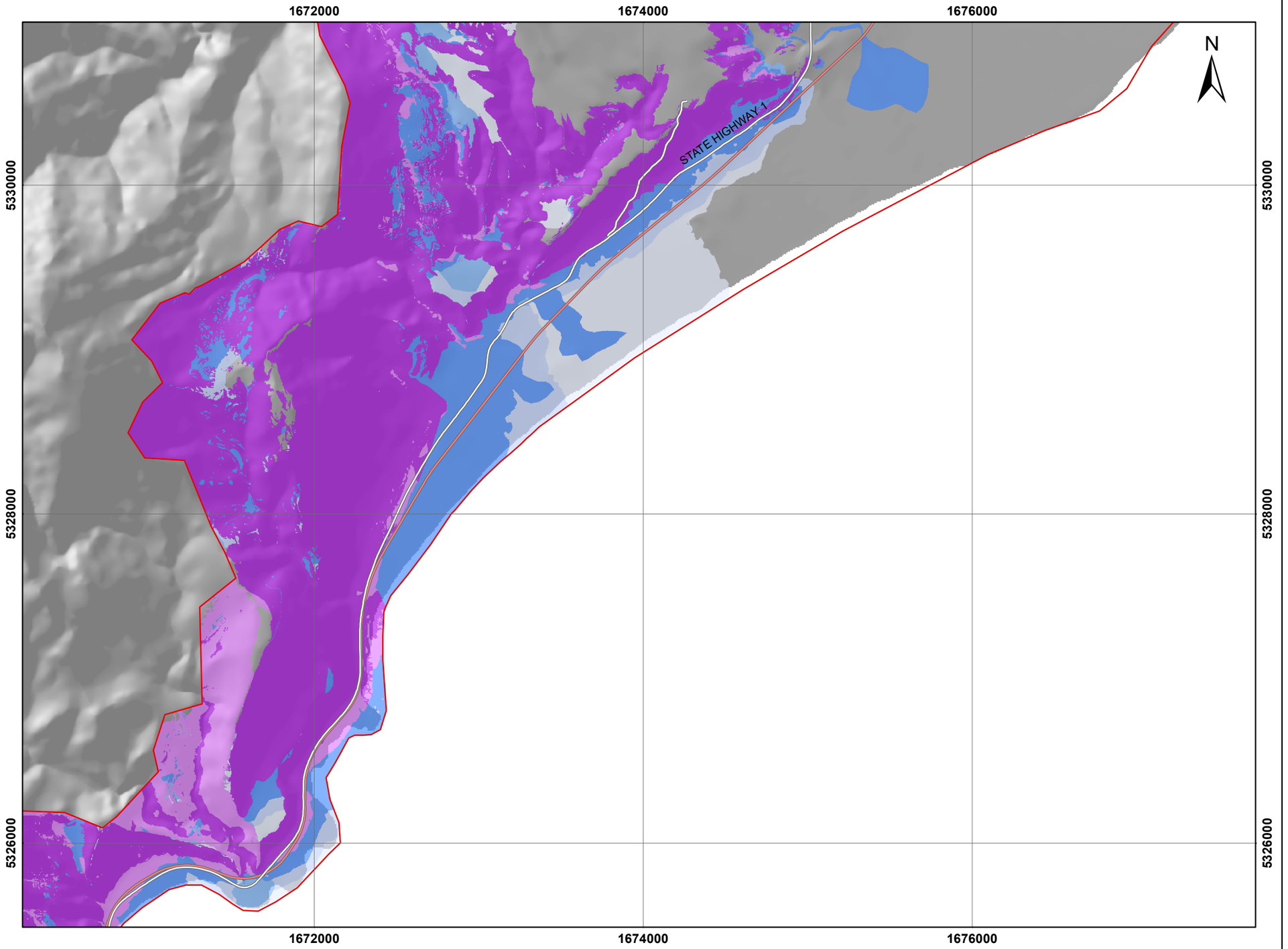
Map 8

FINAL

REPORT: CR2021/89

DATE: Oct 2021





Local personal risk

- 10^{-2} - 10^{-1}
- 10^{-3} - 10^{-2}
- 10^{-4} - 10^{-3}
- 10^{-5} - 10^{-4}
- 10^{-6} - 10^{-5}
- 10^{-7} - 10^{-6}
- Less than 10^{-7}

Roads

Railway

Study area

SCALE BAR: 0 0.5 1 km

EXPLANATION:

The model is based on 84% landslide probability estimates and annual frequencies for 24-hour rainfall adapted for Climate Change as per RSP 8.5 model. It uses a variable value for the vulnerability of a person if hit by a landslide, based on the landslide size and the person's distance from the source.

Background shade model derived from 8 m New Zealand Digital Elevation Model (LINZ Data Service 2012). PROJECTION: New Zealand Transverse Mercator 2000.

DRW: BL

CHK: CM, SDV

GNS SCIENCE TE PŪ AO

Confidential 2021

LOCAL PERSONAL RISK from earthquake- and rainfall-induced landslides Upper scenario

Regional Landslide Risk Analysis Kaikōura

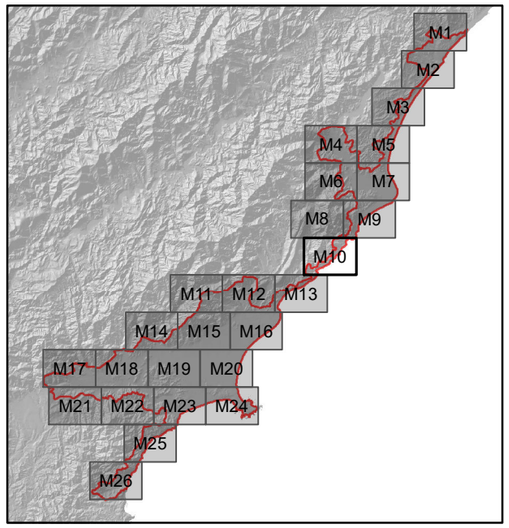
Appendix 4

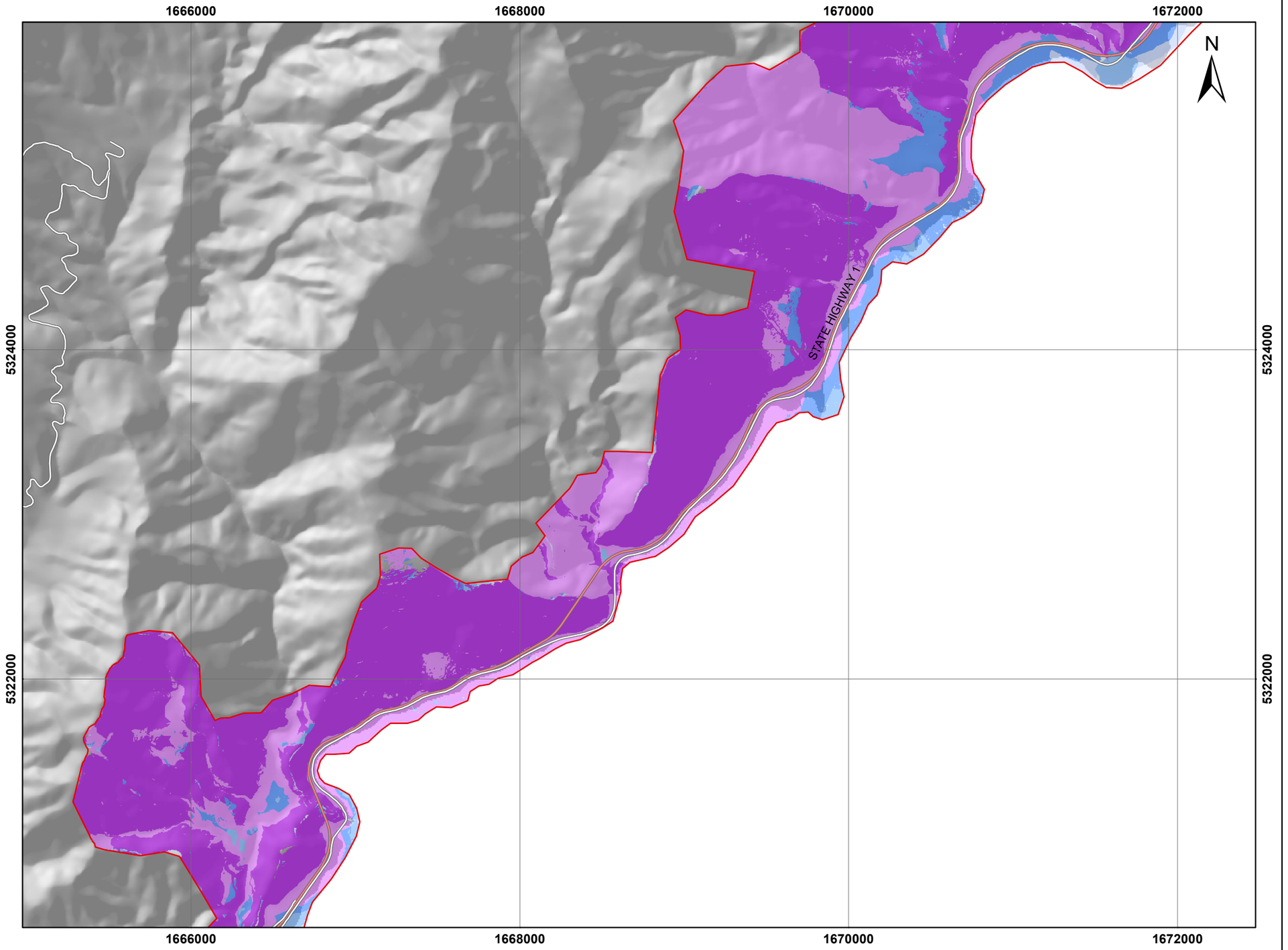
Map 9

FINAL

REPORT: CR2021/89

DATE: Oct 2021





Local personal risk

- 10^{-2} - 10^{-1}
- 10^{-3} - 10^{-2}
- 10^{-4} - 10^{-3}
- 10^{-5} - 10^{-4}
- 10^{-6} - 10^{-5}
- 10^{-7} - 10^{-6}
- Less than 10^{-7}

- Roads
- Railway
- Study area

SCALE BAR: 0 0.5 1 km

EXPLANATION:

The model is based on 84% landslide probability estimates and annual frequencies for 24-hour rainfall adapted for Climate Change as per RSP 8.5 model. It uses a variable value for the vulnerability of a person if hit by a landslide, based on the landslide size and the person's distance from the source.

Background shade model derived from 8 m New Zealand Digital Elevation Model (LINZ Data Service 2012). PROJECTION: New Zealand Transverse Mercator 2000.

DRW: BL

CHK: CM, SDV

GNS SCIENCE TE PŪ AO

Confidential 2021

LOCAL PERSONAL RISK from earthquake- and rainfall-induced landslides Upper scenario

Regional Landslide Risk Analysis Kaikōura

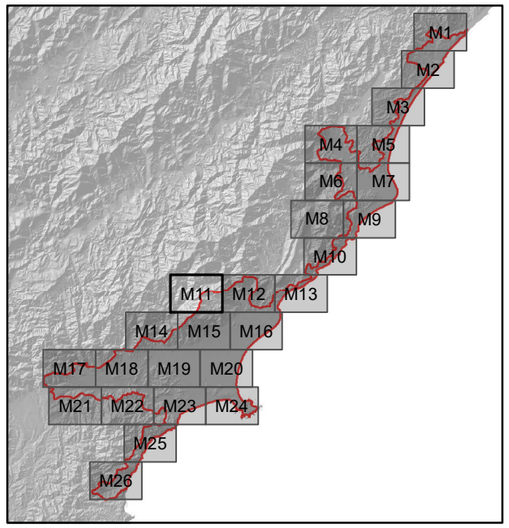
Appendix 4

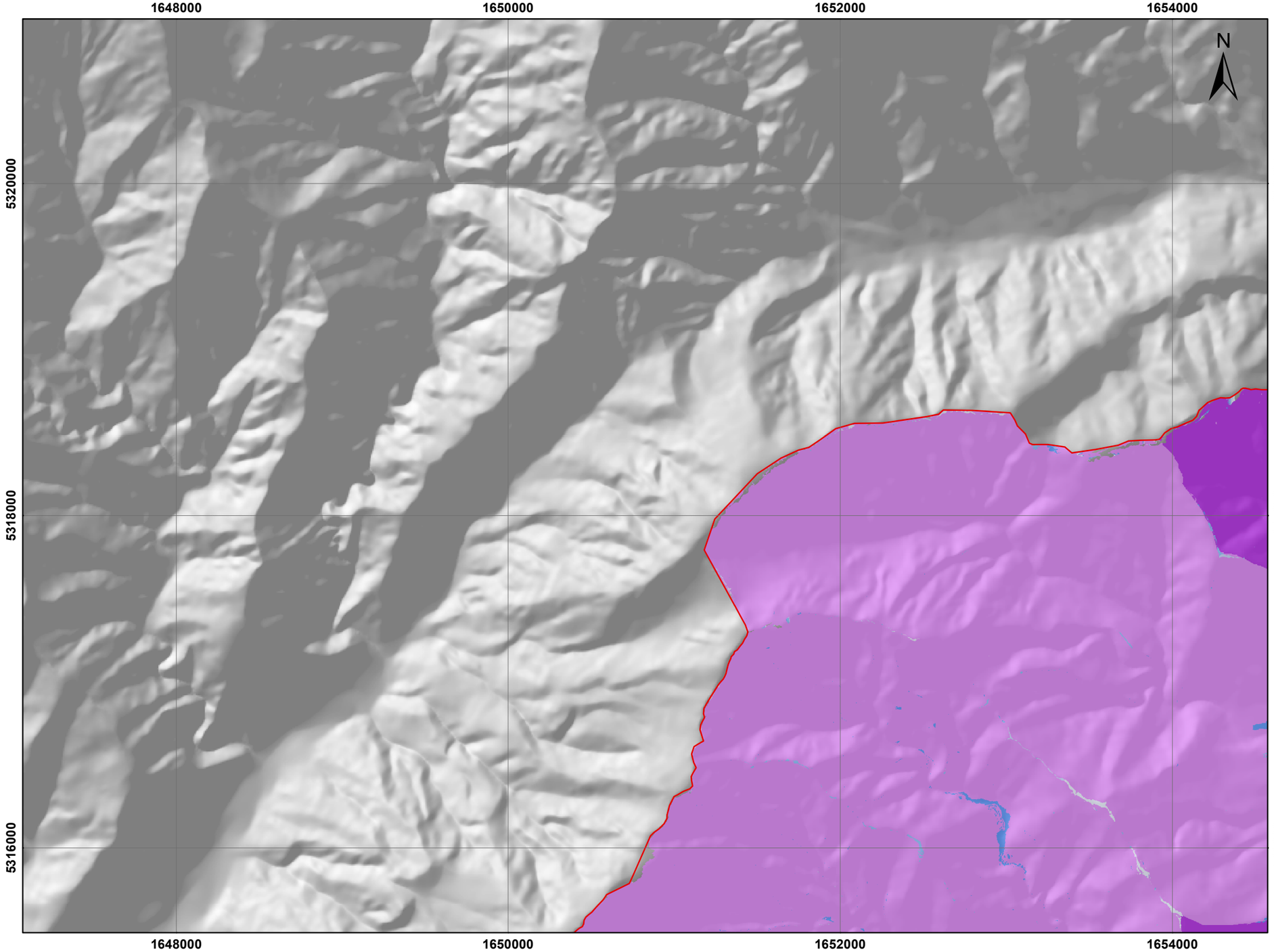
Map 10

FINAL

REPORT: CR2021/89

DATE: Oct 2021





Local personal risk

- 10^{-2} - 10^{-1}
- 10^{-3} - 10^{-2}
- 10^{-4} - 10^{-3}
- 10^{-5} - 10^{-4}
- 10^{-6} - 10^{-5}
- 10^{-7} - 10^{-6}
- Less than 10^{-7}

Roads

Railway

Study area

SCALE BAR: 0 0.5 1 km

EXPLANATION:

The model is based on 84% landslide probability estimates and annual frequencies for 24-hour rainfall adapted for Climate Change as per RSP 8.5 model. It uses a variable value for the vulnerability of a person if hit by a landslide, based on the landslide size and the person's distance from the source.

Background shade model derived from 8 m New Zealand Digital Elevation Model (LINZ Data Service 2012). PROJECTION: New Zealand Transverse Mercator 2000.

DRW: BL

CHK: CM, SDV

GNS SCIENCE TE PŪ AO

Confidential 2021

LOCAL PERSONAL RISK from earthquake- and rainfall-induced landslides Upper scenario

Regional Landslide Risk Analysis Kaikōura

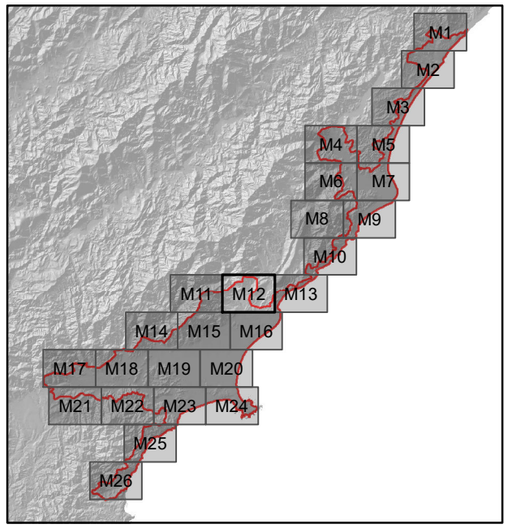
Appendix 4

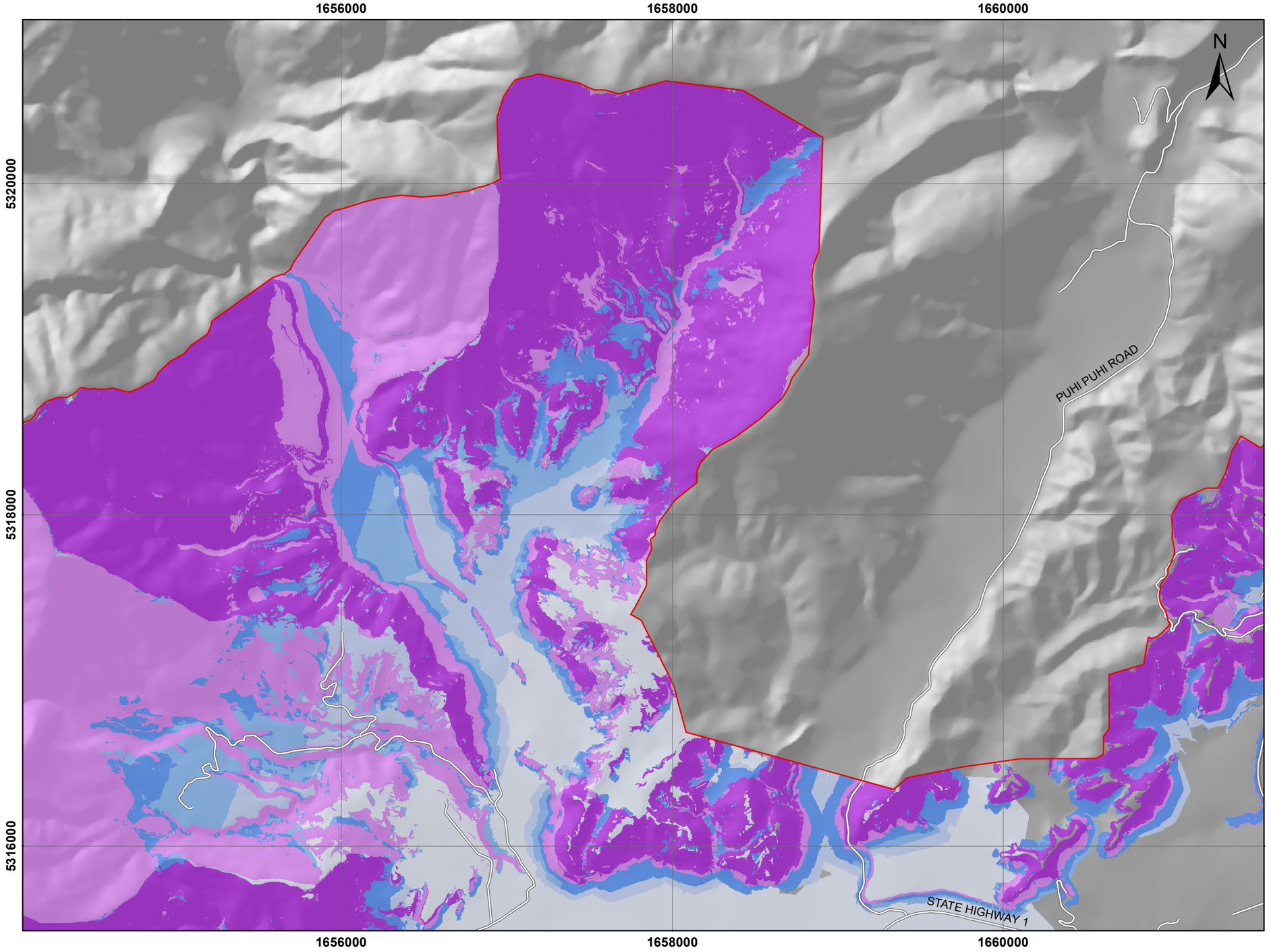
Map 11

FINAL

REPORT: CR2021/89

DATE: Oct 2021





Local personal risk

- 10^{-2} - 10^{-1}
- 10^{-3} - 10^{-2}
- 10^{-4} - 10^{-3}
- 10^{-5} - 10^{-4}
- 10^{-6} - 10^{-5}
- 10^{-7} - 10^{-6}
- Less than 10^{-7}

Roads

Railway

Study area

SCALE BAR: 0 0.5 1 km

EXPLANATION:
The model is based on 84% landslide probability estimates and annual frequencies for 24-hour rainfall adapted for Climate Change as per RSP 8.5 model. It uses a variable value for the vulnerability of a person if hit by a landslide, based on the landslide size and the person's distance from the source.

Background shade model derived from 8 m New Zealand Digital Elevation Model (LINZ Data Service 2012). PROJECTION: New Zealand Transverse Mercator 2000.

DRW: BL

CHK: CM, SDV

GNS SCIENCE TE PŪ AO

Confidential 2021

LOCAL PERSONAL RISK from earthquake- and rainfall-induced landslides Upper scenario

Regional Landslide Risk Analysis Kaikōura

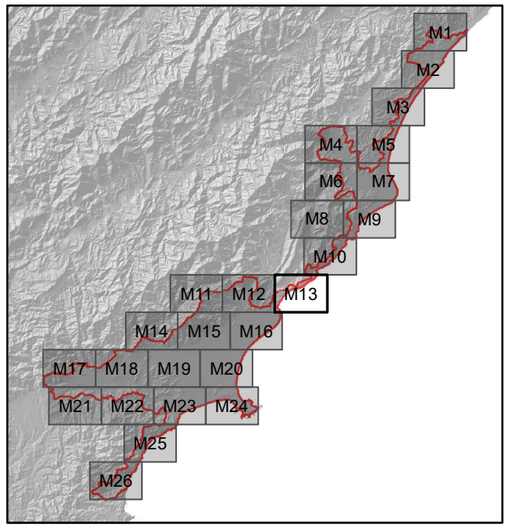
Appendix 4

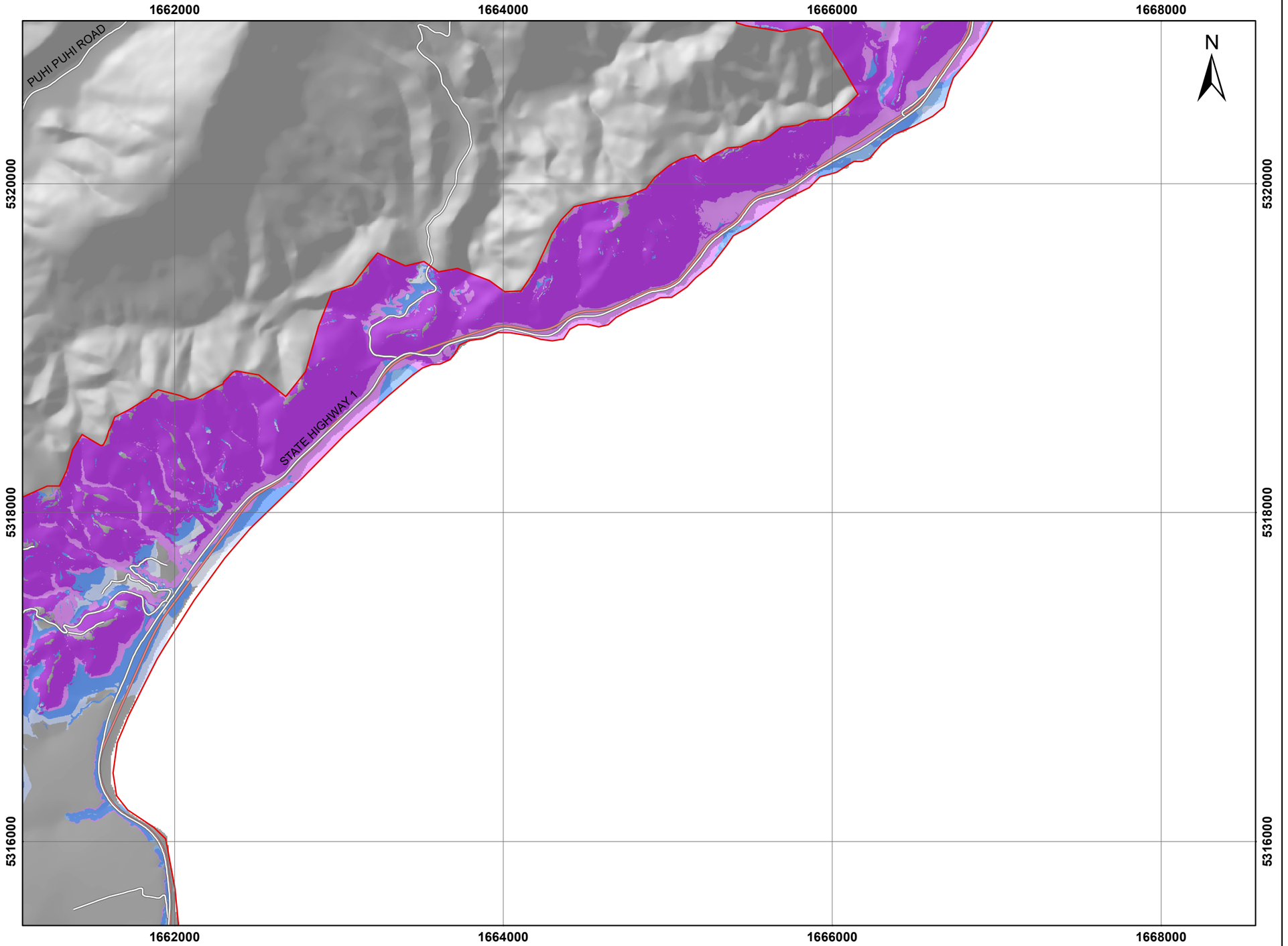
Map 12

FINAL

REPORT: CR2021/89

DATE: Oct 2021





Local personal risk

- 10^{-2} - 10^{-1}
- 10^{-3} - 10^{-2}
- 10^{-4} - 10^{-3}
- 10^{-5} - 10^{-4}
- 10^{-6} - 10^{-5}
- 10^{-7} - 10^{-6}
- Less than 10^{-7}

- Roads
- Railway
- Study area

SCALE BAR: 0 0.5 1 km

EXPLANATION:

The model is based on 84% landslide probability estimates and annual frequencies for 24-hour rainfall adapted for Climate Change as per RSP 8.5 model. It uses a variable value for the vulnerability of a person if hit by a landslide, based on the landslide size and the person's distance from the source.

Background shade model derived from 8 m New Zealand Digital Elevation Model (LINZ Data Service 2012). PROJECTION: New Zealand Transverse Mercator 2000.

DRW: BL

CHK: CM, SDV

GNS SCIENCE TE PŪ AO

Confidential 2021

LOCAL PERSONAL RISK from earthquake- and rainfall-induced landslides Upper scenario

Regional Landslide Risk Analysis Kaikōura

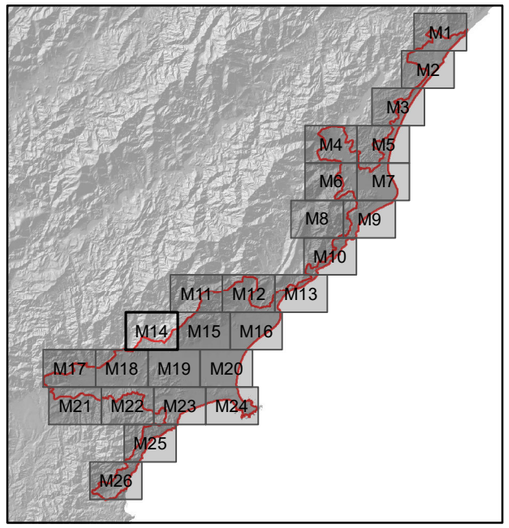
Appendix 4

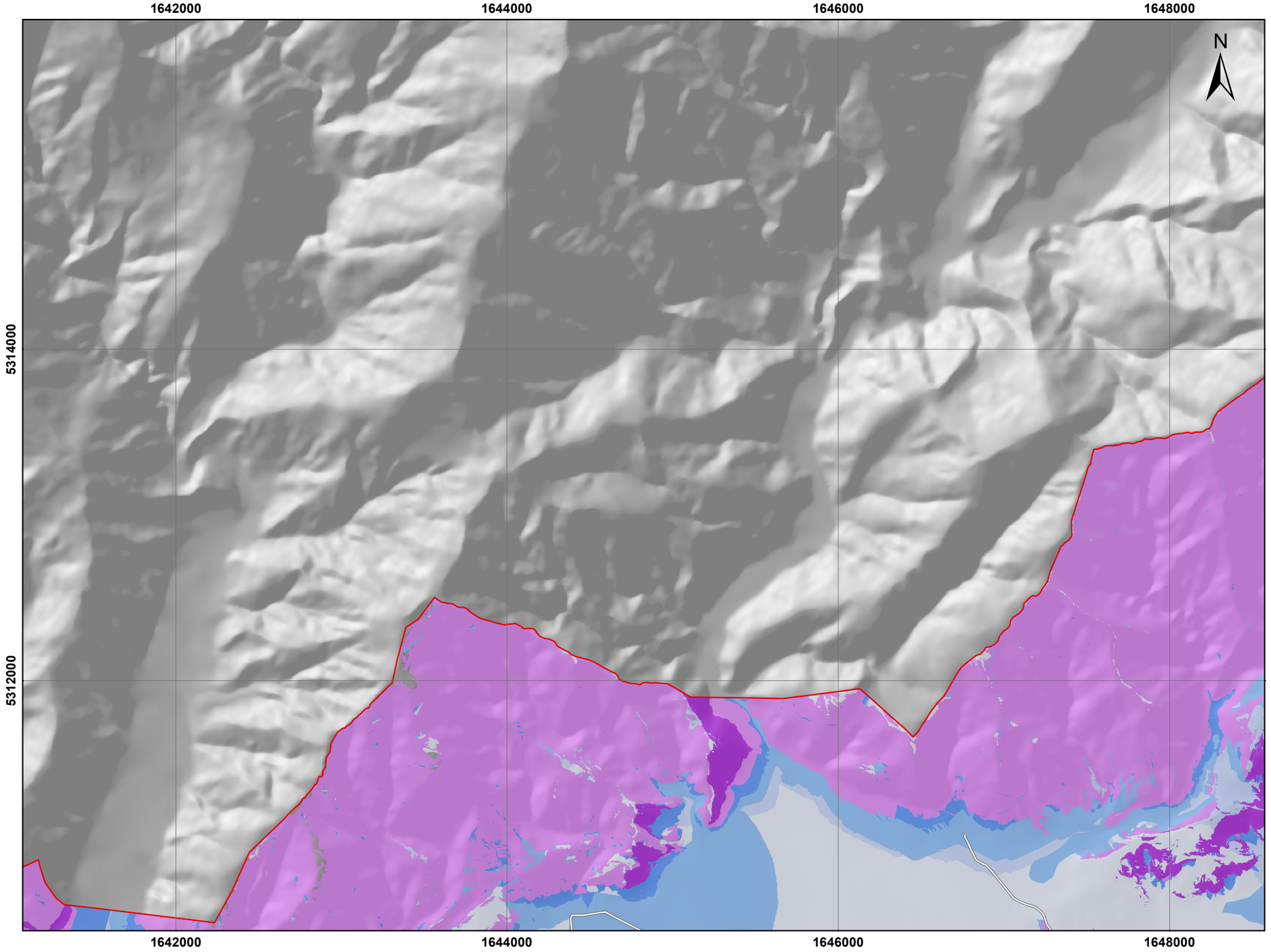
Map 13

FINAL

REPORT: CR2021/89

DATE: Oct 2021





Local personal risk

- 10^{-2} - 10^{-1}
- 10^{-3} - 10^{-2}
- 10^{-4} - 10^{-3}
- 10^{-5} - 10^{-4}
- 10^{-6} - 10^{-5}
- 10^{-7} - 10^{-6}
- Less than 10^{-7}

Roads

Railway

Study area

SCALE BAR: 0 0.5 1 km

EXPLANATION:

The model is based on 84% landslide probability estimates and annual frequencies for 24-hour rainfall adapted for Climate Change as per RSP 8.5 model. It uses a variable value for the vulnerability of a person if hit by a landslide, based on the landslide size and the person's distance from the source.

Background shade model derived from 8 m New Zealand Digital Elevation Model (LINZ Data Service 2012). PROJECTION: New Zealand Transverse Mercator 2000.

DRW: BL

CHK: CM, SDV

GNS SCIENCE TE PŪ AO

Confidential 2021

LOCAL PERSONAL RISK from earthquake- and rainfall-induced landslides Upper scenario

Regional Landslide Risk Analysis Kaikōura

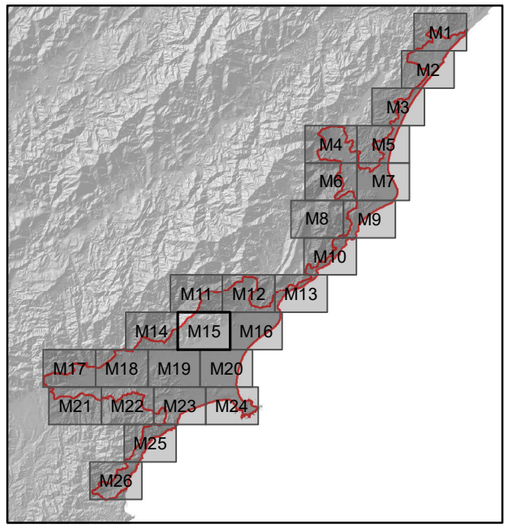
Appendix 4

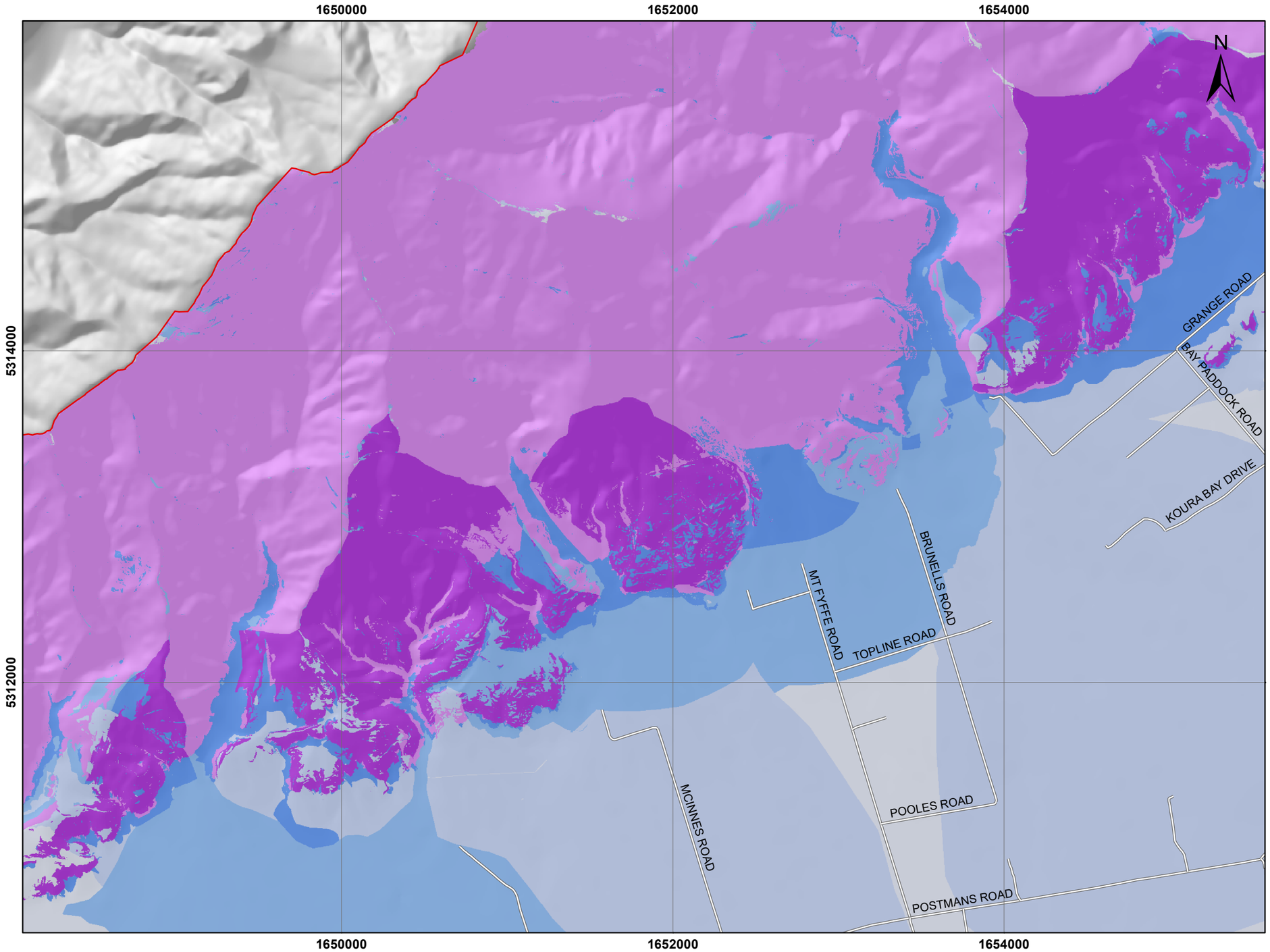
Map 14

FINAL

REPORT: CR2021/89

DATE: Oct 2021





Local personal risk

- 10^{-2} - 10^{-1}
- 10^{-3} - 10^{-2}
- 10^{-4} - 10^{-3}
- 10^{-5} - 10^{-4}
- 10^{-6} - 10^{-5}
- 10^{-7} - 10^{-6}
- Less than 10^{-7}

- Roads
- Railway
- Study area

SCALE BAR: 0 0.5 1 km

EXPLANATION:
The model is based on 84% landslide probability estimates and annual frequencies for 24-hour rainfall adapted for Climate Change as per RSP 8.5 model. It uses a variable value for the vulnerability of a person if hit by a landslide, based on the landslide size and the person's distance from the source.

Background shade model derived from 8 m New Zealand Digital Elevation Model (LINZ Data Service 2012). PROJECTION: New Zealand Transverse Mercator 2000.

DRW: BL

CHK: CM, SDV

GNS SCIENCE TE PŪ AO

Confidential 2021

LOCAL PERSONAL RISK from earthquake- and rainfall-induced landslides Upper scenario

Regional Landslide Risk Analysis Kaikōura

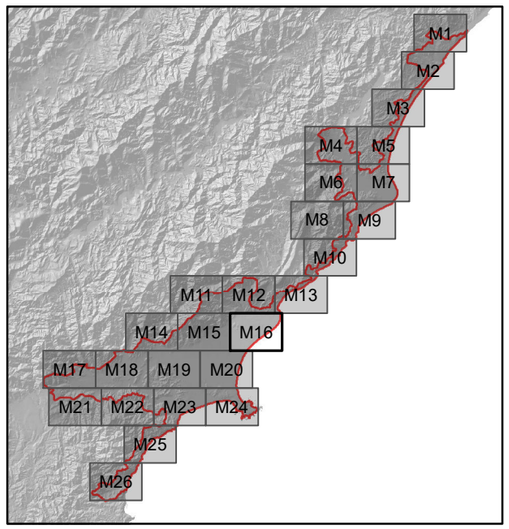
Appendix 4

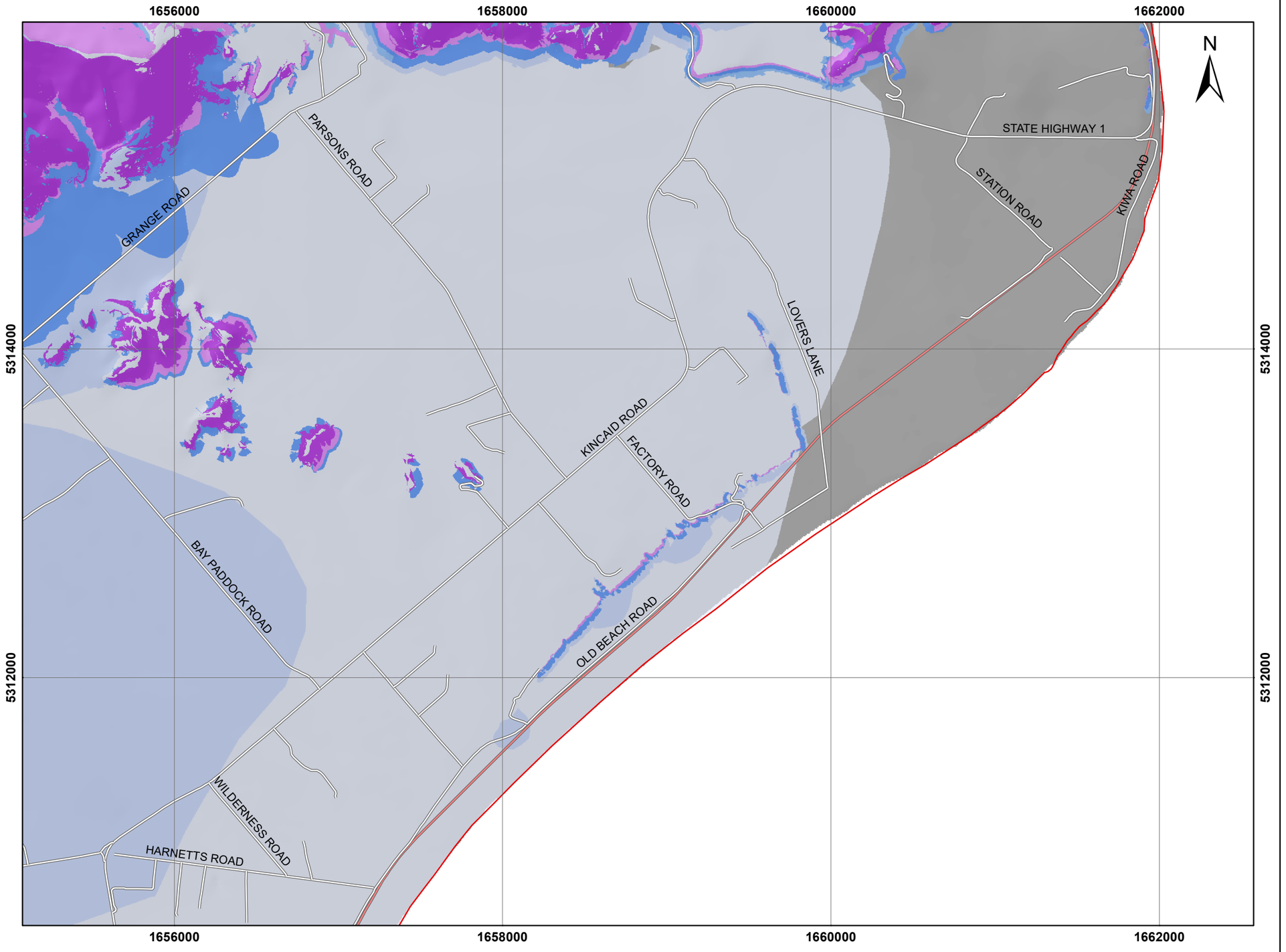
Map 15

FINAL

REPORT: CR2021/89

DATE: Oct 2021





Local personal risk

- 10^{-2} - 10^{-1}
- 10^{-3} - 10^{-2}
- 10^{-4} - 10^{-3}
- 10^{-5} - 10^{-4}
- 10^{-6} - 10^{-5}
- 10^{-7} - 10^{-6}
- Less than 10^{-7}

Roads

Railway

Study area

SCALE BAR: 0 0.5 1 km

EXPLANATION:

The model is based on 84% landslide probability estimates and annual frequencies for 24-hour rainfall adapted for Climate Change as per RSP 8.5 model. It uses a variable value for the vulnerability of a person if hit by a landslide, based on the landslide size and the person's distance from the source.

Background shade model derived from 8 m New Zealand Digital Elevation Model (LINZ Data Service 2012). PROJECTION: New Zealand Transverse Mercator 2000.

DRW: BL

CHK: CM, SDV

GNS SCIENCE TE PŪ AO

Confidential 2021

LOCAL PERSONAL RISK from earthquake- and rainfall-induced landslides Upper scenario

Regional Landslide Risk Analysis Kaikōura

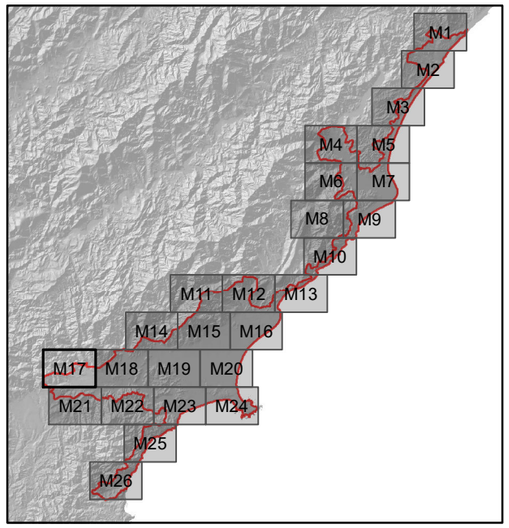
Appendix 4

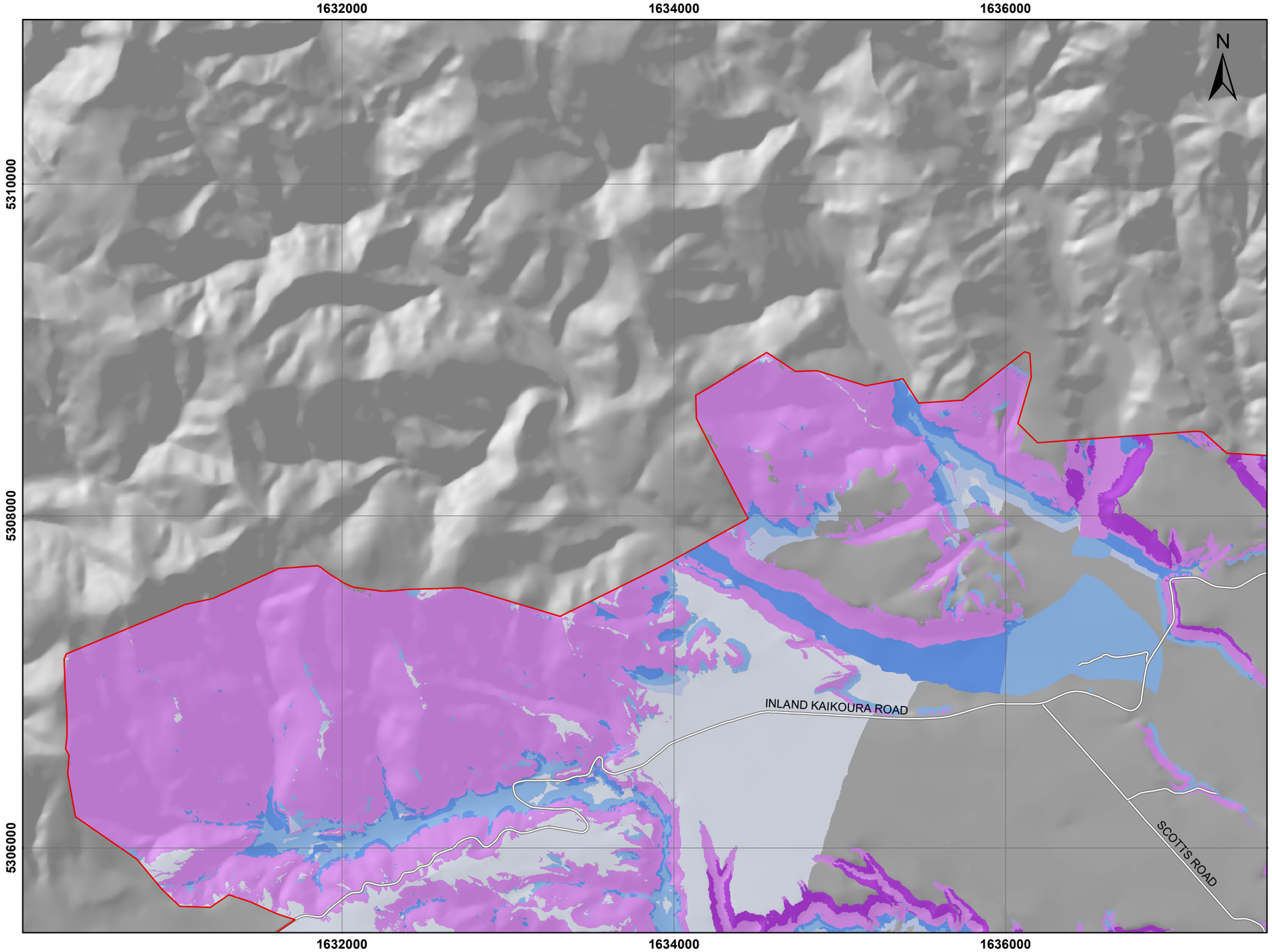
Map 16

FINAL

REPORT: CR2021/89

DATE: Oct 2021





Local personal risk

- 10^{-2} - 10^{-1}
- 10^{-3} - 10^{-2}
- 10^{-4} - 10^{-3}
- 10^{-5} - 10^{-4}
- 10^{-6} - 10^{-5}
- 10^{-7} - 10^{-6}
- Less than 10^{-7}

- Roads
- Railway
- Study area

SCALE BAR: 0 0.5 1 km

EXPLANATION:

The model is based on 84% landslide probability estimates and annual frequencies for 24-hour rainfall adapted for Climate Change as per RSP 8.5 model. It uses a variable value for the vulnerability of a person if hit by a landslide, based on the landslide size and the person's distance from the source.

Background shade model derived from 8 m New Zealand Digital Elevation Model (LINZ Data Service 2012). PROJECTION: New Zealand Transverse Mercator 2000.

DRW: BL

CHK: CM, SDV

GNS SCIENCE TE PŪ AO

Confidential 2021

LOCAL PERSONAL RISK from earthquake- and rainfall-induced landslides Upper scenario

Regional Landslide Risk Analysis Kaikōura

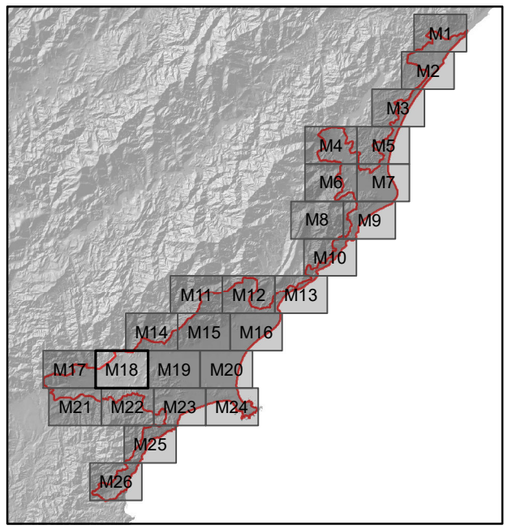
Appendix 4

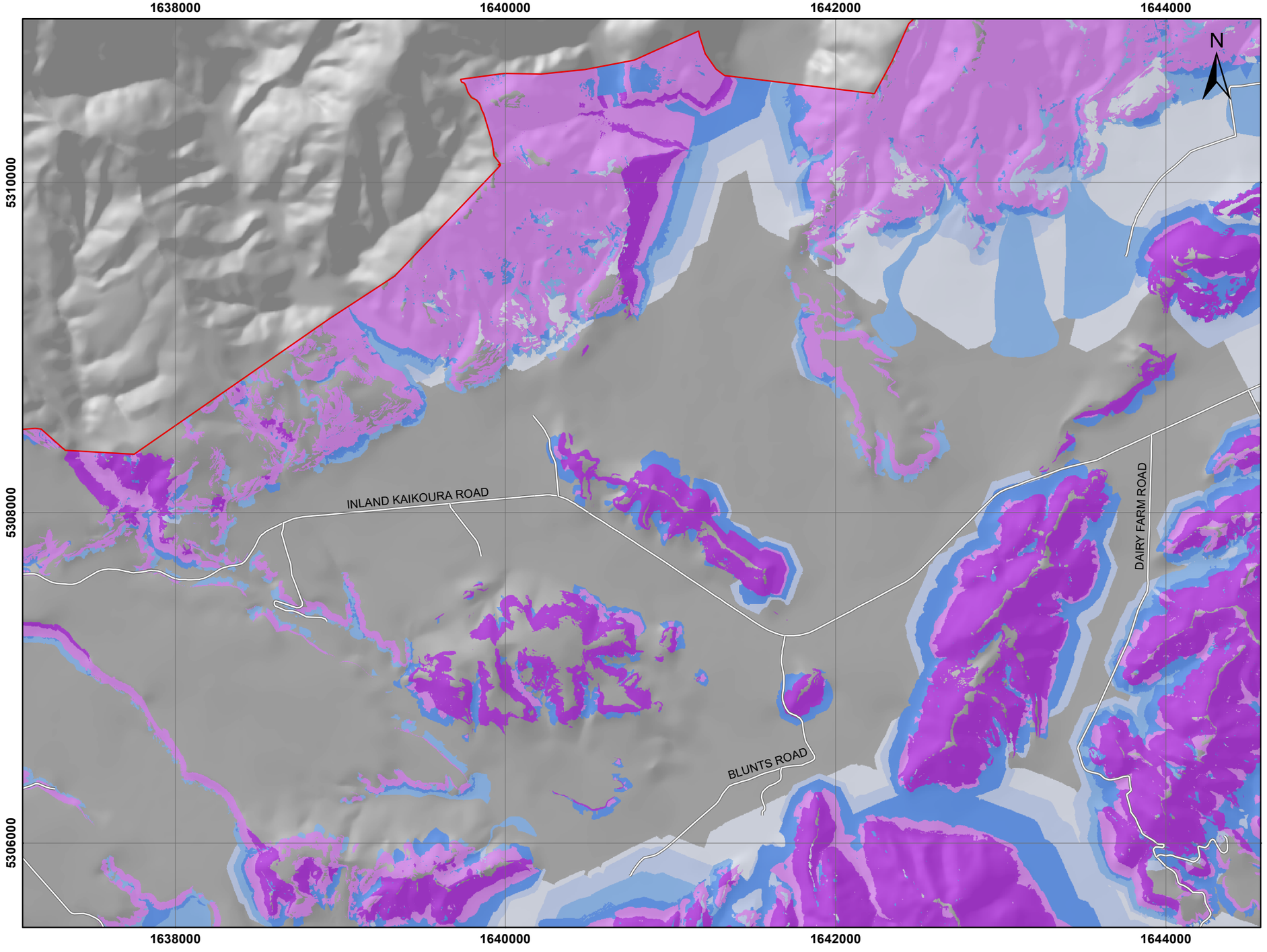
Map 17

FINAL

REPORT: CR2021/89

DATE: Oct 2021





Local personal risk

- 10^{-2} - 10^{-1}
- 10^{-3} - 10^{-2}
- 10^{-4} - 10^{-3}
- 10^{-5} - 10^{-4}
- 10^{-6} - 10^{-5}
- 10^{-7} - 10^{-6}
- Less than 10^{-7}

Roads

Railway

Study area

SCALE BAR: 0 0.5 1 km

EXPLANATION:

The model is based on 84% landslide probability estimates and annual frequencies for 24-hour rainfall adapted for Climate Change as per RSP 8.5 model. It uses a variable value for the vulnerability of a person if hit by a landslide, based on the landslide size and the person's distance from the source.

Background shade model derived from 8 m New Zealand Digital Elevation Model (LINZ Data Service 2012). PROJECTION: New Zealand Transverse Mercator 2000.

DRW: BL

CHK: CM, SDV

GNS SCIENCE TE PŪ AO

Confidential 2021

LOCAL PERSONAL RISK
from earthquake- and rainfall-induced landslides
Upper scenario

Regional Landslide Risk Analysis
Kaikōura

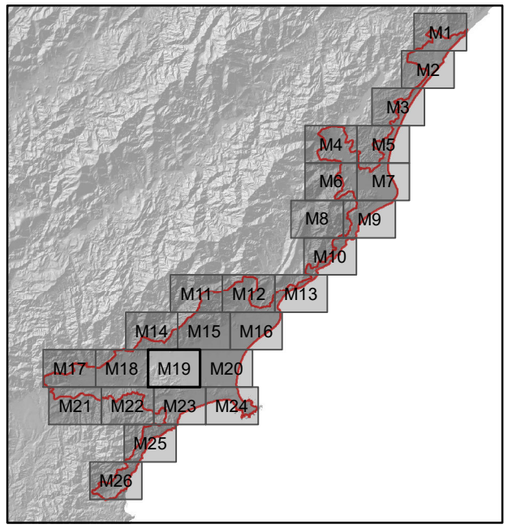
Appendix 4

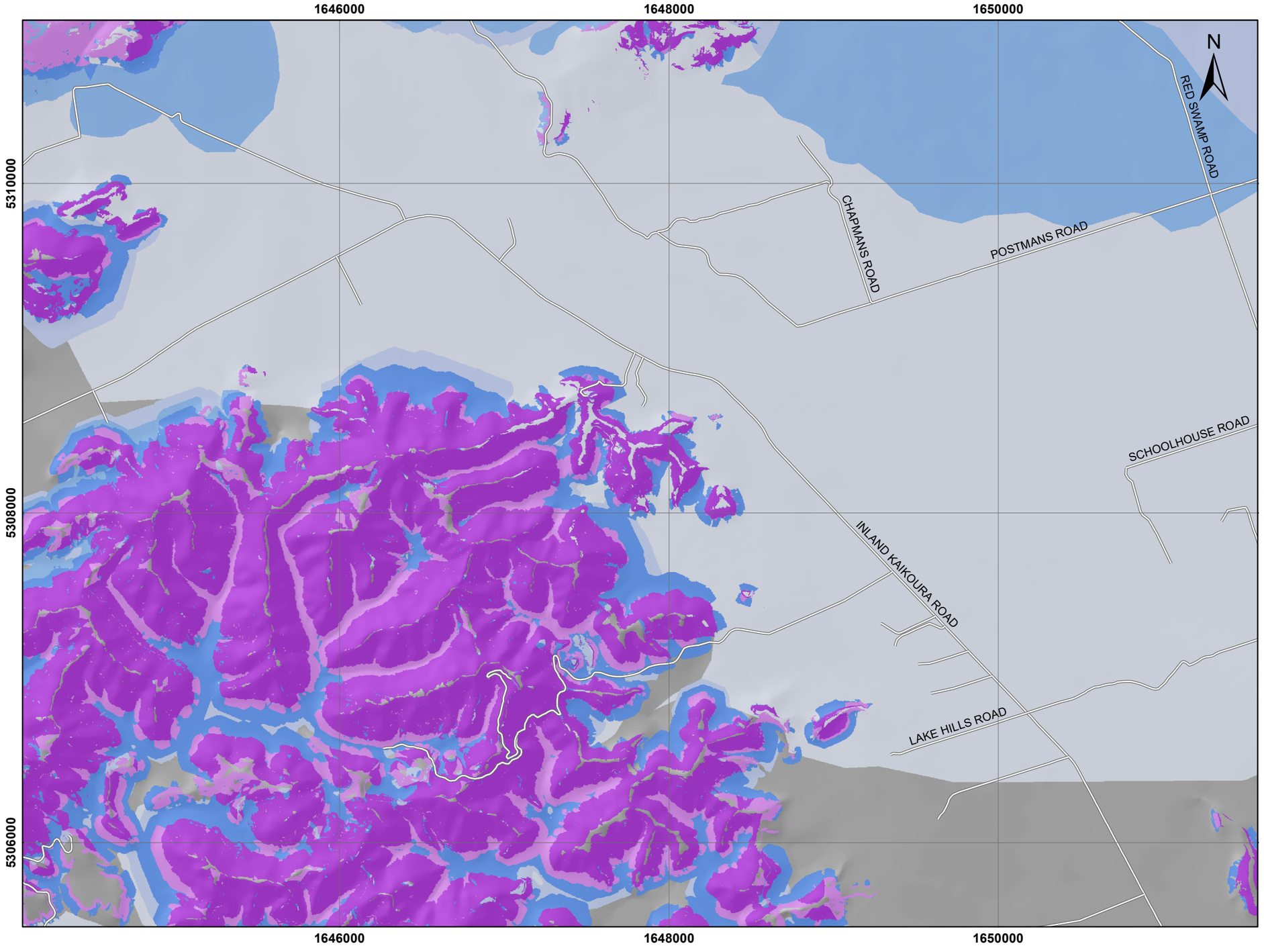
Map 18

FINAL

REPORT: CR2021/89

DATE: Oct 2021





Local personal risk

- 10^{-2} - 10^{-1}
- 10^{-3} - 10^{-2}
- 10^{-4} - 10^{-3}
- 10^{-5} - 10^{-4}
- 10^{-6} - 10^{-5}
- 10^{-7} - 10^{-6}
- Less than 10^{-7}

Roads

Railway

Study area

SCALE BAR: 0 0.5 1 km

EXPLANATION:

The model is based on 84% landslide probability estimates and annual frequencies for 24-hour rainfall adapted for Climate Change as per RSP 8.5 model. It uses a variable value for the vulnerability of a person if hit by a landslide, based on the landslide size and the person's distance from the source.

Background shade model derived from 8 m New Zealand Digital Elevation Model (LINZ Data Service 2012). PROJECTION: New Zealand Transverse Mercator 2000.

DRW: BL

CHK: CM, SDV

GNS SCIENCE TE PŪ AO

Confidential 2021

LOCAL PERSONAL RISK from earthquake- and rainfall-induced landslides Upper scenario

Regional Landslide Risk Analysis Kaikōura

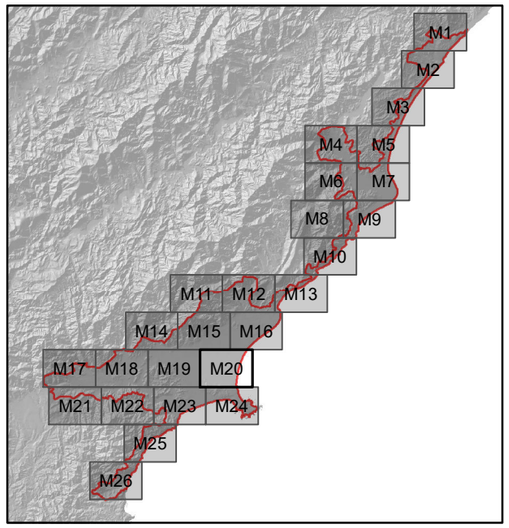
Appendix 4

Map 19

FINAL

REPORT: CR2021/89

DATE: Oct 2021



1652000 1654000 1656000 1658000

5310000

5308000

5306000

N

HARNETTS ROAD
MCINNES ROAD
RED SWAMP ROAD
POSTMANS ROAD
SCHOOLHOUSE ROAD
TITOKI DRIVE
MT FYFFE ROAD
ATHELNEY ROAD
OLD BEACH ROAD
MILL ROAD
HARRIS LANE
RED SWAMP ROAD
HAWTHORNE ROAD
RORRISONS ROAD
BEACH ROAD
LUDSTONE ROAD
GREEN LANE

Local personal risk

- 10^{-2} - 10^{-1}
- 10^{-3} - 10^{-2}
- 10^{-4} - 10^{-3}
- 10^{-5} - 10^{-4}
- 10^{-6} - 10^{-5}
- 10^{-7} - 10^{-6}
- Less than 10^{-7}

- Roads
- Railway
- Study area

SCALE BAR: 0 0.5 1 km

EXPLANATION:

The model is based on 84% landslide probability estimates and annual frequencies for 24-hour rainfall adapted for Climate Change as per RSP 8.5 model. It uses a variable value for the vulnerability of a person if hit by a landslide, based on the landslide size and the person's distance from the source.

Background shade model derived from 8 m New Zealand Digital Elevation Model (LINZ Data Service 2012). PROJECTION: New Zealand Transverse Mercator 2000.

DRW: BL

CHK: CM, SDV

GNS SCIENCE TE PŪ AO

Confidential 2021

LOCAL PERSONAL RISK
from earthquake- and rainfall-induced landslides
Upper scenario

Regional Landslide Risk Analysis
Kaikōura

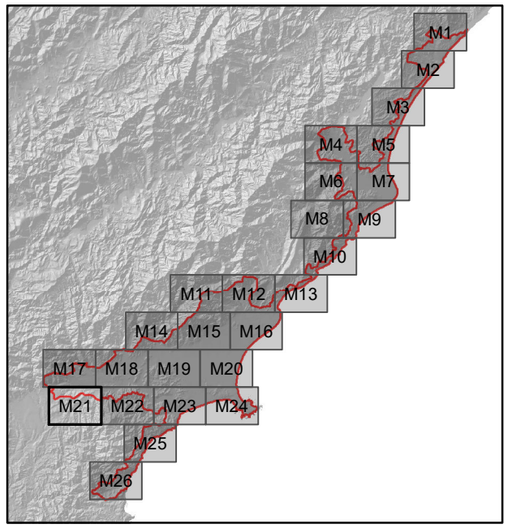
Appendix 4

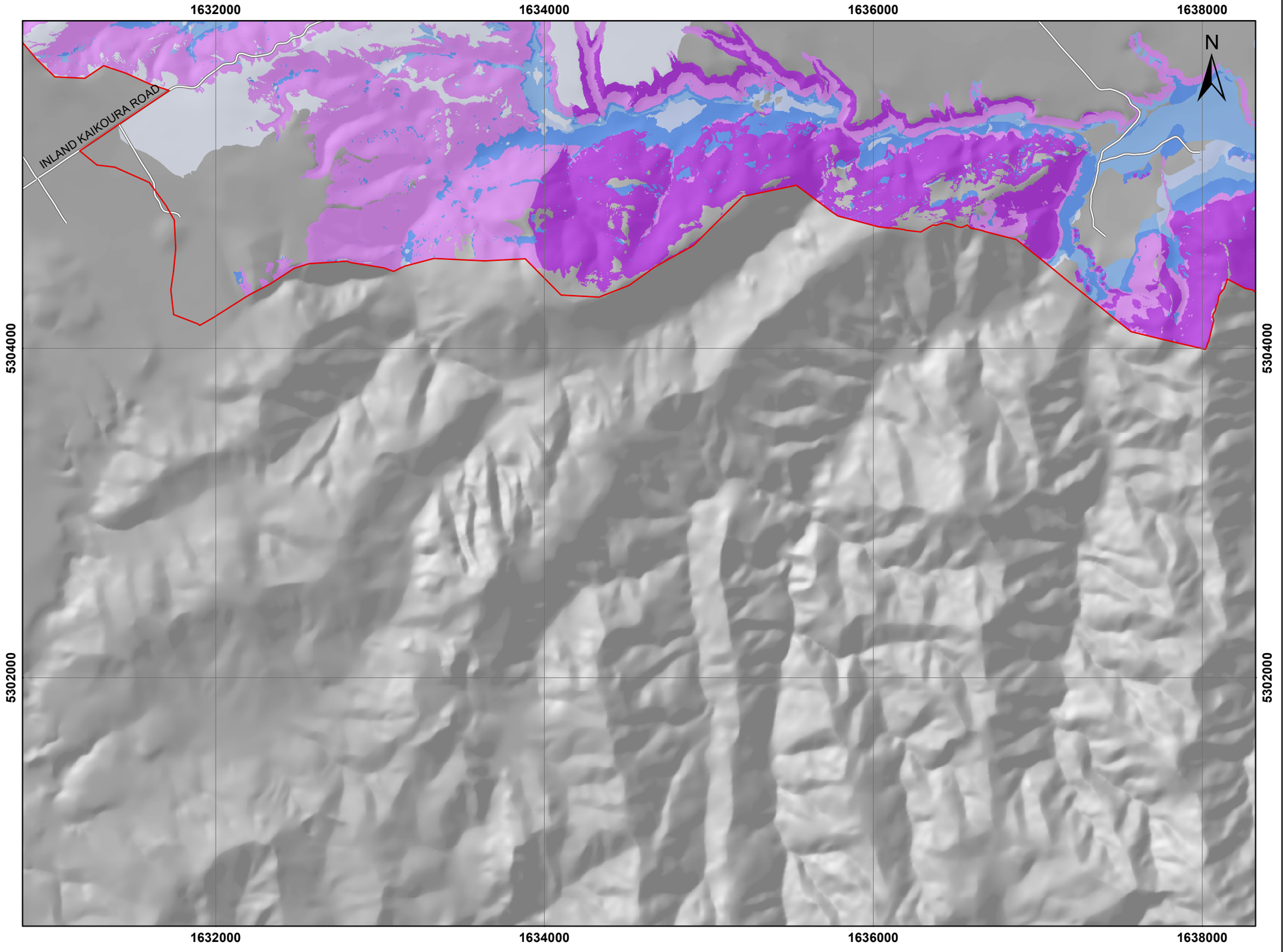
Map 20

FINAL

REPORT: CR2021/89

DATE: Oct 2021





Local personal risk

- 10^{-2} - 10^{-1}
- 10^{-3} - 10^{-2}
- 10^{-4} - 10^{-3}
- 10^{-5} - 10^{-4}
- 10^{-6} - 10^{-5}
- 10^{-7} - 10^{-6}
- Less than 10^{-7}

Roads

Railway

Study area

SCALE BAR: 0 0.5 1 km

EXPLANATION:

The model is based on 84% landslide probability estimates and annual frequencies for 24-hour rainfall adapted for Climate Change as per RSP 8.5 model. It uses a variable value for the vulnerability of a person if hit by a landslide, based on the landslide size and the person's distance from the source.

Background shade model derived from 8 m New Zealand Digital Elevation Model (LINZ Data Service 2012). PROJECTION: New Zealand Transverse Mercator 2000.

DRW: BL

CHK: CM, SDV

Confidential 2021

LOCAL PERSONAL RISK from earthquake- and rainfall-induced landslides Upper scenario

Regional Landslide Risk Analysis Kaikōura

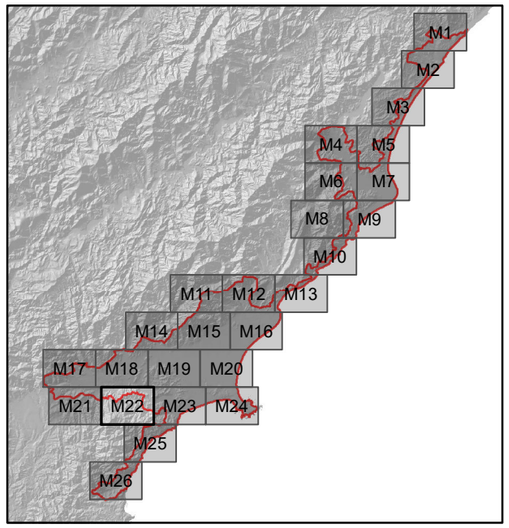
Appendix 4

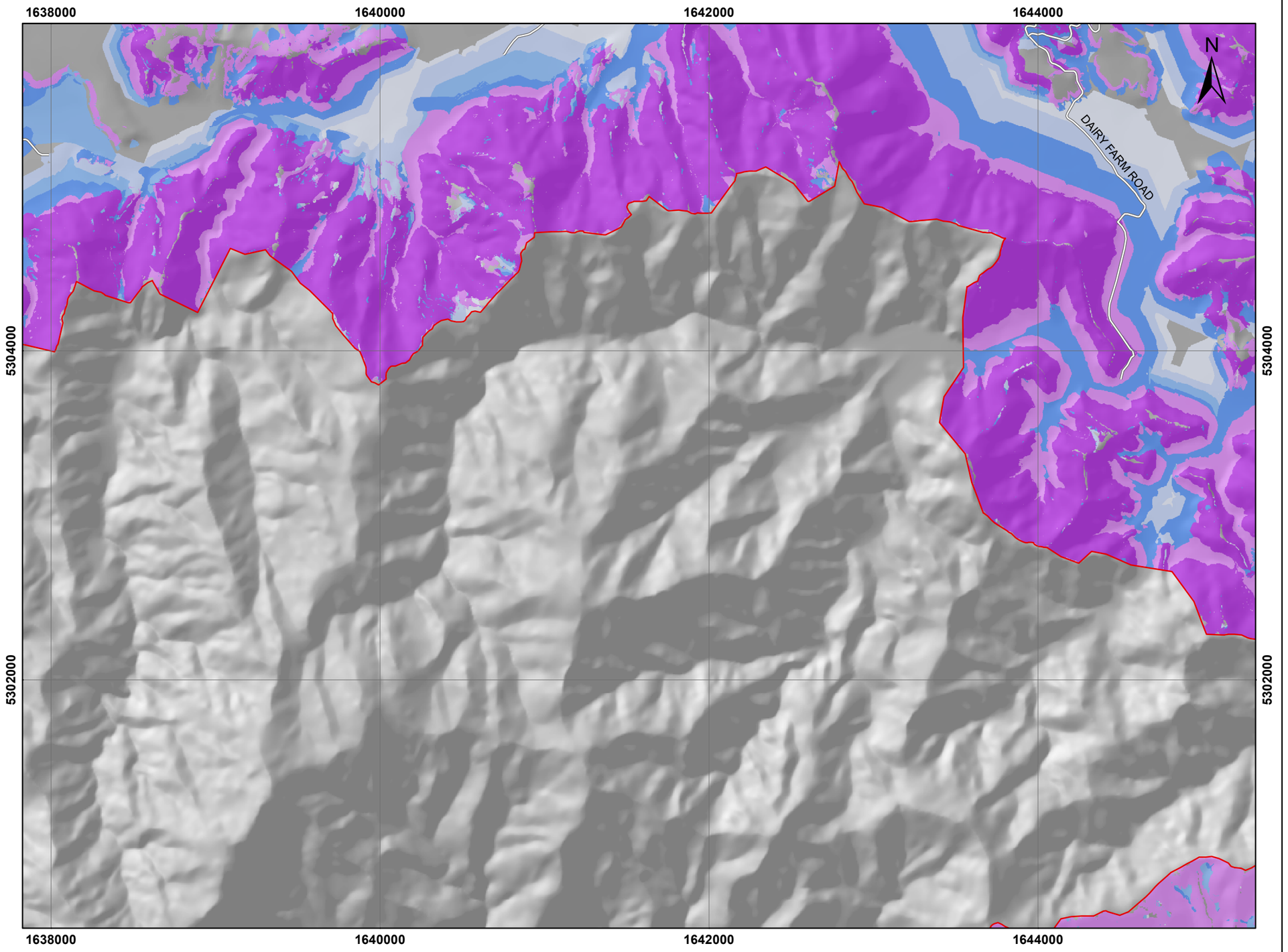
Map 21

FINAL

REPORT: CR2021/89

DATE: Oct 2021





Local personal risk

- 10^{-2} - 10^{-1}
- 10^{-3} - 10^{-2}
- 10^{-4} - 10^{-3}
- 10^{-5} - 10^{-4}
- 10^{-6} - 10^{-5}
- 10^{-7} - 10^{-6}
- Less than 10^{-7}

Roads

Railway

Study area

SCALE BAR: 0 0.5 1 km

EXPLANATION:

The model is based on 84% landslide probability estimates and annual frequencies for 24-hour rainfall adapted for Climate Change as per RSP 8.5 model. It uses a variable value for the vulnerability of a person if hit by a landslide, based on the landslide size and the person's distance from the source.

Background shade model derived from 8 m New Zealand Digital Elevation Model (LINZ Data Service 2012). PROJECTION: New Zealand Transverse Mercator 2000.

DRW: BL

CHK: CM, SDV

GNS SCIENCE TE PŪ AO

Confidential 2021

LOCAL PERSONAL RISK from earthquake- and rainfall-induced landslides Upper scenario

Regional Landslide Risk Analysis Kaikōura

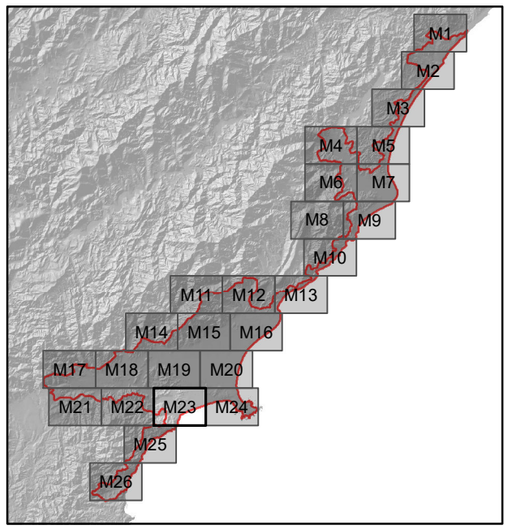
Appendix 4

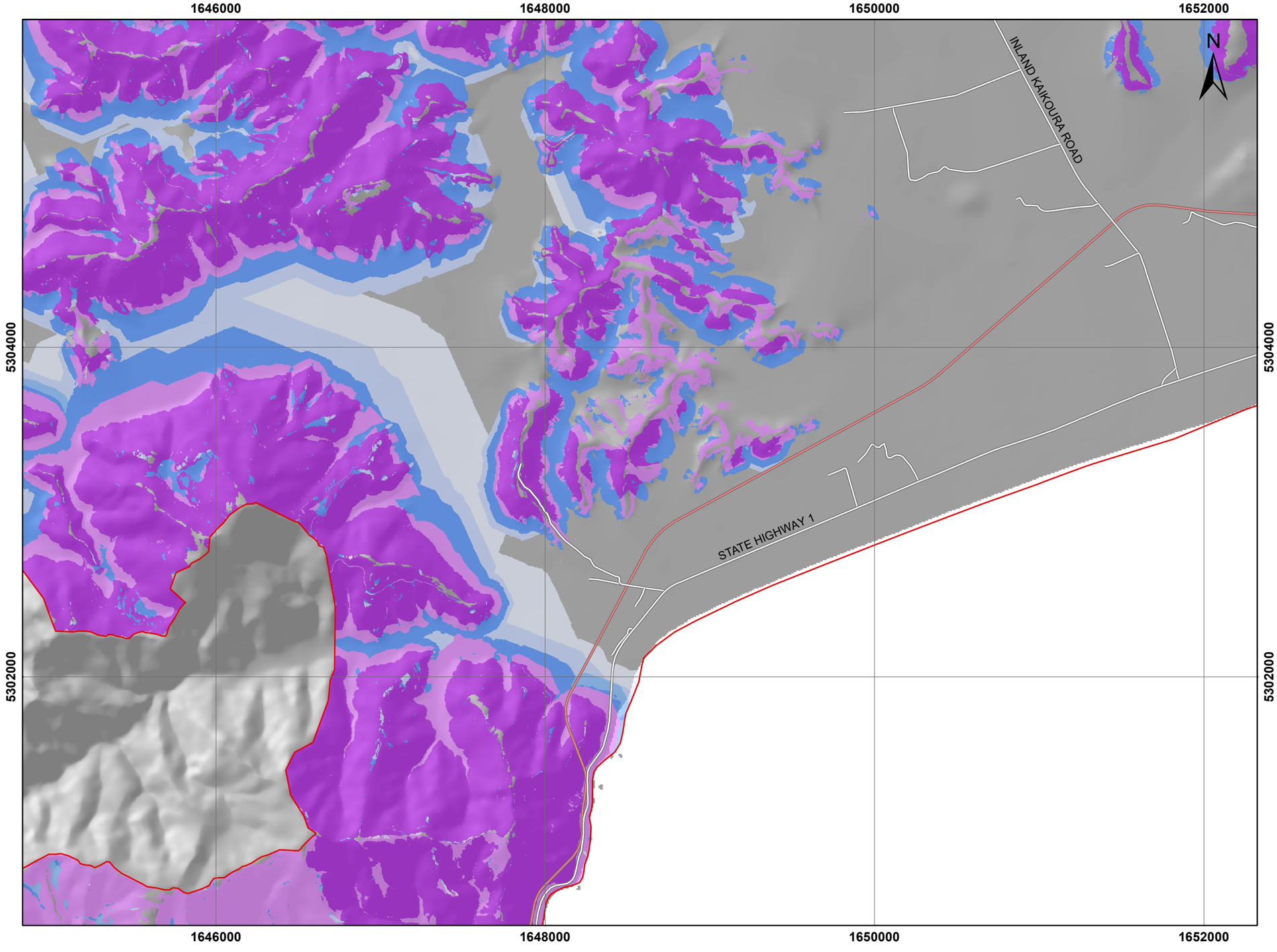
Map 22

FINAL

REPORT: CR2021/89

DATE: Oct 2021





Local personal risk

- 10^{-2} - 10^{-1}
- 10^{-3} - 10^{-2}
- 10^{-4} - 10^{-3}
- 10^{-5} - 10^{-4}
- 10^{-6} - 10^{-5}
- 10^{-7} - 10^{-6}
- Less than 10^{-7}

Roads

Railway

Study area

SCALE BAR: 0 0.5 1 km

EXPLANATION:

The model is based on 84% landslide probability estimates and annual frequencies for 24-hour rainfall adapted for Climate Change as per RSP 8.5 model. It uses a variable value for the vulnerability of a person if hit by a landslide, based on the landslide size and the person's distance from the source.

Background shade model derived from 8 m New Zealand Digital Elevation Model (LINZ Data Service 2012). PROJECTION: New Zealand Transverse Mercator 2000.

DRW: BL

CHK: CM, SDV

GNS SCIENCE TE PŪ AO

Confidential 2021

LOCAL PERSONAL RISK from earthquake- and rainfall-induced landslides Upper scenario

Regional Landslide Risk Analysis Kaikōura

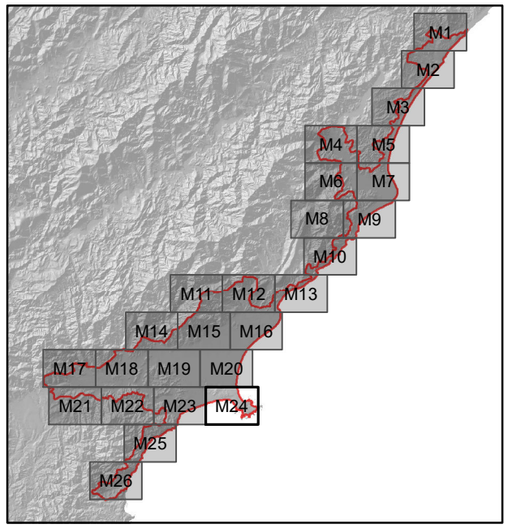
Appendix 4

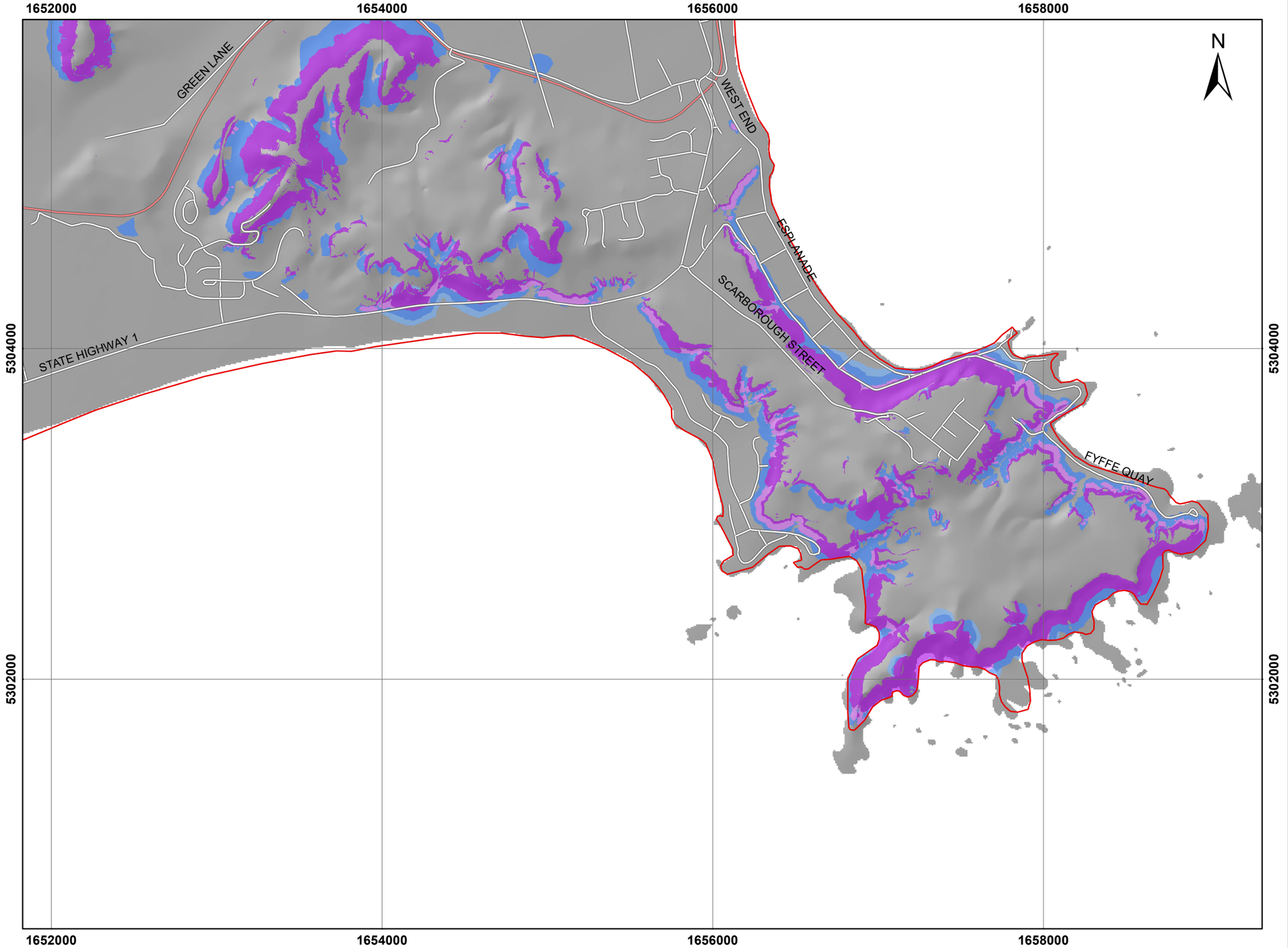
Map 23

FINAL

REPORT: CR2021/89

DATE: Oct 2021





Local personal risk

- 10^{-2} - 10^{-1}
- 10^{-3} - 10^{-2}
- 10^{-4} - 10^{-3}
- 10^{-5} - 10^{-4}
- 10^{-6} - 10^{-5}
- 10^{-7} - 10^{-6}
- Less than 10^{-7}

Roads

Railway

Study area

SCALE BAR: 0 0.5 1 km

EXPLANATION:

The model is based on 84% landslide probability estimates and annual frequencies for 24-hour rainfall adapted for Climate Change as per RSP 8.5 model. It uses a variable value for the vulnerability of a person if hit by a landslide, based on the landslide size and the person's distance from the source.

Background shade model derived from 8 m New Zealand Digital Elevation Model (LINZ Data Service 2012). PROJECTION: New Zealand Transverse Mercator 2000.

DRW: BL

CHK: CM, SDV

GNS SCIENCE TE PŪ AO

Confidential 2021

LOCAL PERSONAL RISK from earthquake- and rainfall-induced landslides Upper scenario

Regional Landslide Risk Analysis Kaikōura

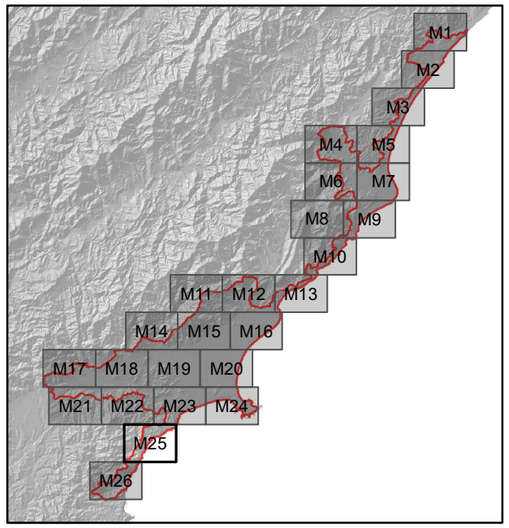
Appendix 4

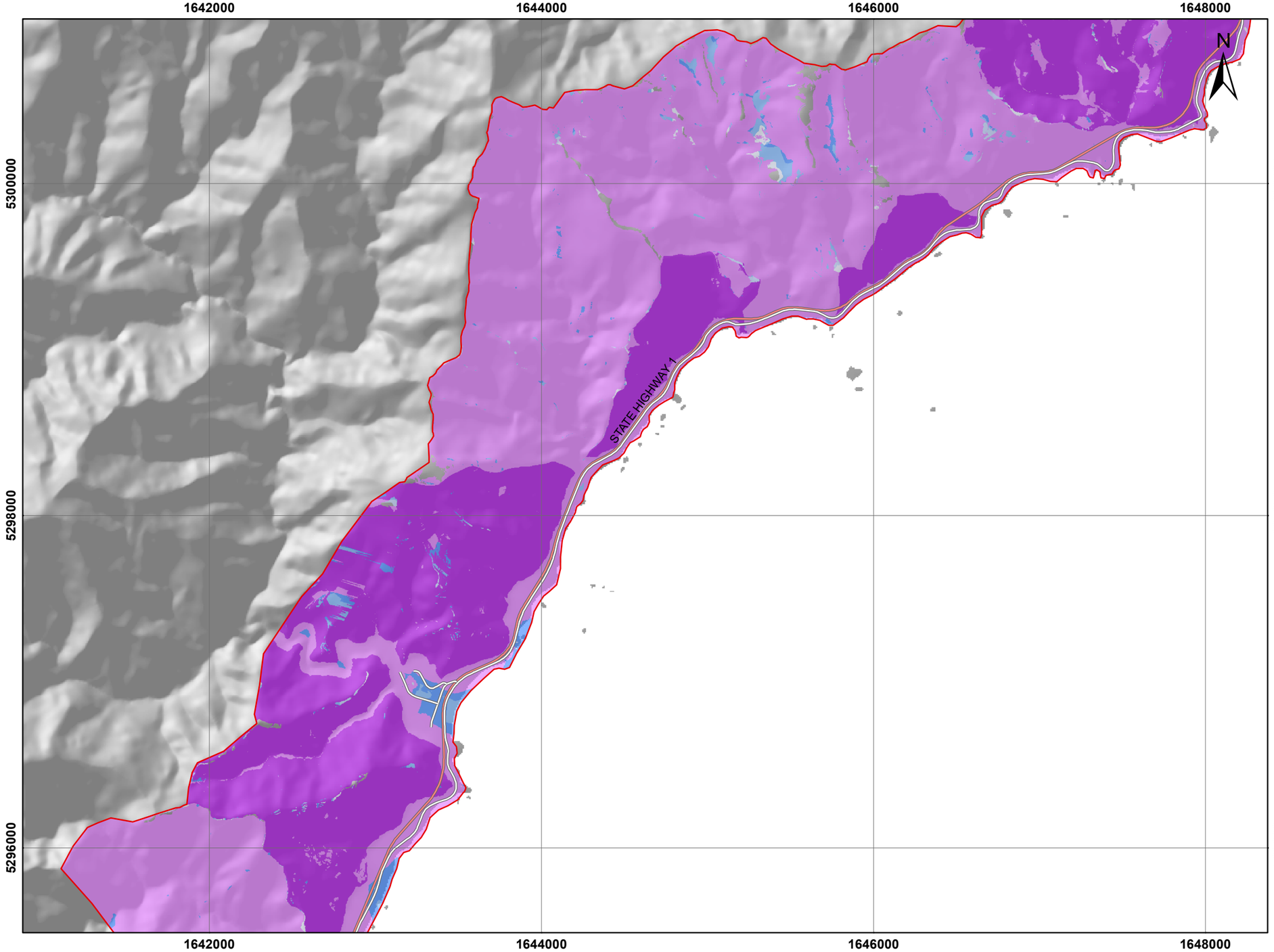
Map 24

FINAL

REPORT: CR2021/89

DATE: Oct 2021





Local personal risk

- 10^{-2} - 10^{-1}
- 10^{-3} - 10^{-2}
- 10^{-4} - 10^{-3}
- 10^{-5} - 10^{-4}
- 10^{-6} - 10^{-5}
- 10^{-7} - 10^{-6}
- Less than 10^{-7}

- Roads
- Railway
- Study area

SCALE BAR: 0 0.5 1 km

EXPLANATION:
The model is based on 84% landslide probability estimates and annual frequencies for 24-hour rainfall adapted for Climate Change as per RSP 8.5 model. It uses a variable value for the vulnerability of a person if hit by a landslide, based on the landslide size and the person's distance from the source.

Background shade model derived from 8 m New Zealand Digital Elevation Model (LINZ Data Service 2012). PROJECTION: New Zealand Transverse Mercator 2000.

DRW: BL

CHK: CM, SDV

GNS SCIENCE TE PŪ AO

Confidential 2021

LOCAL PERSONAL RISK
from earthquake- and rainfall-induced landslides
Upper scenario

Regional Landslide Risk Analysis
Kaikōura

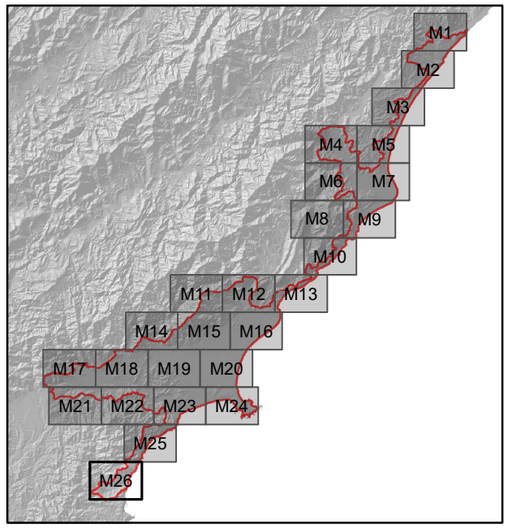
Appendix 4

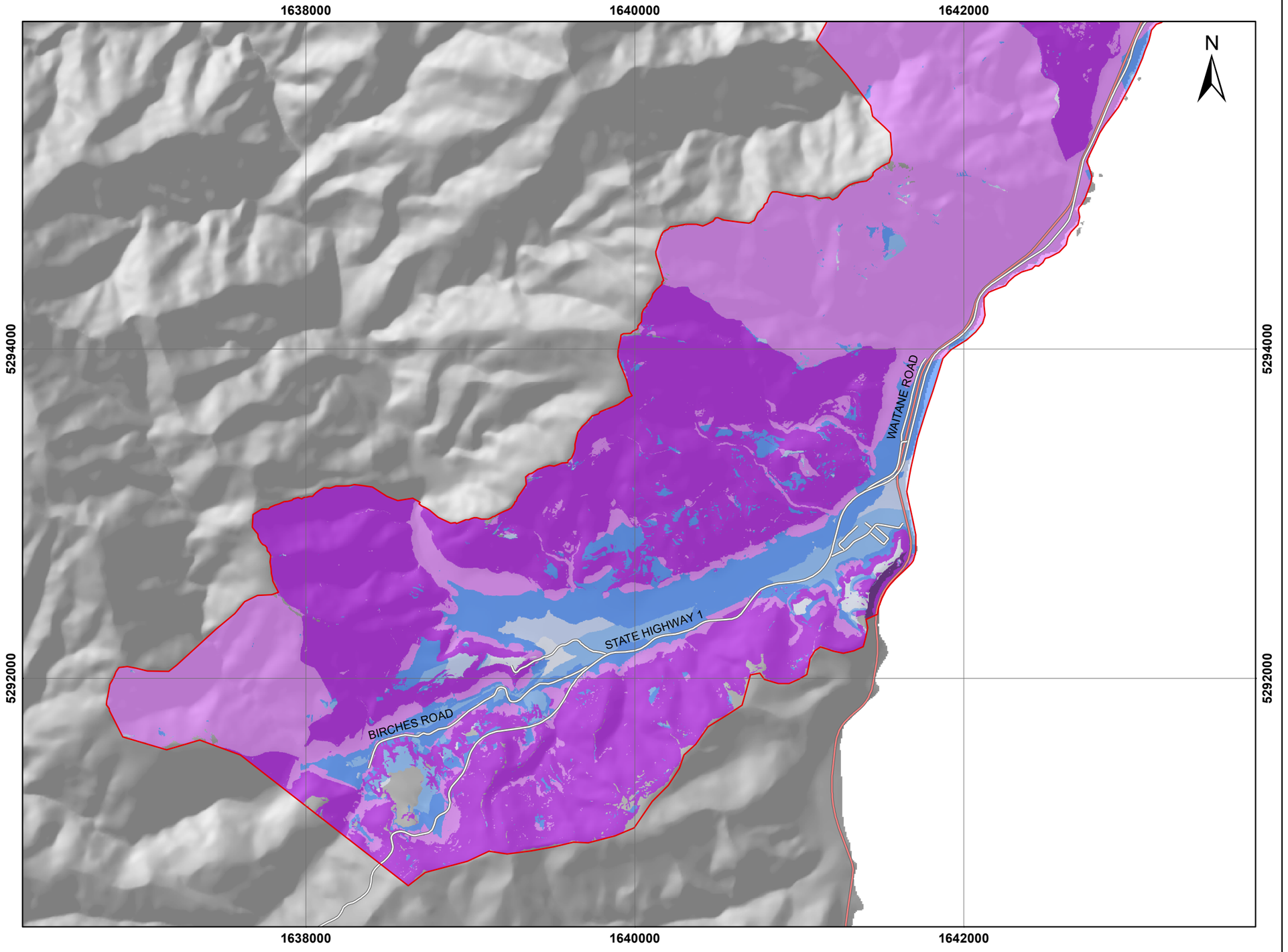
Map 25

FINAL

REPORT: CR2021/89

DATE: Oct 2021





Local personal risk

- 10^{-2} - 10^{-1}
- 10^{-3} - 10^{-2}
- 10^{-4} - 10^{-3}
- 10^{-5} - 10^{-4}
- 10^{-6} - 10^{-5}
- 10^{-7} - 10^{-6}
- Less than 10^{-7}

Roads

Railway

Study area

SCALE BAR: 0 0.5 1 km

EXPLANATION:

The model is based on 84% landslide probability estimates and annual frequencies for 24-hour rainfall adapted for Climate Change as per RSP 8.5 model. It uses a variable value for the vulnerability of a person if hit by a landslide, based on the landslide size and the person's distance from the source.

Background shade model derived from 8 m New Zealand Digital Elevation Model (LINZ Data Service 2012). PROJECTION: New Zealand Transverse Mercator 2000.

DRW: BL

CHK: CM, SDV

Confidential 2021

LOCAL PERSONAL RISK
from earthquake- and rainfall-induced landslides
Upper scenario

Regional Landslide Risk Analysis
Kaikōura

Appendix 4

Map 26

FINAL

REPORT: CR2021/89

DATE: Oct 2021

APPENDIX 5 EXAMPLE SITE-SPECIFIC ASSESSMENT FORM

Example Site Specific Risk Analysis Form

Is the dwelling located on a debris fan? (*Use mapped debris fans from Phase 1 report).*
If Yes, Skip Section A. If No, Answer Section A

Section A: What is the maximum credible volume that could fall from the slope?
(Use the criteria from the Phase 1 report, set out in tbe table below)

Representative volume (m^3)	Minimum local slope relief in the 80 m radius (m)	Source plan area (m^2) for landslide volume
10	3	5
100	22	45
1000	39	410
10,000	51	3800
100,000	66	35,000
1,000,000	71	371,000
10,000,000	83	2,900,000

To determine the maximum credible volume that could fall from the slope? Measure the height and angle of the sklope to answert the following questions:

1. What is the height of the Slope?

_____

2. What is the area of the Slope?

_____

Compare answers to the table. What is the maximum credible volume that could fall from the slope?

_____

Is this smaller or larger than the source area volume in the risk models?

_____

Section B: Do the landslide susceptibility models vary considerably across the site? For example are thar areas of high or low susceptibility above the dwelling? Compare to the susceptibility models in the Phase 2 report.

_____

Could these areas of higher susceptibility deliver debris to the dwelling?

_____

Are there site specific factor that increase the susceptibiliyt? e.g. cracking, loose blocks in the slope? Is there evidence of past landslides at the site?

_____

Section C: Are there site-speciific factors (e.g. vegetation, engineering works (such as bunds), local topographic features) that could prevent the debris from reach the dwelling? For large volumes, these features would have to be large to prevent this.

To determine this, measure the F-angle at the dwelling to the steepest point of the slope above the dwelling.. Use the f-angles for the different volume classes and probability of runout exceedence (50% and 2.3%) in the Phase 2 report.
Is the dwelling within the maximum credible landslide volume f-angle footprint?

For 50%: _____ and For 2.3%: _____

Check obstacle heights used in the Phase 1 report (see table below). Are the site specific factors lower or higher than those used?

_____

Landslide volume class (m^3)	Obstacle height that does not stop runout (m)
10, 100	0
1000	0.5
10,000, 100,000, 1,000,000, 10,000,000	1

Section D: Based on answers to Section A, B and C is the risk higher or lower than the risk models in the Phase 2 report?
Outline reasoning below:

_____



www.gns.cri.nz

Principal Location

1 Fairway Drive, Avalon
Lower Hutt 5010
PO Box 30368
Lower Hutt 5040
New Zealand
T +64-4-570 1444
F +64-4-570 4600

Other Locations

Dunedin Research Centre
764 Cumberland Street
Private Bag 1930
Dunedin 9054
New Zealand
T +64-3-477 4050
F +64-3-477 5232

Wairakei Research Centre
114 Karetoto Road
Private Bag 2000
Taupo 3352
New Zealand
T +64-7-374 8211
F +64-7-374 8199

National Isotope Centre
30 Gracefield Road
PO Box 30368
Lower Hutt 5040
New Zealand
T +64-4-570 1444
F +64-4-570 4657